Surface Engineering of Polymers

Rachel Kate Wells BSc. (Hons.) (Dunelm)

Ph. D. Thesis
Department of Chemistry
University of Durham
1994

ACKNOWLEDGEMENTS

I would like to express my sincere thanks to my supervisor Dr Jas Pal Badyal for his guidance over the past four years.

Thank you to Vicki Ruddick for her help in Chapter 7, and all members of Lab 98 for their support. I would also like to thank all the technical staff for their assistance, in particular George Rowe, Ray Hart, Gordon Haswell, Jim Hodgson, Dr Mike Jones, Bob Coult, Judith Magee and also Dr Tony Royston for his work on the data analysis software.

I am grateful to Kratos Analytical for valence band XPS spectroscopy data, and to Professors R. K. Harris and D. L. H. Williams for making all the facilities at the Department of Chemistry available to me.

I would also like to thank Dr David Perry, my industrial supervisor at B.P. International, Sunbury-upon-Thames.

I acknowledge financial support by the SERC and BP International Limited for a CASE Studentship.

Lastly, I would like to thank Rick (my husband), my parents and all our family for their encouragement and support particularly over the past year.

ABSTRACT

Ultra-violet photons and non-equilibrium plasmas have been used as modification methods to treat polymer surfaces.

The photoreactivity of polystyrene with oxygen and nitrous oxide was found to be linked to the photochemistry occuring at the polymer/gas interface. *In situ* mass spectrometry studies of the photolysis and photo-oxidation of polystyrene enabled possible mechanisms of these reactions to be determined, and perhaps proved for the first time the presence of intermediate phenyl radicals.

Photo-oxidised and plasma oxidised polystyrene surfaces were compared using valence band and core level XPS, and provided another insight into polystyrene surface oxidation processes. The more reactive experimental conditions during plasma treatment were found to produce a less oxidised surface than during photo-oxidation. These observations were attributed to the sputtering characteristics of a plasma environment.

Polyethylene and polystyrene were oxidised by plasma treatment and the aging of the resulting surfaces in air was studied by core level XPS, which showed a gradual loss of surface oxidation after treatment. Valence band XPS of the aged polyethylene surface revealed a uniquely selective surface structure. Oxidised polyethylene rearranged upon aging to give a polypropylene-type structure.

The relative importance of substrate/gaseous molecule photo-reactivity was again highlighted by comparing chromophoric (polystyrene)/nonchromophoric (polyethylene) polymers with chromophoric (hexamethyldisilane)/nonchromophoric (tetramethylsilane) species. Greatest reaction occured when both chromophoric alternatives were used.

Dehydrochlorination of polyvinylchloride was found to depend upon the surrounding atmosphere, vacuum conditions giving the greatest degree of modification. This reaction was monitored by *in situ* mass spectrometry, and indicated that the rate of dehydrochlorination depended upon the initiation mechanism of dehydrochlorination.

MEMORANDUM

The work described in this report is the original work of the author (except where specific reference is made to other sources) and has not been submitted for any other degree.

Work in this thesis has formed the whole, or part of the following publications:

1) *Photo-oxidation of Polystyrene by O_2 and N_2O,* R.K. Wells and J.P.S. Badyal, J. Polymer Science: Polymer Chemistry Edn., 30, (1992), 2677.
2) *Plasma Induced Catalysis at Polymer Surfaces,* R.K. Wells, I.W. Drummond, K.S. Robinson, F.J. Street and J.P.S. Badyal, Chemical Communications, 6, (1993).
3) *Photochemistry at the Organosilane / Polymer Interface,* R.K. Wells and J.P.S. Badyal, Macromolecules, 26, (1993), 3187.
4) *A Comparison of Plasma Oxidized and Photo-Oxidized Polystyrene Surfaces,* R.K. Wells, I.W. Drummond, K.S. Robinson, F.J. Street and J.P.S. Badyal, Polymer, 34, (1993), 3611.
5) *Plasma Oxidation of Polystyrene Versus Polyethylene,* R.K. Wells, I.W. Drummond, K.S. Robinson, F.J. Street and J.P.S. Badyal, Journal of Adhesion Science and Technology, 7, (1993), 1129.

Other Publications:

6) *Modelling of Non-Isothermal Glow Discharge Modification of PTFE using Low Energy Ion Beams,* R. K. Wells, M. E. Ryan, and J. P. S. Badyal, Journal of Physical Chemistry, 97, (1993), 12879.
7) *Plasma Oxidation of Copper-Silver Alloy Surfaces,* J.M. Knight, R.K. Wells and J.P.S. Badyal, Chemistry of Materials, 4, (1992), 640.
8) *Plasma Induced Segregation at Copper-Silver Binary Alloy Surfaces,* Proceedings of 11th International Symposium on Plasma Chemistry, 3, (1993), 956.
9) *A Comparative Study of the Silent Discharge Treatment of Polyethylene, Polypropylene, Polyisobutylene, and Polystyrene,* O.D. Greenwood, R.K. Wells and J.P.S. Badyal, Proceedings of 11th International Symposium on Plasma Chemistry, 3, (1993), 1168.

CONTENTS

CHAPTER 1

GENERAL INTRODUCTION

1. INTRODUCTION

Polymers are extensively used in many areas of everyday life. Traditional materials are increasingly being replaced with less expensive and often better performing polymers (e.g. in car parts and packaging).

A bulk polymer is often chosen for a particular application because of its specific physical properties, such as rigidity and strength. However, the surface of the polymer is often unsuitable for some reason, for example, paint coverage is poor or adhesion to another component fails. Therefore it becomes necessary to modify the physical and chemical properties of the polymer surface whilst retaining the properties of the bulk. Polymer surfaces are important, as it is the surface that comes into contact with the environment in which the polymer is being used.

Surface engineering of polymers is of considerable commercial and academic interest. Many methods of surface modification are available: the addition of surface modifying bulk additives[1], wet chemical[2,3] and flame[4] treatments, photon-induced modifications[5,6,7], physical abrasion[8,9], ion beam treatment[10,11], and plasma treatments[12,13], have all been used. Changes in wettability[14], permeability[15], biocompatibility[16], and adhesion[17,18] are achievable.

All of the above treatments have so far produced a wide range of surface chemical functionalities, and most are poorly understood at the molecular level. The long term goal in this area is to develop highly selective surface modification methods.

In this chapter, a brief overview of polymer surface morphology is given, followed by a summary of surface modification techniques.

2. MORPHOLOGY OF POLYMER SURFACES

The orientation of a polymer at a surface is almost always different from that in the interior; the polymer chains may be lying flat, oriented in the surface plane or, if some special group is attracted to the surface, the orientation may be normal to the plane of the surface[19].

The surface region is generally thought of as being 50-100 Å thick, but the depth of the surface of interest depends upon the nature of the property being studied[19] (wettability may be more surface sensitive than permeability). Measurable thickness depends upon the instrument used and upon its limitations.

Polymer structures and properties are, in general, time and temperature dependant[20,21]. Because of the relatively large size and high molecular weight of synthetic polymer molecules, most polymeric solids rarely achieve true equilibrium. Polymers are therefore non-equilibrium structures and so exhibit a range of relaxation times and properties under normal conditions and in response to changing environments[21]. The above features have long been known to be true for bulk polymer structures, and it is now thought that polymer surfaces are also time, temperature and environment dependant[20].

Surface dynamics permit the interface (i.e the surface of the polymer in contact with the environment) to restructure or reorient in response to different environments. This effect is particularly pronounced in aqueous solutions, where the polarity of the aqueous phase provides a high interfacial free energy driving force for the migration or orientation of polar phases, blocks, segments, or side chains towards the aqueous phase, thereby minimising the interfacial free energy. In a vacuum, air, or other non-polar environment, the polymer orients its apolar components towards the interface again minimising the interfacial free energy.

The time for relaxation in response to a change in environment depends on the intrinsic rigidity of the polymer. In a flexible elastomer, or in general, at temperatures substantially above the glass transition temperature (T_g), surface accommodation will take place in the seconds to hours range. Highly rigid polymers, such as those having inherently stiff chains, and systems in which mobility is restricted through cross linking, may require hours, days or longer to accommodate to environmental changes.

3. SURFACE MODIFICATION TECHNIQUES

3.1 ADDITIVES

Many types of additives may be included during manufacturing of polymers to enhance their properties e.g. those that assist processing, modify bulk mechanical and optical properties, antiaging and surface properties modifiers[1]. Surface property modifiers can be used to alter surface roughness and polarity.

Additives which increase surface roughness are used in order to reduce the intimacy of contact with another component or to induce light scattering and reduce surface gloss. This effect is induced by introducing

into the polymer fine, rigid or rubbery particles. An application of this is in the production of packaging films in order to minimise 'blocking' i.e. the tendency of adjacent film surfaces to stick to one another under pressure.

Additives may form a boundary layer at the surface of polymers resulting from the exudation of the additive from the bulk[1]. This can be exploited to reduce friction and wear, for example by the addition of solid lubricants such as graphite and PTFE powder. In the processing of low density polyethylene, ppm concentrations of oleamide or stearamide (Figure 1) may be included[22]. The amides diffuse to the surface to provide a thin film which is readily sheared.

$CH_3(CH_2)_7CH{=}CH(CH_2)_7CONH_2$ Oleamide

$CH_3(CH_2)_{16}CONH_2$ Stearamide

Figure 1: Molecular formulae of oleamide and stearamide.

The formation of a boundary layer may be used to reduce the build-up of electrostatic charges. Charging of the surface can be decreased by rendering the surface conductive, for example, by inclusion of easily ionisable additives which can migrate to the surface and form conductive paths (e.g. long chain amines and sulphonic acids)[1]. Although easily ionisable compounds such as LiCl may seem an ideal anti-static agent, they may leach out of the system too quickly and therefore be ineffective.

In the absence of a boundary-forming additive, polarity at a polymer surface may be achieved by enriching the regions of the material near the surface with additives whose polarity is substantially different from that of the basic polymer. Inclusion of a substance in the polymer which is sufficiently compatible with the polymer but has a low tendency to crystallise out on the polymer surface may change the surface polarity[1], for example titanates aid the adhesion of polymers to glasses and metals.

Additives are fairly easy to include during polymer processing, but the disadvantages are that relatively large quantities are required and the resulting surface effects may be non-specific.

3.2 WET CHEMICAL TREATMENT

Wet chemical treatments of polymer surfaces usually involve adding a variety of functional groups[3]. The major disadvantages of this method are that the modified layer may be fairly deep and solvents are required. Chromic acid etching of polyethylene and polypropylene resulted in a depth of oxidation of ~300 Å[23]. Various oxygenated functionalities were observed on the polymer surfaces by XPS, giving an overall level of oxidation in which 5% of the carbons in the analysed region had been oxidatively modified. This gave a large (approximately 16 fold) increase in adhesion to the modified surface.

To know if a reagent will react with the polymer surface or if it is able to react internally also, the solubility parameters of the polymer, solvent and reagent are required[24]. Surface reactions occur when the reagent cannot penetrate the polymer or when chemical reactions are faster than diffusion of the reactant into the polymer. Internal reactions occur when a solvent or reagent is able to swell the polymer and diffusion of reactant into the polymer is faster than chemical reaction. An example of this is in the surface sulphonation of polystyrene beads used as ion exchange resins[25]. In initial work, uncontrolled sulphonation lead to the whole polystyrene bead being treated (i.e. surface and bulk). This lead to slow kinetics of ion exchange due to swelling of the beads by water diffusion. If a highly crosslinked polystyrene bead was sulphonated, the sulphate groups were limited to the surface. This blocked transport of water into the bead interior and hence stopped swelling during ion exchange.

If wet chemical processes are used on an industrial scale, the costs of solvent disposal and re-purification make wet chemical methods unattractive.

An extension of the wet chemical technique is surface grafting[3]. This type of chemistry can be fairly specific. It usually involves a radical reaction which attaches functional groups from a solution onto the surface. Surface grafting may be initiated by several types of radiation. γ - Radiation has been used to induce graft copolymerisation of vinyl acetate to Teflon[26]. Another branch of this technique is photo-grafting where UV light is shone at the polymer surface through a solution of the reactant species. Photon induced grafting takes place[3]. This relies upon the polymer and/or the species in solution being reactive under UV, and again the problem of solvent disposal is present. Irradiation of polyethylene through a solution of 2 hydroxyethylmethacrylate (and benzophenone in acetone) resulted in a surface with poly(2 hydroethylmethacrylate) grafted upon it, determined

using XPS[27]. Increased wettability, as determined by contact angle measurements, resulted from this treatment.

3.3 FLAME TREATMENT

Flame treatment is a fairly harsh form of surface modification producing a plethora of reaction products at the surface[4]. The flame is formed by burning a methane and air mixture in a controlled ratio so that the richness of the flame is constant. Typical apparatus is illustrated in Figure 2.

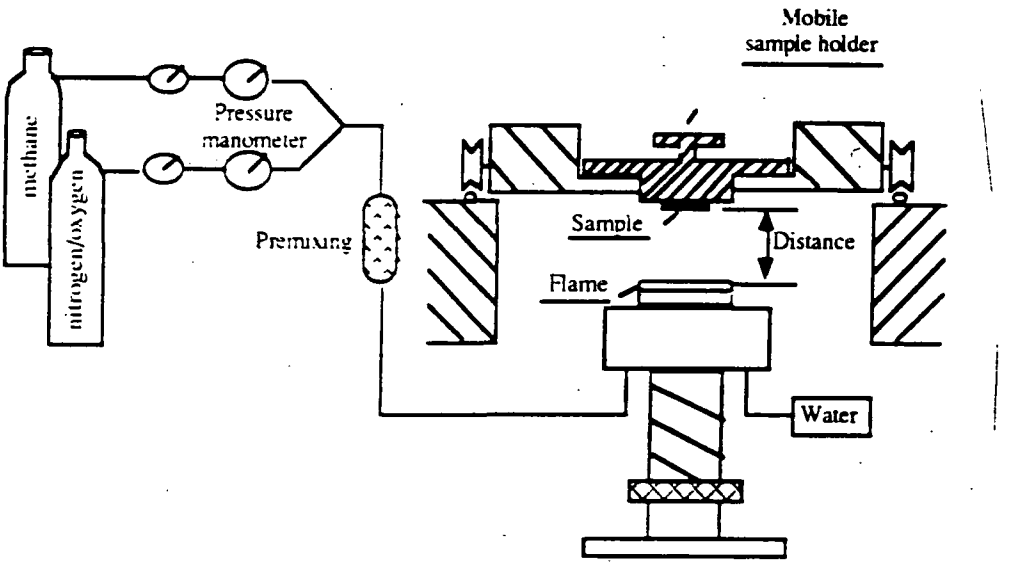

Figure 2: Equipment used in flame treatment of polymer surfaces[4].

The main merit of this method is that it can be carried out at atmospheric pressures, but well defined conditions are necessary to prevent excessive degradation of the polymer[4]. Also, inaccessible 'nooks and crannies' of complex shapes may not get treated[28].

Flame treatment of polyethylene gave a level of oxidation of ~ 5%, i.e. 1 in 20 carbon atoms in the analysed region were modified, with an oxidation depth of 40 - 90 Å. A stable surface resulted which gave no changes in oxidation level (by XPS) or adhesion characteristics even after 12 months storage[2]. Mechanisms of modification are based around the free radicals present in the flame e.g. O·, NO·, ·OH and ·NH, which are thought to abstract hydrogen from the polymer surface to initiate the process[25]. Surface oxidation then propagates by a free radical mechanism with a variety of possible paths leading to a variety of functional groups. The long term stability of the surface of films modified in this manner suggests that surface cross linking also occurs.

3.4 PHYSICAL ABRASION

Sand abrasion may be used to increase the surface roughness of polymer films[8]. A high degree of porosity is obtained and the resulting surface may improve adhesion characteristics by increasing surface area for polymer contact (Figure 3).

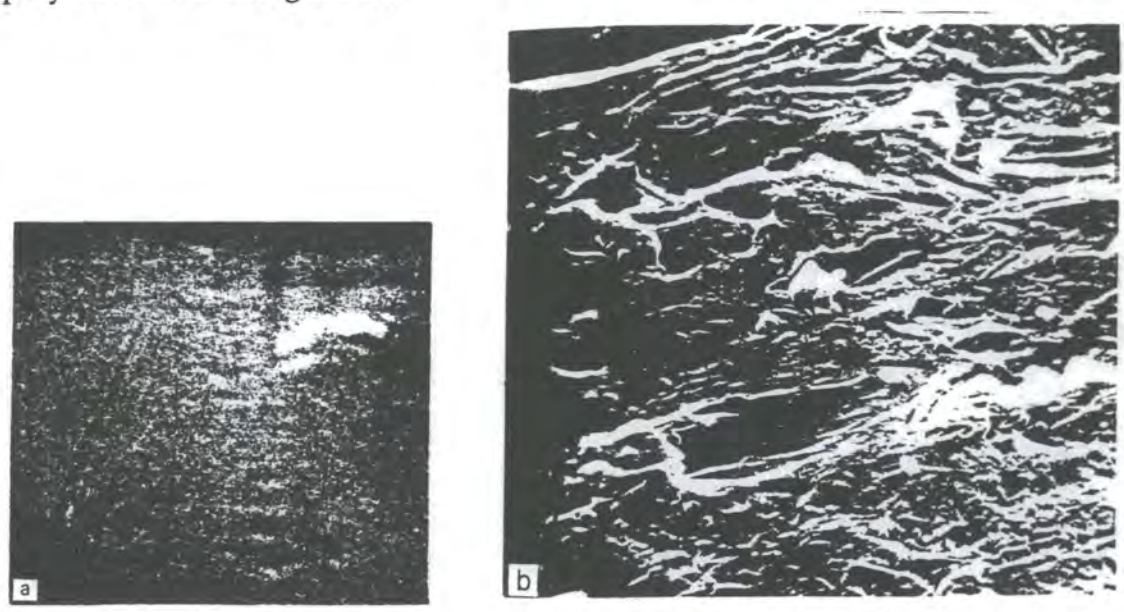

Figure 3: Scanning Electron Micrographs (SEM) of Untreated (left, magnification x 50,000) and sand abraded (right, magnification x 5,000) PET showing an increase in surface roughness in the sand abraded case[8].

An alternative theory is that abrasion of polymer surfaces breaks chemical bonds and produces polymer radicals[9]. In air, the radicals formed react with oxygen or water to form polar groups. When abraded in a liquid, the radicals formed instantaneously react with the molecules of the liquid. Abrasion of polyethylene with emery paper whilst submerged in an epoxy monomer gave characteristic epoxy absorptions in ATR-IR spectra (even after repeated rinsings with solvents)[9].

3.5 PHOTON INDUCED MODIFICATION

Polymer surface modification initiated by UV photons may be achieved with a standard UV source or a laser[29,30,31]. Photo-oxidation[30], ablation[6], or photo-chemical vapour deposition[7] can be initiated depending upon the power and wavelength of the UV source and the presence of reactant species.

The first law of photochemistry (Grotthus - Draper Principle) states that for a photochemical reaction to occur the first event must be the absorption of light by some component of the system[32]. Polymers may absorb light by the following processes[32,33,34]:

a) through chromophores present in the repeat unit of the polymer structure.
b) through isolated impurity chromophores either in the polymer chain or in the matrix.
c) via charge-transfer complexes formed between the polymer and reactant.

Penetration depth depends upon the relative ratio of the refractive indices of the polymer and its surrounding media (e.g. air, vacuum, etc.) and the angle of incidence, the wavelength and intensity of the radiation[35,36] and the concentration of absorbing species.

3.5.1 Photo-oxidation

Generally, photo-oxidative degradation of polymers occurs by free radical mechanisms and can lead to cleavage of the polymer backbone (chain scission)[37,38], crosslinking[39], photo-rearrangement[39], formation of unsaturated units[37] and/or formation of low molecular weight products[40,41]. These processes are responsible for the loss of mechanical and other physical properties of a polymer such as colour, gloss, impact strength and tensile strength. Once started an ageing process on the surface may spread to the bulk via surface cracks.

The detailed mechanism of polymer photo-oxidation is still not fully established, but can be split into 3 basic steps; initiation, propagation and termination[42]. Initiation occurs by absorption of radiation by the polymer by one of the mechanisms described above (see section 3.5.). This basically leads to a radical in or on the polymer chain[42,43,33]:

Polymer ----> P· + P·
(where P· is a polymer alkyl radical).

The oxidation process is propagated by the steps shown below:

P· + O_2 ----> POO·
POO· + PH ----> POOH + P·

Where POO· is a polymer peroxy radical, P and PH are the polymer, and POOH is a polymer hydroperoxide. The hydroperoxide units formed in the first stage can initiate a branching in the mechanism as shown below:

POOH ----> PO· + ·OH
PH + ·OH ----> P· + H_2O
PO· ----> chain scission reactions.

The weak peroxide bond cleaves to give PO·, a polymer alkoxy radical, and a hydroxyl radical, both of which react further as indicated. This is the classical autocatalytic oxidation process for hydrocarbons.

Termination results from the reaction of the radicals on the polymer chain with each other (crosslinking) or with other free radicals in the system to give an inactive product:

POO· + POO· ----> POOP + O_2
POO· + P· ----> POOP
P· + P· ----> P-P

POOP, a polymer peroxide, represents an inherently unstable unit in the modified polymer.

3.5.1.1 Photostabilisation of Polymers.

Photo-oxidation is not always a desirable process; natural ageing of polymers reduces their working lifetime. The introduction of photo-stabilisers into the polymer helps stop initiation and/or propagation of the oxidative process[42].

Photostabilisers can be classified according to their function[42,43,1]:

a) *Absorbers* reduce the number of photons absorbed by internal and external chromophores present in the polymer, usually by absorbing degrading radiation and retransmitting it at a harmless wavelength (e.g. carbon black and derivatives of 2 hydroxybenzophenone[1]).

b) *Excited state quenchers* deactivate photo-excited species in the polymer (e.g. nickel dibutyldithiocarbamate[1]).

c) *Decomposers* deactivate hydroperoxy groups by decomposition (e.g. sulphur compounds such as di-laurylthiodipropionate[1])

d) *Free radical scavengers* interrupt degradative chain processes (e.g. phenolic antioxidants[1])

Other factors are involved in natural deterioration of polymers in the environment, such as temperature, water, micro-organisms and atmospheric pollutants (e.g. gases)[1].

3.5.2 Photo-chemical Vapour Deposition (Photo-CVD)

Photo-CVD involves deposition of films by gas phase photochemical reactions onto a particular substrate[7]. Depending on the wavelength and intensity of the photon source, either the gas, adlayer or substrate will be the predominant absorber. The most common process in Photo-CVD is photo-dissociation, which involves absorption of one or more photons by a molecule which ultimately results in the scission of a chemical bond (usually the weakest in the molecule).

A volatile precursor is introduced into a reactor and radiation is shone through this vapour onto a substrate (often heated) where deposition occurs[7].(Figure 4).

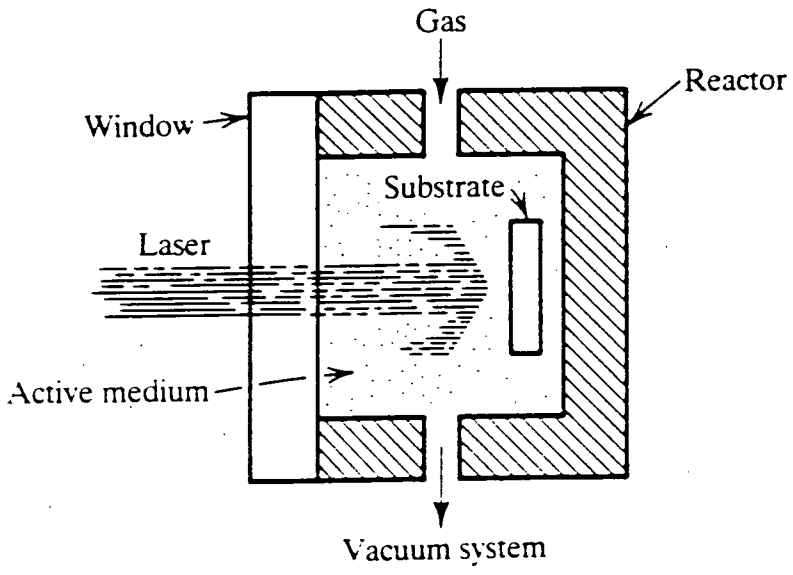

Figure 4: Schematic of Photo-CVD reactor[7].

If a laser is used as the source, the option of 'direct writing' onto the substrate is achievable. A focused laser beam is scanned across the surface. The major drawback is in the low scanning speed of the laser (typically << 100 μms^{-1}). Patterned deposition can be obtained more quickly by projection through a mask, however there will be a loss in spatial resolution of the image. Patterning is used in the deposition of metal films by Photo-CVD for use as interconnects in the microelectronics industry. Another example of Photo-CVD is in the epitaxial growth of III-V semiconductor films (such as AlGaAs) by metal organic CVD (MOCVD)[7].

Photo-CVD has not previously been studied for polymer substrates, however the basic principles should be applicable.

A process similar to Photo-CVD is photopolymerisation. Organic molecules are usually used as monomers for the process, and vinyl and diene monomers, perhalogenated molecules (e.g. C_2F_4) and organosilicone materials have been extensively studied[44]. For example, cyanoethyltriethoxysilane (vapour pressure 0.5 Torr) was photopolymerised onto a heated metal substrate (125°C) with a growth rate of 30 $Åmin^{-1}$.

3.5.3 Ablation

Photo-oxidation and Photo-CVD are photochemical in nature i.e. the absorption of radiation induces a chemical reaction. Ablation is a photothermal process and involves vaporisation of the polymer by a high energy photon source, usually a laser. The required fluence of the laser depends upon the polymer substrate treated[45-47]. This technique is of major industrial importance in the use of self-developing deep UV photoresists in wafer fabrication[48,49](Figure 5).

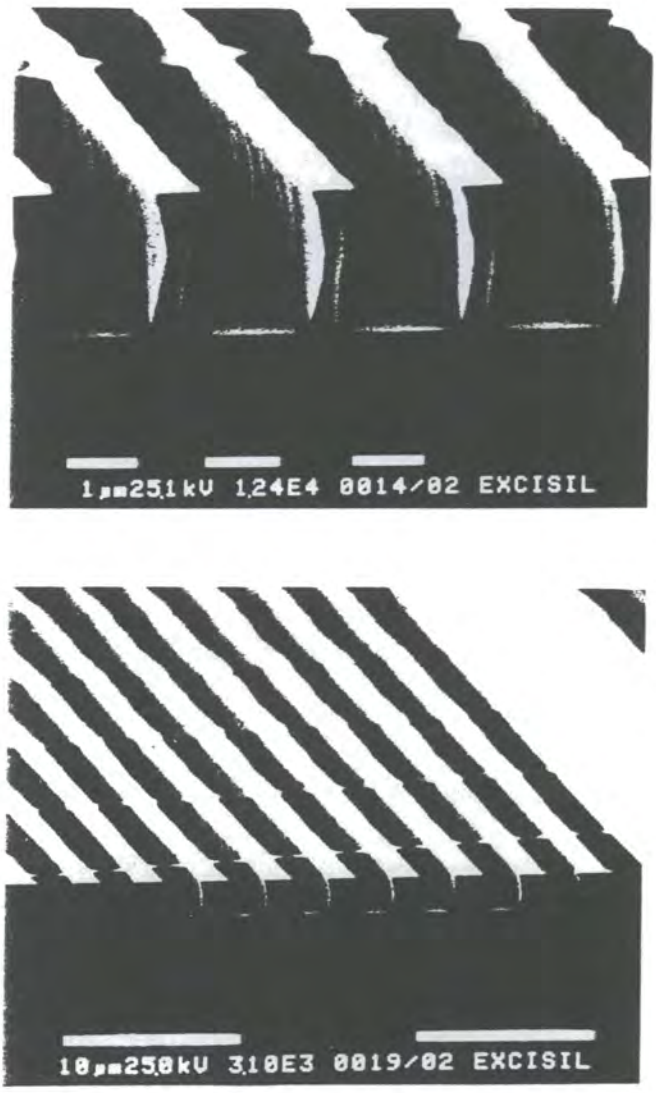

Figure 5: Self-developed submicrometer images produced in a thin film (0.2 μm) of a polysilane (poly(p-tert-butylphenylmethylsilane) by irradiation at 248 nm. Images transferred by oxygen reactive ion etching[50].

Ablation of the resist removes the need for a developing stage in the process (which normally requires solvents), i.e. the number of processing steps is reduced.

3.6 ION BEAM MODIFICATION

3.6.1 Introduction

Chemical modification of polymers by ion beams may be classified into two main types[51]:

i) Reactions induced by energy deposition during the slowing down of the beam particle giving products that do not contain the projectile (even for bombardment with reactive ions)

ii) Reactions between projectile and target molecules (and/or target fragments) giving products containing the projectile. This process is more commonly known as 'ion implantation'[52,53].

3.6.1.1 Energy Loss Mechanisms.

Loss of energy by an incident ion may occur by two processes:[54]

i) Nuclear collision involving direct momentum transfer from the ions of the beam to the atoms of the solid, which results in sputtering, atomic mixing, defect production, or decomposition and new molecule formation.

ii) Electronic collision which may cause excitation and ionisation. Collisions of this nature may cause electron-hole pair generation, secondary electron emission, luminescence, sputtering, defect production, and decomposition and new molecule formation.

3.6.1.2 Stopping Power Cross Section

The energy loss of an incident ion is characterised by the stopping power cross section ε (energy loss in atoms cm^{-2})[55]. This mainly depends on the energy and the atomic number of the incoming ion and on the atomic number of the target atoms.

The stopping power cross section is not constant with ion beam energy; it reaches a maximum value which depends upon the atomic number of each element. Also, the energy loss rate of the ion travelling in the target reaches a maximum as the ion slows down.

For polymers an additive rule for elemental cross section is used; eg. for a polymer of basic repeat unit $C_mH_nO_p$:[55]

$$\varepsilon \text{ (polymer)} = n\,\varepsilon \text{ (H)} + m\,\varepsilon \text{ (C)} + p\,\varepsilon \text{ (O)}$$

3.6.1.3 Range

The volume of polymer affected is usually indicated by the track radius.[56] This mainly depends upon the energy of the primary projectiles and on the energy deposition mechanism.

For heavy ions the concept of track radius is physically better established and for a given energy range a typical size of ion track may be defined. In the keV regime (5 - 400keV) the typical track radii (as determined by primary events) range between 2 and 10 Å[56].

Spatial distribution of energy deposited can be partitioned into two contributions:[51]

i) a core region which is cylinder-like in shape and occurs around and along the ion track where the energy density is very high.

ii) a cloud region around the core area between which occurs the thermalization of the fast secondary electrons coming from the core region. This secondary track has a size range of ~ 50 - 100 Å[51].

A Monte Carlo program for ion beam exposure of resists has been developed to simulate ion trajectories, energy losses and scattering processes in polymers[55]. The program gives a 3-D distribution of the implanted atoms and of the damage caused. It is particularly useful in lithography applications (Figure 6).

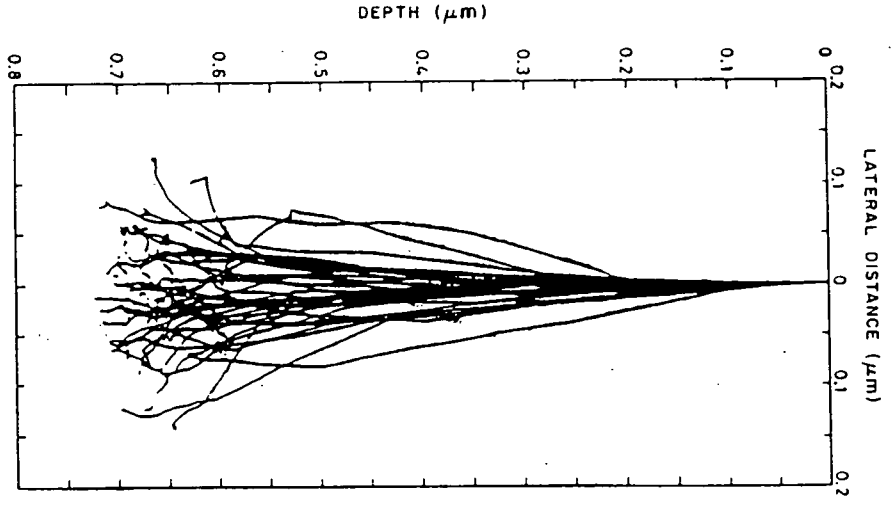

Figure 6: Trajectories of 60 keV protons travelling through PMMA obtained by Monte Carlo program of ion beam resists (PIBER)[55].

3.6.1.4 Time Scale

Time scales for chemical modifications are always much longer than that of the slowing down of the primary ion and of the secondary electrons ($\sim 10^{-13}$s)[51]. Therefore even in fast chemical reactions (which need at least a time corresponding to many vibrational periods to occur) we can assume that when the ion is stopped in the polymer none of the macromolecules along the track has yet reacted. The type and amount of final products will depend on type, spatial distribution and density of the excited species formed by the energy loss of the bombarding particle[51].

3.6.2 Polymer Transformations

In the excited track regions ions (both positive and negative) and excited molecules (both neutral and ions) are present[51]. All of these energetic species can give rise to a variety of chemical transformations such as emission of volatile products[55,57], scission to lower mass macromolecules[58] and aggregation to higher mass macromolecules[59-61].

3.6.2.1 Fluence Regimes

Fluence regimes are distinguished as follows[56]:

i) Single Track: fluence upto 10^{13} ions cm^{-2}.

Tracks are isolated and chemical modifications are confined to the track. Observable changes in the polymer are solubility variations, and modified molecular weight distributions, indicating crosslinking or chain scission.

ii) First overlap: fluence from 10^{13} to ~ 5×10^{14} ions cm^{-2}.

Several types of chemical reactions occur according to the primary structure of the polymer. The surface is saturated with ions and most of the original polymer structure has been modified. Physical properties such as optical and electrical behaviour change.

iii) Re-Implantation Regime: doses between 5×10^{14} to 10^{16} ions cm^{-2}.

A complex 3-D carbon network is formed containing non-negligible quantities of the original polymer heteroatoms (the structure is approximately a heavily doped hydrogenated amorphous carbon). Electrical and optical properties are strongly modified. These modifications depend upon the original chemical structure (Figure 7).

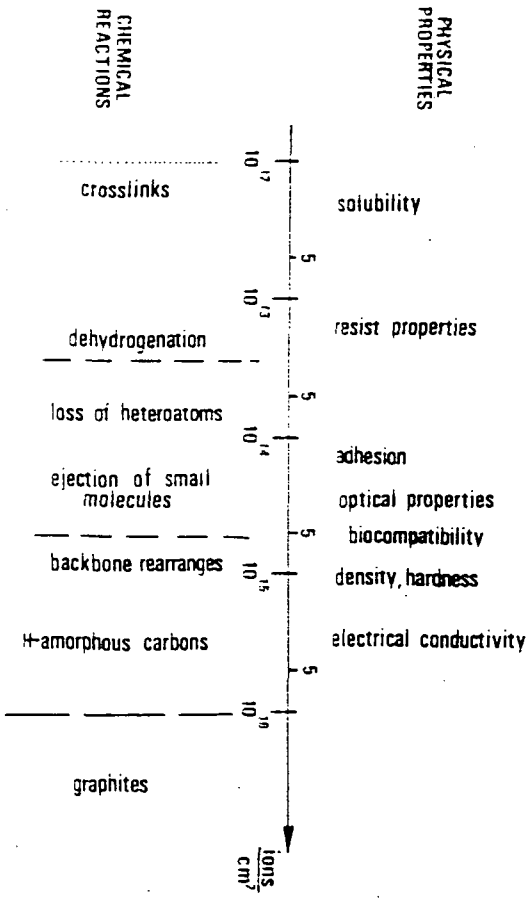

Figure 7: Qualitative trends of ion fluence vs. typical chemical reactions and related physical properties[62].

3.6.2.2 G-Values

G-value is defined as the number of products or events per absorbed 100 eV of energy[59]. In ion beam modification work G-values for crosslinking have been measured and found to depend upon ion energy and

species[59]. For polystyrene, the G - value for crosslinking was larger for He^+ ions than for γ rays and fast electrons[59], for example, with He^+ bombardment the G - value reached a maximum at 0.7 MeV[59].

3.6.2.3 Ion Implantation

For implantation to occur the projectile energy must be in the order of ~20 eV (ie the energy of a few chemical bonds)[51], and implantation or 'doping' is an end-of-track phenomenon. However, even when implantation occurs energy loss processes also occur all along the ion track.

3.6.3 Examples of Ion Beam Modification of Polymers

A brief account of ion beam modification of polystyrene, poly(ethyleneterepthalate) (PET) and poly(etheretherketone) (PEEK) are given below.

3.6.3.1 Polystyrene

Ion bombardment of polystyrene with 100 keV He^+ source yielded a gel or macromolecular solid that was insoluble in all solvents[63-66]. At lower doses the system was characterised by changes in molecular weight distribution[61,65,67].

At high ion fluences the structure of polystyrene approximated to hydrogenated amorphous carbon (by Raman and valence band spectroscopies)[68,69] or heavily damaged highly oriented pyrolytic graphite (HOPG) (valence band studies)[69]. Hydrogen diffused out from the polymer during ion bombardment[69]. There was also some evidence of ordering of target atoms[68].

3.6.3.2 PET

Irradiation of PET induced preferential breaking of the carbonyl group bonds[70]. Low fluences produced amorphisation whereas high fluences caused degradation and carbonisation[70]. Melting temperature and crystallinity were both decreased[70,71].

3.6.3.3 PEEK

High fluence treatments of PEEK gave a highly damaged surface (as studied by Raman spectroscopy)[72]. Below the threshold fluence of 30 MeV mg^{-1} cm^{-2} a type of diamond like carbon (DLC) formed, above this ceiling damaged graphite was produced[72].

3.6.4 Applications

3.6.4.1 Adhesion

Improved adhesion of polymers to metal films by ion beam treatment may be effected in several ways[73-75]:

a) Pre-treatment of the polymer with an ion beam before metal film deposition[73].

b) By 'ion beam mixing' in which a metal film on a polymer is treated with an ion beam. This causes interface mixing and also broadens the interface giving improved adhesion[74].

c) By 'ion beam assisted deposition', in which metal film deposition and ion bombardment are carried out simultaneously[74]. The initial effect with the first few atomic layers of the metal is interface mixing. After the metal film has grown thicker ions don't affect the interface but can alter the crystal structure, inherent stress, and density of the metal[74].

Pre-irradiation of the polymer substrate and subsequent metal film evaporation (even after atmospheric exposure) is just as effective at improving adhesion as post-bombardment of the whole system[73].

3.6.4.2 Lithography

One of the most important recent application of ion beam bombardment is in the processing of polymer resists in the electronics industry[76].

Ion beams give good resolution and sensitivity[55]. Resolution is higher for ion beams than for electron beams because scattering of electrons and creation of secondary electrons (from the primary electron beam interactions) both broaden the effective size of a focused beam as it penetrates a resist. Also, backscattering of electrons from the resist or from the underlying substrate (if the resist film is thin) by an electron beam provides a broad background about the incident beam. These effects limit patterns with very fine dimensions as scattering from one feature smears

into a neighbouring feature with a loss of contrast. Ions scatter much less than electrons giving better resolution of pattern features.

3.7 PLASMA TREATMENT

3.7.1 Introduction

Plasmas are beginning to be used extensively to process surfaces in many areas of modern technology[77]. Types of applications include thin film deposition, surface etching and surface modification[78]. Often the resulting surface is quite unique to this plasma process.

3.7.2 Theory

A plasma is often referred to as the fourth state of matter. It is a partially ionised gas consisting of ions, atoms, metastable atomic and molecular species, electrons and a broad electromagnetic spectrum[79]. In order for a plasma to exist, the number of positive and negative charge carriers must be approximately equal. This criterion is satisfied when the dimensions of the discharged gas volume is much greater than the Debye length[79]:

$$\lambda_D = (\varepsilon_o kT_e/ne^2)^{1/2}$$

where λ_D is the Debye length, ε_o is the permittivity of free space, k is the Boltzman constant, T_e is the electron temperature and n is the electron density. λ_D defines the distance over which a charge imbalance can exist.

Plasma initiation is achieved by the release of electrons (generated by field emission or photo-dissociation) in a volume of gas to which an electric field has been applied[80]. The electric field may be produced by electrodes, inductive/capacitive coupling by an RF field or by microwaves. Electrons are accelerated by the electric field and collide with the gas atoms or molecules. If the electrons have gained enough kinetic energy they will collide inelastically with the gas molecules causing ionisation or dissociation. A cascade of electrons rapidly spreads through the whole gas volume. Not all electrons generated will participate in another inelastic collision. Many are lost by diffusion or drift to boundaries surrounding the plasma by recombination with positive ions and in some cases by attachment to neutrals to form negative ions. A plasma has reached a steady state when electron generation and loss processes balance each other.

3.7.2.1 Plasma Parameters

3.7.2.1.1 Electron Energy Distribution Function (EEDF)

The energy of electrons in a plasma is determined by two parameters[81]: the total electric field the electrons are subjected to, and the type of interactions with other particles in the plasma.

Various types of plasma exist (see 3.7.3) and they usually differ by their electron densities and electron energy distribution, Figure 8.

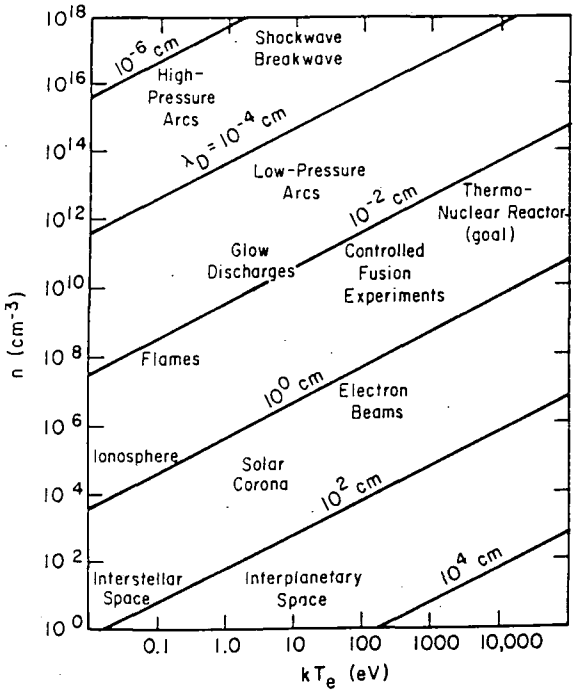

Figure 8: Typical plasmas characterised by their electron energy and density[79].

3.7.2.1.2 Plasma Potential

The potential of a plasma[82] is positive and usually at least several volts more so than the most positive surface in contact with the plasma. This is because electrons usually have a higher mobility in plasmas than ions and will therefore reach the limits of the plasma much more quickly.

3.7.2.1.3 Floating Potential

The floating potential[82] is the potential at which equal fluxes of positive and negative charged species arrive at an electrically floating surface in contact with the plasma.

3.7.2.1.4 Plasma Sheath

As already mentioned, the potential of a plasma is always positive with respect to any surface in contact with the plasma. The initial electron flux to all surfaces is therefore greater than the ion flux. The surfaces in contact with the plasma become negatively charged and a positive space-charge layer or sheath develops in front of these surfaces[82]. In a glow discharge (low pressure, non-equilibrium plasma) the sheath region is dark because there are fewer electrons in the sheath and therefore fewer gas species are excited by electron collisions and consequently fewer species relax and emit radiation. The sheath appears dark relative to the glow discharge.

Positive ions that enter the sheath from the glow region by random thermal motion are accelerated into the electrodes or other surfaces in contact with the plasma. Secondary electrons from the surfaces accelerate through the sheaths into the glow region. The maximum energy with which the ions bombard the surface and the maximum energy with which secondary electrons enter the glow region is determined by the difference between the potential of the surface and the plasma potential. This potential across the sheath is usually referred to as the sheath potential.

3.7.2.2 Plasma Processes.

Many processes occur in a plasma[80,81,83]:

a) Ionisation - electron impact ionisation occurs in a plasma. An example is shown below,

$$e^- + Ar \longrightarrow Ar^+ + 2e^-$$

Recombination of an argon ion with an electron also occurs.

b) Excitation - the energy of the incoming electron excites quantisised transitions between vibrational, rotational and excited states in the molecule, resulting in formation of excited states. For example:

$$e^- + O_2 \longrightarrow O_2^* + e^-$$

c) Dissociation - the molecule is broken into smaller atomic or molecular fragments. The products are usually radicals and are generally more

chemically reactive than the parent gas molecule. Dissociation of CF_4, for example is relied upon in plasma etching or film removal processes:

$$e^- + CF_4 \longrightarrow e^- + CF_3{\cdot}^* + F{\cdot}^*$$

d) Dissociative ionisation - during dissociation, one of the excited species may become ionised e.g.:

$$e^- + CF_4 \longrightarrow 2e^- + CF_3^+ + F{\cdot}^*$$

e) Electron attachment - neutral molecules become negative ions after electron capture, e.g.:

$$e^- + SF_6 \longrightarrow SF_6^-$$

f) Dissociative attachment - e.g.:

$$e^- + N_2 \longrightarrow N^+ + N^- + e^-$$

As well as electron collisions, ion-neutral, excited or metastable-excited and excited atom-neutral collisions occur. Examples are:

g) Symmetrical charge transfer:

$$A + A^+ \longrightarrow A^+ + A$$

h) Asymmetric charge transfer:

$$A + B^+ \longrightarrow A^+ + B$$

i) Metastable-neutral collisions:

$$A^* + B \longrightarrow B^+A + e^-$$

j) Metastable-metastable ionisation:

$$A^* + A^* \longrightarrow A + A^+ + e^-$$

Evidence for these reaction comes from real-time monitoring of discharges by mass and light emission spectrometry.

3.7.3 Types of plasma

3.7.3.1 Equilibrium Plasmas

In equilibrium or 'hot' plasmas, many inelastic collisions occur between electrons and gas molecules resulting in the electron temperature, T_e, and gas and ion temperature, T_i, being approximately equal ($T_e \approx T_i$). This results in a high gas temperature. Examples of equilibrium plasmas are arc and plasma torches used in welding[84].

A thermal plasma arc operates at 500 - 50,000 K[85]. Using the definition:

$$T = E/k$$

where T = temperature in Kelvin, E = energy in Joules and k = Boltzman constant ($1.38066 \times 10^{-23} JK^{-1}$)[86] , the gas energy in this plasma ranges from 0.04 - 4.31 eV.

Another study involving a plasma arc gave an electron temperature of 20,900K (corresponding to 1.8 eV) and gas temperature of 14,200K (1.2 eV).[87] It can be seen that the electron temperature and gas temperature are similar, indicating an equilibrium plasma. The electron density was 1.62 x $10^{23} m^{-3}$.

3.7.3.2 Non-Equilibrium Plasmas

In non-equilibrium plasmas, the electron temperature is much greater than the gas or ion temperature ($T_e/T_i = 10^2$ to 10^3)[88] because fewer inelastic collisions take place than in the equilibrium plasma case. This type of plasma is also known as a low temperature or 'cold' plasma. There are several types of non-equilibrium plasmas; glow discharges, corona discharge, silent discharge, R. F. and microwave discharges.

3.7.3.2.1 Glow Discharge

Low pressure plasmas emit electromagnetic radiation, particularly in the UV and vacuum UV[89,90]. There is a small output in the visible region which gives rise to characteristic colours for plasmas excited in a given system, and hence to the name 'glow discharge'. The stationary glow discharge is a low pressure discharge usually between flat electrodes encapsulated in a tube (Figure 9)

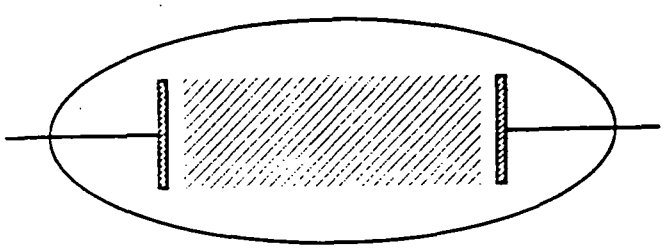

Figure 9: Diagram of a glow discharge system[81].

There is some ambiguity concerning the correct description of glow discharge systems. Thus, operating pressures of < 10 mbar (~ 7.6 Torr) are generally used and electron energies of 0.5 - 2 eV and electron densities of 10^8 - 10^{11} cm^{-3} have been quoted[81]; by contrast, other literature sources quote

electron energies of 1-30 eV and electron densities of 10^9 - 10^{12} cm^{-3} [88]. The electron energy distribution function (EEDF) in a low pressure plasma is a fingerprint of the discharge, and is a good indication of the state of the plasma[91]. Chemical kinetics are sensitive to the EEDF and the electron population plays a central role in coupling power into the desired reactions. Electron energies of ~2 eV have been measured in a glow discharge with the energies of neutrals being 0.025 eV and ions ~0.04 eV[83]. For etching, electron energies of 1 - 10 eV and ion energies of a few tens of meV are used[80].

Glow discharges are used in the lighting industry in neon tubes and new energy efficient light bulbs[81]. This type of plasma is also used to deposit films; for example diamond, refractory metals, epitaxial films, amorphous and polycrystalline films and dielectric films have all been produced by plasma enhanced chemical vapour deposition (PECVD)[82,92]. PECVD has an advantage over thermal CVD in that the deposition temperature is lower, although temperatures of 250-350°C are still required. Plasma assisted etching involves the removal of a substrate by a plasma, as in transfer of resist patterns into a silicon wafer[80].

3.7.3.2.2. Corona Discharge

Corona discharges encompass a high energy electrical discharge through a gas operating at up to atmospheric pressures[81]. The electrode geometry is inhomogeneous; typically a pointed electrode and a plane (Figure 10)

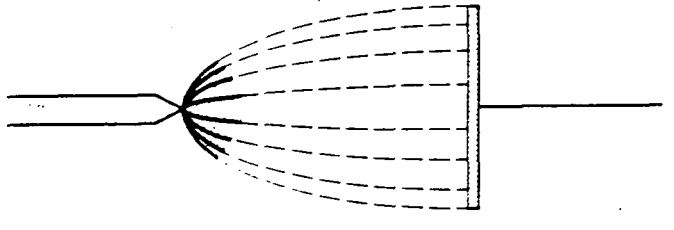

Figure 10: Schematic of corona discharge apparatus[81].

The discharge is inhomogeneous with a localised filamentary glow if the point is negative (negative corona). If the point is positive, the glow is more homogeneous (positive corona). Electron energies in the corona depend on the gas characteristics and the method of generating the corona[93], but range from ~ 1eV - 10 eV (determined by optical emission studies)[81,94]. Electron densities of $10^{13}cm^{-3}$ are present[81]. Ion identities depend upon the polarity of the discharge and the characteristics of the gas[93]. In air atomic oxygen (O·), ozone (O_3) and excited oxygen (O_2^*) are present[95].

Coronas are used to produce charged particles in electrostatic copying machines, and also in the treatment of flue gases and for surface treatment of polymers[81].

3.7.3.2.3. Silent Discharge.

Silent discharge apparatus consists of two flat A. C. high voltage electrodes with at least one of the electrodes covered in a dielectric[81] (Figure 11). Pressures of 1 bar are used with electron energies in the order of 1-10 eV with a density of 10^{14} cm^{-3}.

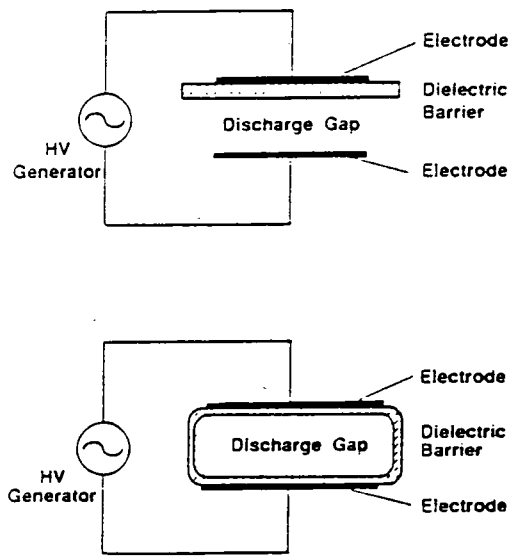

Figure 11: Silent discharge configurations with one (top) or two (bottom) dielectric barriers[96].

3.7.3.2.4 R. F. (Radio Frequency) Discharges.

R. F. Glow discharges are low temperature and low pressure non-equilibrium plasmas, usually operating at 0.01 - 1 Torr[89]. Inductively coupled R.F. plasmas have advantages over normal glow discharges in that

the electrodes are outside the reactor volume and hence electrode erosion and contamination of the plasma with metal vapour is reduced[81] (Figure 12).

Parallel plate reactive ion etchers are used industrially. Ion energy distributions depend upon the r.f. voltage. Most ions lie in the 10 - 30 eV range[97].

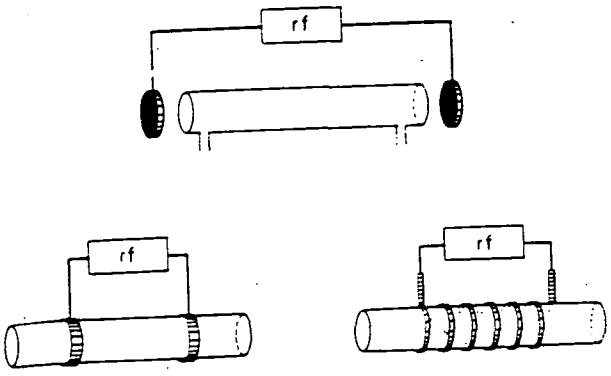

Figure 12: Typical arrangements for r.f. discharges[81].

3.7.3.2.5 Microwave Discharges.

In this case, microwaves in the 0.3 - 10 GHz range cause the electromagnetic field for plasma initiation[81] Operating pressures of between 0.01 and 1.0 Torr are used[89]. The microwave power is led by a coaxial cable or wave guide from the generator (magnetron or klystron) to the resonant cavity which encloses the reactor (Figure 13).

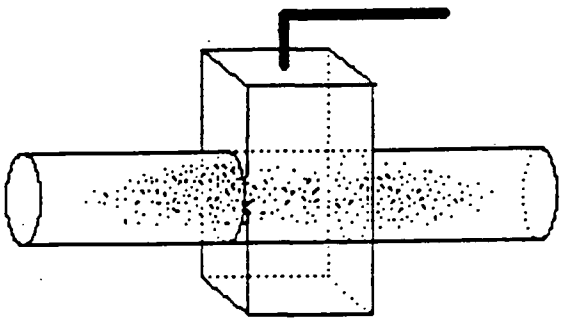

Figure 13: Microwave discharge reactor[98].

Microwave discharges are more difficult to sustain at low pressures (< 1 Torr) than d.c. or r.f. discharges[99]. As a result, high pressures are used and the gas temperatures can rise to several hundred degrees. This often leads to pyrolytic decomposition of the reactants.

3.7.4 Plasmas and Polymers

A low pressure non-equilibrium plasma is required for polymer surface treatment as it produces mild conditions[88]. High pressure, equilibrium plasmas would be too destructive and completely destroy the polymer because of the associated high gas temperatures. Depending upon the polymer, parameters and type of plasma it is possible to achieve crosslinking[95,100], chain scission,[101] chemical changes[13] or thin film deposition[102].

Plasma processes are gaining importance in industry as they give a non-solvent based method for surface activation and enable recycling of the substrate by plasma etching of any overlayers. An industrial process which uses plasmas is the pretreatment of car bumpers before paint spraying[103]. The surface is activated by the plasma, and the functional groups incorporated upon the surface allow good paint coverage. Even 'nooks and crannies' are treated. The main disadvantage is that at the moment batch processes must be used and a low (10^{-2} Torr) working pressure is required.

Corona discharges allow a continuous line process to be used but gives a wide range of surface functionalities[104]. This process has been used for adhesion, printing and wettability applications[105-107].

Plasma interactions can be broadly divided into the areas of plasma modification and plasma polymerisation.

3.7.4.1 Plasma Modification.

Inert gas plasmas mainly result in crosslinking of the polymer via energy transfer from the active species in the plasma and the U.V component of the electromagnetic radiation of the plasma[89]. Excited states of the polymer undergo homolytic bond cleavage to produce free radicals which then crosslink between adjacent polymer chains. An example of crosslinking is in the argon plasma treatment of ethylene-tetrafluoroethylene copolymer. The intensity of the C(1s) signal in the XPS spectrum increases with increasing exposure time. This indicates loss of HF and crosslinking as the surface shrinks due to a reduction of interchain

spacing so that the number of carbon atoms per unit volume in the surface increases.

Oxygen plasma treatment increases the surface free energy or wettability of the polymer by incorporation of oxygenated functional groups[89,108,109]. A more detailed discussion will be given in Chapter 4.

3.7.4.2 Plasma Polymerisation

Plasma polymerisation refers to the formation of a polymeric material under the influence of a plasma[89,102]. The common type of plasma used is a glow discharge. Polymer films may be produced by plasma polymerisation of appropriate monomers either on an inert substrate or by direct interaction with a polymer[89].

3.7.4.3 Surface Dynamics

Many plasma treated surfaces undergo surface rearrangement upon ageing[104,110-118]. Hydrophobic polymers which have been oxygen plasma treated to become hydrophilic may rearrange with time to become hydrophobic again[115]. The corresponding loss of oxygen functionalities depends upon temperature[115], polymer molecular weight[117], environment[113] and the original plasma parameters[114,115]. Rearrangement can be related to surface mobility and hence the extent of crosslinking produced during treatment; extensively crosslinked polymer surfaces age more slowly than less crosslinked surfaces[114].

Knowledge of surface dynamics and therefore ageing of treated polymers is important in an industrial environment as treatment decay can effect adhesion[104,110] and wettability.

The contact angle of a drop of liquid (usually water) with a polymer surface indicates the wettability of the surface and is often used to measure changes in the hydrophilicity of a treated polymer.

The contact angles of conventional polypropylene (PP) which had been treated with an oxygen plasma (50mT, 80W), plasma deposited PP and a methane glow discharge polymer (both of which had been subsequently plasma oxidised as above) were compared as a function of ageing time (in days) in air[114]. The contact angle for the oxidised plasma polymer of methane did not change over a period of 200 days, whereas both types oxidised PP did; the decay in the conventional polymer was faster than for the plasma polymerised PP. This was related to the extent of crosslinking (and hence surface mobility) of each polymer; plasma polymerised methane

having a greater extent of crosslinking than plasma polymerised propylene. Conventional PP had the least degree of crosslinking. Oxidised polypropylene reduces the interfacial free energy by burying polar groups into the bulk.

The hydrophobic recovery of plasma oxidised polystyrene (2 Pa, 100W, 20s) was found to be molecular weight dependant[117]. High molecular weight polymer (Mw = 50,000) aged at any temperature only partly recovered its hydrophobicity (as determined by XPS and contact angles) whereas low Mw (~ 2700) polystyrene returned to untreated polymer at temperatures > 373K. Therefore high Mw is reported to age via molecular motions within the plasma modified layer and low Mw by out-diffusion of untreated polystyrene. Polystyrene recovery occurs by rearrangement of the modified layer and out-diffusion of the untreated bulk (but only for low molecular weight polystyrene and at high temperatures).

4. SUMMARY

A summary of the effects of different polymer surface modifications is shown in Table 1

TREATMENT	EFFECTS	ADVANTAGES	DISADVANTAGES
Additives	Changes in surface roughness, polarity, friction, electrostatics.	Easily added during processing.	Large quantities of chemical used. Fairly non-specific functional groups.
Wet Chemical Treatment	Incorporation of functional groups.	Atmospheric pressure operation, simple apparatus.	Deep modified layer, solvents required. Non-specific functional groups.
Flame Treatment	Incorporation of functional groups.	Atmospheric pressure.	Harsh treatment, non-specific.
Physical Abrasion.	Increase in surface roughness, incorporation of functional groups.	Atmospheric pressure.	Non-specific.
Photon Induced	Incorporation of functional groups. Thin film deposition.	Specific selectivity. Surface sensitive. Direct writing possible.	Vacuum conditions sometimes required.
Ion Beam	Chemical transformation, Molecular weight modification.	Direct writing possible.	Vacuum conditions required.
Plasma Treatment	Incorporation of functional groups. Thin film deposition.	Specific selectivity.	Vacuum conditions sometimes required.

Table 1: Effects of polymer surface modification techniques, advantages and dissadvantages.

The use of a particular treatment depends upon the required surface for a certain application, and the equipment available or the cost of installing new equipment. Vacuum processes usually involve a batch

process, which may be unsuitable to incorporate into a current continous line system.

Surface treatment methods studied in this thesis are photon-induced, and plasma interactions with polymers, with emphasis upon carrying out detailed systematic investigations.

5. REFERENCES

1) L. Mascia, 'The Role of Additives in Plastics', Chapter 4, Edward Arnold (Publishers) Ltd., 1974.
2) D. Briggs, B.M. Brewis, and M.B. Konieczko, J. Mater. Sci., 14, (1979), 1344.
3) D. E. Bergbreiter in 'Chemically Modified Surfaces', ed. H. A. Mottola and J. R. Steinmetz, Elsevier, (1992), 369.
4) E. Papierer, D. Wu and G. Nanse in 'Chemically Modified Surfaces', ed. H. A. Mottola and J. R. Steinmetz, Elsevier, (1992), 369.
5) D.T. Clark and H.S. Munro, Polym. Degrad. and Stab., 3, (1981), 97.
6) S. Srinirason and B. Biaren, Chem. Rev., 89, (1989), 1303.
7) J. G. Edenin 'Thin Film Processes II', ed. J. L. Vossen and W. Kern, Academic Press Inc., (1991), 443.
8) B. Leclerq and M. Sotton, Polymer, 18, (1977), 675.
9) C.H. Lerchenthal, M. Brenman, and N. Yits'hag, J. Polym. Sci., Polym. Chem. Ed., 13, (1975), 737.
10 G. M. Gossedge and P. Cadman, J. Mat. Sci., 14, (1979), 2672.
11) O. Puglisi; Mat. Sci and Eng.; B2, (1989), 167-175.
12) A.R. Blyth and D. Briggs, Polymer, 19, (1978), 1273.
13) A.G. Shard and J.P.S. Badyal, Polymer Commun., 32, (1991), 217.
14) M. Kogoma, H. Kasai, K. Takahashi, T. Moriwaki and S. Okazaki, J. Phys. D, Appl. Phys., 20, (1987), 147.
15) N. Nystrom, P. Jarman, J. Membrane Science, 60, (1991), 275.
16) P. M. Triolo, and J. D. Andrade, J. Biomed. Mat. Res., 17, (1983), 129.
17) E. M. Liston, J. Adhesion, 30, (1989), 199.
18) E. M. Liston, L. Martinu and M. R. Wertheimer, J. Adh. Sci. and Technol., 7, (1993), 1091.
19) L. H. Sperling, 'Introduction to Physical Polymer Science', 2nd edn., Wiley Interscience, 1992.
20) J. D. Andrade in 'Polymer Surface Dynamics', ed. J. D. Andrade, Plenum, New York, 1988.
21) V. D. Fedotov and H. Schneider, 'Structure and Dynamics of Bulk Polymer by NMR Methods', Springer-Verlag, 1989, Chap. 4.
22) B. J. Briscoe and D. Tabor in 'Polymer Surfaces', ed. W. J. Feast and D. T. Clark, Wiley, 1978, Chapter 1.
23) D. Briggs, D. M. Brewis and M. B. Konieczo, J. Mat. Sci., 11, (1976), 1270.
24) W. T. Ford in 'Chemically Modified Surfaces', ed. H. A. Mottola and J. R. Steinmetz, Elsevier, 1992, p155.

25) S. Wu, 'Polymer Interface and Adhesion', Marcal Dekker Inc., 1982, Chapter 9.
26) A. J. Restaino and W. N. Reed, J. Polym. Sci., 36, (1959), 499.
27) S. Edge, S. Walker, W. J. Feast and W. F. Pacynko, J. Appl. Polym. Sci., 47, (1993), 1075.
28) W. Mohl, Adv. Mater., 2, (1990), 57
29) R. K. Wells and J. P. S. Badyal, J. Polym. Sci. A., Polym. Chem. Edn., 30, (1992), 2677.
30) R. K. Wells and J. P. S. Badyal, Macromolecules, 26, (1993), 3187.
31) I. P. Herman, Chem. Rev. ,89, (1989), 1323.
32) J. F. McKeller and N. S. Allen 'Photochemistry of man-made polymers', Applied Science Publishers Ltd., 1979, Chapter1.
33) J. F. Rabek and B. Ranby, 'Photodegredation, Photo-oxidation and Photo-stabilisation of Polymers-Principles and Applications', Wiley, 1975, Chapter 3.
34) J. F. Rabek and J. Sanetra, Macromolecules, 19, (1986), 1679.
35) S. F. Johnston, 'Fourier Transform Infrared: A Constantly Evolving Technology', Ellis Horwood Ltd., 1991, Chapter 17, p304.
36) R. T. Graf, J. L. Koenig and H. Ishida in 'Fourier Transform Infrared Characterisation of Polymers' ed. H. Ishida, Plenum Press, 1987, Chap. 1.
37) G. Geuskens, D. Baeyens-Volant, G. Delaunois, Q. Lu-Vinh, W. Piret and C. David, Eur. Polym. J., 14, (1978), 291.
38) N. A. Wier, P. Kutok and K. Whiting, Polym. Deg. and Stab., 24, (1989), 247.
39) R. Ranby and J. F. Rabek in 'Comprehensive Polymer Science', ed. S. L. Aggorwol and S. Russo, Permagon Press, Chapter 12.
40) B. Mailhot and J-L Gardette, Macromolecules, 25, (1992), 4119.
41) S. H. Lee and E. Ruckenstein, J. Coll. and Int. Sci., 117, (1987), 172.
42) J. F. Rabek, 'Photostabilisation of Polymers - Principles and Applications', Elsevier Applied Science, 1990, p3.
43) D. M. Wiles and D. J. Carlsson in 'New Trends in the Photochemistry of Polymers', ed. N. S. Allen and J. F. Rabek, Elsevier, 1985, Chapter 9.
44) A. N. Wright in 'Polymer Surfaces', ed. W. J. Feast and D. T. Clark, Wiley, 1978, Chapter 8.
45) R. Srinivasan; Appl. Phys. A.; 55, (1992), 269-273.
46) H. Hiraoka; J. Photochem. Photobiol. A., Chem.; 65, (1992), 293-302.
47) M. Bolle; Appl. Phys. Lett.; 60, (1992), 674.
48) O. Nalamasu, F. A. Biocchi and G. N. Taylor in 'Polymers in Microlithography', Chapter 12, Am. Chem. Soc., p189.
49) R. D. Miller, Angew. Chem. Int. Ed. Engl. Adv. Mater., 28, (1989), 1733.

50) R. D. Miller in 'Silicon - Based Polymer Science, A Comparative Resource', ed. J. M. Ziegler and F. W. Gorgon Fearon, American Chemical Society, 1990, Ch 24.
51) O. Puglisi; Mat. Sci and Eng.; B2, (1989), 167-175.
52) J. W. Rabalais; ACS Symposium Series, 162, (1981), 237-246.
53) K. Rossler; Radiation Effects; 99, (1986), 21-70.
54) W. L. Brown; Nuclear Instruments and Methods in Physics Research B, 32, (1988), 1-10.
55) T. Venkatesan, L. Calcagno, B. S. Elman and G. Foti; in 'Beam Modifications of Materials 2, Ion Beam Modification of Insulators', ed. P. Mazzoldi and G.W. Arnold, Elsivier, 1987, Chapter 8.
56) G. Marletta; Surf. + Int. Anal.; 16, (1990), 407.
57) T. Venkatesan, W.L. Brown, C.A. Murray, K.J. Marcantonio and B. J. Wilkens; Polym. Eng. and Sci.; 23, (1983), 931.
58) W. Schnabel and S. Klaumer; Radiat. Phys. Chem.; 37, (1991), 131-134.
59) Y. Aoki, N. Kouchi, H. Shibata, S. Tagawa, Y. Tabata and S. Imamura; Nuc. Inst. and Meth. in Phys. Res.; B33, (1988), 779-802.
60) O. Puglisi, A. Licciardello, L. Calcagno and G. Foti; J. Mater. Res., 3, (1988), 1247.
61) A. Licciardello, O. Puglisi, L. Calcagno, G. Foti; Nuc. Inst. and Meth. in Phys. Res.; B46, (1990), 338-341.
62) S. Pignataro and G. Marletta in 'Metalized Plastics 2', ed K.L. Mittal, Plenum, New York, 1991, p269.
63) Y. Aoki, N. Kouchi, H. Shibata, S. Tagawa, Y. Tabata and S. Imamura; Nuc. Inst. and Meth. in Phys. Res.; B33, (1988), 779-802.
64) O. Puglisi, A. Licciardello, L. Calcagno and G. Foti; J. Mater. Res., 3, (1988), 1247.
65) A. Licciardello, O. Puglisi, L. Calcagno, G. Foti; Nuc. Inst. and Meth. in Phys. Res.; B19/20, (1987), 903-906.
66) W. Schnabel and S. Klaumer; Radiat. Phys. Chem.; 37, (1991), 131-134.
67) L. Calcagno, G. Compagini, G. Foti; Phys. Rev. B.; 46, (1992), 10573.
68) G. Foti and R. Reitano; Nuc. Inst. and Meth. in Phys. Res.; B46, (1990), 306-308.
69) A. Terrasi, G. Foti, Y. Hwu and G. Margaritondo; J. Appl. Phys.; 70, (1991), 1885.
70) R.M. Papaleo, M.A. de Araujo, and R.P. Livi; Nuc. Inst. and Meth. in Phys. Res.; B65, (1992), 442-446.
71) R. M. Papaleo, M. A. Araujo and R. P. Livi; Mat. Res. Symp. Proc.; 157, (1990), 617.

72) C.J. Sofield, S. Sugden, C.J. Bedell, P.R. Graves and L.B. Bridwell; Nuc. Inst. and Meth. in Phys. Res.; B67, (1992), 432-437.
73) P. A. Ingemarsson; Nuc. Inst. and Meth. in Phys. Res.; B44, (1990), 437-444.
74) T. Flottmann and W. Lohmann; in Mettalized Plastics 2, ed K.L. Mittal, Plenum, New York, 1991, p97.
75) P. A. Ingemarsson; in Mettalized Plastics 2, ed K.L. Mittal, Plenum, New York, 1991, p349.
76) H. Ryssel, K. Haberger and H. Kranz; J. Vac. Sci. Thechnol., 19, (1981), 1358-1362
77) J. W. Coburn, IEEE Transactions on Plasma Science, 19, (1991), 1048.
78) E. M. Liston, L. Martinu and M. R. Wertheimer, J. Adh. Sci. and Technol., 7, (1993), 1091.
79) 'Techniques and Applications of Plasma Chemistry', ed. J. R. Hollan and A. T. Bell, Wiley, New York, (1974), Chapter 1.
80) H. W. Lehmann in 'Thin Film Processes II' ed. J. L. Vossen and W Kern, Academic Press, 1991, V-1.
81) B. Eliasson and U. Kogelschatz, IEEE Transactions on Plasma Chemistry', 19, (1991), 6.
82) R. Reiv and W. Kern in 'Thin Film Processes II' ed. J. L. Vossen and W Kern, Academic Press, 1991, IV-1, p525
83) M. Ohring, 'The Materials Science of Thin Films', Academic Press, 1992, Chapter 3.
84) J. L. Shohet, IEEE Transactions on Plasma Science', 19, (1991), 725.
85) M. Hrabovsky and P. Krenk in 'Proceedings of 11th International Symposium on Plasma Chemistry', ed. J. Harry, Vol 1, p315
86) P. W. Atkins, 'Physical Chemistry', Third Edn., Oxford University Press, 1987.
87) S. C. Snyder, G. D. Lassahan and L. D. Reynolds in 'Proceedings of 11th International Symposium on Plasma Chemistry', ed. J. Harry, Vol 1, p380.
88) H. Biederman and Y. Osada, Adv. Polym. Sci., 95, (1990), 57.
89) D. T. Clark, A. Dilks and D. Shuttleworth in 'Polymer Surfaces', ed. W. J. Feast and D. T. Clark, Wiley, 1978, Chapter 9.
90) E. M. Liston ISPC-7, Eindhoven, 1985, 513.
91) N. Braithwaite, Pure and Appl. Chem, 62, (1990), 1721.
92) M. Ohring, 'The Materials Science of Thin Films', Academic Press, 1992, Chapter 4.
93) J-S Chang, IEEE Trans. on Plasma Sci., 19, (1991), 1152.

94) K. Yan, E. M. van Veldhuise and A. H. F. M. Baede in 'Proceedings of 11th International Symposium on Plasma Chemistry', ed. J. Harry, Vol 2, p609.
95) T. Bezigian, Tappi J., March, (1992), 139.
96) U. Kogelschatz, Appl. Surf. Sci., 54, (1992), 410.
97) A. C. Dickenson, D. Field, D. F. Klemperer and P. W. May in 'Proceedings of 11th International Symposium on Plasma Chemistry', ed. J. Harry, Vol 4, p1278.
98) H. Sur, Plasma Chem and Plasma Proc., 9, (1989), 7S
99) A. T. Bell in 'Techniques and Applications of Plasma Chemistry', ed. J. R. Hollahan and A. T. Bell, Wiley, 1974, Chapter 2.'
100) M. Yuzuya, A. Noguchi, H. Ito, S. I. Kondo and N. Noda, J. Polym. Sci., Polym. Chem. Edn., 29, (1991), 1.
101) R. K. Wells, J. P. S. Badyal, I. W. Drummond, F. J. Street and K. S. Robinson, J. Adh. Sci. and Technol., 7, (1993), 1129.
102) H. Yasuda, 'Plasma Polymerisation', Academic Press, 1985.
103) T. A. Wilde, 11th Int. Symp. on Plasma Chem. Proc., Vol 3, (1993), 1198.
104) D. Briggs, D. G. Rance, C. R. Kendall and A. R. Blythe, Polymer, 21, (1980), 895.
105) T. Bezigian, Tappi J., March (1992), 139.
106) B. Leclerq and M. Sotton, Polymer, 18, (1977), 675.
107) K. Jud, Chimia, 44, (1990), 321.
108) W. J. Brennan, W. J. Feast, H. S. Munro and S. A. Walker, Polymer, (1991), 32, 1527.
109) D. T. Clark and A. Dilks, J. Polym. Sci, 17, (1979), 957.
110) D. Briggs, D. G. Rance, C. R. Kendall, V. J. I. Zichy and A. R. Blythe, Polymer, 19, (1978), 1273.
111) T. Yasuda, K. Yoshida and T. Okuno, J. Polym. Sci. B, Polym. Phys., 26, (1988), 2061.
112) T. Yasuda, M. Miyama and H. Yasuda, Langmuir, 8, (1992), 1425.
113) D. X. Piao, Y. Uyama and Y. Ikada, Kobunshi Ronbunshu, 48, (1991), 529.
114) T. Yasuda, A. K. Sharma and H. Yasuda, J. Polym. Sci. B, Polym. Phys., 19, (1981), 1285.
115) M. Morra, E. Occhiello and F. Garbassi, J. Colloid + Int. Sci., 132, (1989), 504.
116) M. Morra, E. Occhiello, L. Pozzi and F. Garbassi, 9th Int. Symp. on Plasma Chem., Pugnochiuso, Italy, Sept. 4-8, 1989, Vol. 3, p. 1595.
117) M. Morra, E. Occhiello, F. Garbassi, D. Johnson, P. Humphrey, App. Surf. Sci., 47, (1991), 235.

118) M. Morra, E. Occhiello, F. Garbassi, G. Morini, P. Humphrey, J. App. Polym. Sci., 42, (1991), 551.

CHAPTER 2

PHOTO-OXIDATION OF POLYSTYRENE BY O_2 AND N_2O

1. INTRODUCTION

Photolysis and photo-oxidation of polystyrene film has been widely investigated[1-7]. Many mechanisms have been proposed for photo-oxidation, however, a better consensus exists concerning the nature of photolysis, that is the processes which result from the interaction of the polymer with light in the absence of any other chemical reagent. Discrepancies which exist between different research findings probably arise because of differing experimental conditions, such as lamp power, wavelength of radiation, exposure time, and different sources of polymer samples with differing defects and impurities.

Various mechanisms have been put forward to explain photo-oxidative degradation of polystyrene in the presence of oxygen[8]. In this chapter the possible role of atomic oxygen is assessed, by comparison of experiments involving irradiation of polystyrene with ultra-violet light in the presence of O_2 or N_2O. N_2O is a source of atomic oxygen under these conditions.

Firstly, a review of polystyrene photolysis and photo-oxidation mechanisms is given, followed by an outline of the excited states of molecular oxygen, and brief summary of previous surface photo-oxidation studies, the latter being grouped by the investigation technique used.

1.1 BACKGROUND

The ultraviolet absorption spectrum of polystyrene is mainly due to the $S_0 - S_1$ transition of the phenyl ring, with an absorption maximum at about 250 nm[9]; the -(CH-CH_2)- backbone of the polymer does not absorb above 200 nm. Weak absorptions are usually found above 290 nm and have been assigned to chromophoric impurities in the polymer chains, for example, carbonyl groups which are introduced during processing or storage of the polymer[10]. The carbonyl groups are believed to arise from a multi-step process in which a hydroperoxide is formed by abstraction of the tertiary allylic hydrogen and recombination, followed by energy transfer processes from an excited chromophore group to the hydroperoxide resulting in carbonyl formation and chain cleavage[11]. Charge transfer complexes between polystyrene and oxygen have also been suggested to absorb in this region[1].

Studies have taken place within two distinct ranges of wavelength; those that cause direct excitation of the phenyl group ($\lambda < 290$ nm)[12], and those which mimic natural weathering ($\lambda > 290$nm)[2].

1.2 PHOTOLYSIS

The action of ultraviolet radiation on polystyrene in the absence of oxygen causes chain scission, cross linking and discolouration[13,14]. The gaseous products formed, as detected by mass spectrometry[3,15] and gas-solid chromatography[13], include molecular hydrogen, carbon monoxide, carbon dioxide and benzene. As polystyrene only contains carbon and hydrogen, the presence of carbon monoxide and carbon dioxide indicates that these photolysis studies must be contaminated in some way, either by impurities in the polymer or through a leak in the vacuum system.

Direct excitation of the phenyl ring occurs at wavelengths of about 250 nm or less[2], and the excited singlet states initially formed are transformed by inter system crossing to the triplet state (Reaction 1)[8,12].

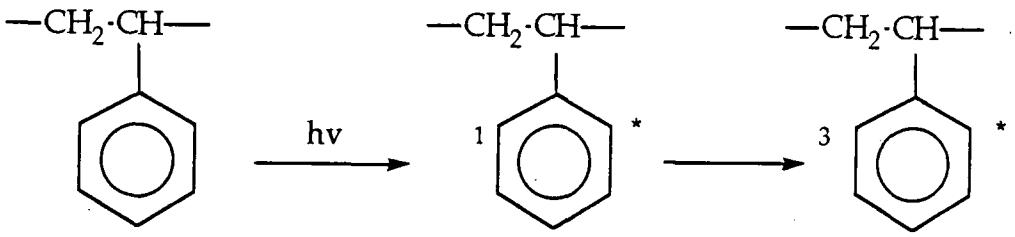

Reaction 1: U.V. excitation of polystyrene[8].

Following this, four types of bond dissociation could occur[4,16] (Reaction 2), only one of which results in chain breaking.

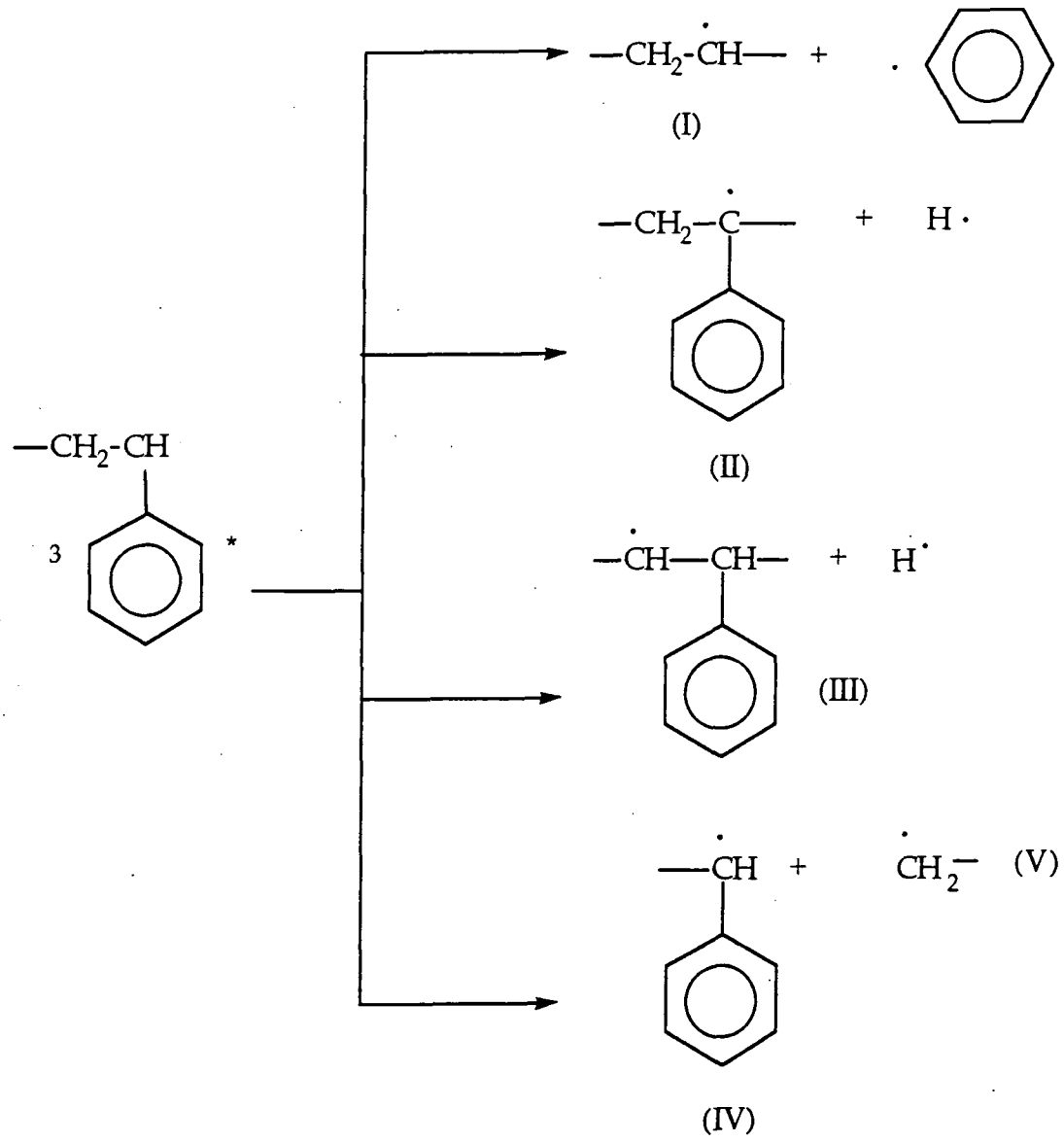

Reaction 2: Dissociation routes for excited polystyrene giving radicals I to V[16].

Grassie and Weir have suggested that the most important step during vacuum photolysis of polystyrene is the scission of C-H bonds[13]. Tertiary C-H bonds in polystyrene are weaker than secondary C-H bonds and C-H bonds within the phenyl ring. Hence it has been suggested[13] that these tertiary C-H bonds are most likely to break during photolysis (i.e. chain radical (II) will predominate). Electron spin resonance (ESR) has yielded direct evidence for the presence of this tertiary radical (II)[17].

Hydrogen radicals are known to be highly mobile and may diffuse out of the polymer matrix in order to recombine to form molecular hydrogen. Phenyl radicals, on the other hand may abstract hydrogen atoms from adjacent polymer molecules to produce benzene[16] (Reaction 3).

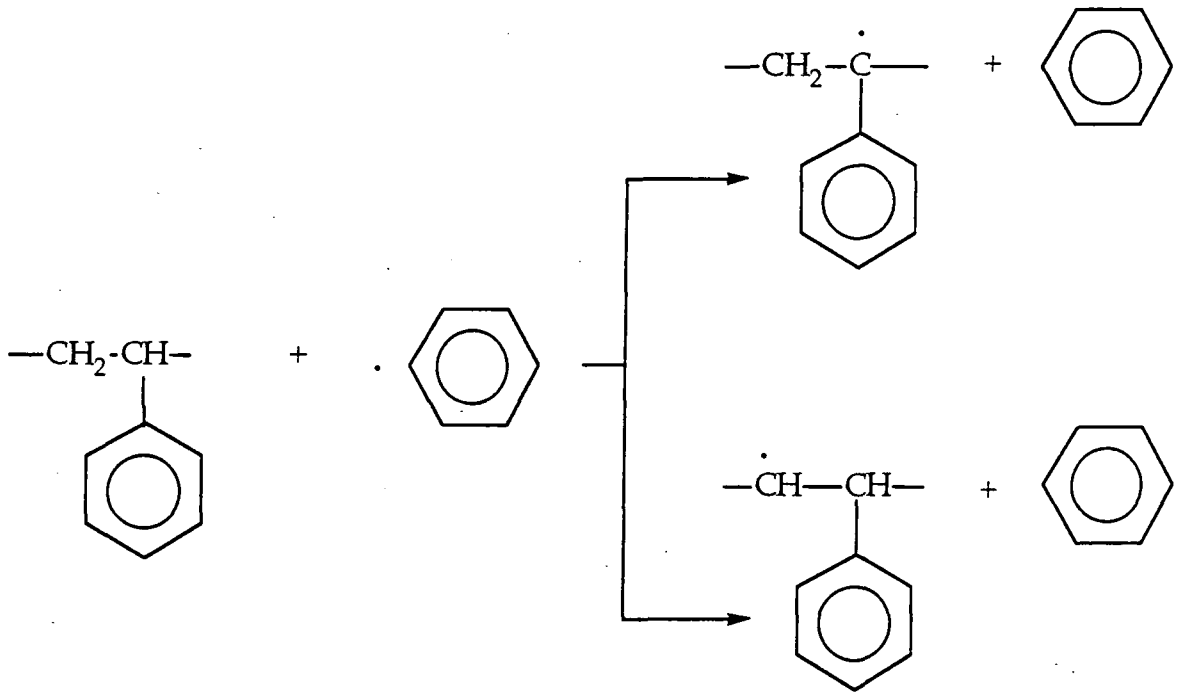

Reaction 3: Mechanism of benzene formation by hydrogen abstraction[16].

Macroradical (III) (in Reaction 2), formed by fission of a secondary C-H bond, may undergo disproportionation and thereby cause main chain scission[16] (Reaction 4).

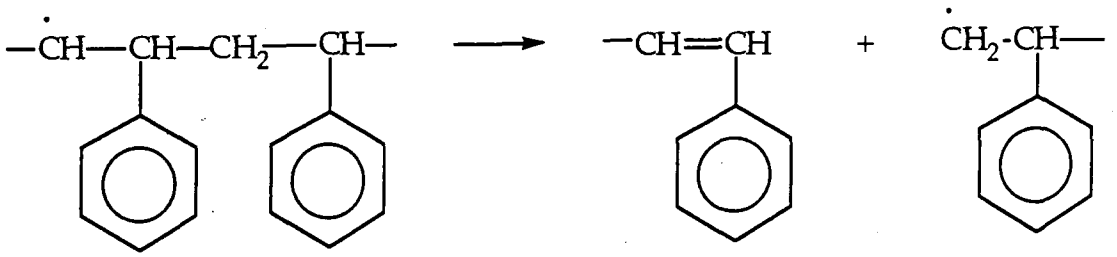

Reaction 4: Chain scission caused by disproportionation of radical III.

The end group radical (IV) could form styrene by a retro addition reaction, 'unzipping', from the polymer backbone (Reaction 5).

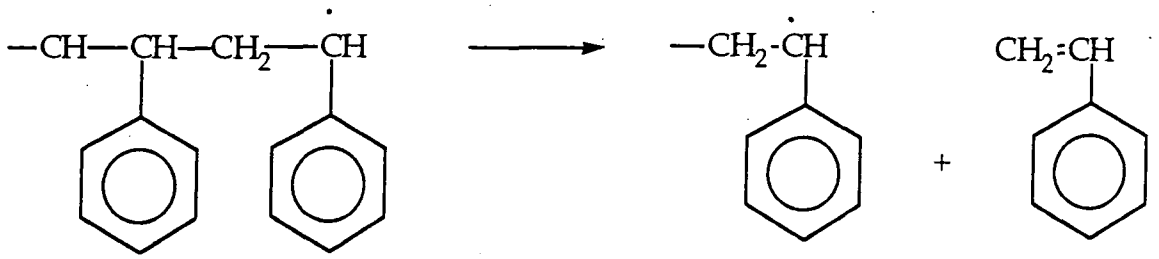

Reaction 5: Mechanism of styrene production[16].

Crosslinking could occur when two macroradicals come close enough together to combine[13,16] (Reaction 6).

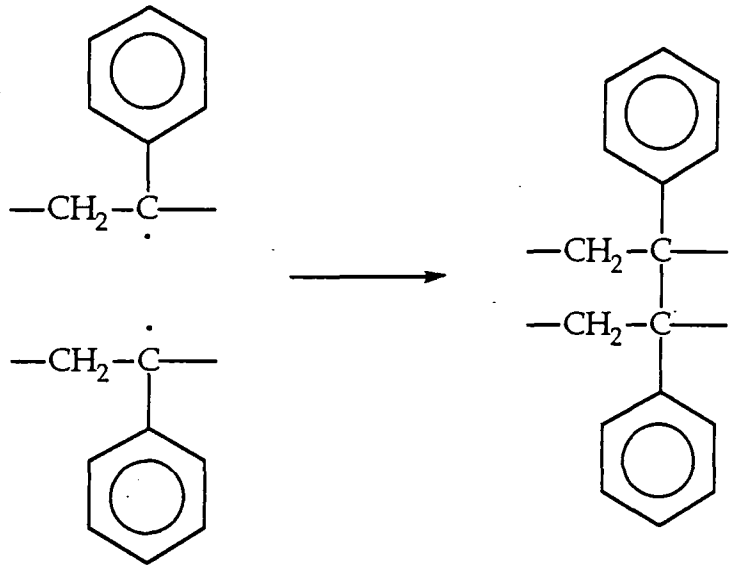

Reaction 6: Mechanism for cross-linking of polystyrene[16].

Yellowing of polystyrene film under ultraviolet light was initially attributed the formation of main chain unsaturation[14], but later studies favoured photo-isomerisation of benzene molecules present in the photodegraded polymer or phenyl rings in polystyrene to fulvene and benzvalene[16].

1.3 PHOTO-OXIDATION

Photo-oxidation of polystyrene film causes yellowing and significant changes in the physical properties of the polymer[16]. Hydrogen, carbon monoxide, carbon dioxide, water, methane, benzene, styrene and benzophenone are amongst the volatile products evolved [3,14,15,18].

Various mechanisms have been put forward to explain photo-oxidative degradation of polystyrene[8], and a major area of debate is the photo-initiation step[12]. Formation of a charge-transfer complex between molecular oxygen and the polymer substrate is one possible initiation route[1,19], and subsequent photolysis of these charge transfer complexes can result in the eventual formation of a polymer radical and a hydroperoxide radical (Reaction 7). An alternative initiation route could be via a polymer radical generated by the photolysis initiation mechanism, which could then

form a peroxy species[2] (Reaction 7). Hydroperoxides have been detected in polystyrene exposed to light and oxygen[7].

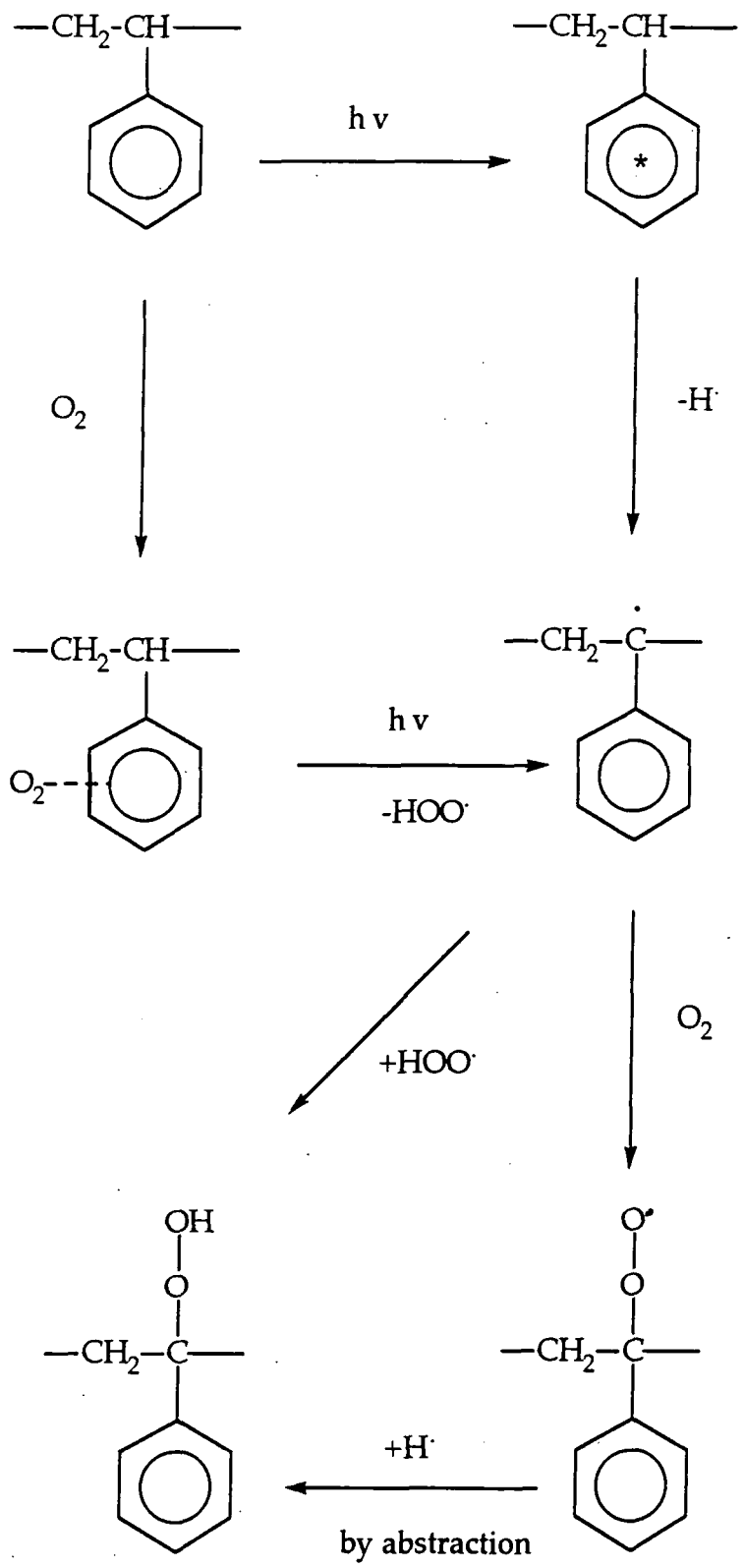

Reaction 7: Photoinitiation in polystyrene.

It has also been suggested that initiation may be achieved by singlet oxygen produced either by intermolecular energy transfer between excited phenyl rings in polystyrene and molecular oxygen, or via a charge-transfer complex (CTC) with molecular oxygen (Reaction 8)[12].

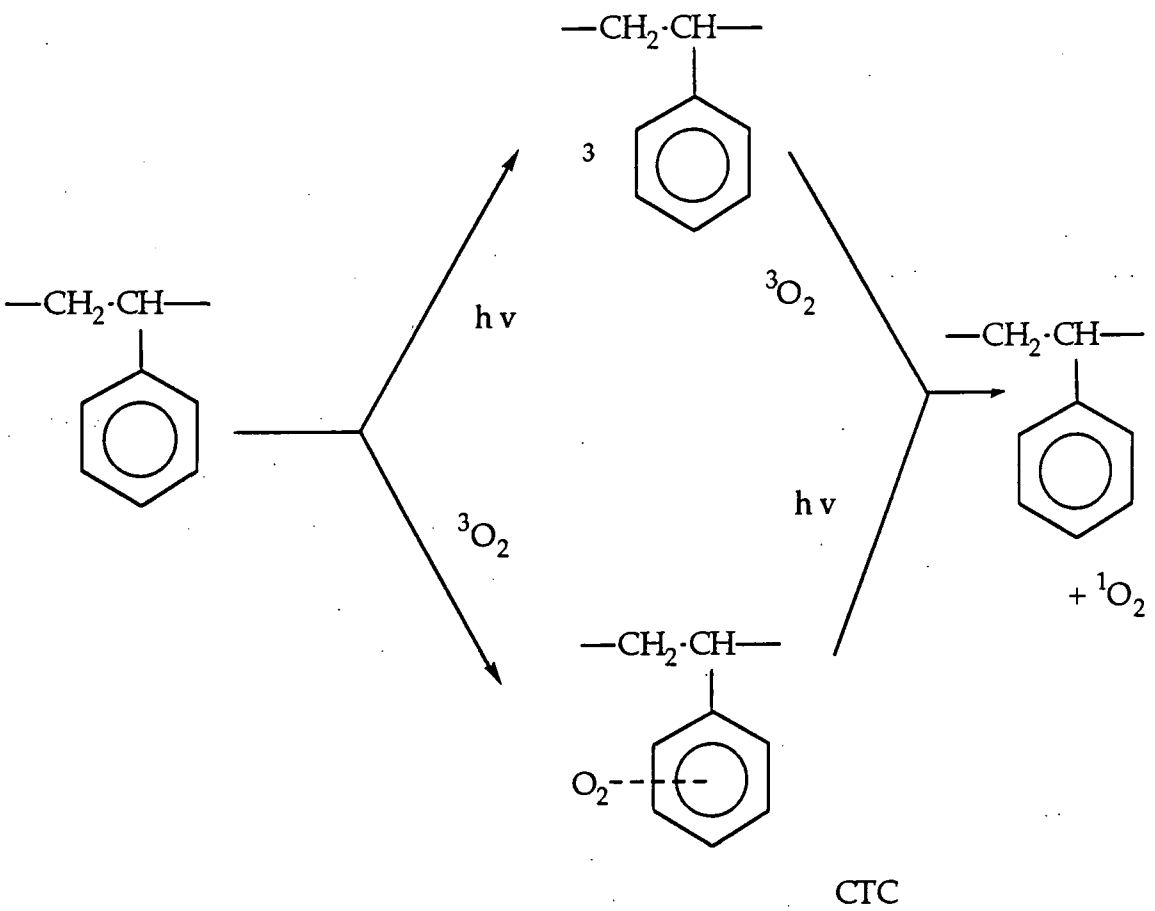

Reaction 8: Singlet oxygen formation[12].

Singlet oxygen so formed, in principal, could then react with ground state polystyrene either on the main chain or the phenyl ring to give a variety of possible oxidation products (Reaction 9), as suggested by Rabek and Rånby[12].

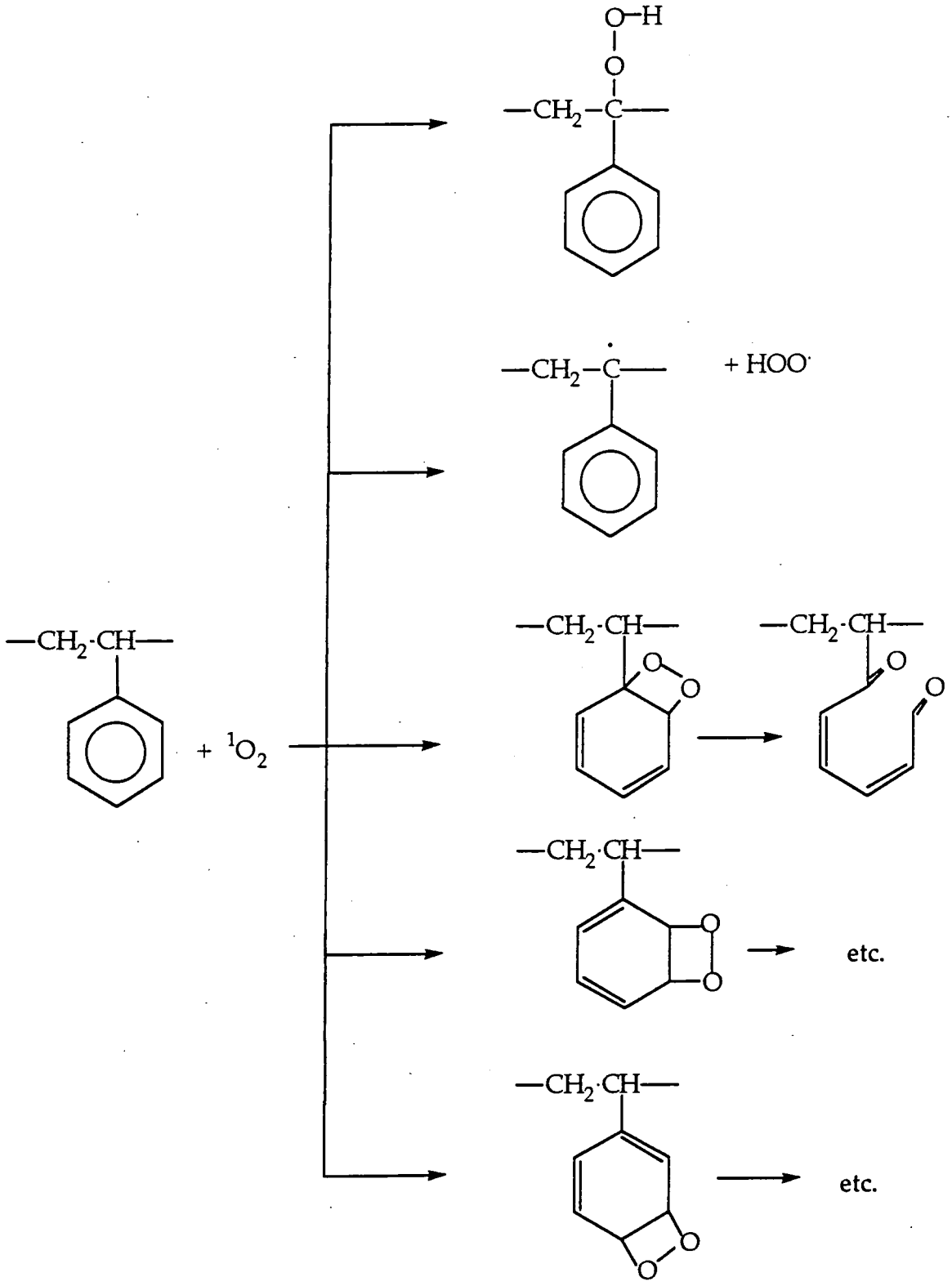

Reaction 9: Reactions of singlet oxygen with polystyrene[12].

Clark and Munro[7] discounted the role of singlet oxygen, since they found no signs of oxidation following exposure of polystyrene films to a stream of singlet oxygen generated from a microwave discharge. Hence they

concluded that any singlet oxygen that may be produced during photo-oxidation has no role in modifying the polymer surface.

Charge-transfer complexes have been detected between oxygen and polystyrene by U.V. spectroscopy[1], their role in initiation has been mentioned earlier. It is thought that such complexes may cause photo-oxidation in the phenyl ring, giving the products illustrated in Reaction 9, but their exact mechanistic role during photo-oxidation has not been established[20].

1.4 EXCITED STATES OF MOLECULAR OXYGEN

In this chapter dealing with photo-oxidation we shall need to discuss the various possible forms of atomic and molecular oxygen and their electronic states in relation to any mechanistic interpretation. A basic description of the structure and bonding in such species is included here and will be refered to in subsequent chapters dealing with oxygen plasmas.

The joining together of two oxygen atoms to form molecular oxygen is illustrated in Diagram 1, showing the distribution of electrons in their molecular orbitals[21]:

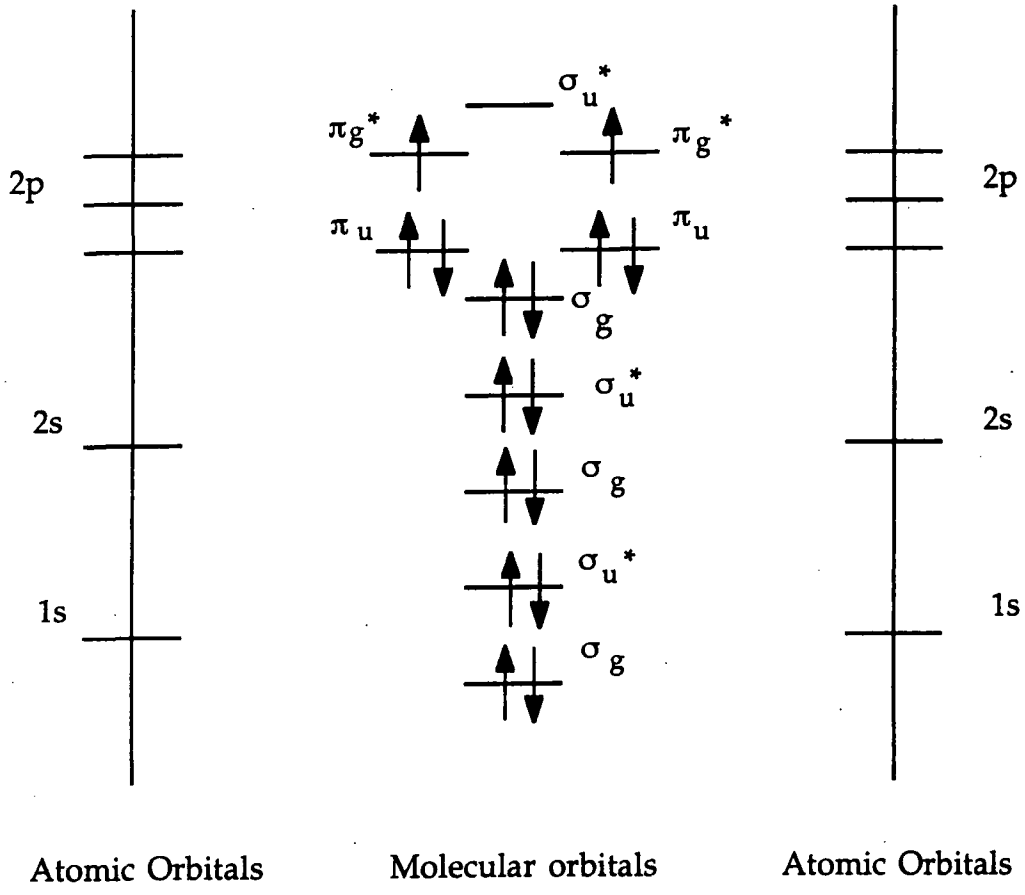

Diagram 1: Occupied molecular orbitals of molecular oxygen[21].

The total description of the occupied molecular orbitals in ground state molecular oxygen can be given as follows[22]: $(\sigma_g 1s)^2$ $(\sigma_u^* 1s)^2$ $(\sigma_g 2s)^2$ $(\sigma_u^* 2s)^2$ $(\sigma_g 2p)^2$ $(\pi_u 2p)^4$ $(\pi_g^* 2p)^2$. This is given the term symbol $^3\Sigma_g^-$. Σ is the symbol for the orbital angular momentum given capital greek letters Σ, Π, Δ, etc. The multiplicity is the total electron spin momentum which may be either 3 , triplet, or 1, singlet, and is twice the value of the total spin plus one (i.e 2s+1 where s = ± 1/2). For homonuclear molecules the subscript 'g' or 'u' is used to indicate whether the total wavefunction is symmetric or antisymmetric with respect to inversion at the co-ordinate origin. The '+' or '-' added to the term symbol refers to the symmetry of the wavefunction with respect to a plane through the nuclei and applies both to homonuclear and heteronuclear diatomic molecules. States which are symmetric are labelled with a superscript '+' and antisymmetric states with a '-'[21].

Energy levels can also be represented as a set of potential energy curves, see Diagram 2.

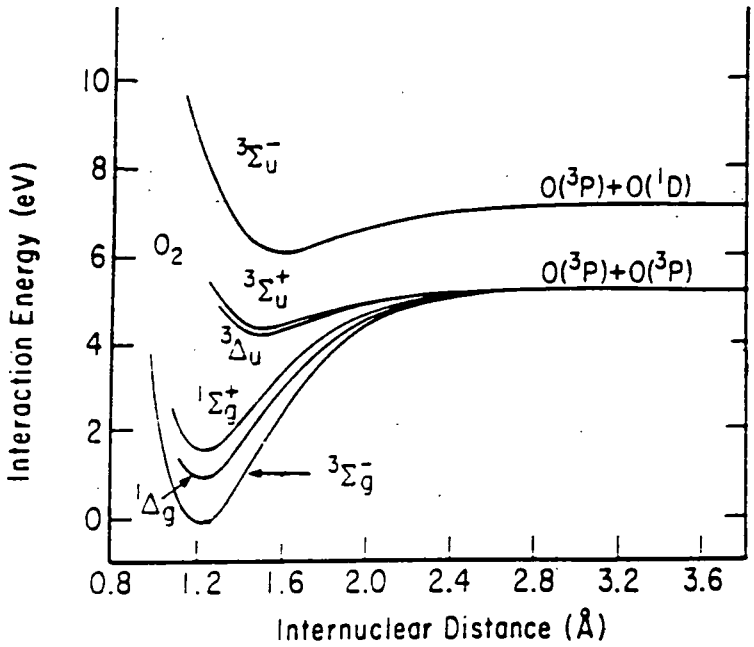

Diagram 2 : Potential energy curves for some states of O_2[22].

Ground state molecular oxygen has an absorption spectrum which falls within certain wavelengths[23]. One of these, the Hertzberg band, is mentioned in the discussion section of this chapter. It originates near 245.4 nm and results from the absorption:

$$O_2(^3\Sigma_g^-) \quad + \quad h\nu \quad \longrightarrow \quad O_2(^3\Sigma_u^+)$$

Promotion to the $^3\Sigma_u^+$ state results in rapid dissociation because the shallow potential well of this state is displaced to larger internuclear distances than the ground state, therefore:

$$O_2(^3\Sigma_g^-) \quad + \quad h\nu \quad \longrightarrow \quad O_2(^3\Sigma_u^+) \quad \longrightarrow \quad 2O(^3P)$$

This process can be visualised pictorially with the use of the potential energy curves for these states of molecular oxygen, Diagram 3.

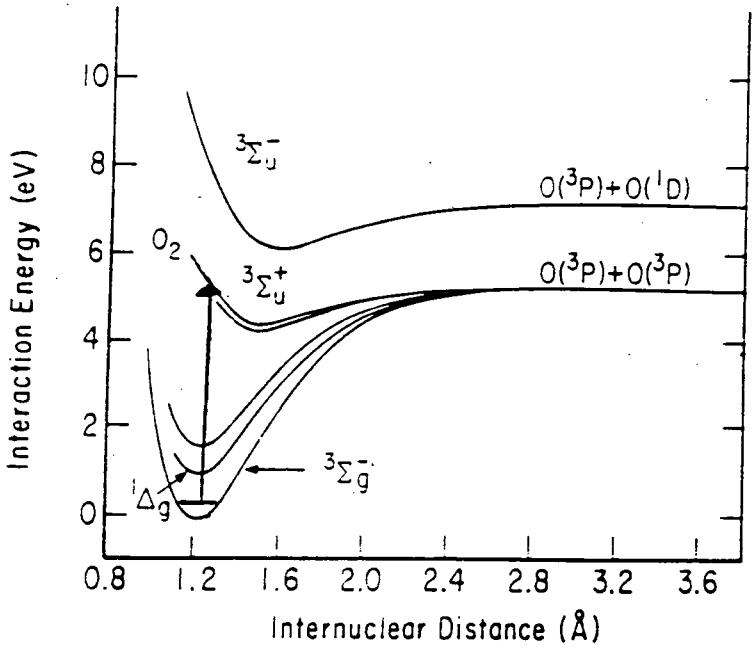

Diagram 3: Potential energy curves showing the formation and subsequent dissociation of $^3\Sigma_u^+$, resulting in production of O (^3P). (Modified from Reference 22)

It is possible to excite other states of molecular oxygen in oxygen plasmas, as in the plasma volume electron collisions occur as well as UV absorbance and hence states of oxygen forbidden by light absorption can result from these electron collisions. Direct triplet to singlet transition are forbidden during light absorption processes, however electron impact processes allow this direct excitation. Hence in an oxygen plasma the excited singlet states of molecular oxygen that are possible are $^1\Delta_g$ and $^1\Sigma_g^+$, as well as the triplet states $^3\Sigma_u^+$, $^3\Sigma_u^-$ and even higher electronic states depending upon the electron energy distribution of the plasma and the cross section (ie the probability) for that state[22], Diagram 4.

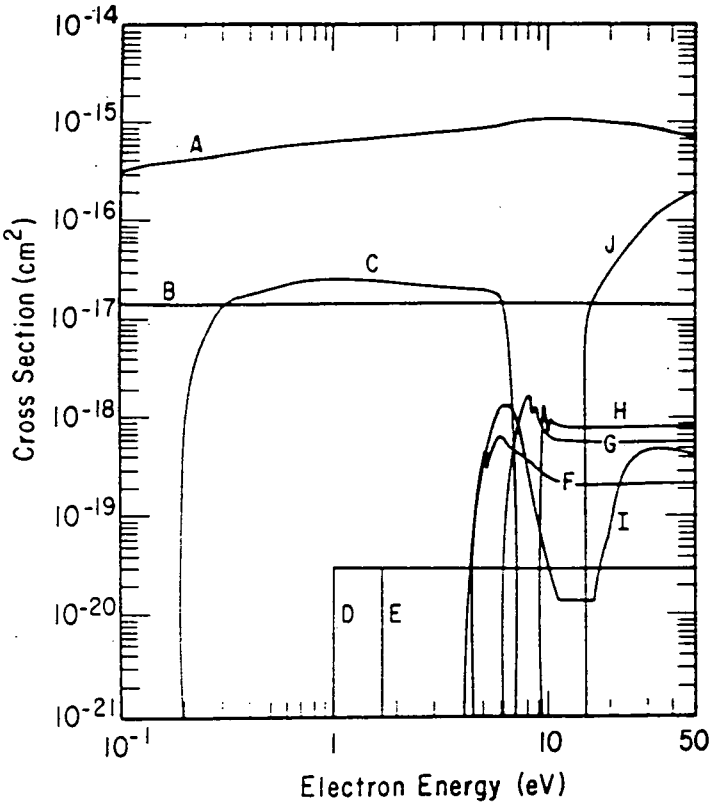

Diagram 4: Elastic and inelastic collision cross-sections for electrons in oxygen; (A) elastic scattering; (B) rotational excitation; (C) vibrational excitation; (D) excitation to the $^1\Delta_g$ state; (E) excitation of the $^1\Sigma_u^+$ state; (F) excitation of the $^3\Sigma_u^+$ state; (G) excitation of the $^3\Sigma_u^-$ state; (H) excitation of higher electronic states; (I) dissociative attachment; (J) ionisation[22].

1.5 LITERATURE REVIEW OF SURFACE PHOTO-OXIDATION STUDIES

1.5.1 XPS Analysis

XPS has been a particularly useful probe of changes in surface chemistry during photo-oxadative modification. The XPS experiment is reviewed in Appendix 1.

Surface photo-oxidation of polystyrene has been extensively studied by Clark and co-workers[7,24,25]. Reactions in air and oxygen showed similar trends[7,25]; C-H percentages as a total of all carbon present decreased as a function of irradiation time, while C-O, C=O, and O-C=O contributions increased, and loss of aromaticity was observed as a decrease in the π-π^* shake-up percentage[7,24,25].

Hydroperoxide formation was thought to occur in either air or pure oxygen atmospheres, the evidence for which was an initial increase of the C-O functionality without concomitant increase in carbonyl and carboxylate groups[7,24]. Hydroperoxy-species were identified by labelling with sulphur dioxide[7].

An increase in light intensity increased the rate of photo-oxidation[7], temperature, however, only had a small effect on photo-oxidation.

An induction period was observed before the formation of C=O and O-C=O features, the initial increase of the former was greater than that of the latter. A steady state was eventually reached where there was a balance between continued photo-oxidation and desorption of low molecular weight species[7,24,25].

Oxidative degradation of the phenyl group and the rate and extent of oxygen uptake were found to be strongly dependant on the partial pressure of oxygen at the gas-solid interface[24].

Continuous and cyclic irradiation were compared in an attempt to mimic the natural situation. The rate of photo-oxidation was found to be a function of the amount of light reaching the surface[24]. Natural weathering was also studied by Clark et al and was found to be similar these to model photo-oxidation experiments[26].

Shard and Badyal studied the vacuum - UV photo-oxidation of polystyrene under oxygen and nitrous oxide atmospheres[27]. The vacuum - UV source was a nitrogen glow discharge, the main lines of which were at 174 and 149 nm. Determination of the surface composition by XPS showed an oxygen atmosphere gave a more oxidised surface than nitrous oxide. The lower oxidation produced using N_2O was attributed to recombination of oxygen radicals in the gas phase to form molecular oxygen (diluted with N_2),

for an oxygen radical to react with the surface close proximity was required. An N_2O environment showed greater selectivity with respect to oxygenated functional group production on the polymer surface; whereas oxygen gave C-O, C=O, O-C-O and O-CO-O groups, N_2O gave a surface exclusively due to atomic oxygen incorporation, i.e. C-O and C=O. There was no nitrogen detected on the surface after photo-oxidation under an N_2O atmosphere. The C-O functionality in the nitrous oxide case was attributed entirely to alcohol groups (C-OH) rather than ether linkages (C-O-C).

1.5.2 Mass spectral Analysis

TOF-SIMS (Time of Flight Secondary Ion Mass Spectrometry) has been used to monitor changes in polystyrene polymer chain length as a function of exposure time[28]. Extended irradiation resulted in the complete destruction of the high molecular weight polymeric material.

A similar study used Cf 252 particle desorption mass spectrometry to monitor the changes of the polystyrene spectrum after photo-oxidation[29]. Photo-oxidation produced changes in both the positive and negative ion spectra. Oxygen incorporation produced a slight increase in intensity of the m/z+ 18 and 19 (H_2O^+ and H_3O^+) and m/z- 16 and 17 (O^- and OH^-). The tropyllium ion , $C_7H_7^+$, m/z 91^+, originates from the rearrangement of C_6H_5-CH_2^+ in the ioniser of the mass spectrometer, and C_6H_5-$CH_2\cdot$ is emitted from polystyrene by breaking the polymer chain. The relative intensity of the tropyllium ion, decreased after photo-oxidation and was interpreted as the formation of a bond α to the phenyl ring, hence inhibiting chain fragmentation. Increases in intensity of the phenyl radical, $C_6H_5^+$, m/z$^+$ 77 and C_6H_5-C_2H_4, or C_6H_5-CO, m/z$^+$ 105, were thought to arise from easily ionised fragments of the oxidation products of polystyrene.

1.5.3 ATR-FTIR Analysis

Infrared analysis samples a much greater depth of the surface than the above techniques. Never-the-less it has been extensively used in such studies.

Evidence for phenyl ring reactions in polystyrene photo-oxidation has been found by monitoring the emergence of phenyl hydroperoxides[30]. Carboxylic acids have also been detected as the major degradation product of polystyrene photo-oxidation[31].

These results refer to much more extensively oxidised systems than we are concerned with in this work.

2. EXPERIMENTAL

A glass reactor with a quartz port (cut off wavelength 180-200 nm) was used for irradiating the sample (Diagram 5). The UV source was an Oriel 200 W low pressure Hg-Xe arc lamp operating at 100 W, which gave a strong line spectrum in the 240 to 600 nm region.

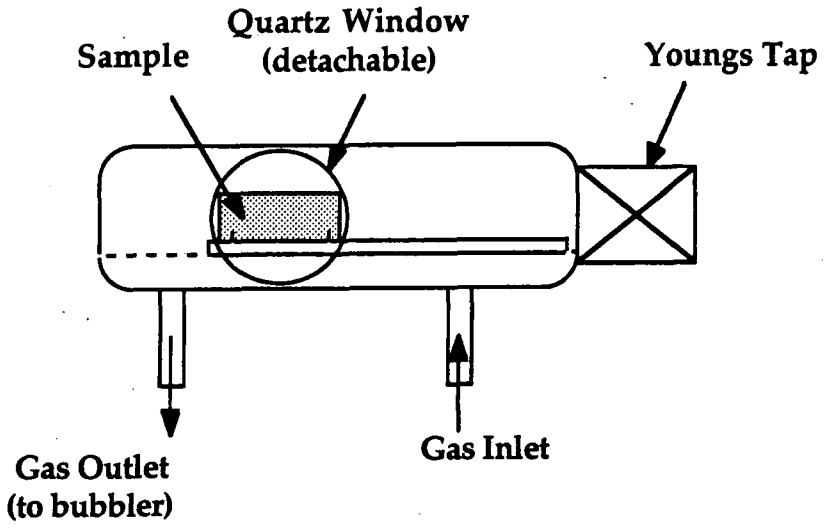

Diagram 5: Schematic of glass reactor used in photo-oxidation studies.

Polystyrene film (Trycite) was degreased with isopropyl alcohol and positioned facing the quartz window. A high flow of N_2O or O_2 (BOC) was passed through the reactor at atmospheric pressure, and was maintained before, during, and after UV irradiation.

X-ray photoelectron spectroscopy (Appendix 1) measurements were recorded using a Kratos ES300 surface analysis instrument (base pressure ≈ 6 x 10^{-10} Torr) (Plate 1). Mg K_α radiation was used as the excitation source with electron detection in the fixed retarding ratio (FRR) analyser mode. XPS spectra were acquired at an electron take-off angle of 30° from the surface normal. Data accumulation and component peak analyses were performed on an IBM PC computer, using Gaussian fits with fixed FWHM (except for the π-π^* transition). All binding energies are referenced to the hydrocarbon component at 285.0 eV[32]. Instrumentally determined sensitivity factors are such that for unit stoichiometry, the C(1s) : O(1s) intensity ratio is ~ 0.55 and the C(1s) : N(1s) value is ~ 0.74.

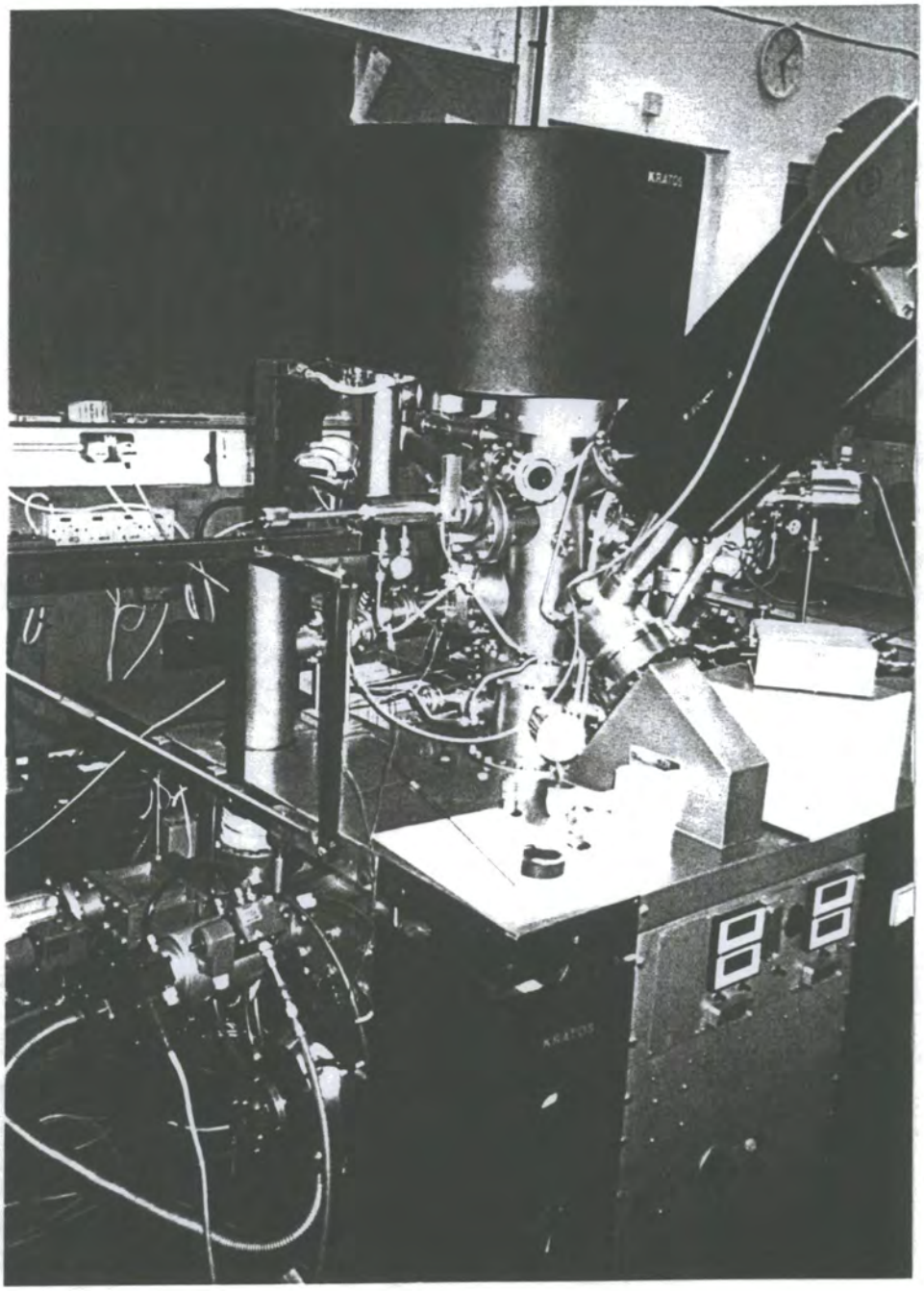

Plate 1: Kratos ES300 surface analysis instrument.

3. RESULTS

3.1 INTRODUCTION

Functional groups at a polymer surface can be identified by XPS. For clean polystyrene film, two peaks are observed in the C(1s) region of the XPS spectrum, Figure 1a: a hydrocarbon component (285.0 eV, 94% of total C(1s) signal, with a FWHM of 2.0 eV) and a distinctive satellite structure at ~291.6 eV (6% of total C(1s) signal), which is associated with low-energy $\pi \rightarrow \pi^*$ shake-up transitions that accompany core level ionization[33]. Chemical species generated at the polymer surface during oxidation can be identified by peak fitting the C(1s) XPS spectra to a range of carbon functionalities, Figure 1b: carbon singly bonded to one oxygen atom as in hydroxyls, ethers, peroxides or hydroperoxides (-C-O- ~286.6 eV), carbon singly bonded to two oxygen atoms or carbon doubly bonded to one oxygen atom (-O-C-O-, -C=O ~287.9 eV, refered to from now on as -C=O for simplicity) and carboxylate groups as observed for acids, esters, peroxyacids or peroxyesters (-O-C=O ~289.0 eV)[34]. Also any loss of aromaticity can be monitored by the decrease in intensity of the $\pi \rightarrow \pi^*$ shake-up satellite[7,24,25].

3.2 CLEAN POLYSTYRENE

A small amount of oxygen was detected in the O (1s) spectrum of the surface of clean polystyrene, O:C ~ 0.01. This oxidation could not be resolved in the C(1s) region. No changes in the C(1s) and O(1s) spectra were detected after exposure to either O_2 or N_2O under normal laboratory lighting for 80 minutes.

3.3 O_2-UV/POLYSTYRENE

Analysis of the XPS data following UV exposure under O_2 reveals that the relative O:C ratio at the polymer surface increases rapidly with time and finally approaches a constant value 0.51 ± 0.03, Figure 2a; this corresponds to approximately one oxygen atom per oxidized carbon atom at the surface. The -CH_x- component of the C(1s) spectra follows this trend, by decreasing to a final contribution of 40% of the total C(1s) peak. A gradual loss of aromaticity was observed with time (as determined by calculating the π-π^* shake-up satellite to -CH_x- peak ratio).

The relative emergence and variation of various carbon-oxygen functionalities with time were monitored by peak-fitting the C(1s) spectra,

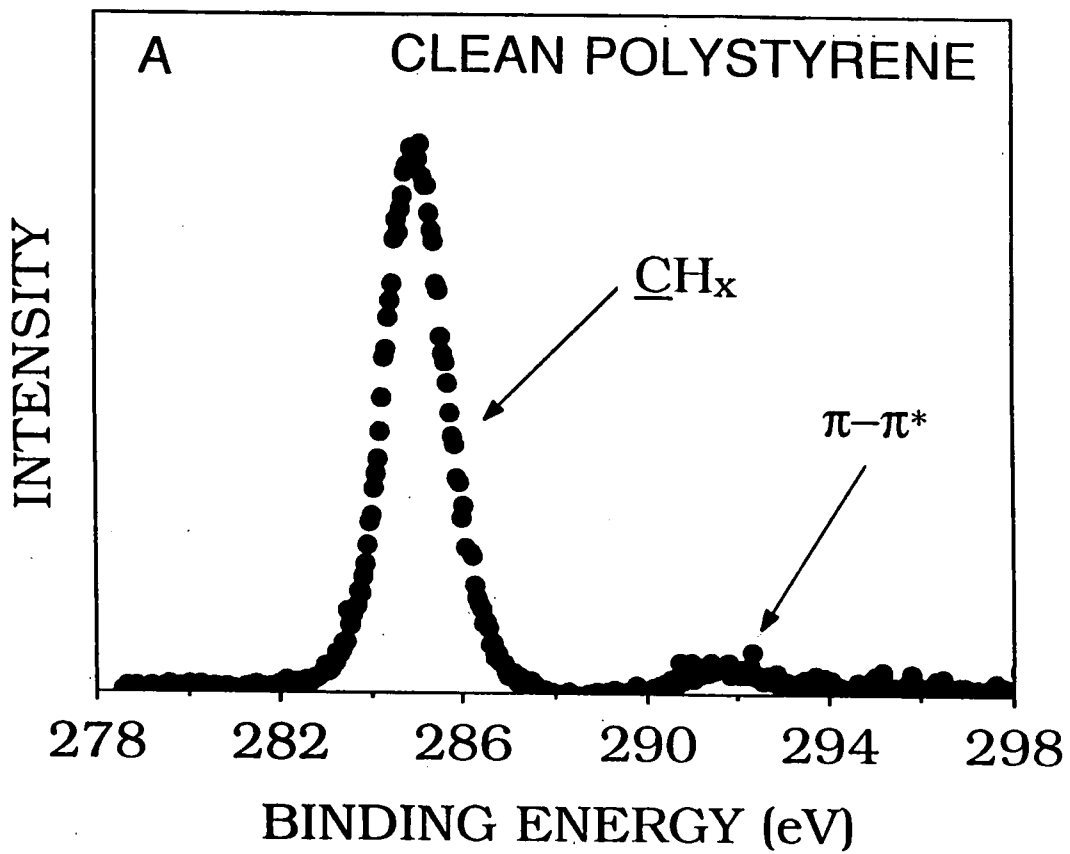

Figure 1a: Peak fit of C(1s) XPS spectrum for clean polystyrene.

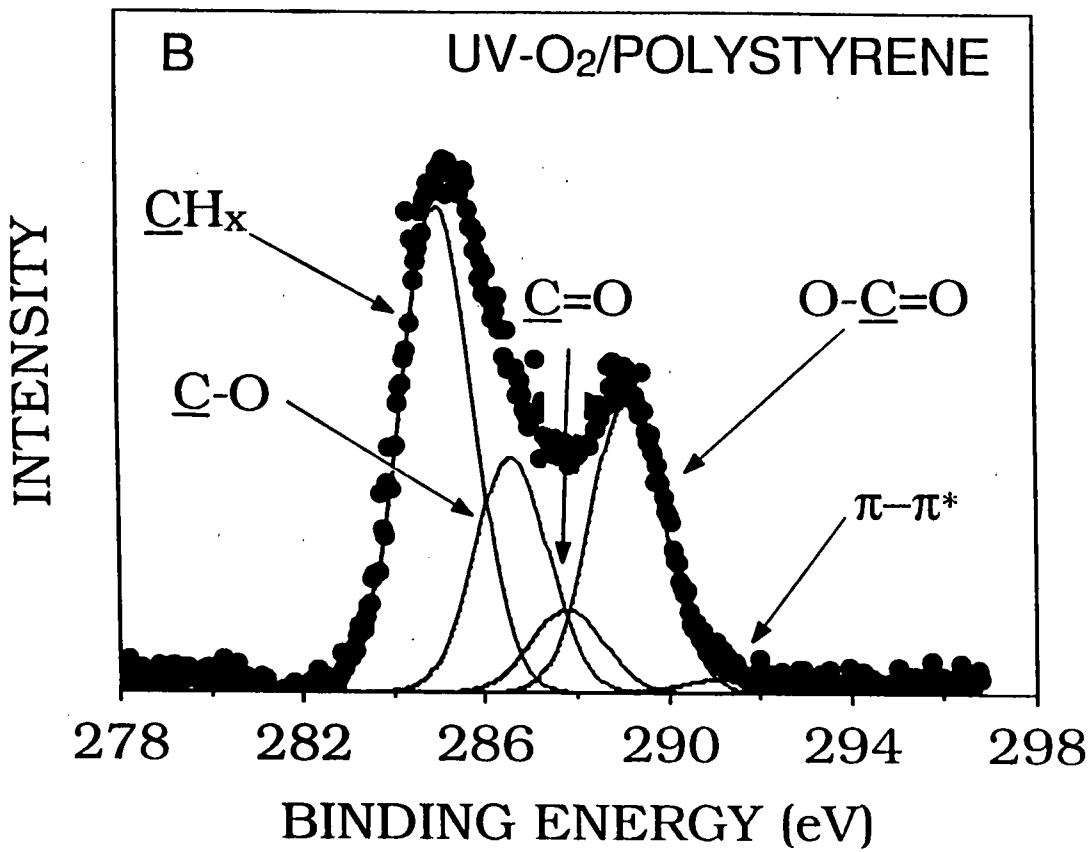

Figure 1b: Peak fit of C(1s) XPS spectrum for O_2-UV oxidized polystyrene.

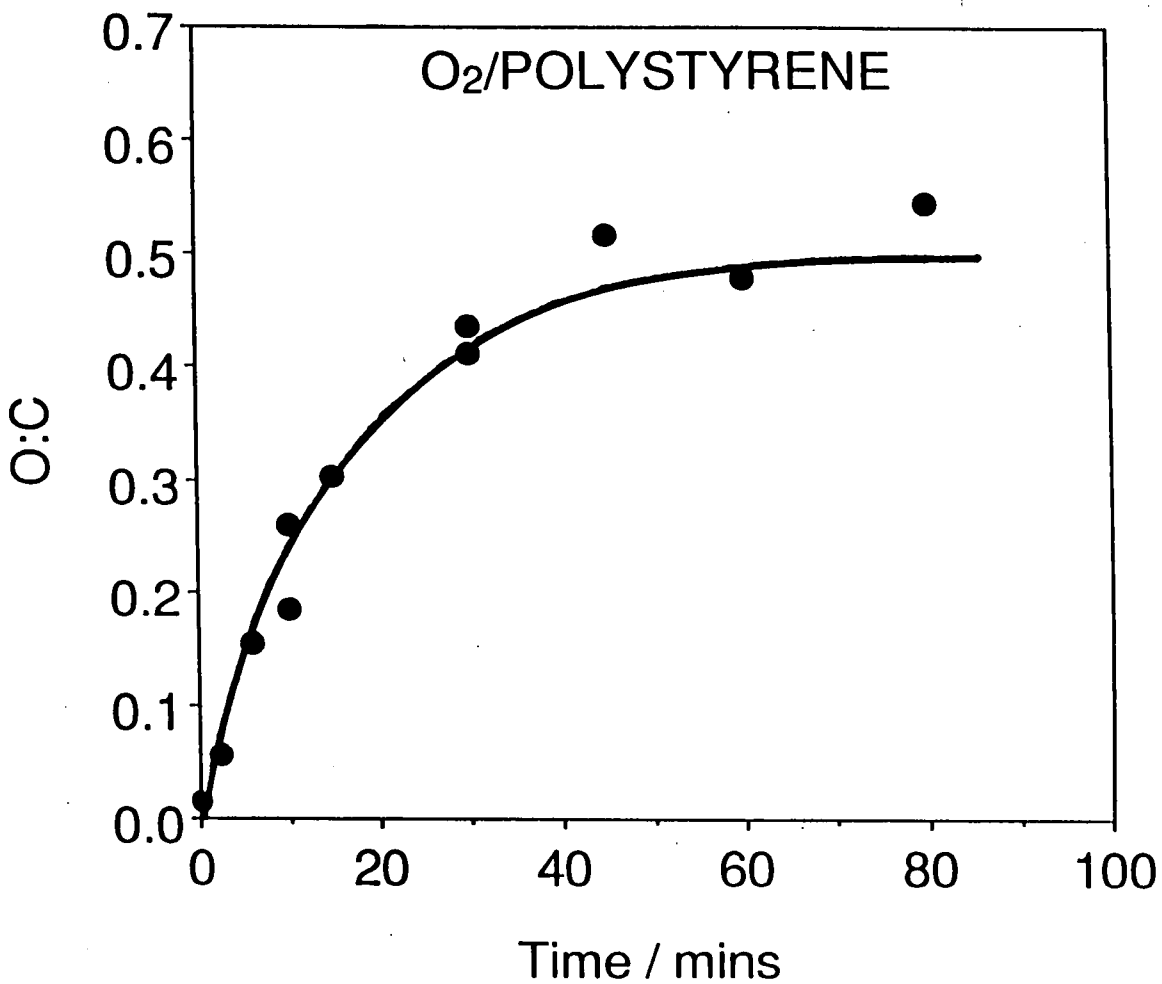

Figure 2a: Summary of O_2-UV/polystyrene experiments: O:C ratio versus time.

Figure 2b. Initially the only form of oxidized carbon present is -C-O-. This species decreases rapidly over the first 10 minutes of UV exposure and then settles down to a value of 35% of the total oxidized carbon present. Concurrently, the -O-C=O functionality at the polystyrene surface increases rapidly over this initial period and subsequently levels off towards 45% of the total oxidized carbon. In addition, the concentration of -C=O and -O-C-O- passes through a maximum and then slowly drops to 20%.

3.4 N_2O-UV/POLYSTYRENE

Photo-oxidation of polystyrene under N_2O generates both oxygen and nitrogen species at the surface. During the first 30 mins, there is an increase in O:C ratio towards a limiting value of 0.17 ± 0.02; whilst the N:C ratio rises to approximately 0.03 ± 0.02 over the same time interval, Figure 3a. The O:N ratio remains virtually constant throughout UV exposure at 6.0 ± 0.6. This suggests that the chemical processes responsible for introducing oxygen and nitrogen functionalities into the polymer surface must be occurring simultaneously.

In order to check for secondary reactions involving N_2 by-product, a control experiment employing N_2 instead of N_2O was performed which yielded no N(1s) signal.

During UV irradiation, the -CH_x- component slowly decreases with time to a limiting value of 72% of the total C(1s) area; this was accompanied by a corresponding attenuation of the π-π^* shake-up satellite. The most prominent component of the oxygenated carbon functionalities is -C-O-, Figure 3b; as a percentage of all of the oxidized carbon environments, it drops from an early value of 80% to 46% after 30 mins. This is compensated by the delayed emergence of the -O-C=O group from 0 to 28% (probably as a consequence of secondary reactions involving N_2O and -C-O-). There is not much variation in the proportion of (-C=O, -O-C-O-) species.

4. DISCUSSION

4.1 O_2-UV/POLYSTYRENE

Irradiation of polystyrene below 280 nm is known to cause the direct excitation of phenyl rings, thereby generating reactive centres and mobile hydrogen radicals[9]. Other parts of the polymer such as -CH- and -CH_2- do not absorb above 200 nm. Attenuation of the C(1s) π-π^* shake-up satellite indicates a loss in aromaticity, this is consistent with excitation and subsequent reaction of the phenyl groups with oxygen, and has previously been observed by Clark et al[7,24,25]. Unfortunately it is not possible to distinguish between total or partial loss of conjugation.

Peak fits for the C(1s) spectra indicate that the -C-O- functionality is predominant during the preliminary stages of oxidation. This induction period before other species appear was also observed by Clark and co-workers[7,24,25].

The low oxygen : oxidized carbon value (far less than one) implies that the first step in photo-oxidation can not exclusively involve a hydroperoxy bond, since one would expect to measure approximately two oxygen atoms per oxidized carbon atom at the surface. Clark et al determined the presence of hydroperoxy species by labelling with sulphur dioxide[7] and concluded that ~ 6% of the C(1s) XPS signal was due to C-OOH.

Further exposure leads to a decrease in the -C-O- species with concurrent growth of -C=O, -O-C-O- and -O-C=O linkages. After 10 minutes, the -C-O- peak approaches a limiting value, whereas the C=O feature passes through a maximum and the -O-C=O species continues to rise until eventually it becomes the predominant species at the polymer surface. Most of these oxidized groups are probably ester linkages since the limiting oxygen : oxidized carbon value is approximately equal to one (i.e. each -O-C=O functionality must also have an associated -C-O- bond); or by sheer coincidence the oxygen : oxidized carbon ratio can be attributed to an equal proportion of C-O-C and O=C-OH groups being present. The latter seems highly unlikely.

These experimental results can be explained in at least two ways:

1) In the first explanation, molecular oxygen is excited and breaks up to give reactive oxygen atoms. Molecular oxygen is known to undergo a very weak absorption corresponding to the forbidden $^3\Sigma_g^- \dashrightarrow {}^3\Sigma_u^+$ transition[35] (See Diagram 3 section 1.4). This is the highest excited molecular state accessible in our experiments and is part of the Hertzberg I bands. These bands have a convergence limit at 242.4 nm which results in the production of $O(^3P)$,

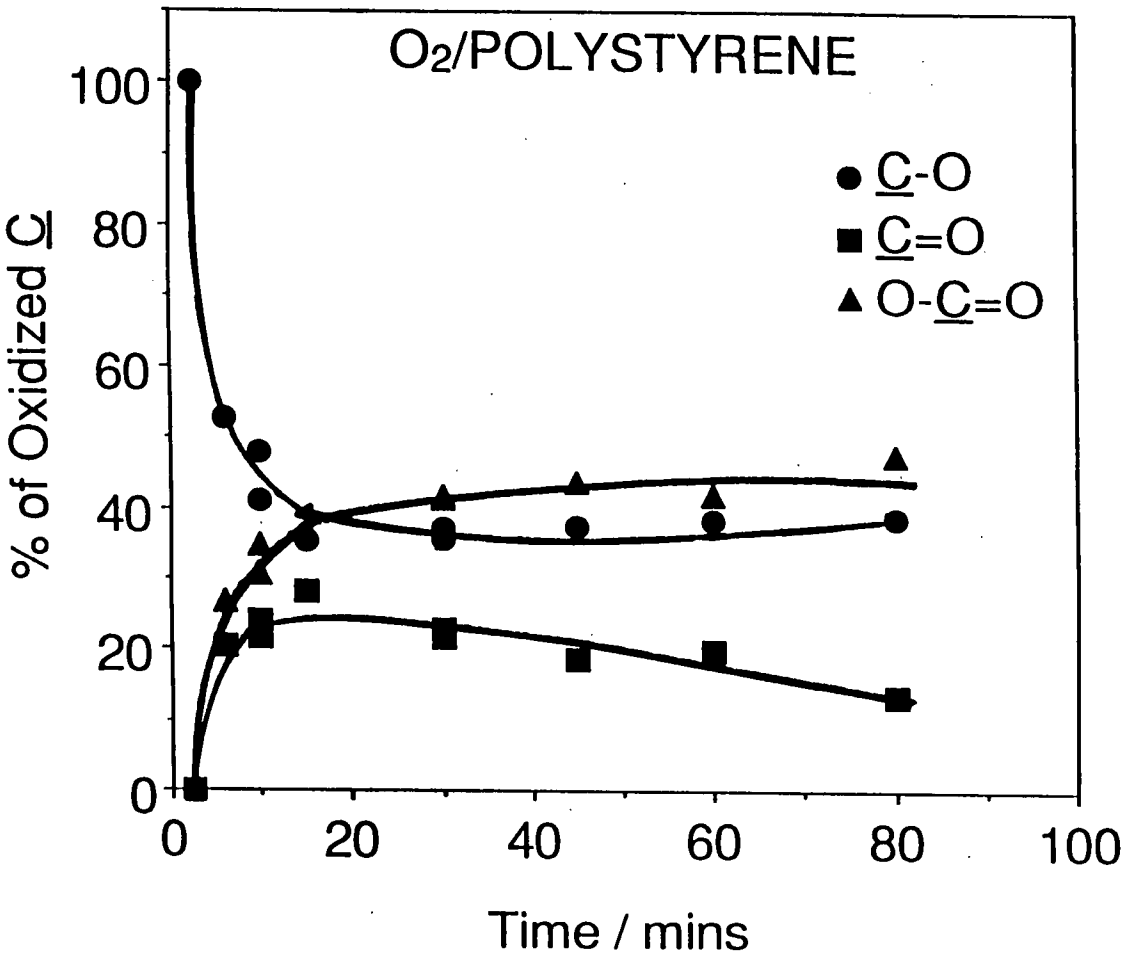

Figure 2b: Summary of O_2-UV/polystyrene experiments:
Relative proportions of oxygenated functionalities as a percentage of total amount of oxidized carbon.

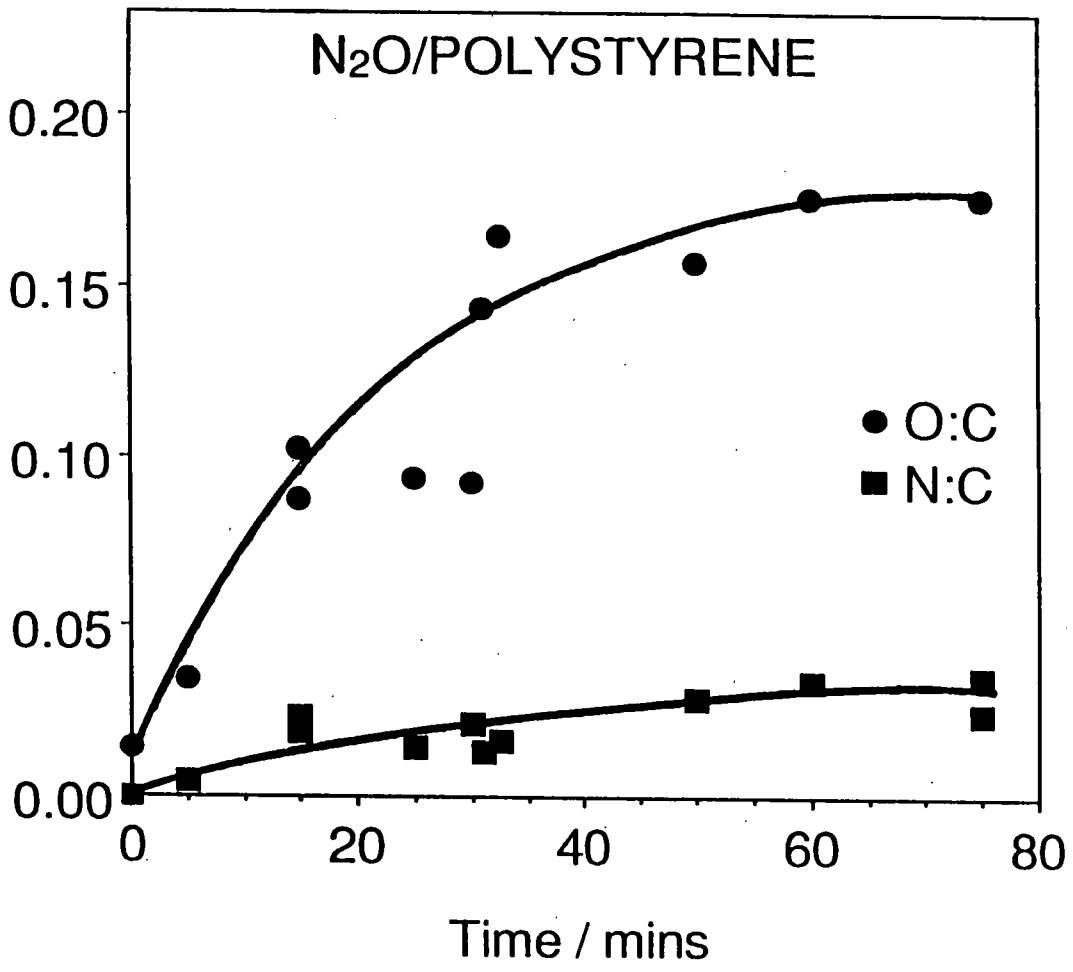

Figure 3a: Summary of N_2O-UV/polystyrene experiments: O:C and N:C ratios versus time.

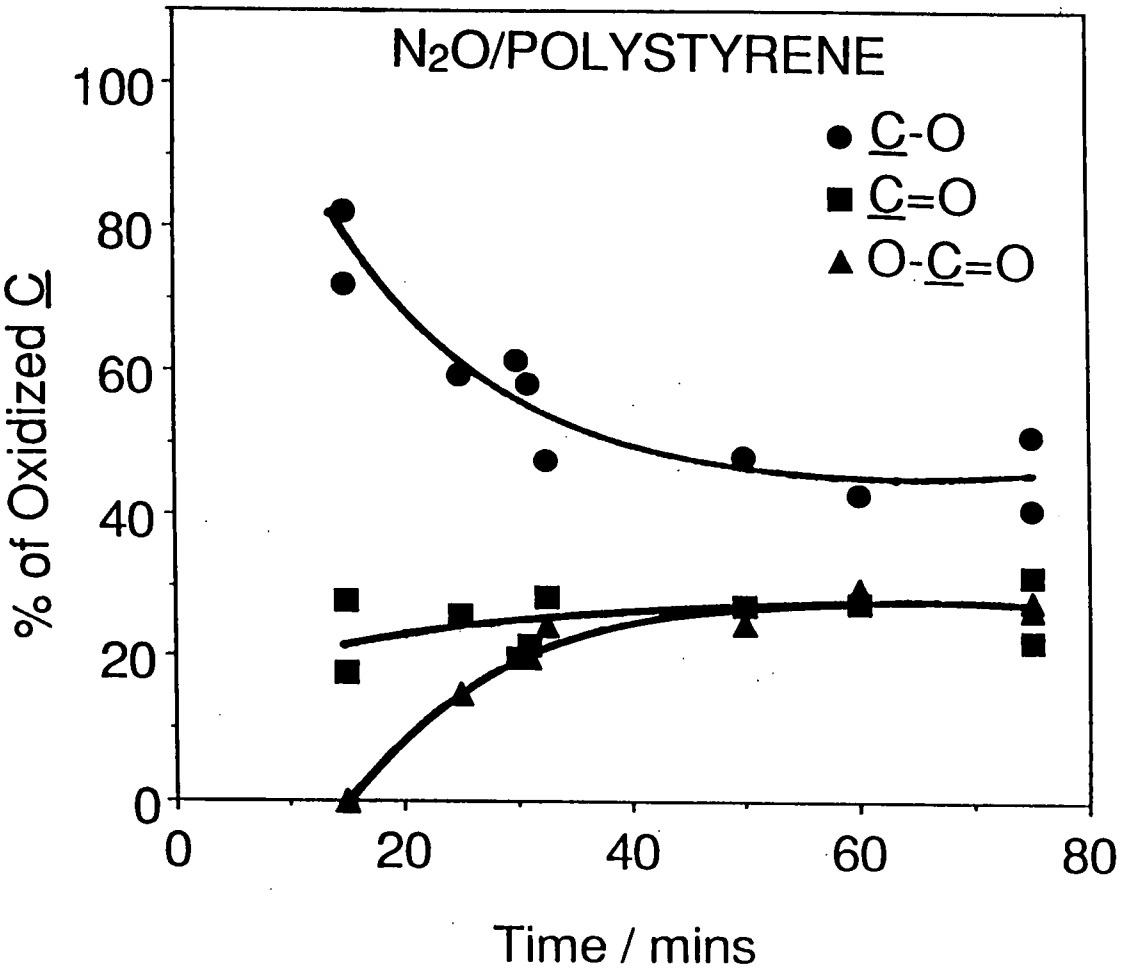

Figure 3b: Summary of N_2O-UV/polystyrene experiments:
Relative proportions of oxygenated functionalities as a percentage of total amount of oxidized carbon.

4. DISCUSSION

4.1 O_2-UV/POLYSTYRENE

Irradiation of polystyrene below 280 nm is known to cause the direct excitation of phenyl rings, thereby generating reactive centres and mobile hydrogen radicals[9]. Other parts of the polymer such as -CH- and -CH_2- do not absorb above 200 nm. Attenuation of the C(1s) π-π^* shake-up satellite indicates a loss in aromaticity, this is consistent with excitation and subsequent reaction of the phenyl groups with oxygen, and has previously been observed by Clark et al[7,24,25]. Unfortunately it is not possible to distinguish between total or partial loss of conjugation.

Peak fits for the C(1s) spectra indicate that the -C-O- functionality is predominant during the preliminary stages of oxidation. This induction period before other species appear was also observed by Clark and co-workers[7,24,25].

The low oxygen : oxidized carbon value (far less than one) implies that the first step in photo-oxidation can not exclusively involve a hydroperoxy bond, since one would expect to measure approximately two oxygen atoms per oxidized carbon atom at the surface. Clark et al determined the presence of hydroperoxy species by labelling with sulphur dioxide[7] and concluded that ~ 6% of the C(1s) XPS signal was due to C-OOH.

Further exposure leads to a decrease in the -C-O- species with concurrent growth of -C=O, -O-C-O- and -O-C=O linkages. After 10 minutes, the -C-O- peak approaches a limiting value, whereas the C=O feature passes through a maximum and the -O-C=O species continues to rise until eventually it becomes the predominant species at the polymer surface. Most of these oxidized groups are probably ester linkages since the limiting oxygen : oxidized carbon value is approximately equal to one (i.e. each -O-C=O functionality must also have an associated -C-O- bond); or by sheer coincidence the oxygen : oxidized carbon ratio can be attributed to an equal proportion of C-O-C and O=C-OH groups being present. The latter seems highly unlikely.

These experimental results can be explained in at least two ways:

1) In the first explanation, molecular oxygen is excited and breaks up to give reactive oxygen atoms. Molecular oxygen is known to undergo a very weak absorption corresponding to the forbidden $^3\Sigma_g^-$ ---> $^3\Sigma_u^+$ transition[35] (See Diagram 3 section 1.4). This is the highest excited molecular state accessible in our experiments and is part of the Hertzberg I bands. These bands have a convergence limit at 242.4 nm which results in the production of $O(^3P)$,

oxygen atoms. Molecular oxygen in the $^3\Sigma_u^+$ state could react intermolecularly with excited polystyrene to yield atomic oxygen species at the polymer surface, these may then become incorporated as -C-O- linkages. Subsequently, these -C-O- groups may react with a second $^3\Sigma_u^+$ oxygen molecule to give -O-C=O species.

2) Alternatively, the $^3\Sigma_g^-$ ground state may react with a radical formed via an oxygen-polystyrene charge transfer complex[1] to produce a peroxy-type of linkage, -C-O-O-, (See Reaction 7, Section 1.2) which could then generate the C=O functionality[16]. The limiting distribution of oxygenated carbon centres in our experiments is comparable to that found at longer wavelengths (greater than 290 nm)[7]; this appears to be consistent with the latter explanation.

In order to differentiate between the two possible reaction pathways, further experiments with N_2O and polystyrene were undertaken.

4.2 N_2O-UV/POLYSTYRENE

In the range 240 - 600 nm, N_2O can undergo dissociation via one of two possible routes[35]:

$$\longrightarrow \quad N_2(^1\Sigma_g^+) + O(^3P) \quad \text{threshold wavelength 741.5 nm;}$$

$$\longrightarrow \quad N_2(^1\Sigma_g^+) + O(^1D) \quad \text{threshold wavelength 340.7 nm.}$$

The threshold wavelength for the absorption of nitrous oxide to give $NO(^2\Pi) + N(^4S)$ is 251.9 nm[35], hence this reaction is also expected to be on-going in the gas phase during UV irradiation and could be a potential route for nitrogen incorporation into the polymer substrate as either C-N or C-ON moieties. NO could also react with oxidized carbon functionalities and thereby create N-containing groups at the surface. However, since the N:C ratio is rather small and constant, it can be concluded that these reaction pathways are in the minority and are probably occurring independently. It was impossible to distinguish between -C-N and -CO-N by XPS because the N(1s) signal was of low intensity. Previous studies did not observe the incorporation of nitrogen in the polymer surface[27]. This is unusual as interaction of UV with N_2O at low wavelengths is just as likely to produce N and NO as at higher wavelengths[23].

A control experiment using polystyrene and N_2 was also performed in order to check whether insufficient flushing of the reactor could cause the molecular nitrogen by-product to react with the polymer substrate. No N(1s) signal was detected by XPS, as ground state N_2 is too stable to react with the surface[35].

Peak fits for the C(1s) spectra show -C-O- as the initial predominant peak (there is also a small amount of -C=O present). The -C-O- peak slowly decreases during the first 30 mins, whilst there is a slight increase in the -C=O component. At a later time, the -O-C=O XPS feature appears and slowly reaches a limiting value. The -C-O- peak remains the major species throughout the experiment. Direct reaction of gas phase $O(^3P)$ and /or $O(^1D)$ photo-dissociation products with the substrate may explain the origins of the high selectivity towards -C-O- functionalities. The experiments of Shard and Badyal[27] showed greater selectivity of oxygenated functional groups with only C-O and C=O being detected during photo-oxidation with N_2O. This may be because of different experimental conditions, the wavelength of the source used was mainly at 174 and 149 nm. The limiting O : C ratio for their experiments was 0.07 ± 0.01, and so a less oxidised surface prevailed as compared to our limiting value of 0.17 ± 0.02. At the wavelengths of Shard and Badyals experiments, C-C bond cleavage also occurs, therefore a different photo-oxidation mechanism results, possibly leading to greater evolution of CO and CO_2 and hence a less oxidised surface.

The final O:C ratio is small in comparison to the O_2-UV/polystyrene values. Extended N_2O oxidation reduces the hydrocarbon component down to about 75% of its original value. This is rather small in comparison to the limiting value of 45% observed for the O_2-UV/polystyrene experiments. All of these observations suggest that photo-oxidation of polystyrene is less vigorous during N_2O exposure. One explanation for this behaviour could be poisoning of the polymer surface by adsorbed nitrogen species, although this would seem unlikely because of the low incorporation of nitrogen species. A second possibility may be that the attack of atomic oxygen species at the substrate is accompanied by formation of stable hydroxyl groups. This has been suggested to occur for shorter wavelength studies[27]. Alternatively the attacking species may be so reactive that there could be total combustion at the surface leading to CO_2, CO and H_2O evolution and no residual oxygenated carbon environments. This latter explanation seems unlikely since one would expect the variation of the O:C ratio as a function of exposure time to pass through a maximum - this was not observed.

Thermodynamically it is easier to cleave the N_2-O bond [$D_O(N_2\text{-}O)$ = 1.67 eV] than the O-O bond in O_2 [$D_O(O\text{-}O)$ = 5.12 eV][35]. These bond dissociation energy values are still applicable when photon induced reactions occur. Our results demonstrate that there is a greater extent of oxidation with O_2, and therefore the major reaction pathway does not involve O-O bond dissociation by the excited polymer to yield atomic oxygen

intermediates. Formation of peroxide linkages or O_2-polystyrene charge-transfer complexes appear to play an important role in the photo-oxidation of polystyrene, rather than atomic oxygen.

5. CONCLUSIONS

Contrary to what might be expected from the known relative reactivities of O_2 versus N_2O, it has been discovered that polystyrene is less susceptible to surface photo-oxidation under N_2O. The dominant reaction pathway for N_2O may be envisaged as atomic oxygen reacting with excited polystyrene centres to yield C-O bonds eventually producing hydroxyls, i.e. the more reactive N_2O hinders subsequent reactions by creating unreactive -OH groups. Molecular oxygen interacts with the excited substrate to produce a peroxy-type linkage or a charge-transfer complex, these species can then participate in polymer oxidation.

6. REFERENCES

1) J.F. Rabek, J. Sanetra, and B. Ranby, Macromolecules, 19, 1674 (1986).
2) N.A. Weir and K. Whiting, Eur. Polym. J., 25, 291 (1989).
3) B.G. Achhammer, J. Polym. Sci., 8, 555 (1952)
4) N. Grassie and N.A. Weir, J. App. Polym. Sci., 9, 963 (1965)
5) B. Ranby and J. Luki, Pure and App. Chem., 52, 295 (1980)
6) H. Hiraoka and L.W. Welsh, Tenth Intl. Conf. Electron and Ion Beams Science and Technol. Proc., 83, 71 (1983).
7) D.T. Clark and H.S. Munro, Polym. Deg. and Stab., 8, 213 (1984).
8) J.F. McKellar and N.S. Allen, 'Photochemistry of Man-Made Polymers', Applied Science Publishers Ltd, London, 1979.
9) G. Loux and G. Weill, J. Chem. Phys., 61, 484 (1964).
10) P.J.Burchill and G.A. George, J. Polym. Sci., Polym. Letts. Edn., 12, 497 (1974).
11) G. Geuskens, D. Baeyens-Volant, G. Delaunois, Q. Lu-Vinh, W. Piret and C. David, Eur. Polym. J., 14, 299 (1978).
12) B. Ranby and J.F. Rabek, 'Photodegradation, Photo-oxidation and Photostabilization of Polymers', Wiley, Bristol, 1975.
13) N. Grassie and N.A. Weir, J. Appl. Polym. Sci., 9, 975, (1965).
14) N. Grassie and N.A. Weir, J. Appl. Polym. Sci., 9, 999, (1965).
15) R.B. Fox and L.G. Isaacs, U.S. Research Lab. Rep. No. 6284 (1965).
16) J.F. Rabek and B. Ranby, J. Polym. Sci., Polym. Chem. Edn., 12, 273 (1974).
17) T.R. Price and R.B. Fox, J.Polym. Sci., Polym. Letts. Edn., 12, 273 (1966).
18) N. Grassie and N.A. Weir, J. Appl. Polym. Sci., 9, 987, (1965).
19) G. Geuskens, D. Baeyens-Volant, G. Delaunois, Q. Lu-Vinh, W. Piret and C. David, Eur. Polym. J., 14, 291 (1978).
20) J.F.Rabek and J. Sanetra, Macromolecules, 19, 1679 (1986)
21) W. G. Richards and P. R. Scott, 'Structure and Spectra of Molecules', Wiley, 1985.
22) J. R. Hollahan and A. T. Bell, 'Techniques and Applications of Plasma Chemistry', Wiley, 1974, Chapter 1.
23) J. G. Calvert and J. N. Pitts, 'Photochemistry', Wiley, 1966, Chapter 3.
24) D.T. Clark and H. S. Munro, Polymer Deg. and Stab., 9, (1984), 63-71.
25) D.T. Clark and J. Peeling, Polymer Deg. and Stab., 3, (1980-81), 97-105.
26) H. S, Munro, D. T. Clark and J. Peeling, Polymer Deg. and Stab., 9, (1984), 185
27) A. G. Shard and J. P. S. Badyal, J. Phys. Chem., 95, (1991), 9436.

28) L. O'Toole, R. D. Short, F. A. Bottino, A. Pollicino and A. Recca, Polymer Deg. and Stab., 38, (1992), 147-154.
29) L. Quinones and E. A. Schweikert, Surf. and Int. Anal., 15, (1990), 503-508.
30) P. C. Lucas and R. S. Porter, Polymer Deg. and Stab., 22, (1988), 175-184.
31) E. P. Otacka, S. Curran and R. S. Porter, J. Appl. Polym. Sci., 28, (1983), 3227.
32) G. Johansson, J. Hedman, A. Berndtsson, M. Klasson, and R. Nilsson, J. Electron Spectr., 2, (1973), 295.
33) D.T. Clark, A. Dilks, J. Polym. Sci. Polym. Chem. Edn., 15, (1977), 15.
34) D.T. Clark, A. Dilks, J. Polym. Sci. Polym. Chem. Edn., 17, (1979), 957.
35) H. Okabe, 'Photochemistry of Small Molecules', Wiley Interscience, New York, (1978).
36) D.R. Snelling, Chem. Phys. Letters, 2, (1968), 346.

CHAPTER 3

AN IN SITU MASS SPECTROMETRY INVESTIGATION OF POLYSTYRENE PHOTOLYSIS AND PHOTO-OXIDATION

1. INTRODUCTION

An investigation into the gaseous photolysis and photo-oxidation products of a polymer could lead to an insight into the mechanistic aspects of these processes, and in this chapter a novel approach is described aimed at understanding the nature of the photochemistry occurring during ultraviolet irradiation of polystyrene film both in vacuum and in oxygen. This involves directing a quadrupole mass spectrometer at the irradiated polymer substrate under ultra high vacuum or in the presence of approximately 1 x 10^{-7} Torr of oxygen, i.e. *in situ*, and thereby detecting all the species which are being evolved from the polystyrene surface or formed in the space between the surface and the entrance to the quadrupole mass spectrometer.

An overview of previous studies is given below, these have mainly relied upon trapping gaseous reaction products and later expanding them into a mass spectrometer, reaction intermediates cannot be detected by this technique. New techniques involving analysis of fragments evolved from an oxidised surface by bombardment with energetic species are discussed as well as more traditional chemical analysis methods. The mechanisms of polystyrene vacuum photolysis and photo-oxidation have been thoroughly covered in Chapter 2.

1.1 MASS SPECTRAL ANALYSIS

The first study of the gaseous reaction products evolved during polystyrene photolysis and photo-oxidation were carried out by Achhammer and co-workers in 1952[1]. Films of the polymer were inserted into quartz exposure tubes, evacuated, sealed and then exposed to various conditions of heat and/or U.V. radiant energy in vacuo or in the presence of oxygen. After various periods of exposure the treatments were interupted and mass spectrometric analyses of the gaseous degradation products were made.

Mass spectrometry showed that both heat and U.V. radiation, in vacuo and in the presence of oxygen, caused an initial evolution of gaseous products, which were attributed to loss of residual solvent and the decomposition of thermolabile impurities in the polymer, such as peroxides. Hydrocarbon trace impurities were thought to be due to the presence of residual solvent, such as methyl ethyl ketone and benzene.

Exposure in oxygen at 118°C gave extensive deterioration of the polymer and, in the latter stages of treatment, evolution of polymer oxidation products such as formic acid, acetic acid and acetaldehyde.

Samples in quartz tubes that had been treated as above were then evacuated and irradiated with UV at 120°C, i.e. vacuum photolysis was carried out on a photo-oxidised sample. Water was the chief volatile product with small amounts of acetone, acetaldehyde and benzaldehyde.

In summary, the mechanism of degradation of polystyrene under the conditions employed consisted of two processes:

1) the loss of volatile materials and decomposition of thermolabile structures resulting from exposure to UV and/or heat in the range 115-120°C both in vacuo and in oxygen.

2) oxidation of the polymer by exposure to ultraviolet radiant energy at 120°C in the presence of oxygen.

Fox and Isaacs also monitored the photolysis and photo-oxidation of polystyrene by mass spectrometry[2]. Thin films of polystyrene were photolysed by 253.7 nm radiation in vacuum and in air at 25°, 80° and 120°C, vacuum conditions were 10^{-5} Torr at all temperatures. The quartz cell containing the polymer film was then heated for 48 hours at 120°C and the volatiles thus evolved expanded into a mass spectrometer for analysis. Exposures in air or oxygen were carried out in an analogous fashion.

During vacuum photolysis, hydrogen was the major volatile product emanating from the polymer itself, of the remaining volatile products, carbon monoxide, carbon dioxide, and methane probably arose from polymer imperfections, such as oxygenated species incorporated during processing and through aging during storage. Benzene and styrene were also present as impurities rather than major photolysis products, it was concluded that these species were impurities as different amounts were evolved for different polymer samples.

Photo-oxidation, in the presence of 20 Torr of oxygen produced carbon dioxide, carbon monoxide, styrene and benzene. Water was also observed in relatively large amounts. Hydrogen, alcohols, hydrocarbons and other oxygenated products were absent.

In all of these previous studies, the photochemical reactions have been carried out in a separate vessel from the mass spectrometer. Gaseous products were trapped and expanded into the mass spectrometer after the reaction. This could only be used for extensive photodegradation. In our experiments, all reactions were carried out *in situ*, thereby enabling the initial stages of photo-oxidation to be examined. A brief review of the mass spectral technique is given in Appendix 1.

1.2 TRADITIONAL CHEMICAL TECHNIQUES

A method of studying gaseous reaction products from a polymer other than by mass spectrometry was developed by Grassie and Weir[3,4]. The only product evolved during photolysis was hydrogen, detected by gas-solid chromatography[3]. During photo-oxidation, water and carbon dioxide were observed via absorption of these species on to anhydrous magnesium perchlorate and Carbosorb respectively[4].

1.3 OTHER TECHNIQUES

More recent studies have focussed on the analysis of a photo-oxidised surface after the reaction is complete by bombarding the polymer surface with energetic species and observing the evolved fragments by mass spectrometry[5,6]. Changes in polystyrene mass spectra after photo-oxidation of the polymer have been studied by time of flight (TOF) -SIMS and Cf 252 particle desorption mass spectrometry[5,6]. TOF-SIMS showed that there was complete destruction of high molecular weight polymeric material at the surface after photo-oxidation for extended irradiation times[5]. Cf-252 particle desorption mass spectrometry showed an increase in oxygenated species emitted from the polymer surface after photo-oxidation, such as H_2O^+, H_3O^+, O^- and OH^-[6]. A decrease in intensity of the tropyllium ion signal after photo-oxidation was interpreted as a consequence of the formation of a bond to the benzylic carbon in polystyrene. An increases in intensity of the phenyl radical signal was attributed to the presence of easily ionised fragments in the oxidation products of polystyrene[6], although this attribution was rather vague.

It was felt that detection of any volatile species formed in the initial stages of photo-oxidative degradation of polystyrene might throw light on the mechanism of the primary steps in the process, as opposed to the overall process, which is what these previous studies provide information about. This was the motivation for our work.

2. EXPERIMENTAL

Experiments were carried out in an ultra high vacuum chamber, base pressure 8 x 10^{-10} Torr, Figure 1 and Plate 1. This was equipped with a VG SX200 quadrupole mass spectrometer which had been multiplexed to an IBM compatible computer. An Oriel low pressure Hg - Xe arc lamp operating at 50 Watts emitting a strong line spectrum in the 240 - 600 nm region was used to irradiate the sample through a sapphire window with a cut-off wavelength between 141 - 161 nm. Polystyrene film (BP) was degreased with iso-propyl alcohol in an ultrasonic bath for 30 seconds and dried prior to introduction into the chamber via a fast insertion lock. The distance between the sample and the quadrupole ion source was optimised at 3 cm; closer proximity caused polymer degradation due to the heat of the ioniser filament.

Data acquisition, i.e. the mass signal intensity, for upto 40 different masses, with respect to time, was executed in real time during the photolysis experiment. In total, 500 data points showing the variation of mass signal intensity during the experiment were collected during each experiment. Prior to each run, the UHV chamber walls were outgassed by exposure to UV, with the polymer film held well back out of the line of sight of the sapphire port. Subsequently the UV shutter was closed and the polymer was pushed into position with line of sight to the UV source and mass spectrometer at an angle of 45^{o} to the vertical, and data acquisition initiated. After 10 minutes the shutter was opened for 10 minutes, and finally closed until data accumulation ended approximately 20 minutes later. The same process of shutter manipulation was used during photo-oxidation but in this case the reaction occured under 9.6 x 10^{-8} Torr of oxygen (BOC 99.97 % minimum purity) introduced into the chamber via a leak valve. These shutter manipulations resulted in the characteristic peak profiles described in the next section. All results were reproducible.

Repeated exposures of the same sample were plotted as mass signal intensity increase vs exposure time (which increased in increments of 10 minutes) over a total of 100 minutes. These are described in more detail for each mass signal in the following section, and all are averages of at least two experiments.

During photolysis, a pressure rise of ~ 5.5 x 10^{-9} Torr was seen when the UV source was on the sample. However, during photo-oxidation a pressure rise was not detected, probably because the rise was small in comparison to the pressure of oxygen present in the reaction chamber.

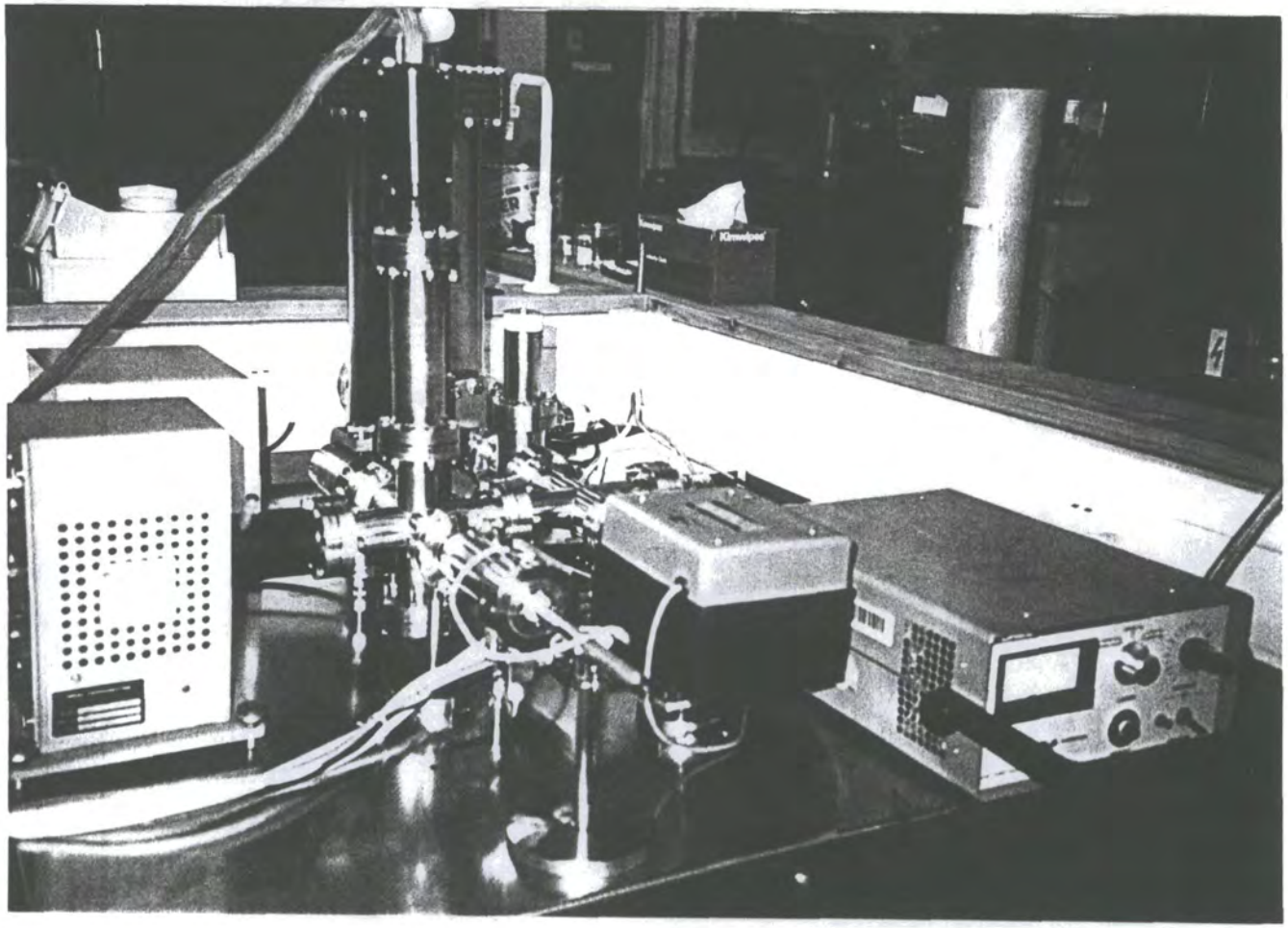

Plate 1 : Ultra high vacuum chamber used for *in situ* mass spectrometry work.

As a blank, experiments were repeated with the polymer out of the line of sight of the mass spectrometer ionisation source and ultra-violet irradiation. Masses 2, 18, 28 and 44 were seen to increase originating from the walls of the chamber, however this increase was negligible in comparison with signals due to photolysis and photo-oxidation experiments.

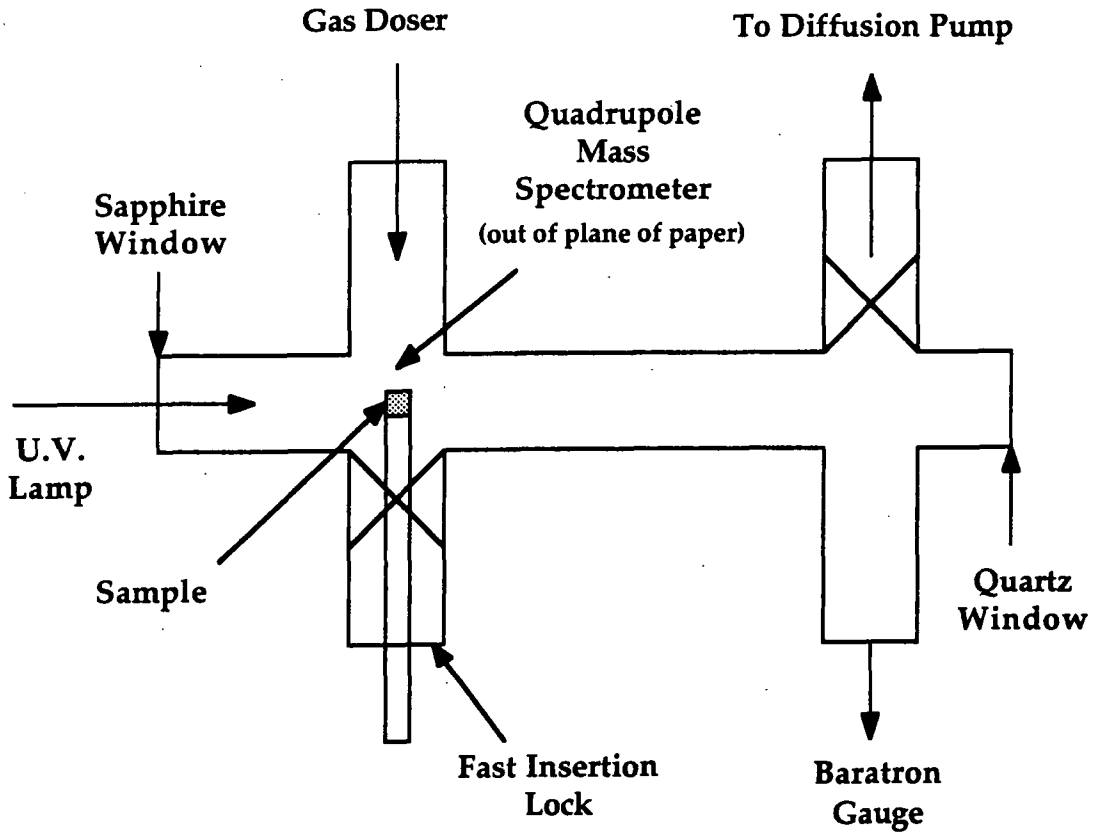

Figure 1: Schematic of ultra high vacuum chamber used.

X-ray photoelectron spectroscopy (XPS) measurements were performed on samples oxidised for 100 minutes in the mass spectrometer chamber. The samples were removed from this chamber, exposed to normal laboratory atmosphere for a minute or so, and inserted into a Kratos ES300 surface analysis instrument (base pressure ~6 x 10^{-10} Torr). MgKα radiation was used as the excitation source with electron detection in the fixed retarding ratio (FRR) analyser mode. XPS spectra were acquired at an electron take-off angle of 30° from the surface normal. Data accumulation and peak area analyses were performed using an IBM compatible computer. Instrumentally determined sensitivity factors are such that for unit stoichiometry, the C(1s) : O(1s) intensity ratio is 1.00 : 0.55 respectively.

3. RESULTS and DISCUSSION

Many different species are ejected from the polystyrene surface during photolysis and photo-oxidation. The same mass signals are observed during both experiments, however a greater yield of products are evolved during photo-oxidation and the relative changes in intensity differ slightly between vacuum photolysis and photo-oxidation experiments. During photolysis the masses listed below were evolved, the numbers in brackets are increases in signal intensity relative to the same gain observed during the 10 minute irradiation period. The intensities are uncorrected for variations of spectrometer sensitivity with mass:

28 (8755 ± 255) > 2 (3310 ± 290) ~ 18 (2995 ± 395) ~ 41 > 44 (2390 ± 160) > 43 (1700 ± 150) ~ 55 ~ 39 ~ 67 ~ 57~ 69 ~ 53 ~ 81 > 77 (532 ± 42) ~ 51 ~ 50 ~ 79 ~ 54 ~ 65 ~ 71 ~ 95 ~ 83 ~ 93 ~ 45 ~ 70 ~ 52 > 78 (344± 13) ~ 91 (356 ± 54) > 105 (260 ± 46) > 104 (117 ± 5) ~ 1 ~ 63 ~ 97 ~ 109 ~ 107 ~ 103 > 76 (49 ± 4) ~ 115

and for photo-oxidation:

28 (27133 ± 2589) > 18 (12433 ± 1074) > 41 (4250 ± 250) > 43 (3350 ± 330) > 2 (1973 ± 412) ~ 55 ~ 39 ~ 57 ~ 69 ~ 51 ~ 67 ~ 81 ~ 91 > 77 (1480 ± 157) ~ 105 (1467 ± 172) > 78 (796 ± 53) ~ 50 ~ 53 ~ 79 ~ 93 ~ 83 ~ 71 > 104 (447 ± 27) ~ 52 ~ 54 ~ 65 ~ 70 ~ 95 ~ 45 ~ 97 ~ 63 ~ 107 ~ 109 > 76 (126 ± 7)~ 103 ~ 115 ~ 1

All of these masses undergo a rise in signal intensity during UV irradiation and subsequently fall in magnitude upon removal of the photon source, eg. mass 2, Figure 2.

In order to compare photolysis and photo-oxidation, mass species directly relating to the polymer structure and oxidative reaction products are the most useful to monitor. Fragments relating to break-up of the polymer chain and oxidation were selected. The most important masses for comparison purposes were found to be: 2, 18, 28, 77, 78, 91, 104 and 105. These mass peaks are assigned as follows: 2 (hydrogen), 77 (phenyl radical) and 78 (benzene)[7]; possible oxidation products are masses 18, and 28 (water and carbon monoxide respectively); fragments indicating polymer chain break down are 91 (tropyllium ion)[8], 104 C_8H_8 (styrene)[9] and 105 C_8H_9 (detected in SIMS of polystyrene)[6,10,11]; other oxidised species are C_7H_4O[8] (also attributed to mass 104) and C_7H_5O[8] (mass 105).

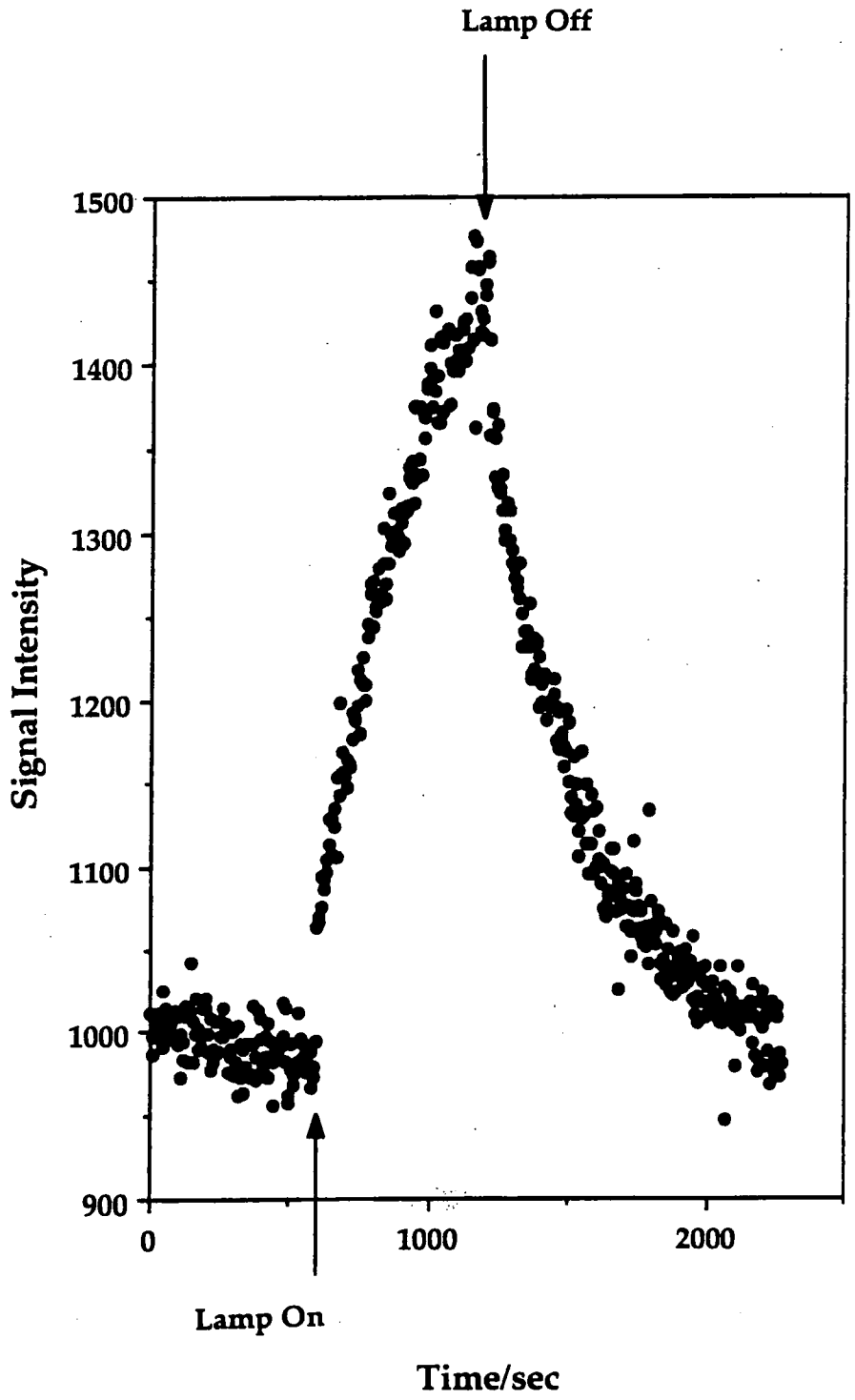

Figure 2: Mass 2 intensity profiles (before, during, and after UV irradiation) for photo-oxidation.

If this short list is used, a more compact ordering of the intensities of peaks for the various species evolved during photolysis and photo-oxidation can be compiled (uncorrected for mass spectrometer sensitivity):

For photolysis:

$$28 > 2 \sim 18 > 77 > 78 \sim 91 > 105 > 104$$

and for photo-oxidation:

$$28 > 18 > 2 > 91 > 77 \sim 105 > 78 > 104$$

Subsequent exposures of previously exposed samples of polystyrene to UV irradiation, both in photolysis and photo-oxidation, resulted in a gradual decrease in mass intensities, e.g. mass 2, Figure 3. This behaviour can be attributed to cross-linking taking place at the polymer surface, together with chain scission, thereby producing a polymer network containing a lower concentration of centres capable of giving volatile products, which will in turn hinder the substrate's susceptibility towards photo-degradation.

XPS analysis of clean polystyrene showed no oxygen incorporation. Measurements on the final photo-oxidised surface (i.e.. after 100 minutes exposure) gave a C (1s) : O (1s) ratio of 0.024 ± 0.010. Only a small amount of oxidation of the polymer had occured during the experiments, as compared to reactions described in Chapter 2, where the limiting value of C (1s) : O (1s) is 0.51 ± 0.03 after 80 minutes. This is due to the different powers of the lamp used and differing pressures of oxygen (50 Watts and 9.6×10^{-8} Torr in these experiments and 100 W and at about 1 Atmosphere pressure in Chapter 2).

3.1 MASS 2

UV irradiation of polystyrene film both in vacuum and oxygen results in a rapid rise in mass 1 (atomic hydrogen) and mass 2 (molecular hydrogen) signals, e.g Figure 2. Molecular hydrogen has been detected in previous vacuum photolysis studies, but has not been found after photo-oxidation reactions[2,4]. This may be due to the time scale of the experiments reported previously, all reaction routes that form molecular hydrogen could be intercepted by oxygen species.

The relative intensities of the peaks for atomic and molecular hydrogen did not appear to change over the duration of the experiments whether the lamp was on or not. This may signifying that although photo-

excitation of the phenyl groups in polystyrene may initiate fission of the benzylic C-H bonds via intramolecular energy transfer[3], the hydrogen radicals so formed are unable to desorb in significant numbers from the polymer surface before participating in reactions, such as the generation of molecular hydrogen by either H· + H· combination or via hydrogen abstraction from neighbouring polymer molecules, and, in the photo-oxidation case, reaction with oxygen containing functionalities formed on the polymer surface (eg hydroperoxide formation[12]).

More hydrogen (mass 2) is given off during photolysis of polystyrene than photo-oxidation, Figure 3. This is consistent with the above rationalization since, during photo-oxidation, an alternative reaction pathway is open to hydrogen radicals other than molecular hydrogen formation.

The mass profile of molecular hydrogen is identical during photolysis and photo-oxidation, evolving rapidly at first and then gradually increasing until the UV source is removed, e.g. Figure 2, when a rapid decrease is followed by a gradual tail towards the background level. Hydrogen continues to desorb from the polymer after irradiation, probably due to species trapped in the sub-surface gradually diffusing out. If the penetration depth of the ultra-violet light could be calculated, knowing the diffusion co-efficient of molecular hydrogen in polystyrene might allow the time for the molecules to escape from that depth to be calculated. This time could then be compared with the time required for the molecular hydrogen signal to drop towards the background level in these experiments. However the absorption depth in films of polystyrene is hard to quantify because of uncertainties concerning the spatial distribution of chromophores, scattering and other complications[13].

The trend of the increase and subsequent slow decrease of the mass signals was not an artifact of pumping speeds, as gas introduced to the chamber via a leak valve was instantaneously pumped away.

3.2 MASS 18

Much more water (mass 18) is evolved during photo-oxidation of polystyrene than photolysis, Figure 4. This has also been noted by previous workers in this field[1].

Water produced during the photolysis of polystyrene can be attributed to water absorbed within the polymer matrix during processing and storage. Polystyrene is particularly susceptible to permeation by water[14]. Attempts to remove this water by storage at 40°C in a vacuum oven overnight and

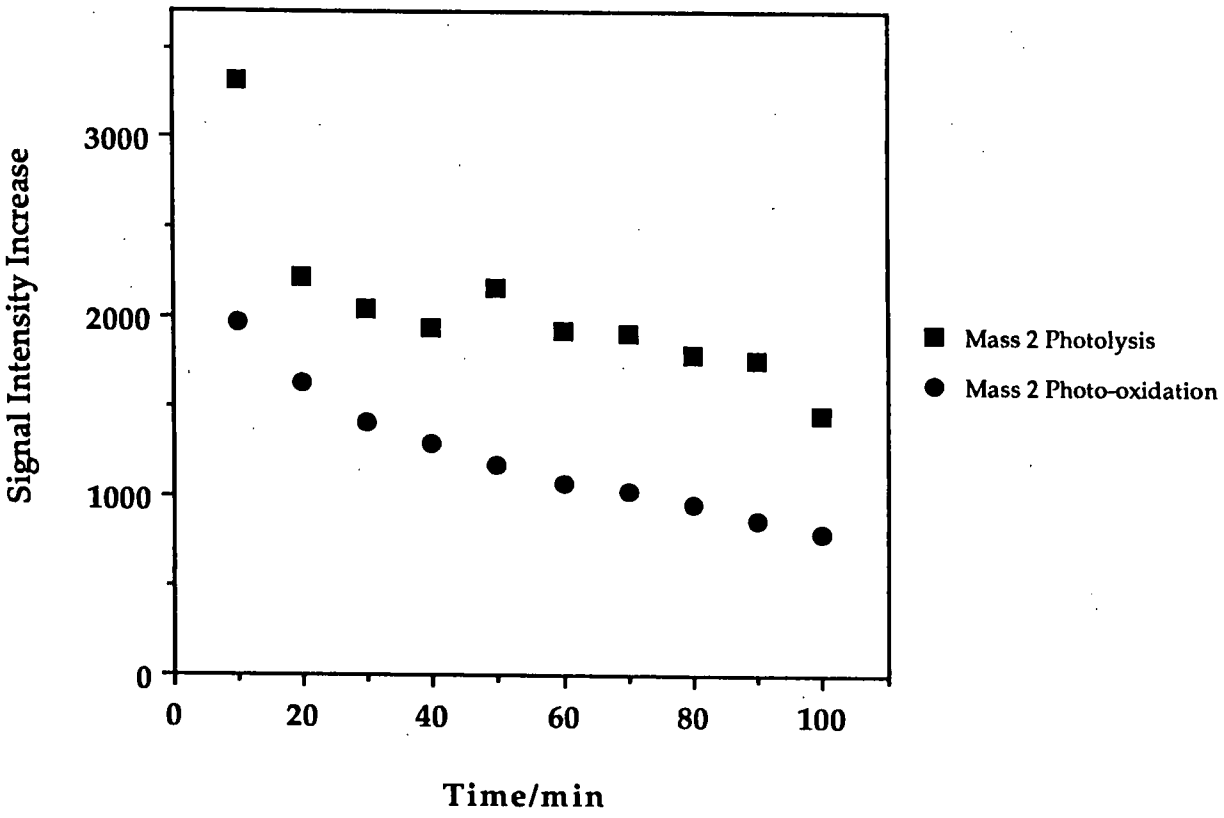

Figure 3: Changes in the mass 2 signal intensity increase as a function of exposure time during photolysis and photo-oxidation.

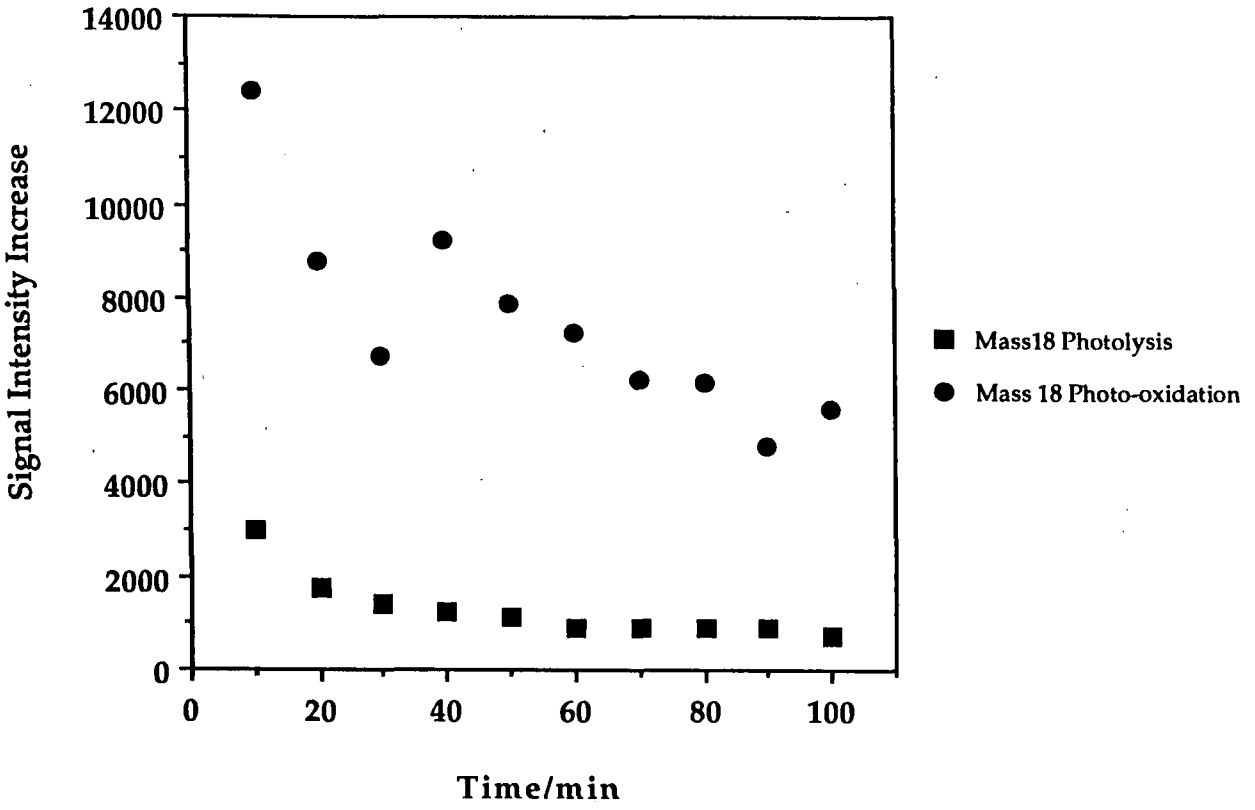

Figure 4: Changes in the mass 18 signal intensity increase as a function of exposure time during photolysis and photo-oxidation.

subsequent pumping for 4 days under UHV in the reaction chamber still gave films which evolved the same amount of water during photolysis. The absorbed water must be strongly trapped in the polymer subsurface and/or bound to the surface. When the polymer is irradiated with UV, any water on the surface of the polymer is thermally excited by local heating (electronic excitation is not possible in the wavelengths accessible in these experiments) and evolved into the mass spectrometer. Also, as overlayers of the polymer are broken down, water trapped within the bulk of the polymer will be free to escape.

During photo-oxidation, water can also be formed by the degradation of the polymer[12]. Breakdown of the hydroperoxy radical according to the mechanism shown in Scheme 1 evolves OH· radicals which may react with hydrogen radicals or abstract hydrogen from nearby polymer chains[12].

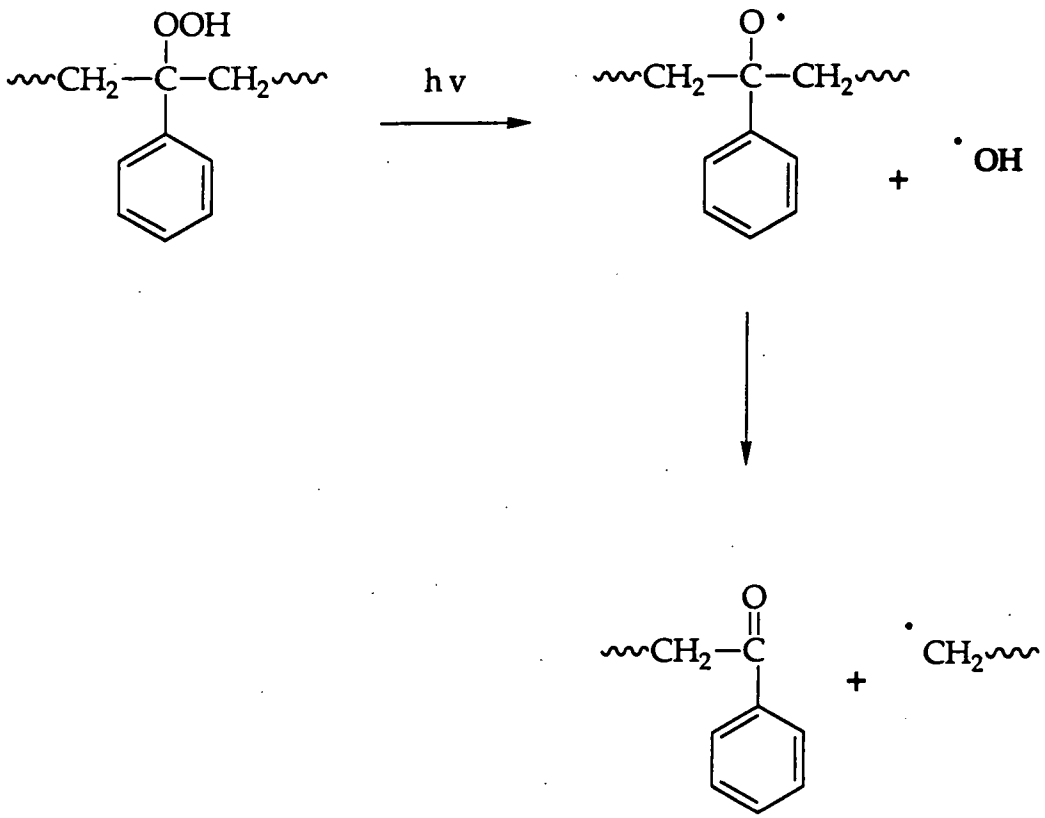

Scheme 1: Photon enhanced degradation of hydroperoxy species in polystyrene[12].

The signal for mass 17 is also observed to increase upon exposure of the polymer to ultra-violet light. However, the relative concentrations of mass 17 and mass 18 did not appear to change over the experiment duration, which is consistent with the view that hydroxyl radicals do not escape from

the polymer surface. The origin of mass 17 is most likely to be due to fragmentation of water in the mass spectrometer[9].

Grassie and Wier suggested an alternative, less favoured, breakdown of the hydroperoxy group in Scheme 1 to produce HOO· radicals[15]. This may give hydrogen peroxide by the following mechanisms (Scheme 2)[15]:

$$HO_2\cdot + RH \longrightarrow R\cdot + H_2O_2$$
$$HO_2\cdot + HO_2\cdot \longrightarrow O_2 + H_2O_2$$

Scheme 2 : Reactions of hydroperoxy radicals[15].

Once formed, hydrogen peroxide may decompose in the presence of UV to form hydroxy radicals. These may subsequently abstract hydrogen radicals from the polymer chains or combine with atomic hydrogen to give water (Scheme 3)[16].

$$H_2O_2 \xrightarrow{U.V} 2OH\cdot \xrightarrow{2H\cdot} 2H_2O$$

Scheme 3 : Hydrogen peroxide decomposition in the presence of U.V[16].

An alternative route for water formation has been proposed involving a six-membered transition state for hydroperoxy degradation (Scheme 4)[17]:

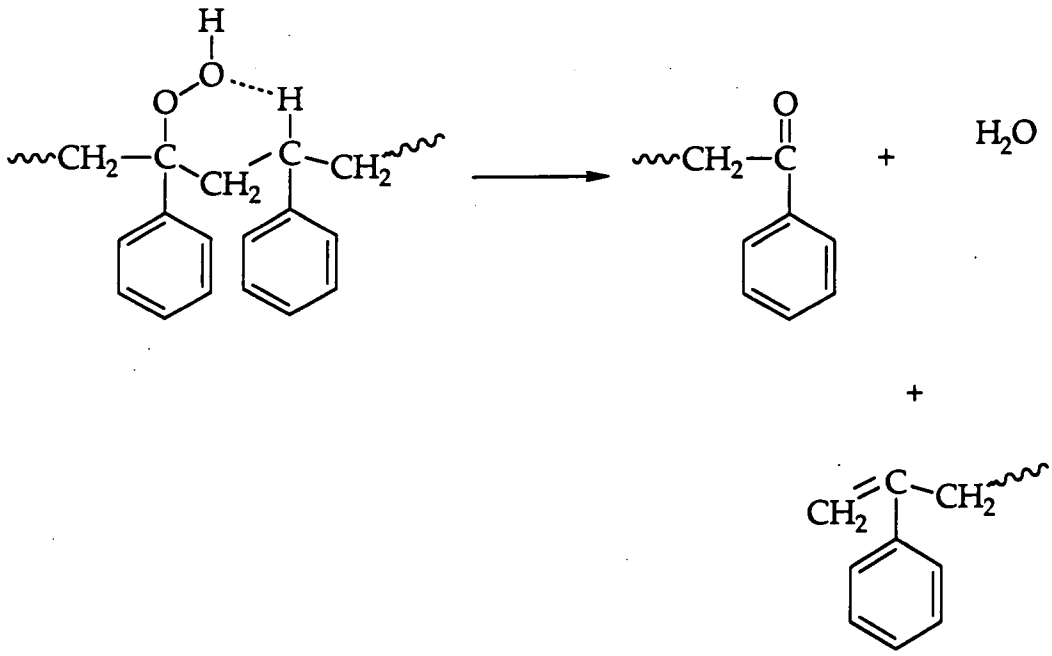

Scheme 4: Water formation via a six-membered transition state[17].

Molecular oxygen adsorbed on the surface of the polymer may react with atomic hydrogen produced during the reaction to give HOO·. This may subsequently react as described in Scheme 2.

3.3 MASS 77 and 78

Benzene, mass 78, and phenyl radicals, mass 77, are detected in abundance during photolysis experiments[7]. The signal intensity profiles of such species is similar to that described for hydrogen evolution (Figure 2). Fragmentation of benzene molecules within the ion source of the quadrupole mass spectrometer also yield peaks at mass 52, 51, and 77 (each with approximately 20% of the mass 78 intensity)[9]. However, the increase in signal strength of mass 77 upon exposure to ultraviolet radiation is greater than mass 78, and cannot, therefore, be attributed to benzene fragmentation in the ion source alone, but must possess a major contribution from desorbing phenyl radicals. Also, mass 77 is not a major fragment in the mass spectrum of polystyrene[18] or polyalkylated benzenes[19]. Hence the phenyl radicals seen here are almost certainly a product of photolysis and photo-oxidation.

Another study detected benzene as a photo-oxidation product[2]. However, other research findings[1] attributed the discovery of benzene in the reaction products to residual solvent or impurities. This was ruled out in our experiments as the amount of benzene evolved was consistent between different experiments under identical conditions but using different polymer samples. Impurities usually differ in concentration for each polymer sample[2].

Evolution of benzene during polystyrene photolysis is consistent with previous theories[20,21]. Photo-excitation of the phenyl ring in the polymer is believed to cause C_6H_5-C bond rupture, thereby creating a phenyl radical. Such phenyl radicals must have limited mobility within the bulk polymer before they form benzene via either hydrogen abstraction from adjacent polymer chains or combination with hydrogen radicals. Alternatively some of these phenyl species may react with macro-radicals in their vicinity. These results are the first direct evidence for this mechanistic description[3,22].

Profiles for masses 77 and 78 are identical during photolysis and photo-oxidation. Comparison of the post irradiation peak profiles for phenyl radicals (mass 77) and molecular benzene (mass 78) reveals that the benzene signal intensity drops much more rapidly than that observed for the phenyl species, Figure 5. Therefore, it seems reasonable to suggest that

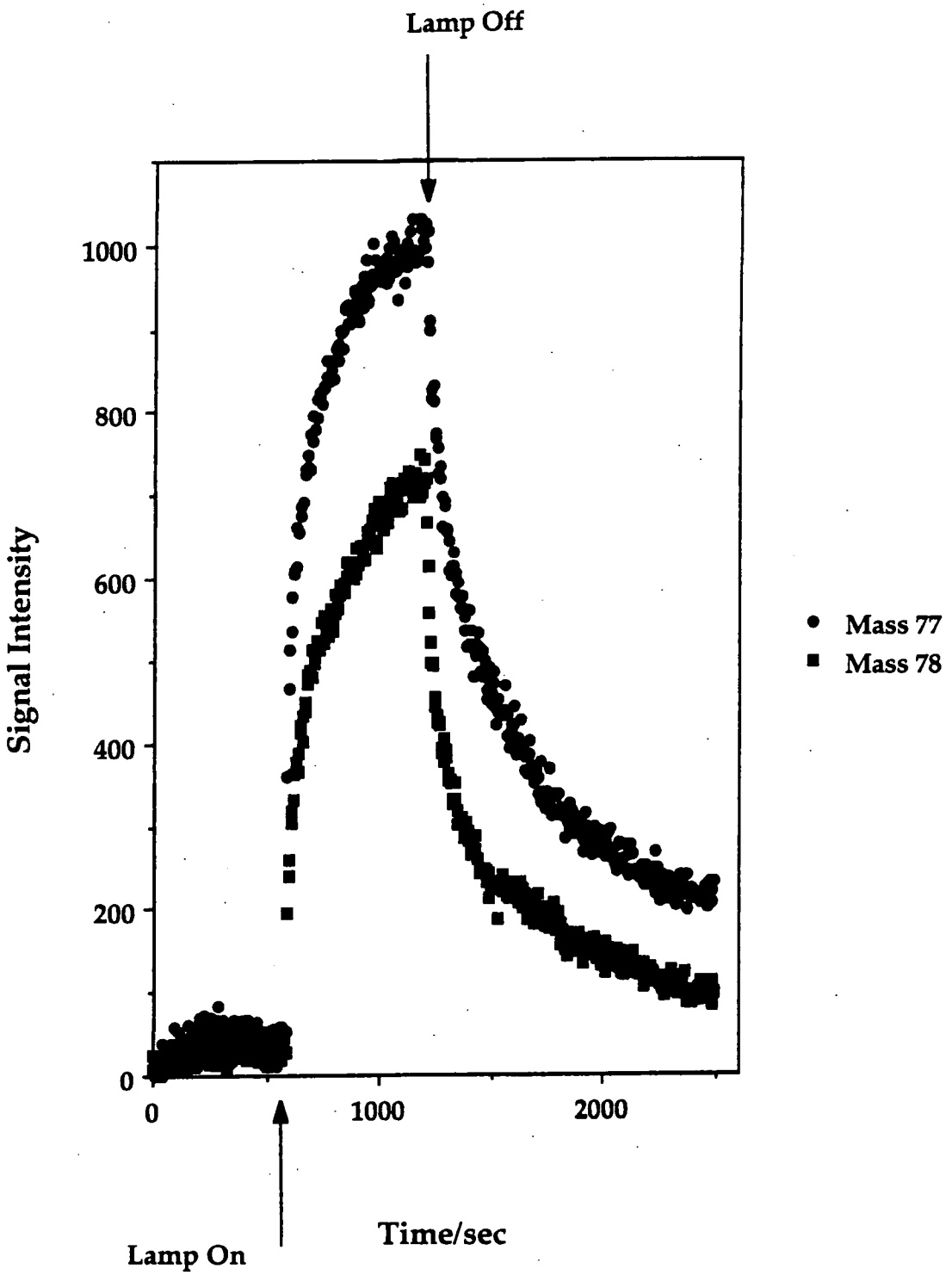

Figure 5: Mass 77 and 78 intensity profiles (before, during, and after UV irradiation) for photolysis.

both combination of phenyl radicals with atomic hydrogen and hydrogen abstraction by the phenyl radicals from neighbouring polymer chains are strongly coupled to the presence of UV.

More intense signals for masses 77 and 78 are observed during photo-oxidation of polystyrene than photolysis, Figures 6 and 7. Photo-oxidation must cause a greater extent of polymer chain break-up than photolysis. This would enable greater vibrational excitation and hence easier release of the phenyl side groups. Abstraction of hydrogen from nearby polymer chains or combination with hydrogen radicals subsequently produces benzene. As previously discussed, molecular hydrogen is also produced at the same time by a similar mechanism. As more benzene is produced during photo-oxidation than photolysis, but less molecular hydrogen is seen in photo-oxidation than photolysis, there must be another factor involved in benzene production during photo-oxidation. Phenyl radicals are much larger than hydrogen radicals and would therefore be trapped in the polymer network to a greater extent once detached from the polymer. This bulkiness would mean that phenyl radicals are in the vicinity of polymer C-H bonds for a longer period of time than hydrogen radicals, and therefore would be more likely to abstract hydrogen. This would imply that the combination of atomic hydrogen with other species is a minor reaction pathway in the photo-oxidation of polystyrene. Trapped benzene gradually escapes after irradiation as seen in the peak profile.

3.4 MASS 91

In the mass spectra of polystyrene mass 91 is usually attributed to the tropyllium ion ($C_7H_7^+$)[6,8,10,11], which is formed in a rearrangement reaction of $C_6H_5CH_2^+$ in the mass spectrometer[19]. Detection of this mass during photon induced reactions of polystyrene must indicate polymer backbone cleavage. Mass 91 is detected in greater abundance during photo-oxidation than during photolysis which is consistent with a greater degree of main chain scission during photo-oxidation, Figure 8.

In these experiments, mass 91 may be produced directly during photolysis, may be a fragment of oligopolystyrenes in the mass spectrometer[18] or may be formed from α branched aromatic hydrocarbons[8,19]. However, fragmentation of styrene, mass 104, in the ion source of a mass spectrometer produces mainly mass 103 (with a third of the intensity of the mass 104 signal)[9], so mass 91 is not a major fragment of styrene, which may be evolved during these reactions. Whichever

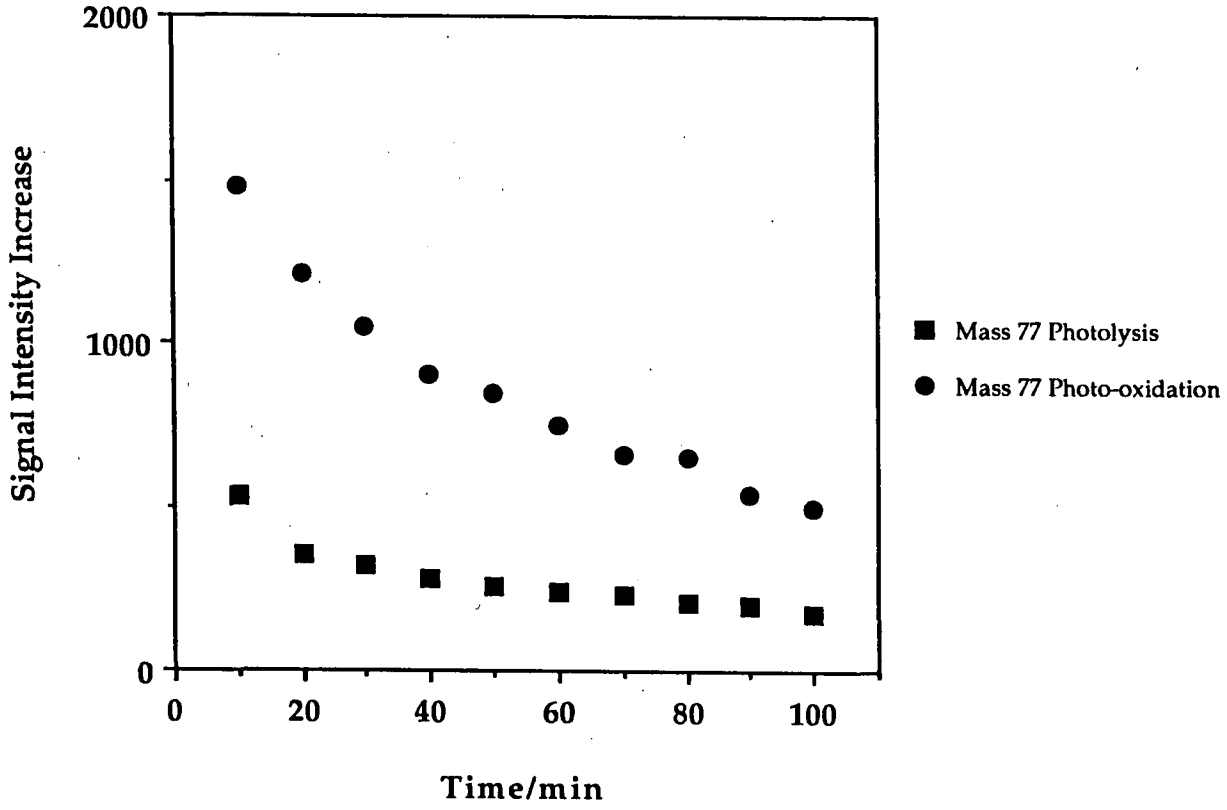

Figure 6: Changes in the mass 77 signal intensity increase as a function of exposure time during photolysis and photo-oxidation.

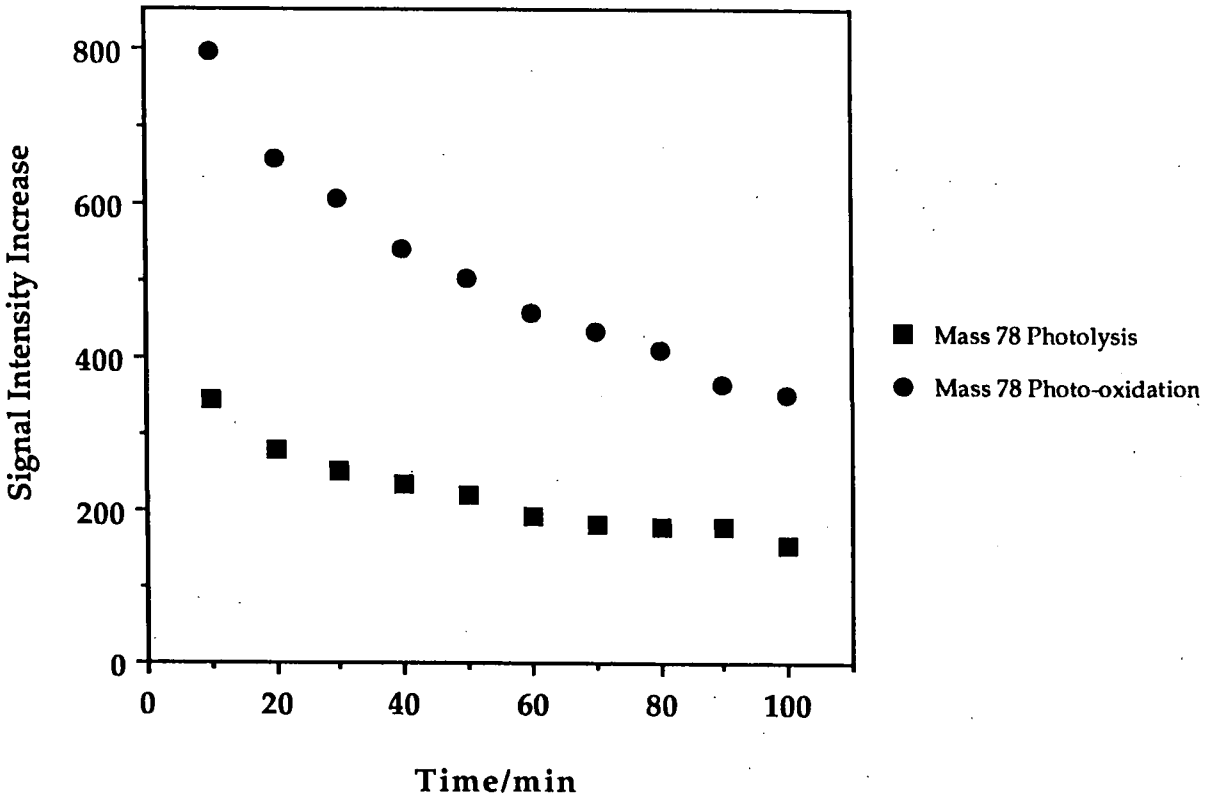

Figure 7: Changes in the mass 78 signal intensity increase as a function of exposure time during photolysis and photo-oxidation.

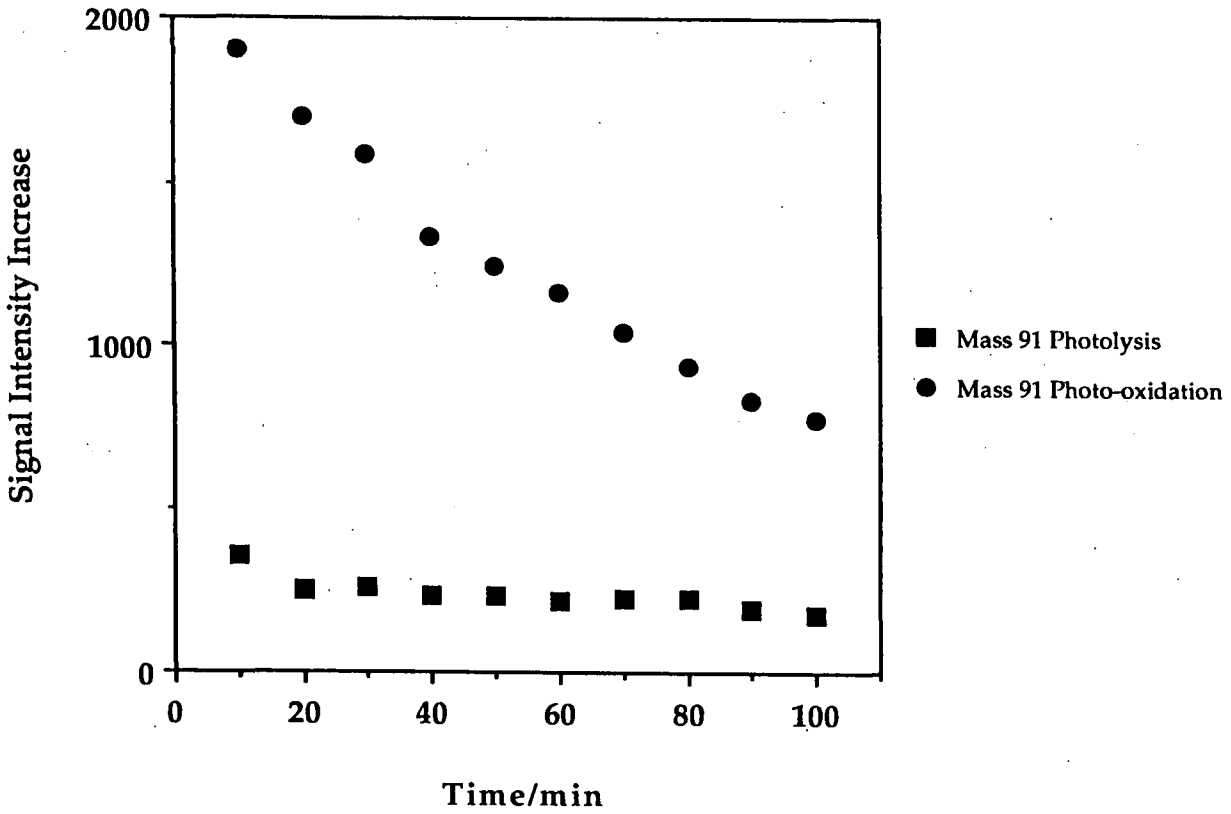

Figure 8: Changes in the mass 91 signal intensity increase as a function of exposure time during photolysis and photo-oxidation.

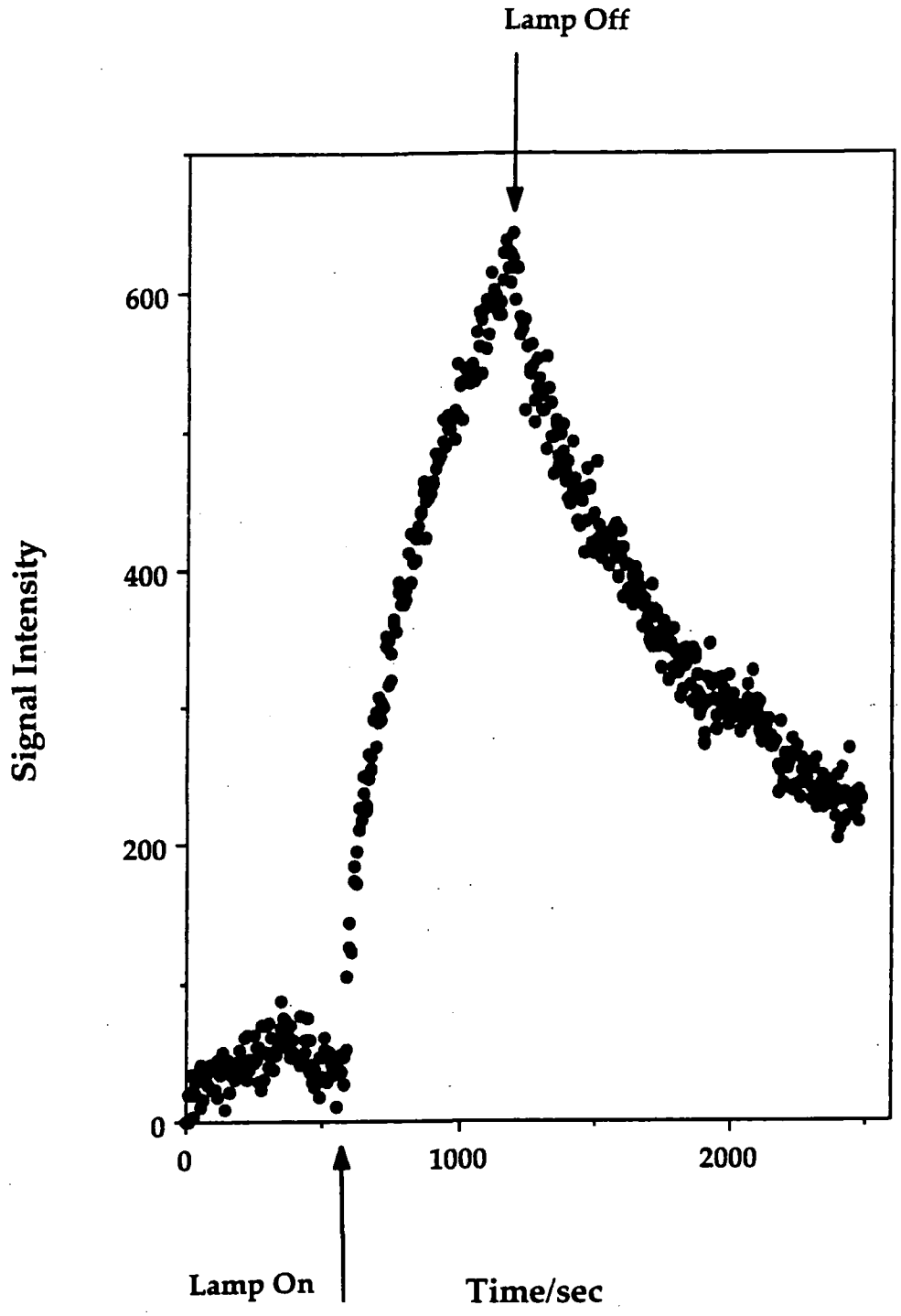

Figure 9: Mass 91 intensity profile (before, during, and after UV irradiation) for photloysis.

mechanism is correct, it is clear that the polystyrene chain is broken during reaction.

The mass profile for 91 is the same during photolysis and photo-oxidation, e.g. Figure 9. Initially the mass signal rises rapidly then gradually continues to increase until UV irradiation is terminated, when the signal very slowly decreases towards the background level. The decrease of the mass 91 signal is slower than in the case of hydrogen, this could be due to mass 91, or the polystyrene fragment that will produce it in the mass spectrometer, being sterically more bulky than hydrogen and therefore taking longer to escape from the polymer.

A previous study of the SIMS spectra of untreated and photo-oxidised polystyrene concluded that cross-linking occured during photo-oxidation and this accounted for the relative decrease of the mass 91 signal in the photo-oxidised sample[6]. The decrease in mass 91 was attributed to crosslinking at carbons α to the phenyl ring.

3.5 MASS 104 and 105

The mass fragments 104 and 105 were evolved from polystyrene with greater intensities during photo-oxidation than photolysis, Figures 10 and 11. The fragments for 104 and 105 arising from photolysis must be C_8H_8[8] and C_8H_9[8] as polystyrene contains no oxygen containing functionalities, and therefore this indicates main chain breaking.

During photo-oxidation, however, these masses may also be due to the oxygenated species C_7H_4O[8] and C_7H_5O[8] which might also arise from extensive breakdown of the polymer structure.

The respective mass profiles for 104 and 105 are identical during photolysis and photo-oxidation. Mass 104 gradually increases upon exposure of the polymer to UV light and upon removal of the light source the intensity of the signal drops quickly and continues to decrease towards the background level in a similar manner to mass 78, e.g. Figure 12. Mass 105, e.g. Figure 13, increases rapidly upon exposure to UV and upon termination of irradiation gradually decreases to the background level. The drop in mass 104 is much faster than that in 105. In comparison to 77 and 78 peak profiles, this infers that mass 104 production is strongly coupled to the presence of UV.

During photolysis styrene, C_8H_8 (mass 104), could be formed by the following retro addition or 'unzipping' reaction[12] Scheme 5:

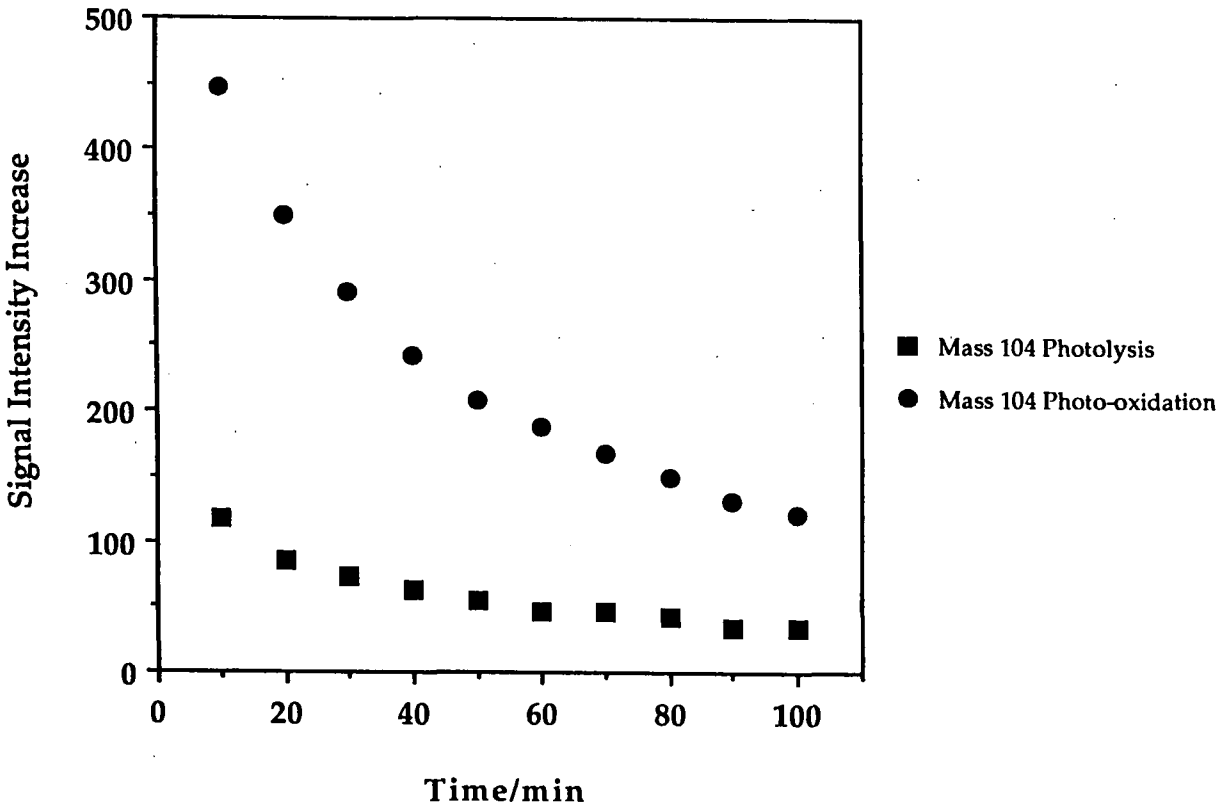

Figure 10: Changes in the mass 104 signal intensity increase as a function of exposure time during photolysis and photo-oxidation.

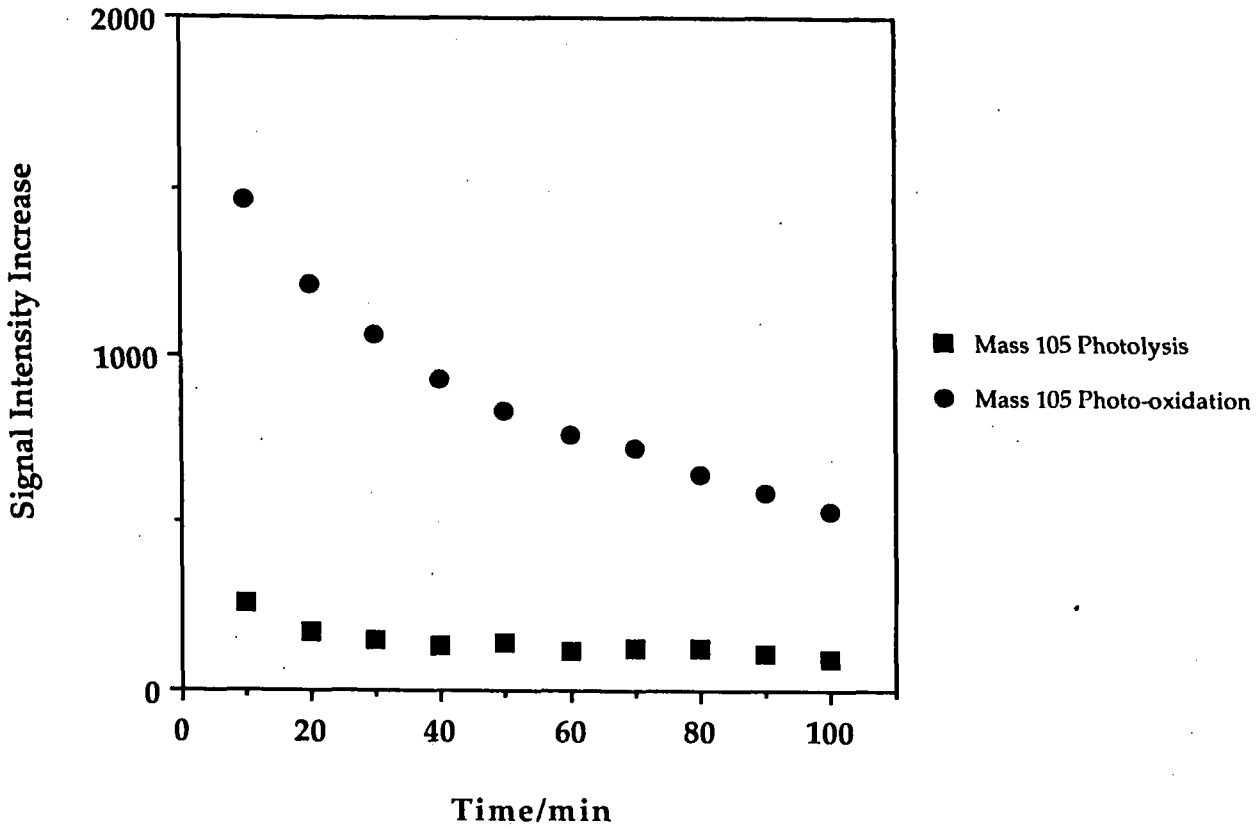

Figure 11: Changes in the mass 105 signal intensity increase as a function of exposure time during photolysis and photo-oxidation.

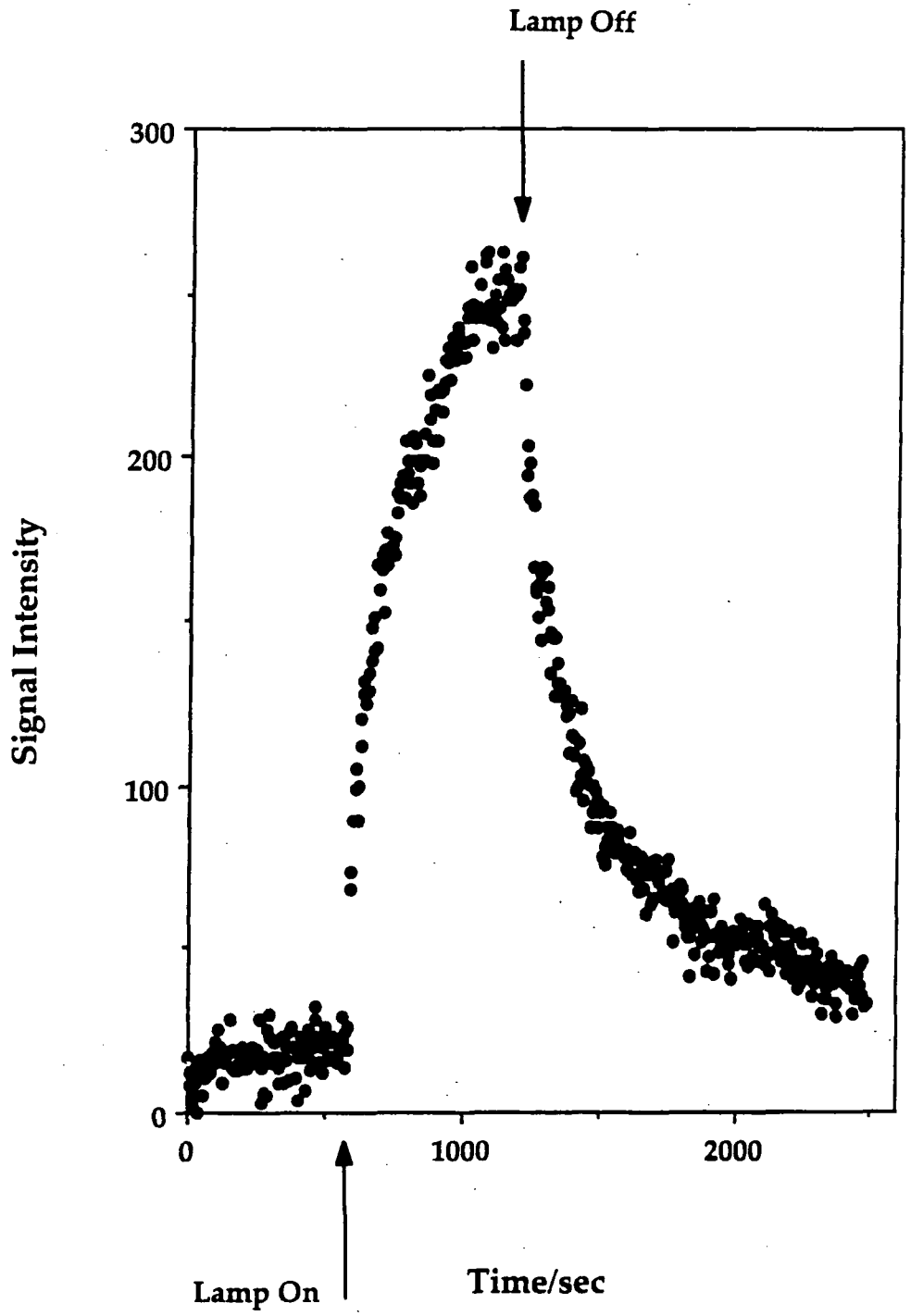

Figure 12: Mass 104 intensity profile (before, during, and after UV irradiation) for photolysis.

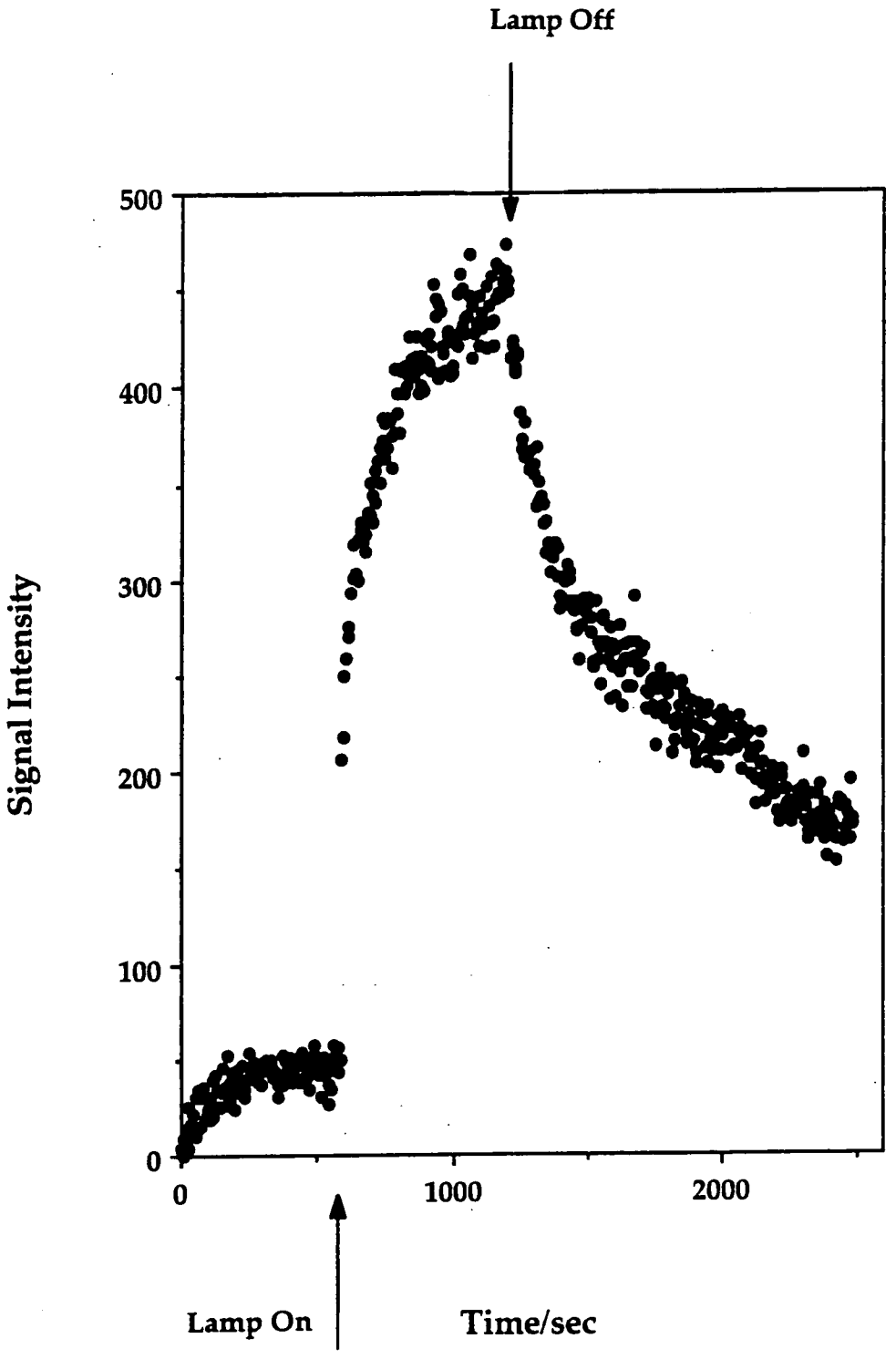

Figure 13: Mass 105 intensity profile (before, during, and after UV irradiation) for photolysis.

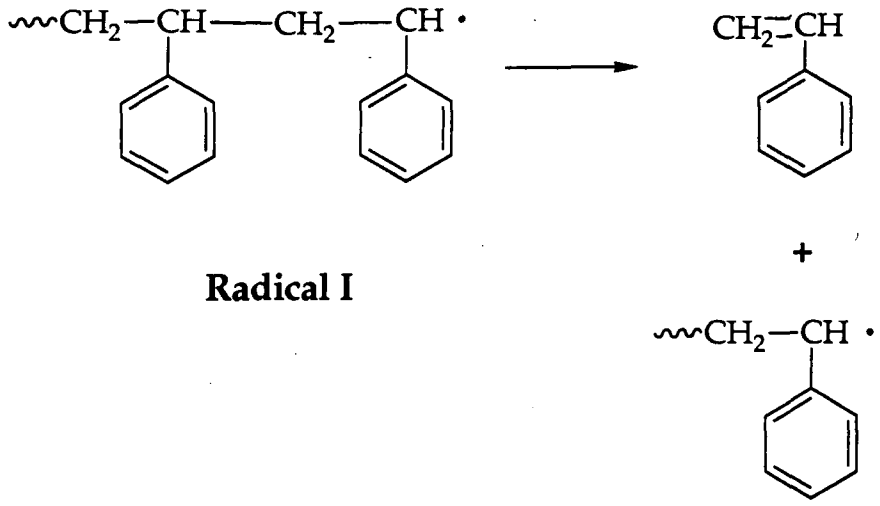

Radical I

Scheme 5: 'Unzipping' of a polystyrene radical to produce styrene[12].

Radical I is produced from polystyrene by intermolecular energy transfer from excited phenyl groups to break the C-C main chain bond[12]. This reaction would also produce primary radicals (see below). Reaction of styrene with atomic hydrogen may give C_8H_9, mass 105, which is a major fragment during SIMS analysis of polystyrene[6,10,11]. Styrene may also be eliminated during photo-oxidation from a primary alkyl chain end radical produced above or by scission of the hydroperoxide radical as seen in Scheme 1.

During photo-oxidation, however, mass 105 is more likely to be C_7H_5O formed by α-cleavage, Norrish type 1, of a chain end carbonyl group[22], Scheme 6:

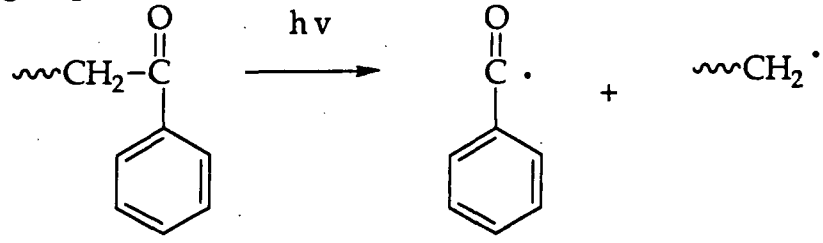

Scheme 6 : Cleavage of a carbonyl end group to give mass 105, C_7H_5O[22].

The alternative decomposition pathway for the carbonyl end group is formation of a phenyl radical and a ketone end group radical[22].

Mass 105 is present in the standard mass spectrometric analysis of polystyrene[18] and is also a common fragment of α branched aromatic hydrocarbons and aromatic ketones[19]. Therefore, these species may be due to fragmentations of larger species in the mass spectrometer, but they still indicate that main chain cleavage has occured. The slow decrease in the

signal after the UV source was shuttered may still be explained as slow escape of bulky species from the subsurface.

The greater amounts of both masses 104 and 105 evolved during photo-oxidation over photolysis indicates a much greater degree of polymer fragmentation by chain scission during photo-oxidation.

3.6 MASS 28

Mass 28 is given off with the greatest intensity increase during photolysis and photo-oxidation of polystyrene. Comparison of results shows that more mass 28 is given off during photo-oxidation, Figure 14.

Mass 28 can be attributed to either carbon monoxide (CO) or C_2H_4. To identify which of these species mass 28 is due to, the fragmentation patterns of CO and C_2H_4 within the ion source of the mass spectrometer must be studied. CO produces mainly fragment 28, whereas C_2H_4 fragments to 28, and also 27 (with approximately a sixth of the intensity of the 28 signal)[9].

Polystyrene does not contain any oxygenated functionalities, therefore during photolysis the only fragment that can be due to mass 28 is C_2H_4. Confirmation of this was seen by studying the fragmentation patterns during photolysis. Mass 27 was observed in abundance. This species must be evolved from backbone scissions, as a result of intermolecular energy transfer from the phenyl rings.

During the photo-oxidation experiments the observed fragmentation patterns indicated that mass 28 was primarily due to CO. Carbon monoxide has been shown to be a major reaction product of polystyrene photo-oxidation in the past[1,2], and is also the major species detected in these experiments. A possible route for formation of CO is cleavage of the fragment formed in Scheme 6 see Scheme 7[23]. It can be seen that this route also produces phenyl radicals.

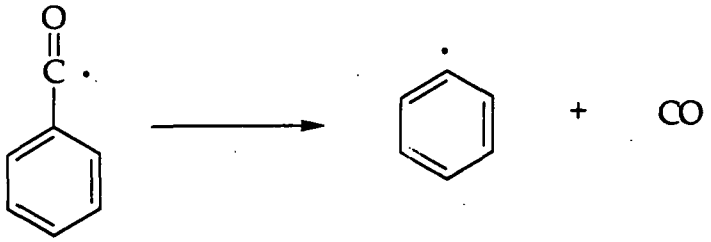

Scheme 7: Mechanism of CO generation during polystyrene photo-oxidation[23].

3.7 MASS 44

Mass 44 was detected during the photolysis of polystyrene, however in the case of photo-oxidation, the relative increase in mass 44 was too small to measure in comparison with the background signal from the reaction chamber. Mass 44 may be due to the species CO_2 or C_3H_8, identification is achieved by studying fragmentation patterns for these molecules; CO_2 gives mainly mass 44 with a main fragment of 28, and C_3H_8 has a main fragment of mass 29[9].

Correlation with these fragmentation patterns indicates that polystyrene mainly gave C_3H_8 during photolysis. The origin of such species is obscure but it seems most likely that they arise from impurities.

3.8 OTHER MASSES

A wide range of hydrocarbon fragments were also emitted from the polystyrene surface during photolysis. These are believed to be produced during extensive break-up of the polymer chain. Masses 41, 43, 55, 57, 69, 97 are all observed in significant amounts and have been previously identified in the SIMS spectra of hydrocarbon polymers, (e.g polyethylene and polypropylene[11]) and are attributed to fragment types C_nH_{2n+1} and C_nH_{2n-1}.

Masses 39 ($C_3H_3^+$), 51 ($C_4H_3^+$), 63 ($C_5H_3^+$), and small amounts of 103 ($CH_2{=}C^+Ph$) and 115 ($C_9H_7^+$ probably a bicyclic aromatic species) are also detected and have previously been reported as fragments in the SIMS spectrum of polystyrene[6,10,11] (as well as the previously mentioned masses 77 and 91).

Masses observed in this work which are not observed during SIMS analysis of hydrocarbon polymers are significant amounts of 67 ($C_5H_7^+$), 53 ($C_4H_5^+$), 81 ($C_6H_9^+$) and smaller quantities of 50 ($C_4H_2^+$), 79 ($C_6H_7^+$), 54 ($C_4H_6^+$), 65 ($C_5H_5^+$), 71 ($C_5H_{11}^+$), 95 ($C_7H_{11}^+$), 70 ($C_5H_{10}^+$), 52 ($C_4H_4^+$), 107 ($C_8H_{11}^+$), 93 ($C_7H_9^+$), 83 ($C_6H_{11}^+$), 109 ($C_8H_{13}^+$), and 76 ($C_6H_4^+$)[8].

During photo-oxidation alternative assignments may be made to include oxygenated species for masses 43 ($C_2H_3O^+$), 55 ($C_3H_3O^+$), 57 ($C_3H_5O^+$), 69 ($C_4H_6O^+$), 103 ($C_5H_9O_2^+$), 81 ($C_5H_5O^+$), 71 ($C_4H_7O^+$), 95 ($C_5H_3O_2^+$), 109 ($C_7H_9O^+$), 107 ($C_4H_7O^+$) and 93 ($C_6H_5O^+$)[8].

Mass 45 ($C_2H_5O^+$)[8] was identified during photolysis and photo-oxidation. There are a number of potential explanations for the origins of this oxygen - containing product during photolysis, these include the photolysis of impurities within the film, or the desorption of absorbed gases from the laboratory atmosphere (although the sample was allowed to outgas

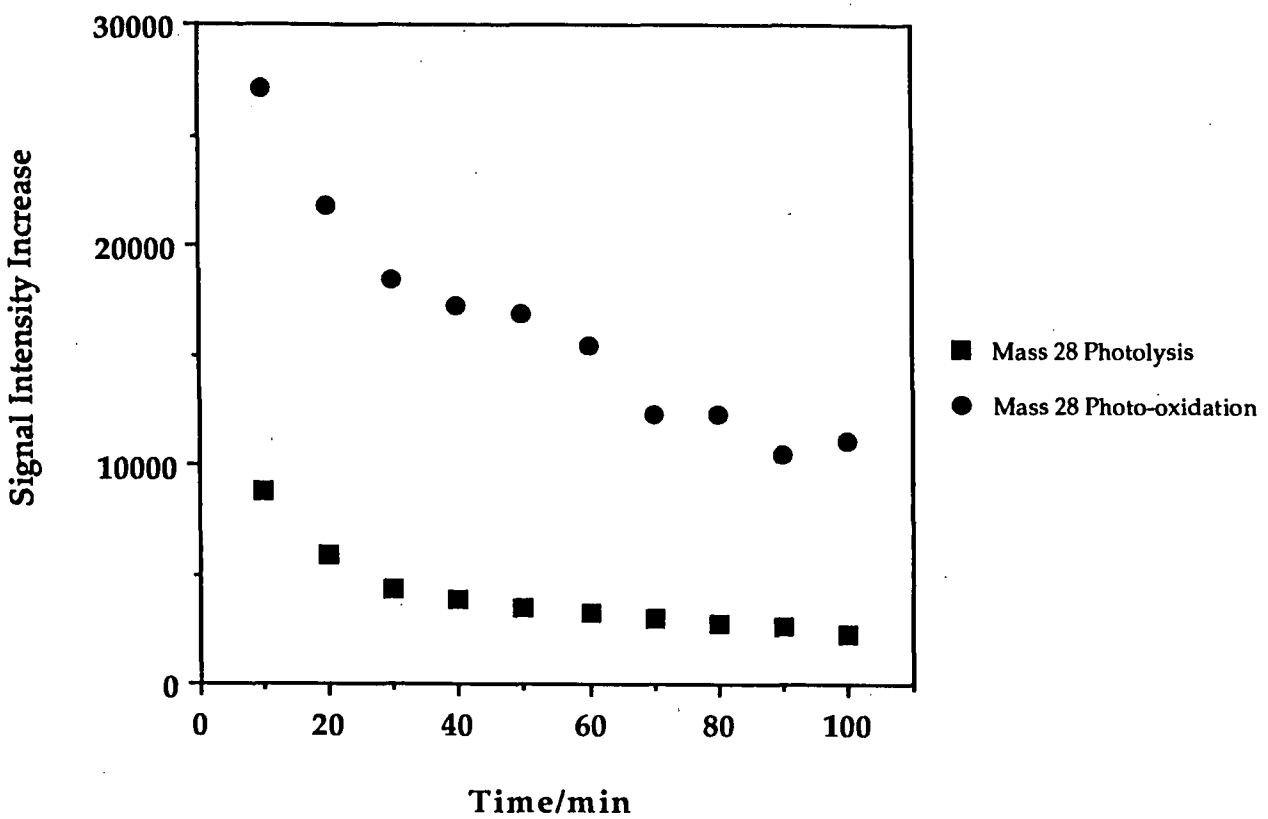

Figure 14: Changes in the mass 28 signal intensity increase as a function of exposure time during photolysis and photo-oxidation.

under ultra high vacuum for several days), or alternatively this could be as consequence of a slight degree of oxidation in air during storage.

4. CONCLUSIONS

Photo-oxidation causes a greater extent of polymer damage by chain scission than photolysis. Absorption of ultraviolet radiation by phenyl rings in polystyrene can cause the direct formation of phenyl radicals and atomic hydrogen by intramolecular energy transfer. The resulting phenyl radicals may subsequently abstract hydrogen radicals from adjacent polymer chains to form benzene. The remaining polymer radicals can undergo cross-linking, or combine with atomic hydrogen. Many phenyl radicals, however do not encounter such hydrogen atoms, and therefore desorb from the polymer surface instead. Atomic hydrogen may subsequently combine to form molecular hydrogen.

Reactions involving polystyrene (PS) photolysis can be summarised as follows:

PS -- UV --> Ph·

PS -- UV --> H· (via intramolecular energy transfer)

Then:

Ph· + PS ---> Benzene + PS· (H· abstraction)

Ph· + H· ---> Benzene

H· + H· ---> H_2

PS· + PS· ---> Crosslinking.

Polystyrene photo-oxidation is a much more complicated process than photolysis. Many different reaction pathways are feasible for production of the masses observed during photo-oxidation

5. REFERENCES

1) B. E. Achhammer, M J Reiney, L. A. Wall + F. W. Reinhart, J. Polym. Sci. 8, (1952), 555.
2) R.B. Fox and L.G. Isaacs, NRL Report, 6284, (1965)
3) N. Grassie and N. A. Weir, J. Appl. Polym. Sci, 9, (1965), 975.
4) N. Grassie and N. A. Weir, J. Appl. Polym. Sci, 9, (1965), 999.
5) L O'Toole, R. D. Short, F. A. Bottino, A. Pollicino and A. Recca, Polymer Deg. and Stab., 38, (1992), 147.
6) L. Quinones and E. A. Schweikert, Surf. and Int. Anal., 15, (1990), 503.
7) R. K. Wells, J. P. S. Badyal and A. Royston, J. Phys. Chem., (in press)
8) R. M. Silverstein, G. C. Bassler and T. C. Morrill, 'Spectrometric Identification of Organic Compounds', 4th Edn., Wiley, 1981.
9) A. Cornu and R. Massot, Compilation of Mass Spectral Data, 2nd Ed., Heyden and Son.
10) G. J. Leggett, J. C. Vickerman, D. Briggs, M. J. Hearn, J. Chem. Soc. Faraday. Trans., 88, (1992), 297
11) D. Briggs, A. Brown and J. C. Vickerman, Handbook of Static Secondary Ion Spectrometry, Wiley, 1989.
12) J. F. Rabek and B. Ranby, J. Polym. Sci., 12, (1974), 273.
13) Personal communication, A. Beeby, Durham University Chemistry Department.
14) 'Kirk - Othmer Encyclopedia of Chemical Technology', 4 th Edn., ed. J. I. Kroschwitz, Wiley, New York.
15) N. Grassie and N.A. Weir, J. Appl. Polym. Sci., 9, (1965), 987.
16) J. G. Calvert and J. N. Pitts, 'Photochemistry', Wiley, 1966.
17) G. Geuskens, D. Baeyens-Volant, G. Delaunois, Q. Lu-Vinh, W. Piret and C. David, Eur. Polym. J., 14, (1978), 291.
18) J. B. Pausch, Anal. Chem., 54, (1982), 90A.
19) H. Budzikiewicz, C. Djerassi and D. H. Williams, 'Mass Spectrometry of Organic Compounds', Holden-Day Inc, 1967.
20) G. Loux and G. Weill, J. Chem. Phys., 61, (1964), 484.
21) N. A. Weir and K. Whiting, Eur. Polym. J., 25, (1989), 291.
22) J. F. McKellar and N.S. Allen, 'Photochemistry of Man-Made Polymers', Applied Science Publishers Ltd, London, 1979.
23) A. Gilbert and J. Baggott, 'Essentials of Molecular Photochemistry', Blackwell Scientific Publications, 1991.

CHAPTER 4

A COMPARISON OF PLASMA OXIDIZED AND PHOTO-OXIDIZED POLYSTYRENE SURFACES

1. INTRODUCTION

Oxidation of polymer surfaces can be used to enhance their susceptibility towards adhesion and wettability[1,2]. Although the extent and stability of such treatments have been widely studied, the precise mechanistic details remain a much debated issue[3,4]. The purpose of this study was to pin-point the subtle differences in oxidative chemistry between photo-oxidized polystyrene surfaces and their plasma oxidized counterparts. For a valid comparison, the experimental parameters have been optimized such that the greatest degree of oxidation is obtained for each treatment[5,6]. This is an important aspect in terms of understanding the activation of polystyrene surfaces for adhesion purposes, since it is not clear to potential end-users whether these treatments are synonymous, or if they impart different functionalities to the surface. Up until now, this choice has been empirical.

The chemical nature of modified polystyrene surfaces has been evaluated by X-ray core level and valence band spectroscopies. These techniques are widely recognized as being complementary tools for the analysis of polymer surfaces[7]. The former is routinely used for locating highly electronegative/positive heteroatoms within a polymeric structure[8]; however it is incapable of distinguishing between different types of hydrocarbon segments belonging to a specific polymeric backbone. In this context, the XPS valence band region can usually provide a much better description[7]. Most polymers possess a unique set of molecular orbitals, and therefore they will exhibit their own characteristic valence band spectra.

An introduction to the processes occuring in an oxygen plasma is given here followed by a review of the plasma oxidation of polystyrene (photo-oxidation has already been covered in Chapter 2) and the XPS - valence band analysis of virgin and modified polymer surfaces.

1.1 GENERAL INTRODUCTION TO OXYGEN PLASMAS.

1.1.1 Theory

Oxygen plasmas consist of singlet molecular oxygen, atomic oxygen, ions, electrons, electromagnetic radiation and neutral species[9]. At low electron energies (<1eV), the principal processes which occur in the plasma are the excitation of rotational and vibrational levels of oxygen in its electronic ground state via inelastic collisions with electrons. With electron energies above 1 eV it is possible to populate higher electronic states.

Chapter 2 gave an introduction to excited molecular oxygen species, these species may also be present in an oxygen plasma, Diagram 1.

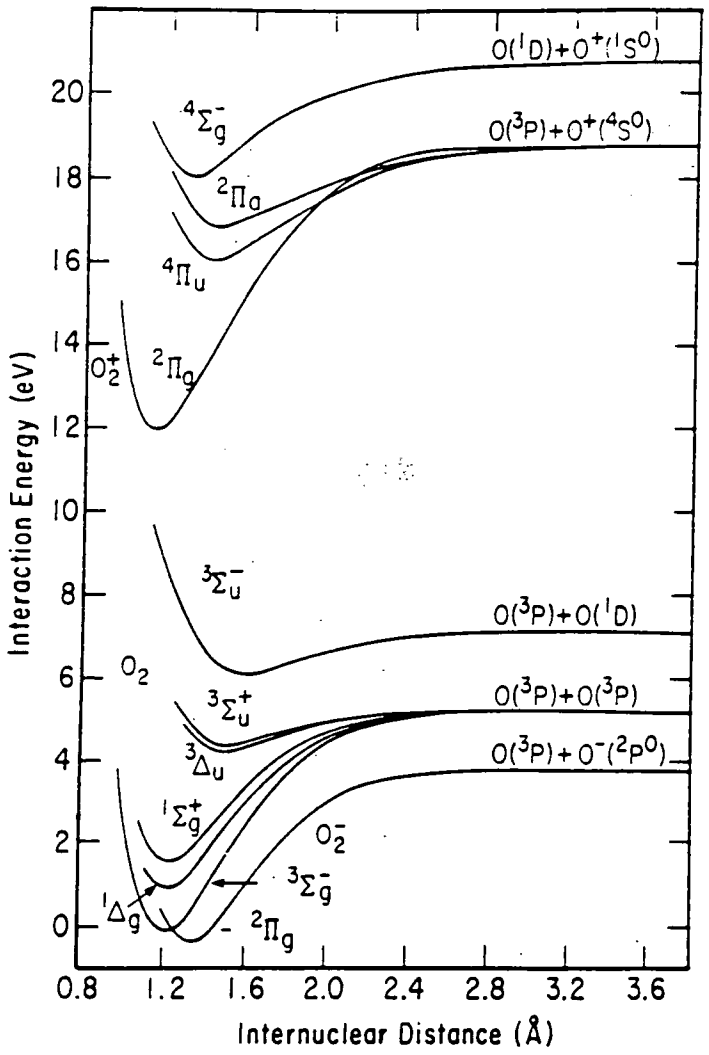

Diagram 1 : Potential energy curves for some states of O_2^-, O_2, and O_2^+.[9]

The main excited states in an oxygen discharge are the $^1\Delta_g$, $^1\Sigma_g^+$, $^3\Delta_u$ and $^3\Sigma_u^+$, all of which dissociate into ground state atoms. Oxygen in the $^1\Delta_g$ state is known as 'singlet' oxygen, this species is particularly long lived and participates in a number of chemical reactions in oxygen discharges. Extensive excitation leads to the ionisation of the oxygen molecule and the formation of O_2^+ in the Π_g state.

Oxygen is also able to form negative ions by direct electron attachment[9]:

$$2O_2 + e^- \longrightarrow O_2^- + O_2$$

the neutral O_2 carries away the attachment energy. Dissociative attachment also occurs:

$$O_2 + e^- \longrightarrow O^- + O\cdot$$

and fragmentation:

$$O_2 + e^- \longrightarrow O^- + O^+ + e^-$$

In an oxygen glow discharge, most of the electromagnetic radiation present is at 1302 Å (130.2 nm) and is due to the relaxation of the first excited state of the oxygen radical[9]. This wavelength is capable of breaking C-C or C-H bonds[10]. Of the organic surface reactions occuring in a plasma reactor, 50% are caused by vacuum ultra-violet photochemistry[10]. The top most surface reactions (10s of Å) are dominated by direct reactions with ions, and free radicals, while the reactions below the surface (100s of Å) are dominated by VUV (vacuum ultra violet) radiation. But both forms of energy transfer result in the formation of the same types of free radicals in the material.

Initial steps in plasma oxidation of simple hydrocarbons involve radical reactions[9]:

$$RH + O\cdot \longrightarrow R'\cdot + R''O\cdot \qquad (1a)$$

$$RH + O\cdot \longrightarrow R\cdot + \cdot OH \qquad (1b)$$

$$RH + 2O\cdot \longrightarrow R\cdot + H\cdot + O_2 \qquad (2)$$

$$RH \xrightarrow{U.V.} R\cdot + H\cdot \qquad (3)$$

Reactions 1 are an oxygen abstraction reactions. Reactions 2 and 3 are bond dissociation reactions driven by the absorption of the dissociation energy of molecular oxygen (5.12 eV) and UV radiation respectively.

Once initiated, ensuing reactions are similar to thermal and photo-chemical oxidation of hydrocarbon polymers. The dominant reactions are[9]:

$$R\cdot + O_2 \longrightarrow ROO\cdot$$

$$ROO\cdot + R'H \longrightarrow ROOH + R'\cdot$$

$$2ROOH \longrightarrow R'{=}O + H_2O + ROO\cdot$$

$$ROOH \longrightarrow RO\cdot + \cdot OH$$

$$RO\cdot + R'H \longrightarrow ROH + R'\cdot$$

$$RH + \cdot OH \longrightarrow R\cdot + H_2O$$

$$R\cdot + HO\cdot \longrightarrow ROH$$

Munro and Beer proved that oxygen radicals are involved in oxygen plasma reactions with polymers (in this case polyethylene)[11], by adding iodine, a free radical scavenger, into the plasma volume. Iodine formed oxidised products in the plasma volume which deposited on the polymer surface and prevented the surface being oxidised. The iodine contaminant was easily removed by washing with simple solvents leaving a relatively unoxidised surface.

Remote plasma treatment involves positioning of the polymer substrate away from the main plasma[12,13]. This reduces the number of reaction pathways and sputter damage is excluded as the substrate is not surrounded by the plasma[12]. Only the longest lived plasma species (micro second lifetimes) are able to reach the sample surface and react. In remote oxygen plasma treatment weak plasma conditions mean a greater control of plasma/polymer interactions[13]. Plasma diagnostics using a Langmuir probe (which can measure electron and ion densities) showed that a very low concentration of cations and no electrons were present in a remote oxygen plasma. Oxygenated functionalities were detected on a polyethylene surface exposed to the remote plasma and the rate of formation of functional groups at the polymer surface was controlled by the low concentration of plasma species at the sample surface.

1.1.2 Effects and Applications

Oxygen plasmas generally cause chain scission and therefore a decrease in the molecular weight of the polymer. The treated surfaces are very polar, completely water wettable and receptive to reactive adhesives.

Most untreated polymers have a water contact angle of 95-60°, however, after plasma treatment with an oxidizing gas the contact angle decreases to less than 40°, with some surfaces being so wettable that the contact angle cannot be measured. Surface energy increases from 25 to 50 $dynescm^{-1}$ for untreated polymers to greater than 73 $dynescm^{-1}$ after plasma treatment.[10]

During adhesion processes it is believed that upon curing the adhesive can covalently bond to the plasma treated interphase by reacting with the surface oxygen species[10].

Excellent wetting characteristics but poor bonding of a polymer surface occurs if the polymer has a thick layer of oil or wax on the surface. This will become wettable upon plasma treatment but upon adhesion there will be no direct interaction between this oil layer and the polymer as a weak boundary layer exists. It is essential in plasma modification to optimise

treatment time for the process. In applications to improve adhesion, over treatment may cause 'ash' to form on the surface and cause a different type of boundary layer. During processing, optimization of the treatment conditions minimises the two problems outlined previously and reduces wasted production time and so increases throughput[10].

Oxygen plasmas are used in the microelectronics industry to remove planarising layers from integrated circuits[14]. Polymers which have a tendency to crosslink in an oxygen plasma, for example polyacrylic acid, are much more suitable for the planarising layer in a multi layer process as they undergo anisotropic etching. Polymers which undergo chain scission and depolymerisation are more likely to produce isotropic (undercut) profiles, Diagram 1.

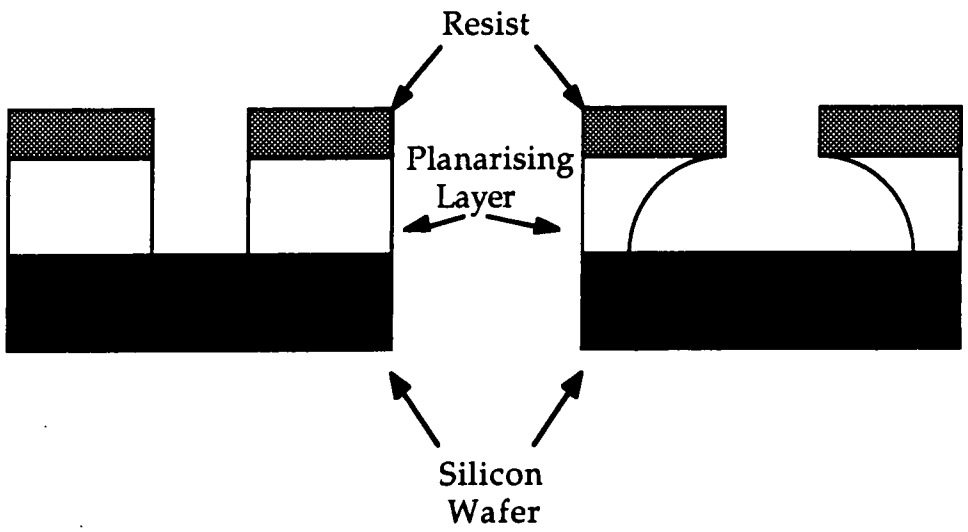

Diagram 1: Anisotropic (left) and isotropic (right) etching.

1.2 LITERATURE REVIEW OF PLASMA OXIDATION OF POLYSTYRENE

Treatment of polystyrene with an oxygen plasma gives incorporation of oxygenated functional groups into the surface[15-18] and loss of aromaticity, noted as a decrease or dissapearance of the π-π^* shake-up satellite in the C(1s) XPS spectrum[16,18]. The surface is thought to eventually reach a steady state where evolution of CO, CO_2 and H_2O and ablation balances renewal of the virgin polymer sublayer[17,18].

Plasma oxidised surfaces usually change with time, the hydrophilic surface becoming hydrophobic as in the untreated surface[4]. This has been observed with polystyrene, and reorientation was postulated to occur by rotation of the oxidised functional groups into the subsurface and also

diffusion of untreated polymer out of the bulk and onto the surface. A more detailed description is given in Chapter 1, section 3.7.4.3.

The etch rate of polystyrene in an oxygen plasma was found to be independent of molecular weight, but dependant upon the temperature of the sample[19]. The etch rate showed a step-like increase in rate when the polymer reached its glass transition temperature[19].

1.2.1 Plasma vs Photo-oxidation of Polystyrene.

A comparison of the plasma oxidation and VUV photo-oxidation of polystyrene was carried out and analysed by core level XPS[18]. A less oxidised surface was observed following oxygen discharge treatment than subsequent to photo-oxidation. This was attributed to the extensive ablation occuring during plasma treatment.

1.3 POLYMER SURFACES STUDIED BY XPS-VALENCE BAND SPECTROSCOPY.

Valence band spectra of simple polymers, such as hydrocarbons, can be found discussed in depth in many good review articles[20-22](See also Appendix 1). Here, for convienience, the valence band region of polyethylene, polypropylene and polystyrene are discussed together. Experiments involving polyethylene are addressed in Chapter 5 where the reason for inclusion of polypropylene in this review will become apparent.

In polyethylene, overlap of the C(2s) orbitals along the polymer backbone results in bonding and anti-bonding molecular orbitals observed at respectively ~ 17 eV and ~ 11 eV in the valence band spectrum[20]. The C(2p) and H(1s) orbitals involved in the C-H bond contribute towards the weak broad structure seen below ~ 10 eV. The relative intensities of these features are dependent upon the ionization cross sections of the various molecular orbitals.

The attachment of a methyl side chain to the main polyethylene backbone introduces an extra feature in the middle of the C(2s)-C(2s) region at ~14.5 eV[20-23].

For polystyrene, the alkyl backbone makes only a minor contribution to the valence band spectrum, since these levels have a density of states with rather broad structure, and the number of such levels is much lower in comparison to those associated with the phenyl groups. As a result, the sharp features of the benzene spectrum predominate[22,24]. Identification of polystyrene with differing tacticities has also been attempted using a

comparison of experimental and theoretical valence band spectra[25]. Isotactic and syndiotactic polystyrene gave subtle differences in the photoelectron spectra in the form of small shoulders on main peaks, however the theoretical simulations were indistinguishable. It was therefore concluded that it would be inaccurate to attribute these changes to the different tacticities when perhaps surface contaminants were responsible.

Any structure which contains oxygen displays a XPS valance band spectrum where O(2s) normally appears at ~25-27 eV, O(2p) electrons associated with oxygen lone pairs in π and non-bonding molecular orbitals, and O(2p)-H(1s), and O(2p)-C(2p) bonds occur below 10 eV[20].

Recent articles focus on more complex systems, for example, elucidation of the electronic structure of poly(etheretherketone) was achieved by comparison with a theoretical simulation of the valence band spectrum and with the spectrum of the model compound bis(4-phenoxyphenyl)methanone[26]. It was found that the spectrum of this compound was virtually identical to that of the polymer, and so it was thought that the ground state of the polymer remains localised with no long range electronic interaction along the chain.

1.3.1 Surface modification.

The first study using the modification of the valence band of a polymer by surface treatment as an analytical probe was the chromic acid etching of polyolefins[27]. The valence band spectrum of polypropylene was little effected by the treatment, but the spectrum for polyethylene was increasingly altered as etching time continued. Modification was seen as a decrease in intensity of the C(2s)-C(2s) band and the subsequent appearance then increase in the O(2s) region. It appears that modification of polyethylene does not alter the surface beyond recognition as the characteristics of the original clean polymer were still observable.

A subsequent experiment on the flame treatment of polyethylene gave the same extent of oxidation as severe chromic acid etching[28]. Valence band spectra mirrored this effect, the basic polymeric unit still visible after modification indicating incomplete alteration of the surface.

The valence states of Ar^+ bombarded polystyrene have been probed using synchrotron radiation[29]. It was found that a treatment of 10^5 ions/cm^2 gave polystyrene a valence band structure approximating to that of amorphous carbon. 'Outgassing' of hydrogen was monitored by a quadrupole mass spectrometer on the deuterated polymer analogue.

Deposition of copper onto poly(ethyleneterephthalate) was followed by synchrotron photoemission to give the valence band spectrum[26]. Valence Effective Hamiltonian, VEH, band structure and Density of Valence State, DOVS, calculations were used to try and understand the features of the spectrum. It was concluded that copper atoms interact with oxygenated functionalities on the polymer surface to form Cu-O-C features at the interface. The metallic state is achieved at low coverages, and at higher coverages Cu atoms bond preferentially to the metal-polymer complex to give clusters.

1.3.1.1 Oxygen plasma treatment.

Burkstrand monitored the plasma oxidation of ABS (acrylonitrile-butadiene-styrene copolymer) and polypropylene through their XPS valence band spectra[30]. The original features of the polymers were still observed after plasma treatment but there was also incorporation of oxygen as seen by the increase in the O(2s) feature in the spectrum.

Gerenser recorded the valence band spectrum of oxygen plasma treated polyethylene[31]. The main C(2s)-C(2s) features could still be seen in the spectrum, and a feature at 5.6eV attributed to the O(2p) lone pair orbital. The valence band spectra were cut off before the O(2s) peak could be observed so limiting the usefulness of the data. The plasma modified surfaces were stable with little or no change after 72 hours in a vacuum chamber, but in the laboratory atmosphere ~ 25% of oxygen incorporation was lost and 1% of nitrogen adsorbed. Angle resolved XPS indicated that there was formation of a hydrocarbon layer on the polymer surface which would account for the apparent loss of oxygen. No explanation is given for the origin of this hydrocarbon layer, but is probably arises due to surface aging. The polymer orients its polar groups into the sub-surface, hence giving the impression of a hydrocarbon overlayer. This type of aging has been detected for polymers in other studies[32].

Briggs et al studied the remote oxygen plasma treatment of polyethylene and polypropylene by XPS valence band spectroscopy before and after treatment[33]. After treatment the original features of the polymer were still visible i.e. the C(2s) features were still apparent, however, additional peaks corresponding to O(2s) and O(2p) (lone pair electrons in a π or non-bonding molecular orbital and O(2p)H(1s) and O(2p) C(2p)) were also observed. This implied that although plasma treatment had caused oxidation of the polymer there were still enough runs of undamaged polymer chain to give the characteristic polymer peaks in the spectrum.

Remote nitrogen plasma treatment also retained enough of the original fingerprint XPS-VB character so that identification of the polymer was possible[33]. For polyethylene, however, a weak additional band at ~ 14.5 eV was also present. This was attributed to creation of some polymeric side chains by cross linking. Angle resolved studies showed the feature was more pronounced at shallower sampling depths.

It was thought that oxygen plasma treatment of polymers resulted in runs of the original polymer interspaced by C-O, C=O and O-C=O groups. Nitrogen plasma treatment produced the same oxygenated functionalities as in the oxygen plasma case together with C-N (amines), C-N (imines), C≡N (nitriles) and O=C-N (amides).

2. EXPERIMENTAL

Polystyrene (Tricite) film was cleaned in an ultrasonic bath with isopropyl alcohol and subsequently dried in air. Research grade quality oxygen (BOC) was used without any further purification.

Plasma oxidation was carried out in a cylindrical glass reactor which was inductively coupled to a 13.56 MHz RF generator via an externally wound copper coil[34]. A strip of polymer was located in the glow region i.e. in the centre of the coil. The reaction vessel was initially evacuated by a two stage rotary pump to a base pressure of better than 4×10^{-3} Torr, then oxygen was passed through the chamber at a pressure of 0.2 Torr for 10 mins. Subsequently the plasma was ignited and left running for 5 mins, longer periods resulted in no further changes at the polymer surface as measured by XPS.

A glass reactor with a quartz port (cut off wavelength 180 - 200 nm) was used for the photo-oxidation experiments. The UV source was an Oriel 200 W low pressure Hg-Xe arc lamp operating at 100 W. This gave a strong line spectrum in the 240 to 600 nm region. Polystyrene film was positioned facing the quartz window, and a high flow of oxygen was passed through the reactor at atmospheric pressure. This was maintained before, during, and after UV exposure. The limiting O(1s) : C(1s) ratio was achieved after 80 mins of UV irradiation.

High resolution core level and valence region spectra were taken on a Kratos AXIS HS instrument in the development laboratories of Kratos at Manchester. This state-of-the-art instrument was equipped with a monochromatic Al Kα (1486.6 eV) X-ray source and a novel magnetic immersion lens system - giving high resolution and high sensitivity. The

X- ray power was limited to ~240 W (14 kV, 17 mA) to limit radiation damage. Uniform charge neutralization with little energy shift was effected with a low energy electron source. These measurements were taken with the surface normal of the sample being aligned with the axis of the electron spectrometer. All binding energies are referenced to the hydrocarbon component (-$\underline{C}_xH_y$-) at 285.0 eV[35], and the instrumentally determined sensitivity factors are such that for unit stoichiometry, the C(1s) : O(1s) intensity ratio is ~ 0.36.

3. RESULTS

Figures 1(a) and 2(a) show the XPS C(1s) core level and valence band spectra of clean polystyrene respectively. The major feature in the C(1s) core-level region is the hydrocarbon component at 285.0 eV; an additional satellite structure at ~291.6 eV is also apparent, which arises from low energy π-π^* shake-up transitions accompanying core level ionization[3]. The alkyl backbone in polystyrene makes only a minor contribution to the XPS valence band region, since the density of states for these levels spans a rather broad structure, and the number of such levels is much lower in comparison to those associated with the phenyl groups. As a result, the sharp features analagous to the benzene spectrum predominate[20,24].

Polystyrene readily undergoes oxidation, this reactivity may be attributed to the fact that this polymer contains phenyl centres; for instance these aromatic rings can act as chromophores leading to photo-oxidation[18]. Detailed chemical information about the modified polymer surfaces was obtained by fitting the C(1s) XPS spectra to a range of carbon functionalities, Figure 1(b) + (c) : carbon adjacent to a carboxylate group ($\underline{C}$-CO_2 ~ 285.7 eV), carbon singly bonded to one oxygen atom ($\underline{C}$-O ~286.6 eV), carbon singly bonded to two oxygen atoms or carbon doubly bonded to one oxygen atom (O-$\underline{C}$-O or $\underline{C}$=O ~287.9 eV), carboxylate groups (O-$\underline{C}$=O ~289.0 eV), and a peak at ~290.4 eV perhaps due to carbonate carbons (O-$\underline{C}$O-O)[36]. Loss of aromaticity at the polystyrene surface could be monitored by the attenuation in intensity of the π–π^* shake-up satellite. On comparing the C(1s) spectra of photo-oxidized and plasma-oxidized polystyrene, it is evident that the former treatment leaves a much greater proportion of -$\underline{C}O_2$- functionalities at the surface. Furthermore the O(1s) : C(1s) ratio was found to be 0.38 after photo-oxidation, whereas it was only 0.27 following exposure to an oxygen glow discharge. A greater extent of oxygen incorporation after photo-

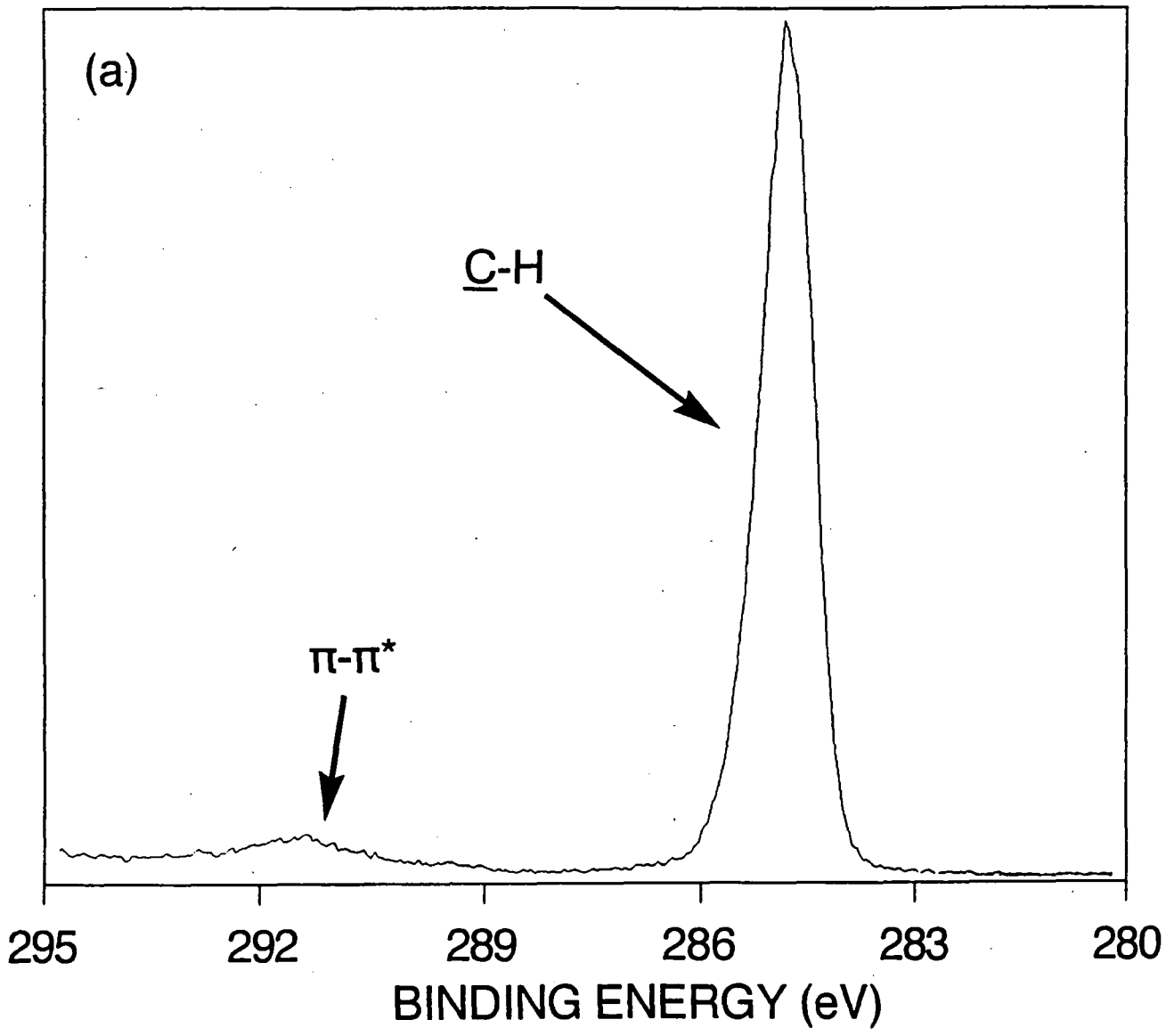

Figure 1a: XPS C(1s) region of clean polystyrene.

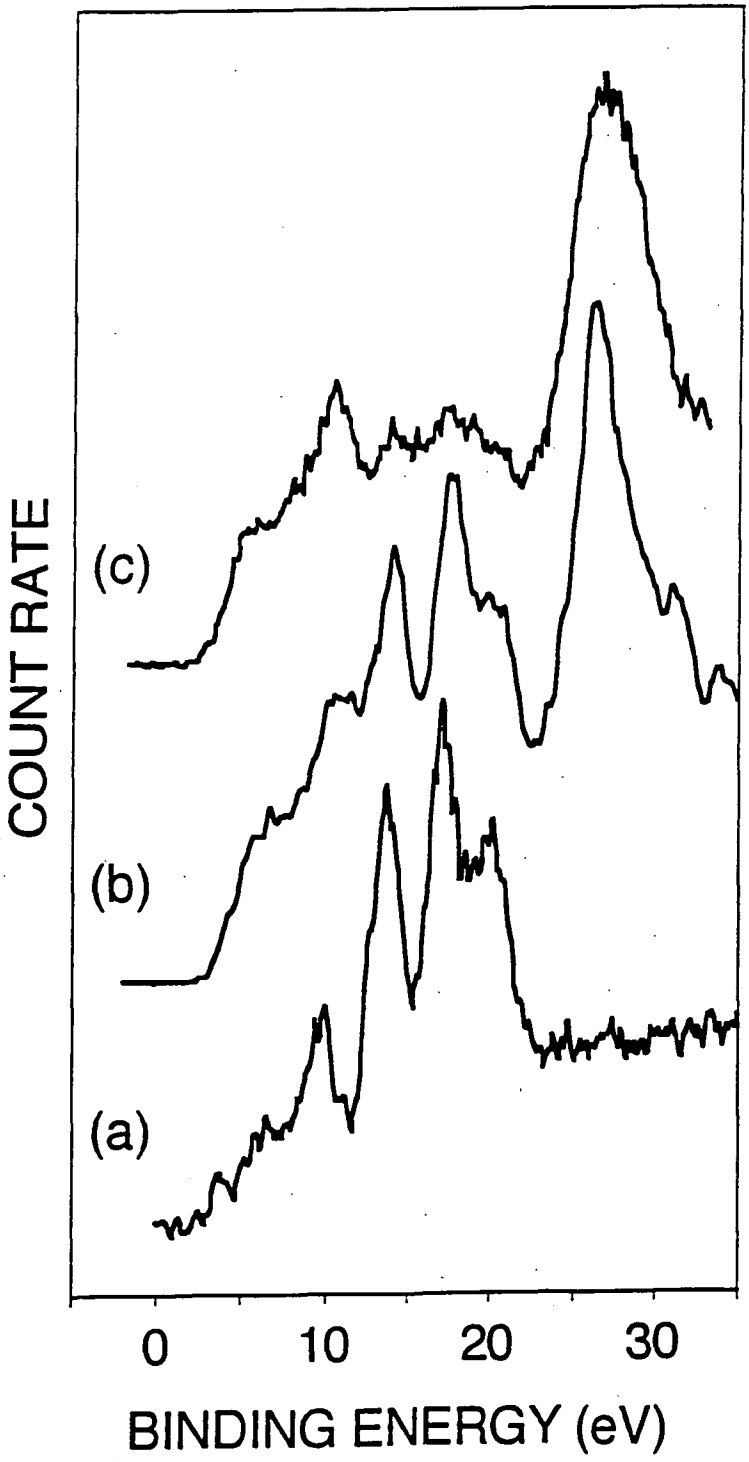

Figure 2: XPS valence band spectra of: (a) clean polystyrene; (b) 1W plasma oxidized polystyrene; and (c) photo-oxidized polystyrene.

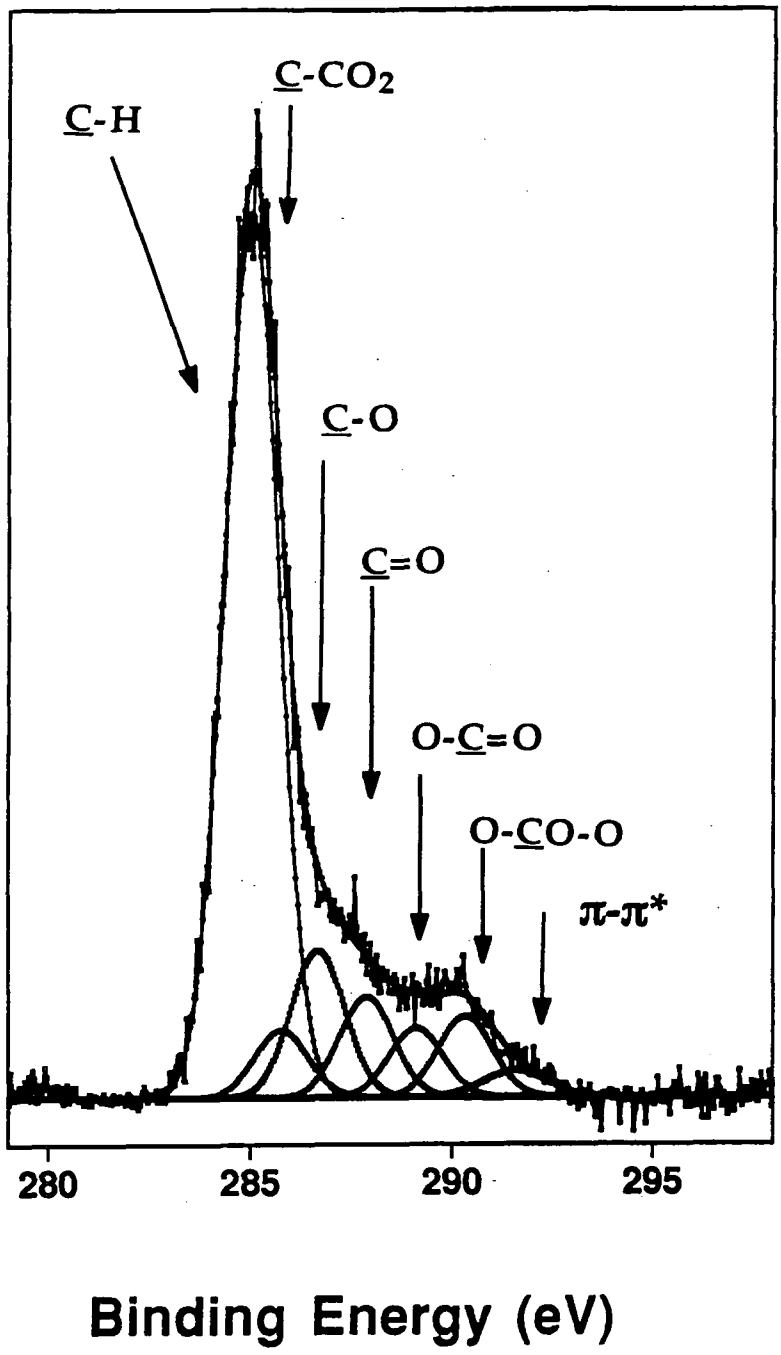

Figure 1b: XPS C(1s) region of 1W plasma oxidized polystyrene.

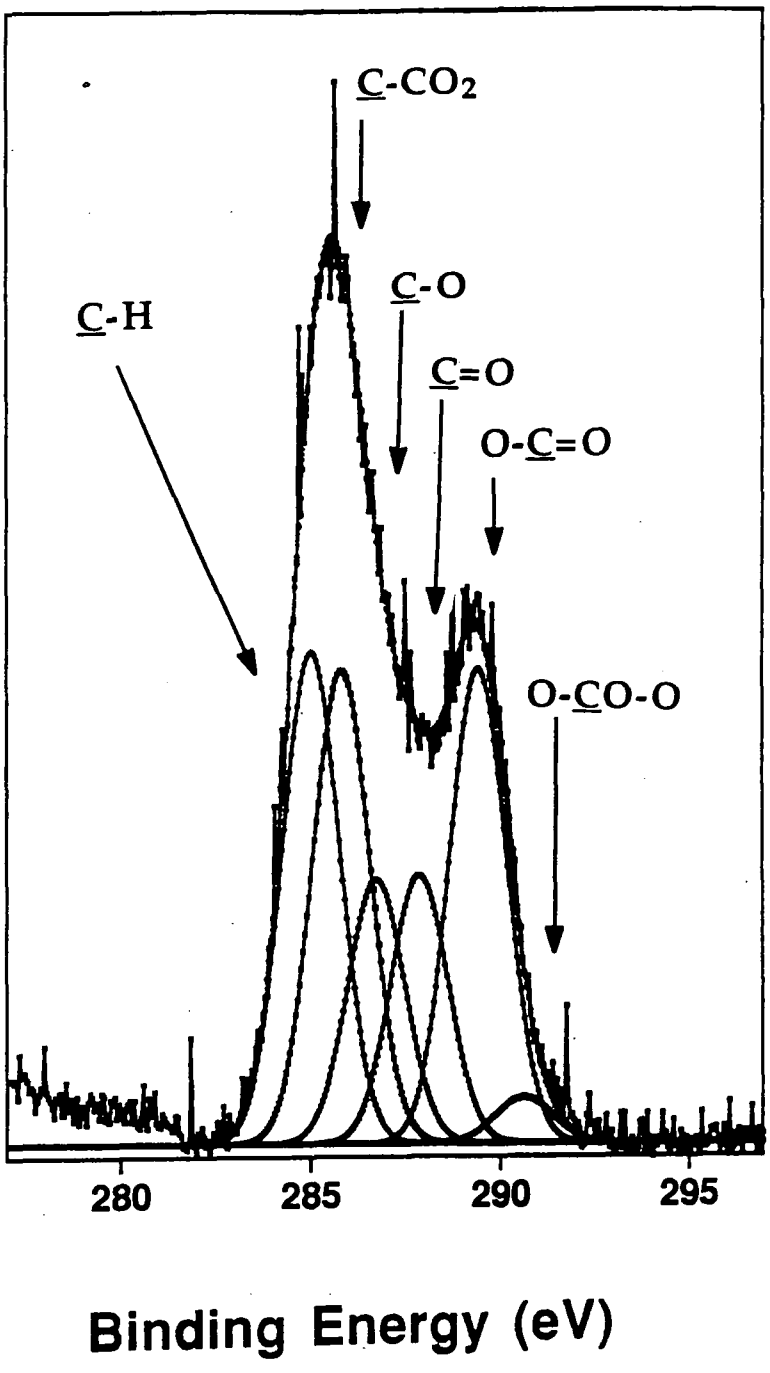

Figure 1c: XPS C(1s) region of photo-oxidized polystyrene.

oxidation than after plasma oxidation is consistent with previous studies by Shard and Badyal[18].

The valence band spectra offer a deeper insight into the extent of disruption of the polystyrene structure following surface oxidation. Polystyrene valence band features are not clearly evident for the photo-oxidized surface and, if present, only exists in low abundance. This implies that most of the phenyl centres have undergone some reaction of modification during UV irradiation in the presence of oxygen. In marked contrast to this behaviour, the characteristic phenyl ring features are clearly visible for the plasma oxidized surface. The C(1s) π-π^* shake-up satellite mirrors the aforementioned trends, however these signal intensities are much weaker in comparison, and also overlap to some extent with the C(1s) binding energy for a signal at ~290.4 eV possibly associated with carbonate species (O-CO-O). O(2s) photoelectrons usually appear at a binding energy of around 25-27 eV ; whereas O(2p) electrons from oxygen lone pairs in π and non-bonding molecular orbitals, and O(2p)-H(1s), and O(2p)-C(2p) bonds occur below 10 eV[20]. A significant amount of O(2s) is clearly evident for both types of oxidized surface.

4. DISCUSSION

One of the merits of studying XPS rather than UPS valence band spectra is that in XPS spectra the relative photo-ionization cross-sections of molecular orbitals with major 2s character are greater than their 2p counterparts[22]. This is of a significant benefit, since the 2s bands are much easier to interpret than the corresponding 2p features[20]. The C(2s)-C(2s) region can be used as a fingerprint for the molecular orbitals of a specific polymer.

In the case of polystyrene, reaction at the phenyl centres can cause an extensive breakdown of the parent polymer and a high degree of oxidation[37]. This is clearly evident from the valence band spectra of the treated surfaces. In these studies, photo-oxidation has been shown to be more disruptive towards the polystyrene surface than plasma oxidation. In the former case, it is the phenyl centres which strongly absorb in the UV region and therefore subsequently undergo reaction[38]. Consecutive oxidation steps will all converge on the eventual desorption of CO_2 gas, this is consistent with the intense signal in the C(1s) spectra due to the carbon bonded to two oxygens.

A pure oxygen plasma is known to comprise of ions, atoms, ozone, and metastables of atomic and molecular oxygen, as well as electrons and a broad electromagnetic spectrum[39]. Therefore in addition to photo-oxidation taking place at the surface, there will also be a variety of concurrent ablative processes occurring. The net outcome of these competing degradation pathways is a less oxidized surface.

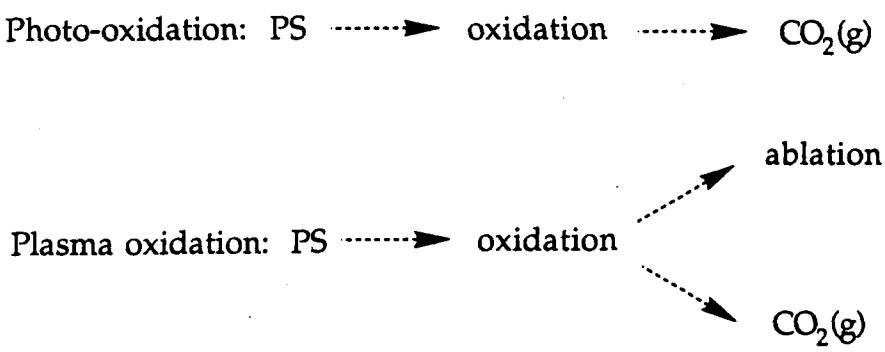

5. CONCLUSIONS

The apparent paradox of a more reactive oxygen glow discharge generating a less oxidized surface can be attributed to the inherent sputtering characteristics of a plasma, which continuously unveils fresh polystyrene substrate. Whereas during straightforward short wavelength UV photo-oxidation, all reaction pathways culminate in the eventual desorption of carbon dioxide and water.

6. REFERENCES

1) J.M. Burkstrand; J. Vac. Sci. Technol., 15, (1978), 223.
2) W.L. Wade; R.J. Mammone; and M. Binder; J. Appl. Polym. Sci., 43, (1991), 1589.
3) D.T. Clark and A. Dilks; J. Polym. Sci. Polym. Chem. Edn., 15, (1977), 15.
4) M. Morra; E. Occhiello; F. Garbassi; D. Johnson and P. Humphrey; Appl. Surf. Sci. , 47, (1991), 235.
5) R.K. Wells and J.P.S. Badyal; J. Polym. Sci. Polym. Chem. Edn.,30, (1992), 2677.
6) R.K. Wells; I.W. Drummond; K.S. Robinson; F.J. Street; and J.P.S. Badyal; J. Adhes. Sci. Tech., 7, (1993), 1129.
7) J.J. Pireaux; J. Riga; P. Boulanger; P. Snauwaert; Y. Novis; M. Chtaib; C. Gregoire; F. Fally; E. Beelen; R. Caudano; and J.J. Verbist; J. Electr. Spectr. and Rel. Phen., 52, (1990), 423.
8) D.T. Clark and D. Shuttleworth; J. Polym. Sci. Polym. Chem. Ed., 18, (1980), 27.
9) M. Hudis in 'Techniques and Applications of Plasma Chemistry' ed. J. R. Hollahan and A. T. Bell, Wiley, 1974, Chapter 3
10) E. M. Liston, J. Adh., 30, (1989), 199.
11) H. S. Munro and H. Beer, Polymer Comm., 27, (1986), 79.
12) R. Foerch, N. S. McIntyre and D. H. Hunter, J. Polym. Sci., Polym. Chem. Edn., 28, (1990), 193.
13) J. Behnisch, A. Hollander, and H. Zimmerman, J. Appl. Polym. Sci., 49, (1993), 117.
14) F. D. Egitto, V. Vukanovic and G. N. Taylor in 'Plasma Deposition, Treatment and Etching of Polymers', Academic Press, 1990, Chapter 5.
15) I. Tepermeister and H. H. Swain, J. Vac. Sci + Technol., 10, (1992), 3149.
16) P. M. Triolo and J. D. Andrade, J. Biomed. Mat. Res., 17, (1983), 129.
17) D. T. Clark, A. Dilks, and D. Shuttleworth in 'Polymer Surfaces', ed. D. T. Clark and W. J. Feast, Wiley, 1978, Chapter 9.
18) A. G. Shard and J. P. S. Badyal, J. Phys. Chem., 95, (1991), 9436.
19) O. Joubert, P. Paniez, M. Pons and J, Pelletier, J. Appl. Phys., 70, (1991), 997.
20) J.J. Pireaux; J. Riga and J.J. Verbist in: 'Photon, Electron and Ion Probes for Polymer Structure and Properties', D.W. Dwight; T.J. Favish and H.R. Thomas; (Eds) ACS Symposium Series 162, (1981), 169-201.
21) K. Seki in Optical Techniques to Characterize Polymer Systems, ed. by H. Bassler, p115, Elsevier, 1989.
22) W.R. Salanek; CRC Crit. Rev. Solid State Mater. Sci., 12, (1985), 267.

23) G. Beamson and D. Briggs, 'High Resolution XPS of Organic Polymers - The Scienta ESCA300 Database', Wiley, 1992.
24) A. Chilkoti; D. Castner; and B.D. Ratner; Appl. Spectros., 45, (1991), 209.
25) E. Orti, J.L. Bredas, J.J. Pireaux, N. Ishihara, J. Elect. Spect. Rel. Phenom., 52, (1990), 551.
26) R. Lazzaroni, N. Sato, W.R. Salaneck, M.C. Dos Santos, L.J. Bredas, B. Tooze, D.T. Clark, Chem. Phys. Lett., 175, (1990), 175.
27) D. Briggs, D.M. Brewis, M.B. Konieczo, J. Mat. Sci, 11, (1976), 1270.
28) D. Briggs, D.M. Brewis, M.B. Konieczo, J. Mat. Sci, 14, (1979), 1344.
29) A. Terrasi, G. Foti, Y. Hwu, G. Margaritondo, J. Appl. Phys., 70, (1991), 1885.
30) J. Burkstrand J. Vac. Sci. and Technol., 15, (1978), 223.
31) L. J. Gerenser, J. Adh. Sci and Technol., 1, (1987), 303.
32) M. Morra, E. Occhiello, F. Garbassi in 'Metallised Plastics II' ed. K. Mittal, Plenum, NY, 1991, p363.
33) R. Foerch, G. Beamson, D. Briggs, Surf. and Int. Anal., 17, (1991), 842.
34) A.G. Shard; H.S. Munro and J.P.S. Badyal; Polym. Commun., 32, (1991), 152.
35) G. Johansson; J. Hedman; A. Berndtsson; M. Klasson and R. Nilsson; J. Electron Spectr., 2, (1973), 295.
36) D.T. Clark and A. Dilks; J. Polym. Sci. Polym. Chem. Edn., 17, (1979), 957.
37) A.G. Shard and J.P.S. Badyal; Macromol., 25, (1992), 2053.
38) J. F. Rabek and B. Ranby; J. Polym. Sci. Polym. Chem. Edn. 12, (1974), 273.
39) J. R. Hollahan; A. T. Bell, Eds.; 'Techniques and Applications of Plasma Chemistry'; Wiley: New York, (1974).

CHAPTER 5

A COMPARISON OF THE PLASMA OXIDATION OF POLYSTYRENE AND POLYETHYLENE

1. INTRODUCTION

Surface modification by glow discharge treatment is a useful means for increasing the surface energy of polymers and improving their adhesion properties[1,2]. Plasma oxidation, as discussed previously, is a complex process in which degradation of the substrate and reaction with ions, atoms, ozone, and metastables of atomic and molecular oxygen, as well as electrons and a broad electromagnetic spectrum occurs. Investigation by surface-sensitive techniques such as X-ray photoelectron spectroscopy (XPS)[3] and secondary ion mass spectrometry (SIMS) [4,5] have revealed that the extent of reaction and the stability of the modified surface are critically dependent upon glow discharge characteristics (e.g. reactor configuration, electromagnetic excitation frequency, substrate location, etc.). However, a very poor understanding exists concerning exactly what occurs during the exposure of a polymer substrate to an oxygen glow discharge, and how the surface subsequently behaves during ageing[6]. In this chapter, we compare the relative reactivities of polyethylene and polystyrene towards an oxygen plasma under identical experimental conditions. The surface chemistry has been monitored by X-ray core level and valence band spectroscopies; these techniques are widely recognised as being complementary tools for the surface analysis of polymers[7]. The former is routinely used for determining the presence of heteroatoms, elemental compositions are readily established and, in more favourable cases, it can give more detailed structural information within a polymeric structure[8]. The XPS valence band region, in favourable cases, provides detailed information about structure and bonding from a different perspective[7]. Often, the valence electronic levels can serve as a fingerprint for a specific polymeric structure. In this study both regions of the spectra have been used to interpret the chemistry observed.

A comprehensive review of polystyrene plasma oxidation was given in the previous chapter, the details of plasma oxidation of polyethylene were also briefly discussed as were the valence band analyses of these polymers.

Below, a summary is given of the main points of interest for polyethylene plasma oxidation and other important features are introduced, such as ageing of plasma oxidised polyethylene and polystyrene and comparisons of the extent of oxidation for these polymers.

1.1 PLASMA OXIDATION OF POLYETHYLENE

Plasma oxidation of polyethylene introduces oxygenated functional groups onto the polymer surface[9-16]. In some cases it has been shown that the polymer structure is not fully destroyed following plasma oxidation, as the features of the polymer valence bands are still visible by XPS-valence band spectroscopy[13,17].

1.2 AGEING

1.2.1 Polyethylene

Monitoring of water contact angles on a polymer surface has shown that oxygen plasma treated polyethylene undergoes some degree of hydrophobic recovery upon ageing, however, the original contact angle of untreated polymer is not usually reached[18]. This recovery process was not detected by monitoring the XPS O(1s) : C(1s) ratios, because of the larger sampling depth of this technique[18], therefore the recovery reaction must be very surface sensitive.

Oxidation of polyethylene using an $^{18}O_2$ plasma enabled the analysis of the surface by Static SIMS[18]. The inclusion of ^{18}O instead of ^{16}O onto the polymer surface eliminates contributions to the oxygen containing mass signals from sources other than the plasma, such as natural ageing during processing and storage and also the absorption of water from the atmosphere. Analysis of the surface by SSIMS and determination of the $CH^-/^{18}O^-$ ratio allowed ~ 1nm in depth of the polymer to be monitored[18]. For oxygen plasma treated polyethylene this ratio was seen to increase with increasing ageing time, indicating surface rearrangement. As the oxygen 18 - containing surface rotates into the bulk, the $^{18}O^-$ signal decreases and hence the $CH^-/^{18}O^-$ ratio increases[18].

1.2.2 Polystyrene

The ageing of plasma oxidised polystyrene was described in Chapter 1, section 3.7.4.3, and Chapter 4, section 1.2. A brief summary is given below.

The ageing mechanism of polystyrene is thought to be molecular weight dependant[6,19-21]. At low molecular weights and high temperatures, ageing occurs by diffusion of untreated polystyrene from the bulk to the surface region, but for high molecular weights, where diffusion is restricted,

ageing is believed to proceed via molecular motions within the plasma modified layer.

1.3 PLASMA OXIDATION OF POLYETHYLENE IN COMPARISON TO POLYSTYRENE

1.3.1 Literature Review

Plasma oxidation of polystyrene has been found to create a more oxidised surface than for polyethylene for the same experimental conditions and treatment times[9,10,22].

Clark and Dilks found that plasma oxidation of polystyrene gave a greater degree of oxidation and more carbonate structures, as detected by XPS, than in the case of polyethylene[10]. In order to investigate further, a helium/oxygen plasma was used to oxidise both polymers. Both polymers showed the same trend in oxidation and also reached the same degree of oxidation under these conditions. Therefore it seemed that the difference in molecular structure of the polymers did not matter in the He/O_2 plasma environment. It was concluded that in the mixed plasma the excited and ionised helium part of the plasma caused crosslinking near the polymer surface, and therefore produced a similar molecular structure for both polymers, hence leading to similar oxidation trends.

Shard and Badyal attributed the greater degree of oxidation of polystyrene than polyethylene to the aromatic rings in polystyrene[9], the phenyl rings were said to be easily susceptible to oxidation.

1.3.2 Does Morphology Effect Reactivity?

Could the physical natures of polyethylene and polystyrene, i.e. the relative degrees of crystallinity, be the cause of the different extents of reaction in the polymers? Polystyrene is usually amorphous but Low Density Polyethylene, LDPE, is usually partly crystalline.

There is evidence that amorphous regions of polymers are more readily plasma etched than the crystallites at the surface[23]. Scanning electron microscopy, SEM, of photo-oxidised or laser ablated polymers such as PET[24] and polystyrene[25] also show evidence of crystallites left on the surface after reaction.

The experiments of Clark and Dilks described in the above section provide evidence that can be interpreted on the basis that the different reactivities of polyethylene and polystyrene are due to the different

molecular structures of the two polymers. If the crystallinities of the polymers effected the reactions then one would expect different oxidation levels with both plasma gases.

Other studies have confirmed that molecular structure is the most important effect in plasma oxidation, some aromatic polymer photo-resists (e.g. poly(α methylstyrene) are more resistant to plasma etching than their aliphatic counterparts (e.g. poly(butene sulphone)[26]. This difference was attributed, in this case, to weak backbone bonds which undergo scission more easily when exposed to the plasma.

The above discussion suggests that the effect of preferential amorphous reactivity in the case of polystyrene can be discounted in the experiments conducted in this study. The differences in reactivity between polyethylene and polystyrene can be mainly attributed to variations in molecular structure.

2. EXPERIMENTAL

Additive-free, low-density polyethylene (ICI, 2 cm^2 x 0.1 mm, M_w = 250,000, 65%w/w crystalline), and polystyrene (ICI, 2 cm^2 x 0.1 mm, M_w = 100,000, amorphous) pieces were cleaned in an ultrasonic bath with isopropyl alcohol and dried in air. Research-grade-quality oxygen (BOC) was used without any further purification.

A 13.56 MHz RF generator was inductively coupled to a cylindrical glass reactor (4.5 cm diameter, 490 cm^3 volume) via an externally wound copper coil; this arrangement was used for the plasma treatments[27]. A strip of polymer was positioned in the centre of the coils (i.e. within the glow region). The reaction vessel was initially evacuated by a two-stage rotary pump to a base pressure of less than 1 x 10^{-2} Torr. Then oxygen was passed through the chamber at a pressure of 0.2 Torr and a constant flow rate of 2.0 cm^3min^{-1} for 10 min, followed by plasma modification for 5 min (longer exposures resulted in no further changes to the polymer surface as determined by XPS). The substrate temperature was not monitored during the glow discharge treatment, but immediately after treatment there was no evidence of significant heating.

Two different electron spectrometers were used for surface analysis of the treated films. Low-resolution core level X-ray photoelectron spectra were acquired on a Kratos ES300 surface analysis instrument, which collected electrons in the fixed retarding ratio (FRR) analyser mode. Unmonochromatized Mg K_α radiation (1253.6 eV) was used as the

excitation source. These measurements were taken with an electron take-off angle of 30° from the surface normal. Data accumulation and component-peak analysis were performed on an IBM PC computer. All binding energies are referenced to the hydrocarbon component (-$\underline{C}_xH_y$-) at 285.0 eV[28], and the instrumentally determined sensitivity factors are such that for unit stoichiometry, the C(1s) : O(1s) intensity ratio is ~0.55.

High-resolution core level and valence region spectra were taken on a Kratos AXIS HS instrument. This instrument was equipped with a monochromatic Al Kα (1486.6 eV) X-ray source and a novel magnetic immersion lens system that yields high resolution and high sensitivity. Uniform charge neutralisation with little energy shift was effected with a low-energy electron source.

3. RESULTS

3.1 UNTREATED POLYETHYLENE AND POLYSTYRENE

Only one C(1s) XPS peak is seen for untreated polyethylene at 285.0 eV, which can be associated with the -$\underline{C}H_2$- linkages present in the polymer[29]. In the valence band region, overlap of the C(2s) orbitals along the hydrocarbon backbone yields bonding (~ 19 eV) and anti-bonding (~ 13 eV) molecular orbitals[30], Figure 1(a). The C(2p) and H(1s) orbitals involved in the C-H bond contribute towards the weak, broad structure seen below ~ 10 eV. The relative intensities are dependent upon the ionisation cross sections of the various molecular orbitals.

In addition to a hydrocarbon component at 285.0 eV, the XPS spectrum of clean polystyrene displays a distinctive satellite structure at ~291.6 eV, which arises from low-energy π --> π^* shake-up transitions accompanying core level ionisation[3], Figure 2(a). The alkyl backbone in polystyrene makes only a minor contribution to the XPS valence band region because the density of states for these levels span a rather broad structure, and the number of such levels is much lower in comparison to those associated with the phenyl groups. As a result, sharp features similar to those in the XPS-VB benzene spectrum predominate[30,31], Figure 3(a).

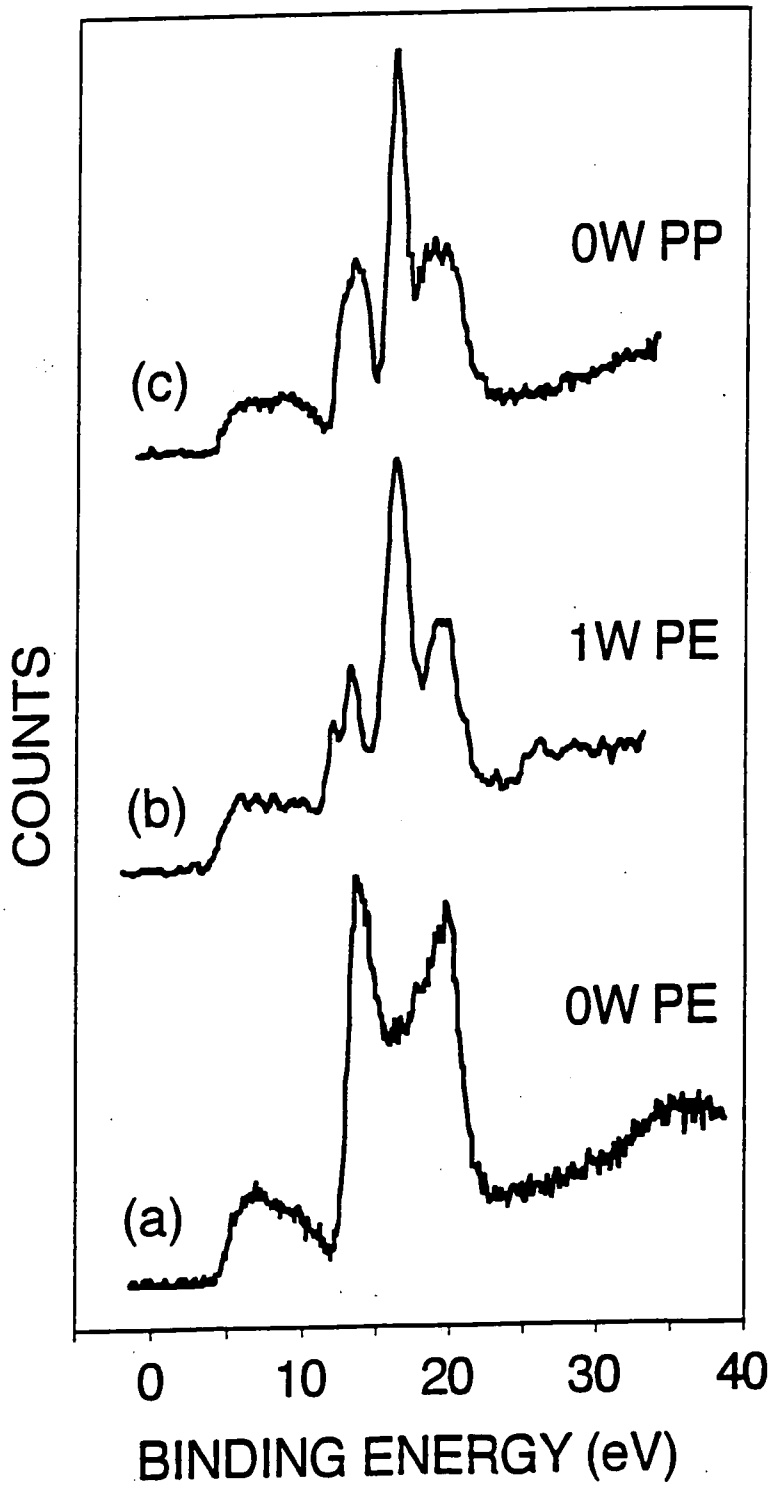

Figure 1: XPS valence band spectra of: (a) clean polyethylene; (b) 1W plasma oxidized/aged polyethylene (10^5 min); and (c) clean polypropylene. (The surface normal was tilted 30° away from the axis of the spectrometer).

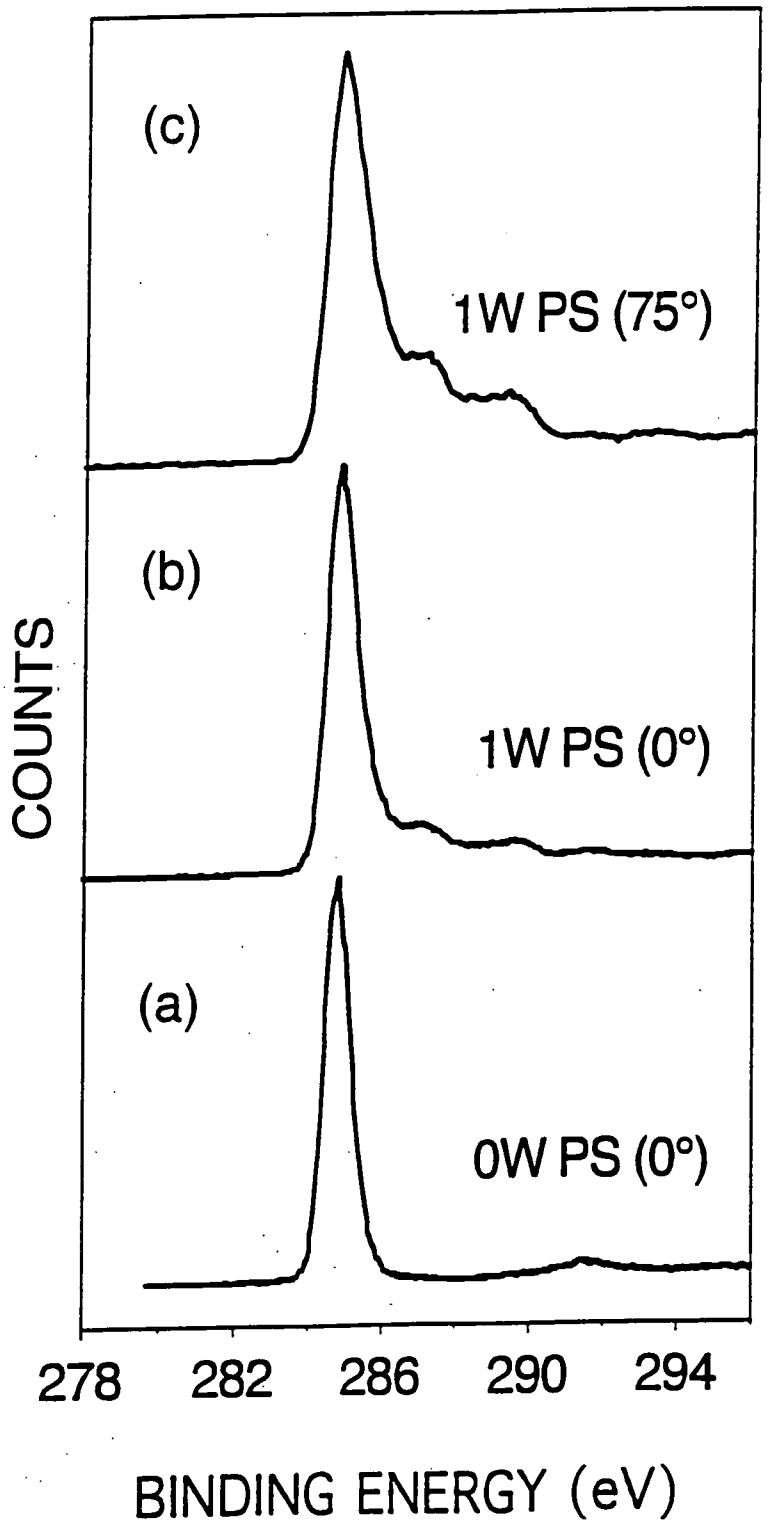

Figure 2: C(1s) region of (a) clean polystyrene; (b) 1W plasma oxidized/aged polystyrene (10^5 min, the surface normal was aligned with the axis of the spectrometer); and (c) 1W plasma oxidized polystyrene/aged (10^5 min, the surface normal was tilted 75° away from the axis of the spectrometer).

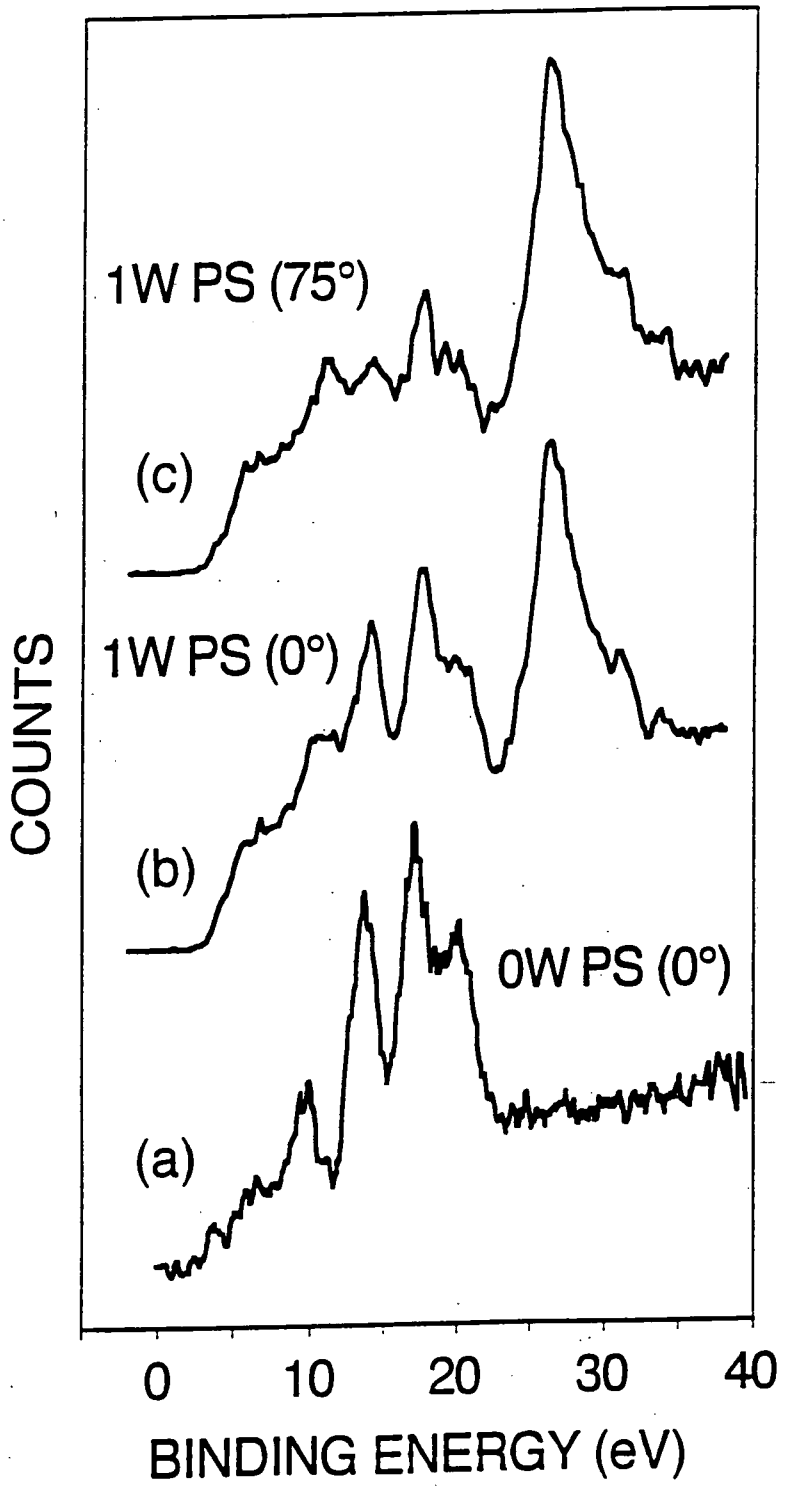

Figure 3: XPS valence band spectra of: (a) clean polystyrene; (b) 1W plasma oxidized/aged polystyrene (10^5 min, the surface normal was aligned with the axis of the spectrometer); and (c) 1W plasma oxidized/aged polystyrene (10^5 min, the surface normal was tilted 75° away from the axis of the spectrometer).

3.2 THE EXTENT OF SURFACE OXIDATION AS A FUNCTION OF GLOW DISCHARGE POWER

Detailed chemical information about the modified polymer surfaces was obtained by fitting the C(1s) XPS spectra to a range of carbon functionalities: carbon adjacent to a carboxylate group (C-CO_2 ~ 285.7 eV), carbon singly bonded to one oxygen atom (C-O ~286.6 eV), carbon singly bonded to two oxygen atoms or carbon doubly bonded to one oxygen atom (O-C-O or C=O ~287.9 eV), carboxylate groups (O-C=O ~289.0 eV), and carbonate carbons (O-CO-O ~290.4 eV)[10]. The C(1s) envelope for plasma oxidised polystyrene is shown in Figure 2(b). Loss of aromaticity in the polystyrene film could be monitored by the decrease in the intensity of the π --> π^* shake-up satellite.

The O(1s)/C(1s) ratios of these samples were determined immediately after plasma oxidation as a function of glow discharge power, Figure 4. A significant quantity of oxidised functionalities was measured at the polyethylene surface following exposure to an oxygen plasma. This is consistent with previous results in the literature[9-16]. The O/C ratio passes through a maximum with increasing wattage; presumably this trend reflects a greater amount of sputtering occurring at higher plasma powers.

Polystyrene undergoes a relatively higher degree of oxidation in comparison with polyethylene. This is also in agreement with previous results[9,10,22]. The O/C ratio is found to be virtually independent of glow discharge power. These observations can be attributed to the fact that this polymer contains phenyl centres, which are known to be reactive, e.g. as chromophores leading to photo-oxidation[32].

3.3 AGEING OF PLASMA OXIDISED SURFACES

The O(1s) and C(1s) core level spectra of plasma-oxidised polyethylene indicate a significant loss of oxygen from the surface on storing in air, Figure 5. Loss of oxygen from the surface has been observed by Ochiello et al using a SIMS analysis[18]. XPS valence band spectra (Figures 1(b) and 3(b)) of aged plasma-oxidised polymers are shown because the changes with respect to the untreated surfaces are so marked and clear-cut. The limiting valence band spectrum (Figure 1(b)) of plasma-oxidised polyethylene (aged over 10^5 min) are markedly different in appearance to the characteristic spectrum of a clean polyethylene surface, Figure 1(a). The major new feature in the C(2s) vicinity overlaps exactly with the extra peak reported for polypropylene. Briggs et al saw this feature with remote nitrogen treated polyethylene but to

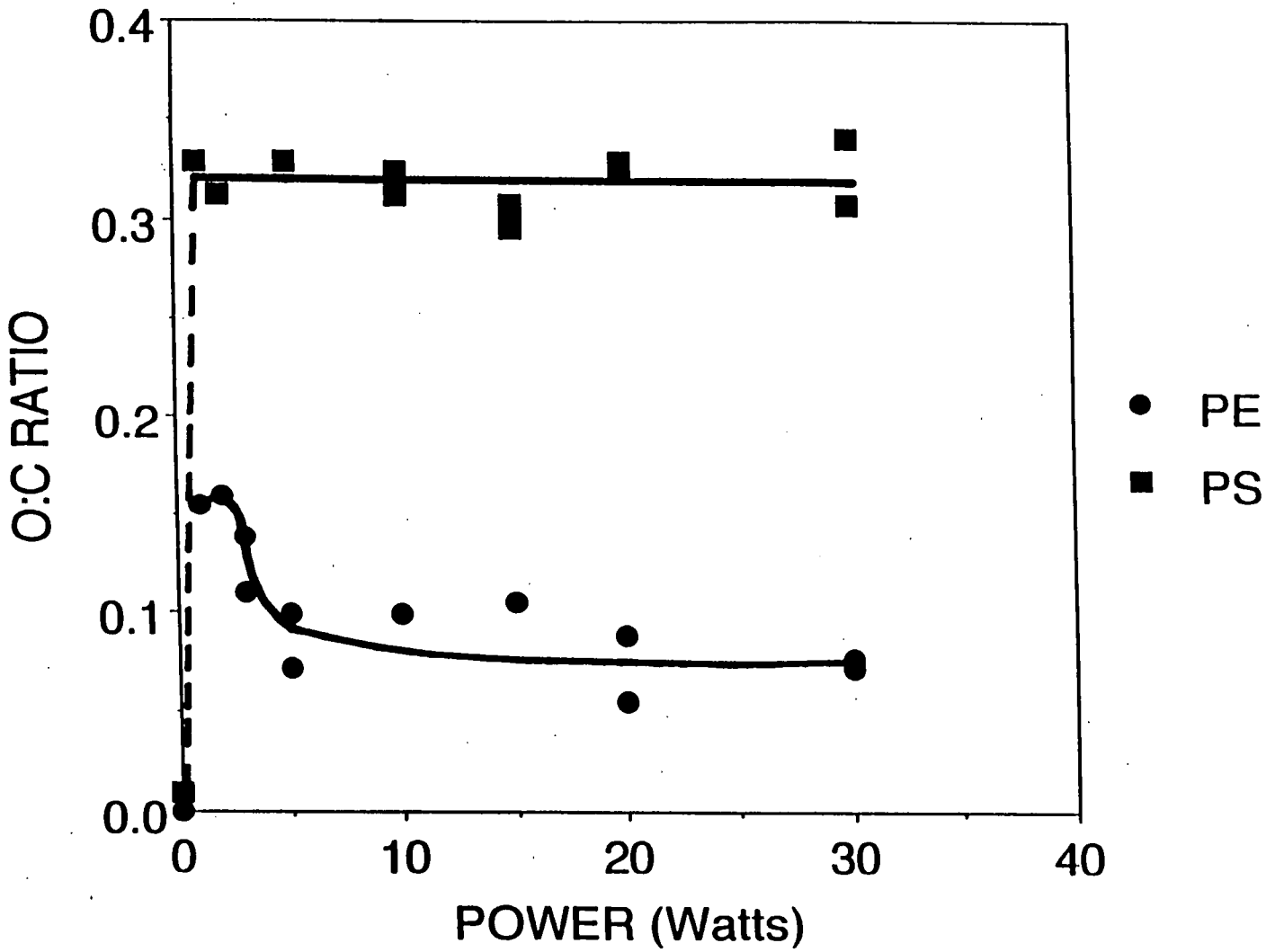

Figure 4: O:C ratio (± 0.01) as a function of the oxygen plasma power (determined by measuring the O(1s) and C(1s) peak areas). (The surface normal was tilted 30° away from the axis of the spectrometer).

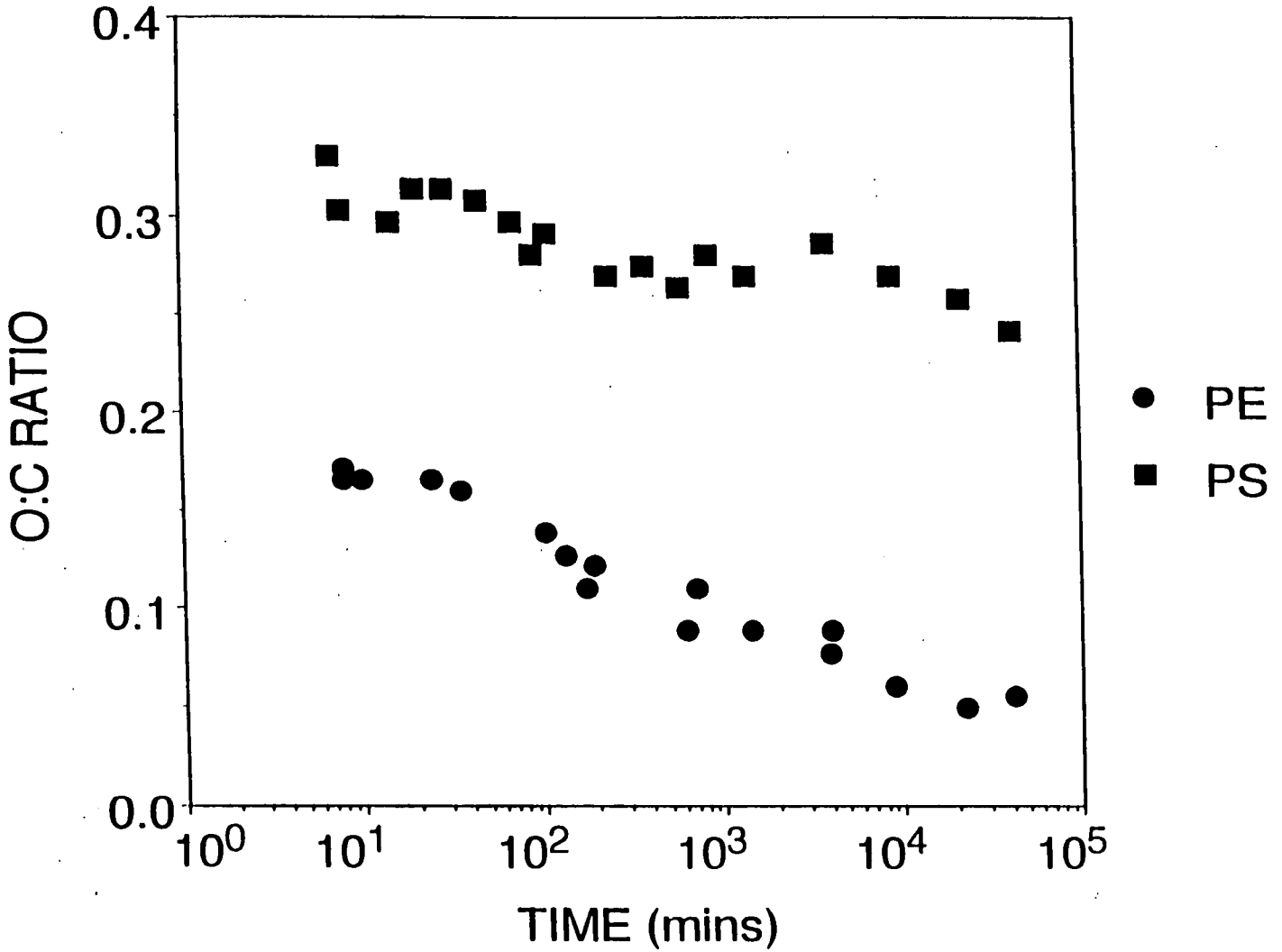

Figure 5: Dependence of the O:C ratio (± 0.01) on the length of storage time following a 1W plasma oxidation treatment (determined by measuring the O(1s) and C(1s) peak areas). (The surface normal was tilted 30° away from the axis of the spectrometer).

a lower extent[17]. The relative intensities of the outer C(2s) features are also consistent with a polypropylene-type of structure (i.e. the attachment of a methyl side chain to the main polyethylene backbone introduces an extra feature in the middle of the C(2s)-C(2s) region at ~16 eV[30], Figure 1(c)). A slight splitting is evident in the polyethylene band at ~ 13 eV; this could be a manifestation of head-to-head and head-to-tail linkages in the polypropylene structure[30] or a mixture of iso- and syndio- tactic polypropylene[33]. O(2s) features are known to appear at ~25-27 eV; whereas O(2p) electrons associated with oxygen lone pairs in π and non-bonding molecular orbitals, O(2p)-H(1s), and O(2p)-C(2p) bonds, all occur below 10 eV[30]. A small amount of O(2s) is still evident for the plasma oxidised / aged polyethylene surface.

C(1s) and O(1s) core-level XPS spectra show that 1W treated polystyrene film ages at a much slower rate than the corresponding 1W plasma-oxidised polyethylene surface. Angle resolved core level and valence band measurements are consistent with the hypothesis that there is a greater degree of oxidation at the surface, Figure 2(c); thus, very little of the polystyrene valence band structure, Figure 3(a) is detectable at high grazing electron-emission angles, Figure 3(c).

4. DISCUSSION

In this study the extent of polyethylene surface modification appears to result in a more well-defined set of resultant molecular orbitals (i.e. selectivity) compared to previous valence-band investigations[13,17]. This discrepancy is probably due to different experimental parameters and reactor configurations (e.g. remote oxygen plasma treatment[15,17]). Also polystyrene is found to undergo a greater degree of oxidation than polyethylene[10,34].

The major advantage of studying XPS rather than UPS valence band spectra is that the photo-ionisation cross section for molecular orbitals with major 2s character is greater than for molecular orbitals with dominant 2p character[35]; this is of a significant benefit, because the 2s bands are easier to interpret than their 2p counterparts[13,36]. The C(2s)-C(2s) band can serve as a fingerprint for the electronic structure of a polymeric system. The very strong valence band spectral features observed for plasma oxidised/aged polyethylene can be attributed to either extensive crosslinking or to rearrangement taking place at the polymer surface to form a polypropylene-type of structure as depicted on the next page:

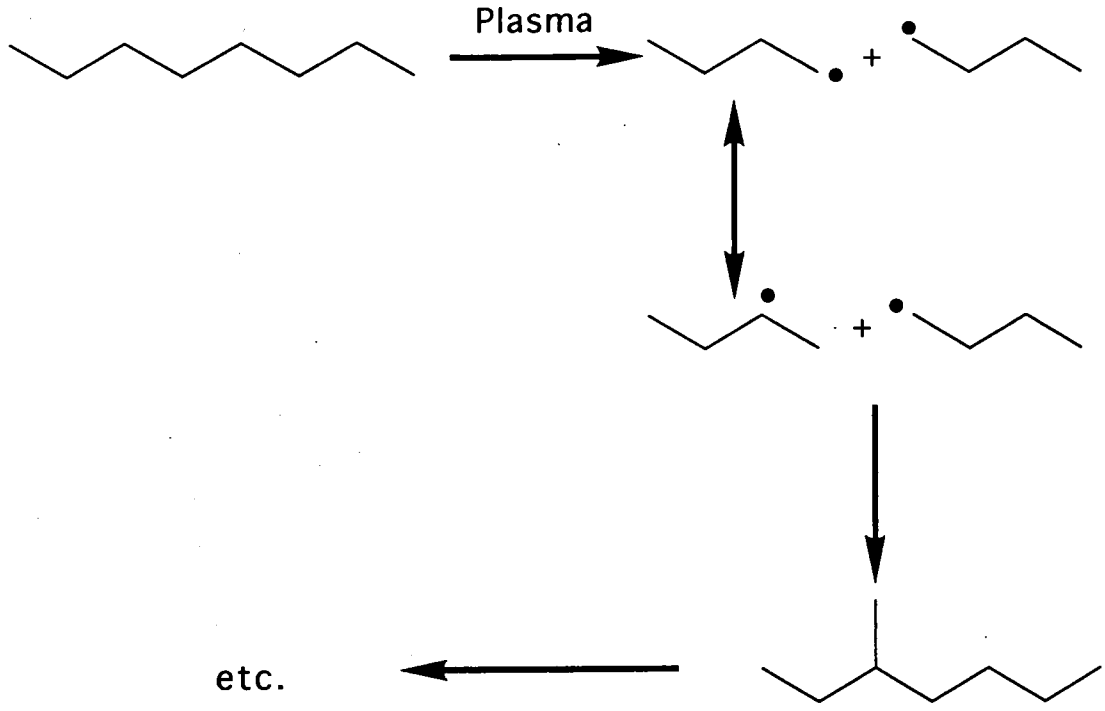

The plasma would be expected to rupture the polyethylene chains to form primary free radicals, which are energetically unstable with respect to their secondary isomers[37]. Therefore these species will undergo rearrangement, and subsequent recombination may occur between a secondary free radical and a neighbouring primary or secondary radical. This sequence of steps results in the generation of a polyethylene backbone to which methyl side groups are attached at random. The resulting atactic chain sequences would be expected to give amorphous material of a greater mobility than the starting polyethylene chains. In plasma treatments it is generally assumed that reaction of the ionic species occurs at the immediate surface whereas the vacuum UV component can penetrate to the subsurface layers (see Chapter 4 introduction). Thus, a hypothesis could be advanced that the UV component results in homolytic C-C bond cleavage and rearrangement to give more mobile chain segments which migrate to the surface during the ageing process.

To a first approximation, the valence band spectrum of a polymer based upon a polyethylene backbone to which a short chain is fixed can be considered to be a simple summation of the individual constituents, i.e. polyethylene + attached group[38]. Therefore, the XPS valence band spectrum of a polyethylene chain with randomly attached methyl side groups would be expected to bear a strong resemblance to the valence region spectrum reported for polypropylene. The loss of oxygenated species from the surface with ageing may be a direct consequence of the creation of this new structure in the subsurface region. Alternatively, ageing may occur via migration of

the oxygenated moieties towards the subsurface, agglomeration into very localised pockets in the surface (phase separation), or simply fragmentation and desorption into the gas phase. Examination of the valence band spectra of a whole range of other hydrocarbon polymers supports this assignment[39] (the closest analogue is found to be a polyethylene backbone with two methyl side groups on each carbon centre, i.e. polyisobutylene; however, the polyisobutylene binding energies differ significantly, but their minor presence could explain the origins of the slight splitting seen in the ~13 eV band). Heterolytic fragmentation or formation of carbocations via oxidation of initially formed radicals can not be discounted but might be expected to lead to unsaturated C-C bonding via proton loss. No evidence for such a process was detected so if it occurs it would seem to be a minor component of the process.

In the case of polystyrene, activation of the phenyl centres by the oxygen plasma offers numerous reaction pathways which can lead to a considerable breakdown of the parent polymer and a greater degree of oxidation[9]. Electromagnetic radiation from the glow discharge can penetrate below the surface to cause photo-excitation of the phenyl groups, and extensive crosslinking reactions may subsequently occur within the subsurface region. This may be the reason why plasma oxidised polystyrene is much more resistant to ageing than its polyethylene counterpart.

5. CONCLUSIONS

These systematic studies have shown that the plasma oxidation of polyethylene followed by ageing results in either a polypropylene-type surface structure, or else implies that some kind of crosslinking has taken place. It should be noted that these results are the first example of such a highly selective reaction occurring at a polymer surface under the influence of a glow discharge. Furthermore, the plasma modification of polyethylene surfaces is found to be much more critically dependent on the process parameters employed than is the case for polystyrene. Polystyrene experiences a greater degree of oxidation and is much more resistant to subsequent loss of surface oxygen. This can be attributed to the unsaturated / chromophoric phenyl groups in polystyrene being highly vulnerable towards plasma activation.

6. REFERENCES

1) J.M. Burkstrand, J. Vac. Sci. Technol., 15, (1978), 223-226.
2) W.L. Wade, R.J. Mammone and M. Binder, J. Appl. Polym. Sci., 43, (1991), 1589-1591.
3) D.T. Clark and A. Dilks, J. Polym. Sci. Polym. Chem. Ed., 15, (1977), 15-30.
4) J. Lub, F.C.M. van Vroonhoven, D. van Leyen and A. Benninghoven, Polymer, 29, (1988), 998-1003.
5) D. Briggs, Br. Polym. J., 21, (1989), 3-15.
6) M. Morra, E. Occhiello, F. Garbassi, D. Johnson and P. Humphrey, Appl. Surf. Sci., 47, (1991), 235-242.
7) J. J. Pireaux, J. Riga, P. Boulanger, P. Snauwaert, Y. Novis, M. Chtaib, C. Gregoire, F. Fally, E. Beelen, R. Caudano, and J. J. Verbist, J. Electr. Spectr. Rel. Phen., 52, (1990), 423-445.
8) D.T. Clark and D. Shuttleworth, J. Polym. Sci. Polym. Chem. Ed., 18, (1980), 27-46.
9) A.G. Shard and J.P.S. Badyal, Macromolecules, 25, (1992), 2053-2054.
10) D. T. Clark and A. Dilks, J. Polym. Sci., Polym. Chem. Edn., 17, (1979), 957.
11) Y. Yao, X. Liu, Y. Zhu, J. Appl. Polym. Sci, 48, (1993), 57.
12) P. M. Triolo and J. D. Andrade, J. Biomed. Mat. Res., 17, (1983), 129.
13) L.J. Gerenser, J. Adhesion Sci. Techol., 1, (1987), 303-318.
14) H. S. Munro and H. Beer, Polymer Comm., 27, (1986), 79.
15) R. Foerch, N.S. McIntyre and D.H. Hunter, J. Polym. Sci. Polym. Chem. Ed., 28, (1990), 193-204.
16) J. Behnisch, A. Hollander, and H. Zimmerman, J. Appl. Polym. Sci., 49, (1993), 117.
17) R. Foerch, G. Beamson and D. Briggs, Surf. Interface Anal., 17, (1991), 842-846 .
18) M. Morra, E. Occhiello, L. Gila, F. Garbassi, J. Adh., 33, (1990), 77.
19) M. Morra, E. Occhiello, P. Chinquina, F. Garbassi, Polymer Preprints, 31, (1990), 308.
20) M. Morra, E. Occhiello, F. Garbassi in 'Metallised Plastics II' ed. K. Mittal, Plenum, NY, 1991, p363.
21) M. Morra, E. Occhiello, P. Chinquina, F. Garbassi, Polymer, 33, (1992), 3007.
22) D. T. Clark, A. Dilks, and D. Shuttleworth in 'Polymer Surfaces', ed. D. T. Clark and W. J. Feast, Wiley, 1978, Chapter 9.
23) J. Friedrich, J. Gahda and M. Photil, Acta Polymer, 31, (1980), 310.on ILL

24) Y. Novis, J.J. Pireaux, A. Brezini, E. Petite, R. Caudano, P. Lutgen, G. Feyden and S. Lazare, J. Appl. Phys, 64, (1988), 365.
25) Y. Novis, R. Demeulemeester, M. Chtaib, J.J. Pireaux, R. Caudano, Br. Polym. J., 21, (1989), 147.
26) F. D. Egitto, V. Vukanovic and G. N. Taylor in 'Plasma Deposition, Treatment and Etching of Polymers', ed. R. d'Agostino, Academic Press Inc.
27) A.G. Shard, H.S. Munro and J.P.S. Badyal, Polym. Commun., 32, (1991), 152-154.
28) G. Johansson, J. Hedman, A. Berndtsson, M. Klasson, and R. Nilsson, J. Electr. Spectr. Rel. Phen. , 2, (1973), 295-317.
29) M.H. Wood, M. Barber, I.H. Hillier and J.M. Thomas, J. Chem. Phys. 56, (1972), 1788-1789.
30) J.J. Pireaux, J. Riga and J.J. Verbist in: 'Photon, Electron and Ion Probes for Polymer Structure and Properties', D.W. Dwight, T.J. Fabish and H.R. Thomas (Eds), ACS Symposium Series No. 162, pp. 169-201, Amer. Chem. Soc. Washiington D.C. (1981).
31) A. Chilkoti, D. Castner and B.D. Ratner, Appl. Spectros., 45, (1991), 209-217.
32) A.G. Shard and J.P.S. Badyal, J. Phys. Chem., 95, (1991), 9436-9438.
33) J. Delhalle, R. Montigny, C. Demanet and J.M. Andre, Theoret. Chim. Acta, 50, (1979), 343-349.
34) P.M. Triolo and J.D. Andrade, J. Biomed. Mater. Res., 17, (1983), 129-147.
35) U. Gelius in 'Electron Spectroscopy', D.A. Shirley (Ed), p. 311. North-Holland, Amsterdam (1972).
36) W.R. Salaneck, CRC Crit. Rev. Solid State Mater. Sci., 12, (1985), 267-296.
37) J. McMurray 'Organic Chemistry', 2nd Ed. pp. 180-207. Brooks/Cole, Belmont, USA (1988).
38) J.J. Pireaux, J. Riga, R. Caudano, J.J. Verbist, J. Delhalle, J.M. Andre and Y. Gobillon, Physica Scripta, 16, (1977), 329-338.
39) G. Beamson and D. Briggs: 'High Resolution XPS of Organic Polymers: The Scienta ESCA300 Database', J. Wiley, Chichester, (1992).

CHAPTER 6

PHOTOCHEMISTRY AT THE ORGANOSILANE / POLYMER INTERFACE

1. INTRODUCTION

Polymeric surfaces can be tailored to enhance a wide range of interfacial properties, such as wettability[1], hydrophobicity[2], adhesion[3], and biocompatibility[4]. Such target surfaces may be attained in a variety of ways. These include the use of coronas[5], plasmas[6], and photochemical methods[7]. In the case of the latter technique, the most important criterion to bear in mind is that at least one of the reactants must be capable of becoming photo-reactive during irradiation, i.e. either the incident moiety or the polymer substrate itself.

A systematic study has been undertaken with the aim of examining the relative photo-reactivities of chromophoric (hexamethyldisilane) / non-chromophoric (tetramethylsilane) gaseous molecules with chromophoric (polystyrene) / non-chromophoric (polyethylene) substrates. Hexamethyldisilane ($[CH_3]_3Si\text{-}Si[CH_3]_3$) contains a weak Si-Si linkage which can readily undergo a $\sigma(Si\text{-}Si) \rightarrow \sigma^*(Si\text{-}Si)$ transition during UV absorption[8]. Tetramethylsilane ($Si[CH_3]_4$) is very similar to hexamethyldisilane in terms of molecular structure, except it does not possess a Si-Si bond, and is therefore a relatively weak chromophore in comparison. Polyethylene is based upon extended alkane chains, $-(CH_2)_n-$, and is generally considered to be the simplest of polymers. Polystyrene comprises of phenyl rings attached to alternate carbon centres along a polyethylene backbone, these aromatic centres absorb strongly in the UV region[9]. The various combinations of organosilane molecules with polymer substrate have been exposed to ultraviolet (UV) irradiation, and the resultant surfaces have been subsequently characterized by X-ray photoelectron spectroscopy (XPS). A pertinent aspect of this investigation is to address whether there is any mutual enhancement of the extent of surface modification, when both the organosilane gas and the polymeric substrate are strongly absorbing in the UV region. The desired system could be tailored for the microelectronics industry in the wafer fabrication process, a detailed explanation of which is given below.

1.1 BACKGROUND TO WAFER FABRICATION

Wafer fabrication in the microelectronics industry is the method of imaging a silicon wafer in order to produce an integrated circuit[10]. The wafer is first covered with a planarising carbon-containing polymer film to smooth the substrate surface by covering any previous steps in the fabrication process, and then a layer of resist material is placed upon this

planarising layer[11]. A resist is a material used in this process that is able to form an image when exposed to some form of radiation through a mask containing the required pattern; ultra-violet light, ion beams or electrons are among the types of radiation used. Upon exposure, the resist material is changed so that the exposed region becomes either more or less soluble in organic solvents. These resists are classified according the nature of the resulting pattern; those which become more soluble are termed 'positive working' resists as the image is directly transferred to the substrate, those which become less soluble are termed 'negative working' resists as the image would be in negative form once transferred to the wafer, Diagram 1. This negative imaging is corrected by using the negative of the actual pattern required as a mask.

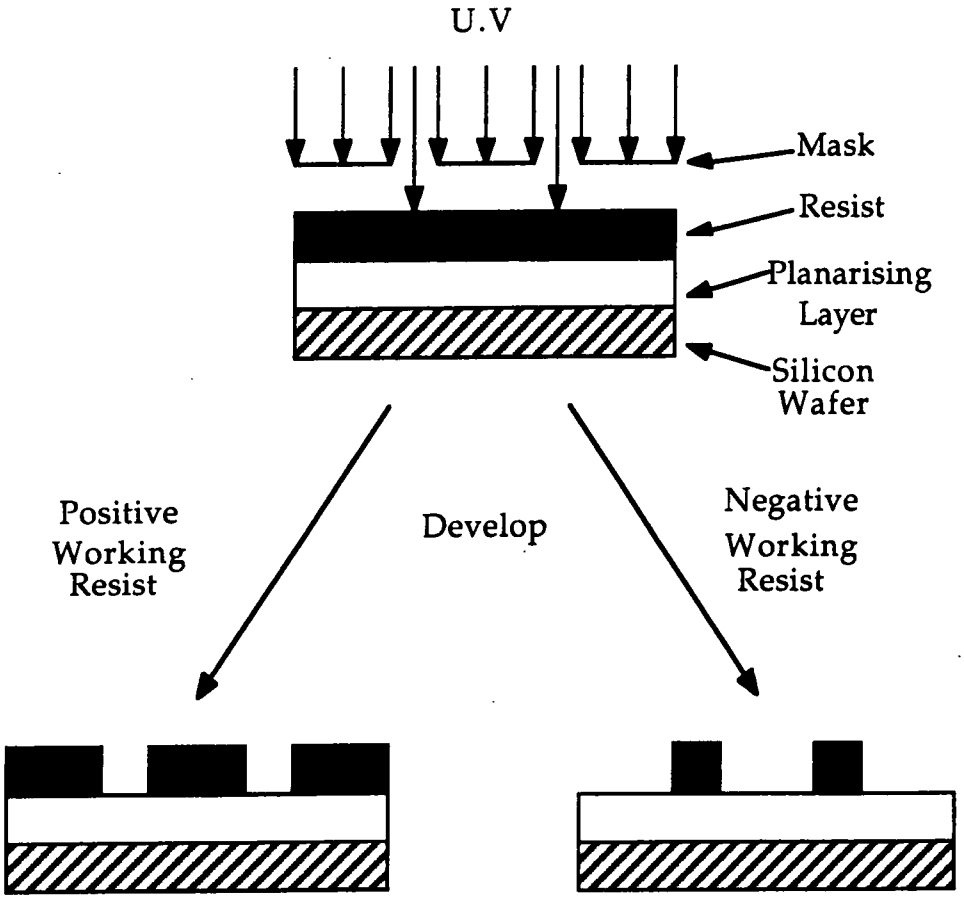

Diagram 1: Schematic of positive and negative working resists.

The long term goal in this field is to reduce the number of processing steps in fabrication and hence reduce processing time and costs.

1.1.1 Polysilane resist materials

Polysilanes posess a number of unique characteristics that make them suitable for many lithographic applications[11,12]. These polymers are soluble, castable into high quality optical films, thermally stable, imageable over a broad spectral range and resistant to oxygen etching in plasma environments.

Polysilanes undergo a decrease in molecular weight upon exposure to ultra-violet light; and are hence positive resist materials[11,13,14]. Images may be developed by classical wet-development processes or an all-dry technique involving photo-ablative imaging.

1.1.1.1 Classical Development.

In the classical process, the polysilane is patterned in a conventional fashion, i.e. through a mask, and the images are developed to the planarising layer using an organic developer. These images can be subsequently transferred to the substrate, silicon wafer by an oxygen -reactive ion-etching (O_2-RIE) treatment, effectively an oxygen plasma[15].

Resistance to oxygen etching is particularly important for multi-layer resist schemes using O_2-RIE techniques for image transfer. O_2-RIE processes have been proposed for the production of high resolution images[11]. This image transfer technique requires an image-forming polymer that is considerably more stable in oxygen plasma environments than normal carbon based polymers, i.e. the planarising layer, so as to serve as an effective etch barrier for the protection of unexposed regions during the pattern transfer step. Upon exposure to an oxygen plasma polysilanes form a thin, highly resistant silicon oxide, SiO_x, etch barrier because of their high silicon content. Therefore the thin polysilane top layer plays a dual role by serving as the imaging layer and as the barrier layer in the subsequent image transfer process, Diagram 2.

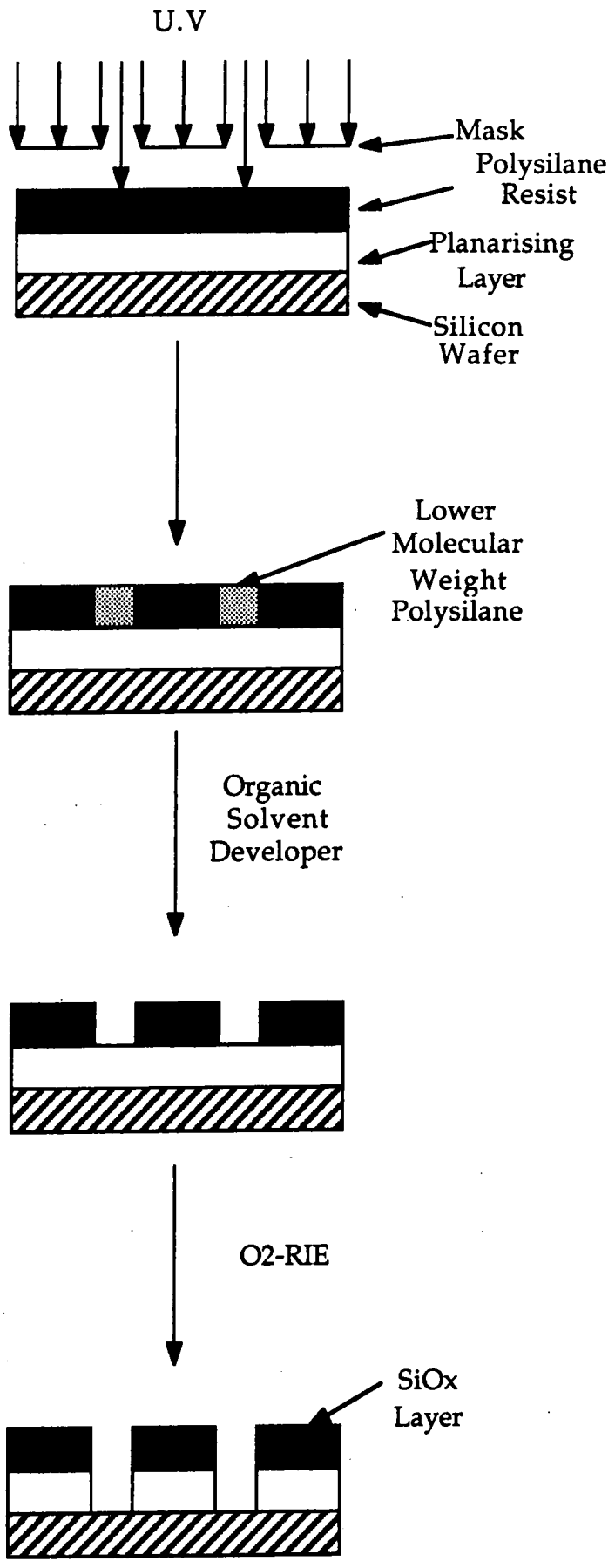

Diagram 2 : Classical development of a polysilane resist.

1.1.1.2 Polysilane Self-Development

Polysilanes, such as poly(p-tert-butylphenylmethylsilane), have been produced that can undergo self-development upon exposure to high flux light sources such as UV excimer lasers[11,16], Diagram 3.

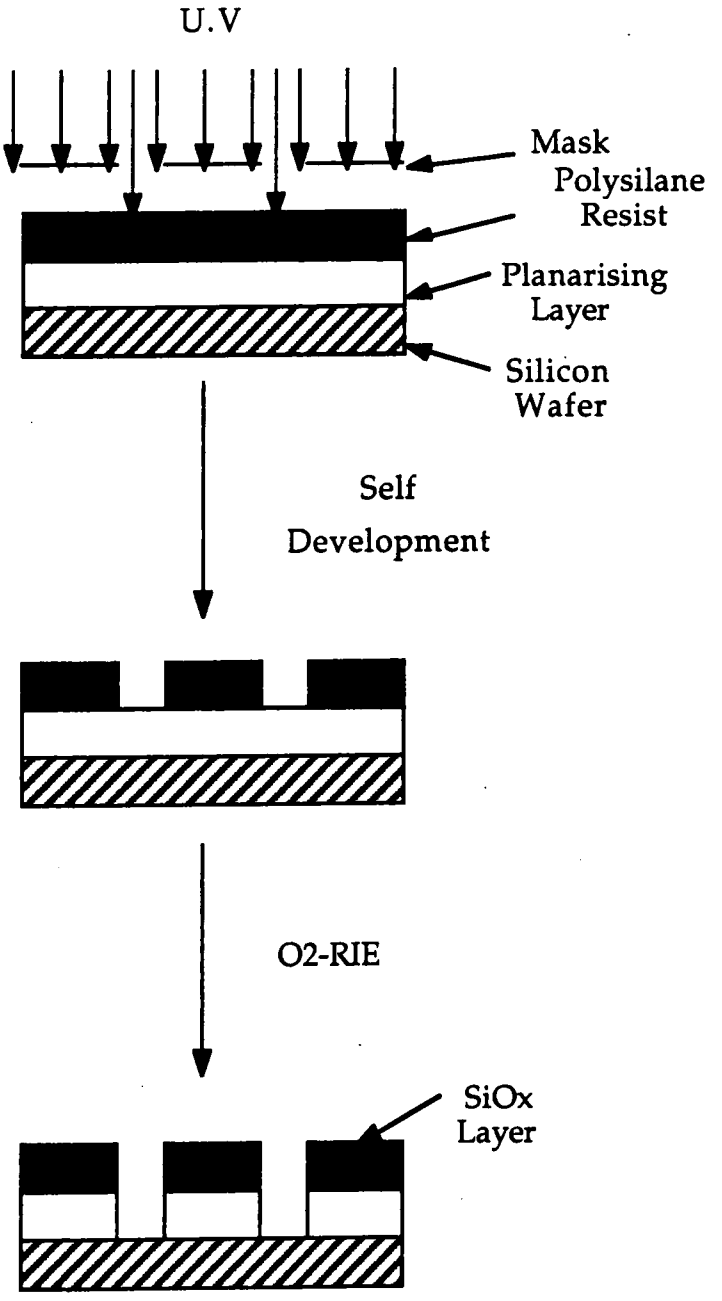

Diagram 3 : Polysilane self-development.

These polymers are attracting considerable interest since if the procedure were used industrially the use of solvents for development would become redundant. The mechanism involved is laser-induced volatilisation; ablation of the polysilane in fragments in this case ranging from one to at least five monomer units[11].

1.1.2 Plasma Polymerisation and Wafer Fabrication

In future, plasmas may be used during wafer fabrication to deposit both the carbon and silicon containing polymer films. Diagram 4 shows the conventional method of preparing the wafer surface before fabrication. Casting of the polymeric layers depends upon the use of solvents.

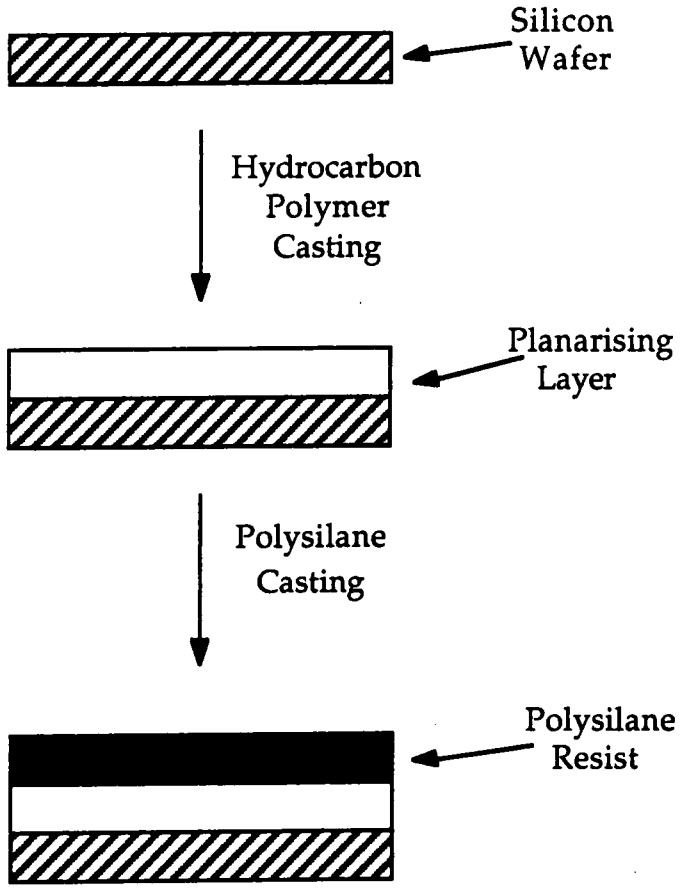

Diagram 4 : Conventional method of casting polymers prior to fabrication.

These solvent steps may be removed if the polymers were deposited upon the wafer surface by using a plasma containing the required precursor, Diagram 5.

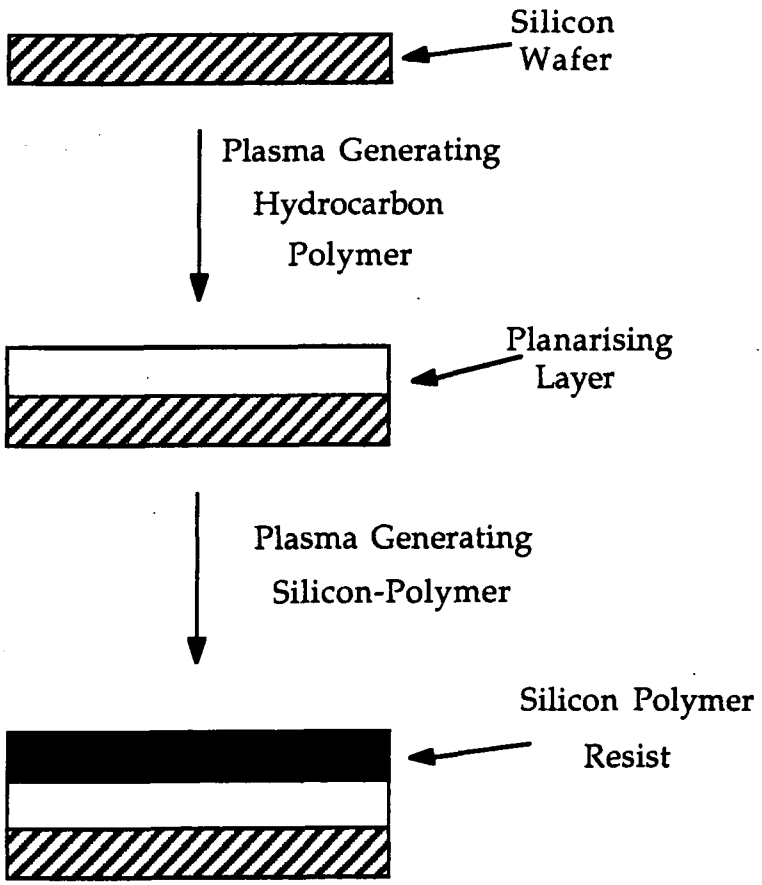

Diagram 5 : Schematic of the plasma deposition of polymers prior to wafer fabrication.

Careful control of the plasma conditions will be required upon deposition of the hydrocarbon polymer layer as the plasma may damage the substrate surface if energetic ions are present.

Badyal and Fonseca studied the plasma polymerisation of hexamethyldisilane onto polyethylene film by XPS[17]. Silicon species were also detected by ATR-FTIR as Si-H, Si-CH_3, Si-O-Si, Si-O-C functionalities, the presence of oxygen was probably due to the reaction of trapped radicals with oxygen and moisture during sample transfer to the spectrometer. The reaction of the silicon-containing polymer to radiation has not yet been studied, and it may still be necessary to develop the resist using conventional organic solvents if ablation does not occur.

Nguyen et al also studied the plasma preparation of organosilicon polymers in relation to wafer fabrication[18]. The monomers used in this case were silazanes and siloxanes which contain nitrogen and oxygen species respectively as well as carbon, hydrogen and silicon. The plasma polymers were to be used as intermediate etch barriers in a trilevel fabrication scheme. A photo-resist was deposited on top of the plasma polymer and patterned in the usual manner, the image being transferred to the plasma polymer by

Freon (CF_4)-RIE and subsequently through the planarising layer by O_2-RIE. This system takes more processing steps than the bilevel scheme of Badyal and Fonseca, the plasma polymer of HMDS would act as an imaging layer and an etch barrier combined, Diagram 6.

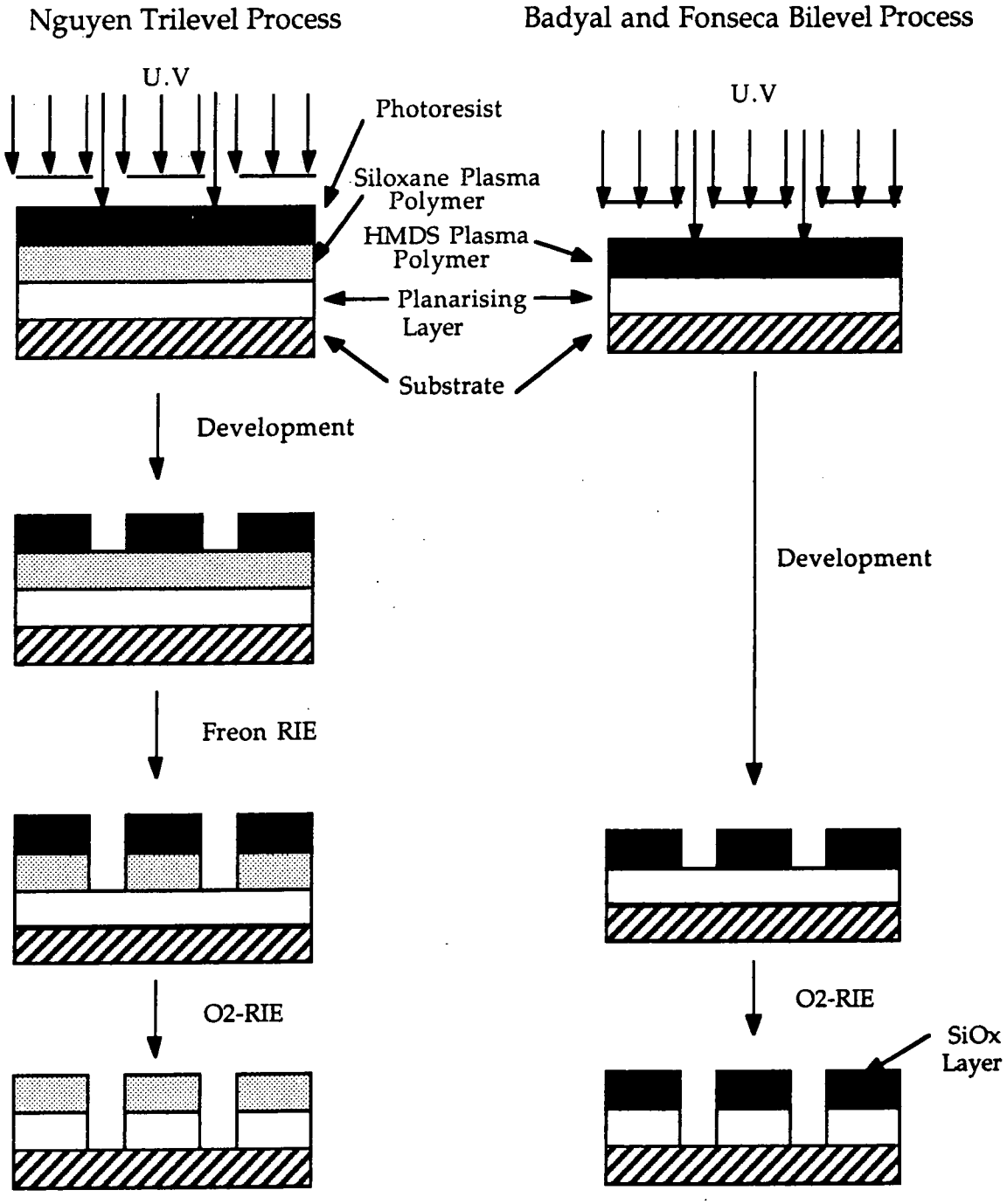

Diagram 6: Trilevel vs Bilevel schemes in wafer fabrication.

1.2 OBJECTIVES OF THE WORK DESCRIBED IN THIS CHAPTER

It may be possible to put down a patterned resist on the planarising polymer layer in one step by the use of a suitable organosilane precursor and a reactive planarising polymer. This process would be even more beneficial than the self-developed polysilane technique, as a further solvent step is taken out of the process by eliminating the casting of the polysilane film.

Shining UV light through a mask onto a carbon-containing polymer planarising layer in the presence of an organosilane precursor may cause reaction at the polymer/organosilane interface. The silicon-containing species deposited upon the planarising layer would image the pattern of the mask, Diagram 7.

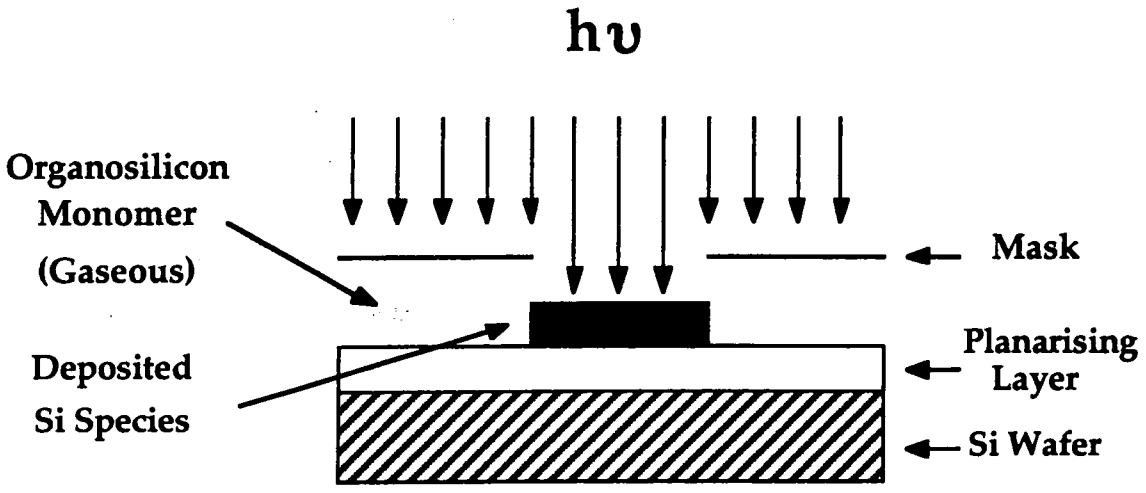

Diagram 7 : Proposed scheme for direct deposition of silicon-containing species upon a planarising layer.

This silicon-containing layer will effectively produce the pattern of a negative working resist and be resistant to O_2-RIE. The planarising layer will be etched away to transfer the pattern to the silicon wafer. Ultimately one may use direct writing of the pattern with a laser to produce very high resolution patterns, with a theoretical limiting resolution of the wavelength of light used. In this chapter we have studied the reaction of polyethylene and polystyrene, possible models for planarising layers, with HMDS and TMS, possible organosilane precursors, to investigate how the nature of the solid/gas reactivity will effect the formation of a silicon containing layer on the carbon-containing polymer.

2. EXPERIMENTAL

UV irradiation was carried out in a glass walled reactor with a detachable quartz window (cut off wavelength 180-200 nm)[19] (Diagram 8). A low pressure Hg-Xe arc lamp (Oriel) was used as the photon source, operating at 50 W, this gave a strong line spectrum from 240 to 600 nm. Low density polyethylene (ICI) and polystyrene (ICI) films were cleaned in an ultrasonic bath with isopropyl alcohol and subsequently dried in air. A small piece of polymer film was positioned in direct line-of sight to the quartz window. The reactor was evacuated down to a base pressure of 3×10^{-2} Torr using a two stage rotary pump equipped with a liquid nitrogen trap and then isolated from the pumping system. Vapour of either of hexamethyldisilane (Aldrich, 98% pure) or tetramethylsilane (Aldrich, 99.9% pure) vapour (both of which had been further purified by freeze - pump - thaw cycles) was introduced into the reactor from a monomer tube to give a pressure of 0.4 Torr. The sample was then irradiated in this static atmosphere for a given time interval. Following completion of exposure, the lamp was switched off, and after a further 5 mins, the reactor was evacuated back down to its base pressure.

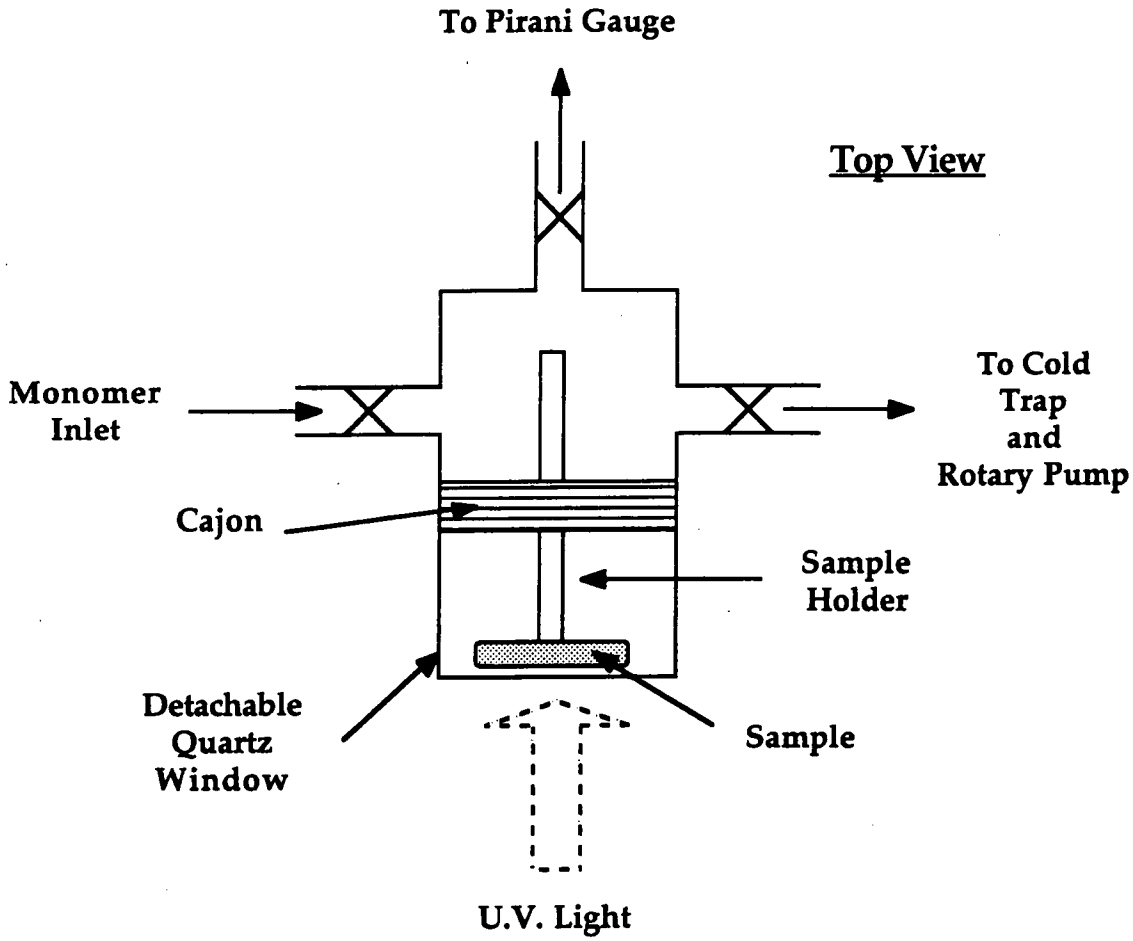

Diagram 8: Schematic of glass reactor used.

Core level X-ray photoelectron spectra were acquired on a Kratos ES300 surface analysis instrument, this collected electrons in the fixed retarding ratio (FRR) analyser mode. Mg K_α radiation (1253.6 eV) was used as the excitation source. XPS measurements were taken with an electron take-off angle of 30° from the surface normal. Data accumulation and component peak analysis were performed on an IBM PC computer. All binding energies are referenced to the hydrocarbon component (-$\underline{C}_xH_y$-) at 285.0 eV[20], and the instrumentally determined sensitivity factors were such that for unit stoichiometry, the C(1s) : O(1s) : Si(2p) intensity ratios are 1.00 : 0.55 : 1.02.

Ultraviolet absorption spectra of the organosilicon monomers were recorded on a Perkin Elmer Lambda 2 UV/VIS double beam spectrometer (190-1100 nm).

3. RESULTS AND DISCUSSION

3.1 INTRODUCTION

Clean polyethylene exhibits only one C(1s) peak at 285.0 eV, which can be attributed to the -$\underline{C}H_2$- linkage in the basic polymer unit -$(CH_2)_n$- [21]. In addition to a hydrocarbon component at 285.0 eV, the XPS spectrum of clean polystyrene displays a distinctive satellite structure at ~291.6 eV (with 7% of the total C(1s) signal) this arises from low energy π - π^* shake-up transitions of the phenyl rings accompanying core level ionization[22], Figure 1(a). An absence of surface impurities was found for both of these polymers, Figure 2(a).

Polystyrene absorbs light strongly below 280 nm via its phenyl ring chromophores[9], whereas pure polyethylene is non-absorbing above 200 nm[23]. UV absorption spectra of hexamethyldisilane (HMDS) and tetramethylsilane (TMS) are shown in Figure 3. HMDS absorbs strongly in the ultraviolet region at wavelengths shorter than ~250 nm , whereas the absorption threshold for TMS is shifted towards ~220 nm. Since the Hg-Xe UV lamp has a cut-off below 230 nm (with lines at 237.8, 248.2, and 253.7 nm), it can be assumed that only the HMDS molecule and the polystyrene substrate will undergo photo-excitation in these experiments.

3.2 HEXAMETHYLDISILANE / POLYSTYRENE

Exposure of polystyrene to ultraviolet light in a hexamethyldisilane atmosphere results in the appearance of a Si(2p) peak at 101.4 ± 0.2 eV. This binding energy corresponds to silicon bound to carbon[24], Figure 2(b). The amount of silicon present at the polymer surface increases from zero up to a maximum value of ~17% after 40 minutes of UV irradiation, Figure 4. No further change was detected for longer exposure times. A corresponding attenuation in the C(1s) π - π^* shake-up satellite of polystyrene was observed, Figure 1(b), possibly indicating that the phenyl centres were participating in the photochemistry or being covered up by a silicon-containing layer. A small amount of O(1s) signal was also detectable after irradiation (~3%). However this was not resolvable as oxygenated functionalities in either the C(1s) or Si(2p) envelopes, and was therefore probably picked up during transfer of the sample from the irradiation vessel to the electron spectrometer.

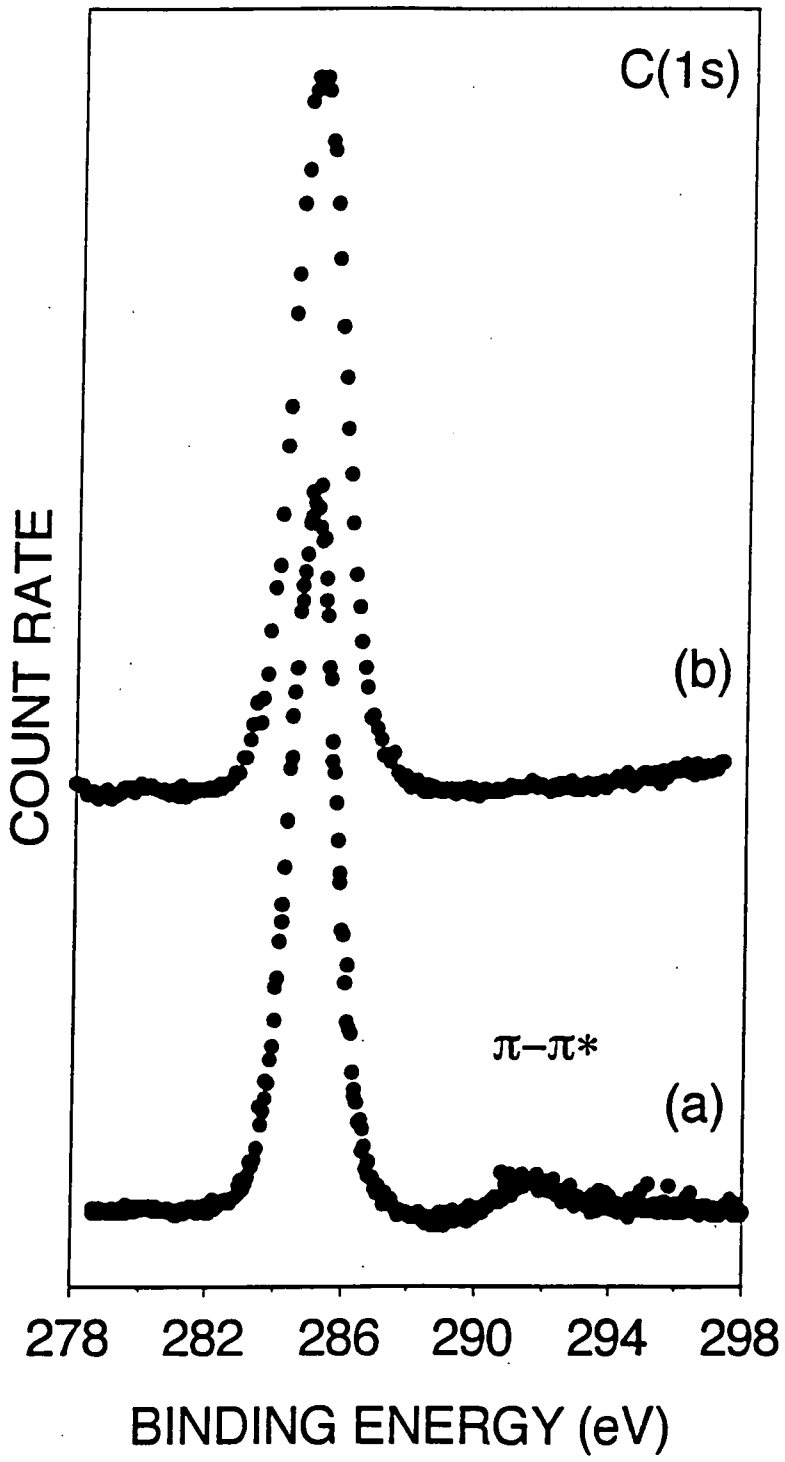

Figure 1: C(1s) XPS spectra of: (a) clean polystyrene; and (b) UV irradiated polystyrene in the presence of hexamethyldisilane.

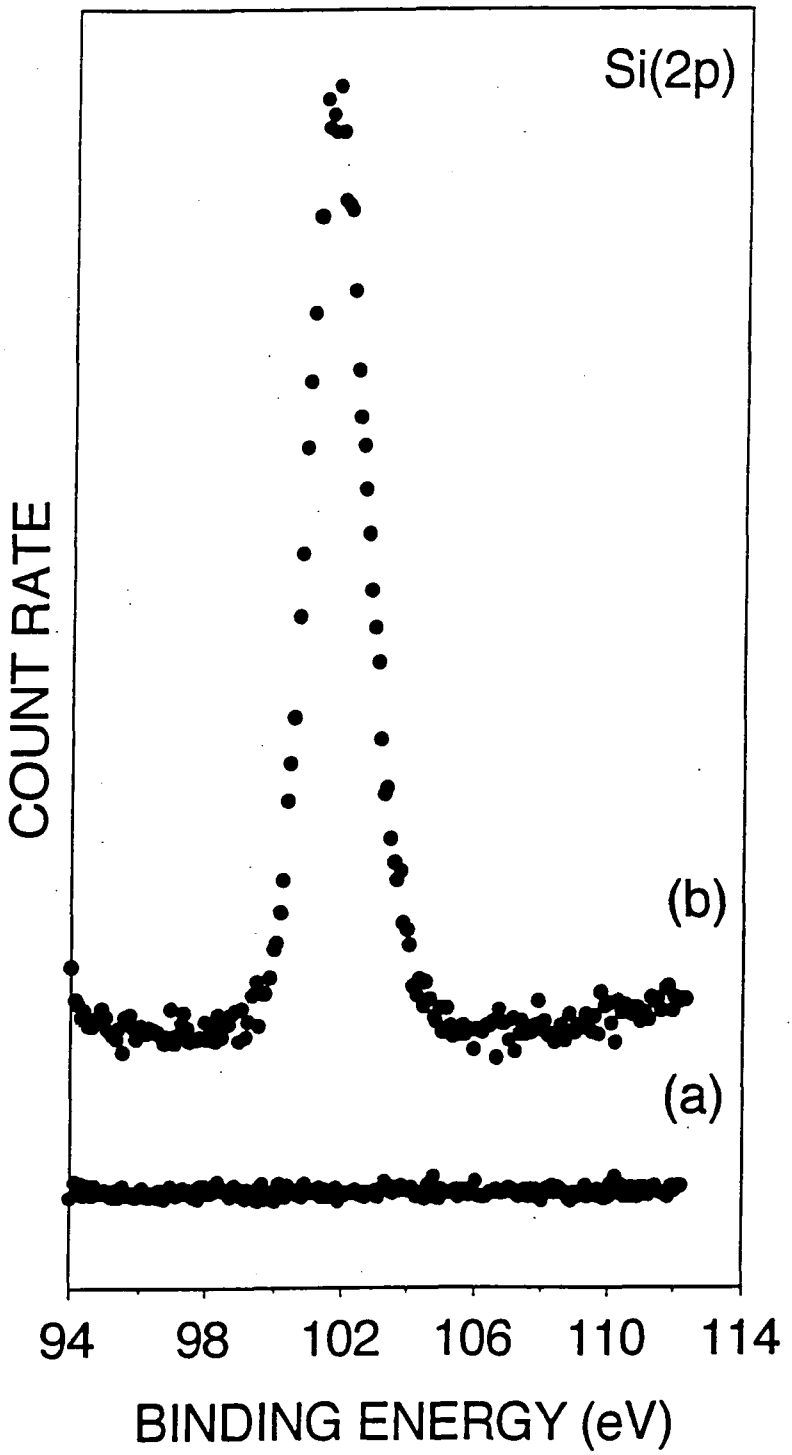

Figure 2: Si(2p) XPS spectra of: (a) clean polystyrene; and (b) UV irradiated polystyrene in the presence of hexamethyldisilane.

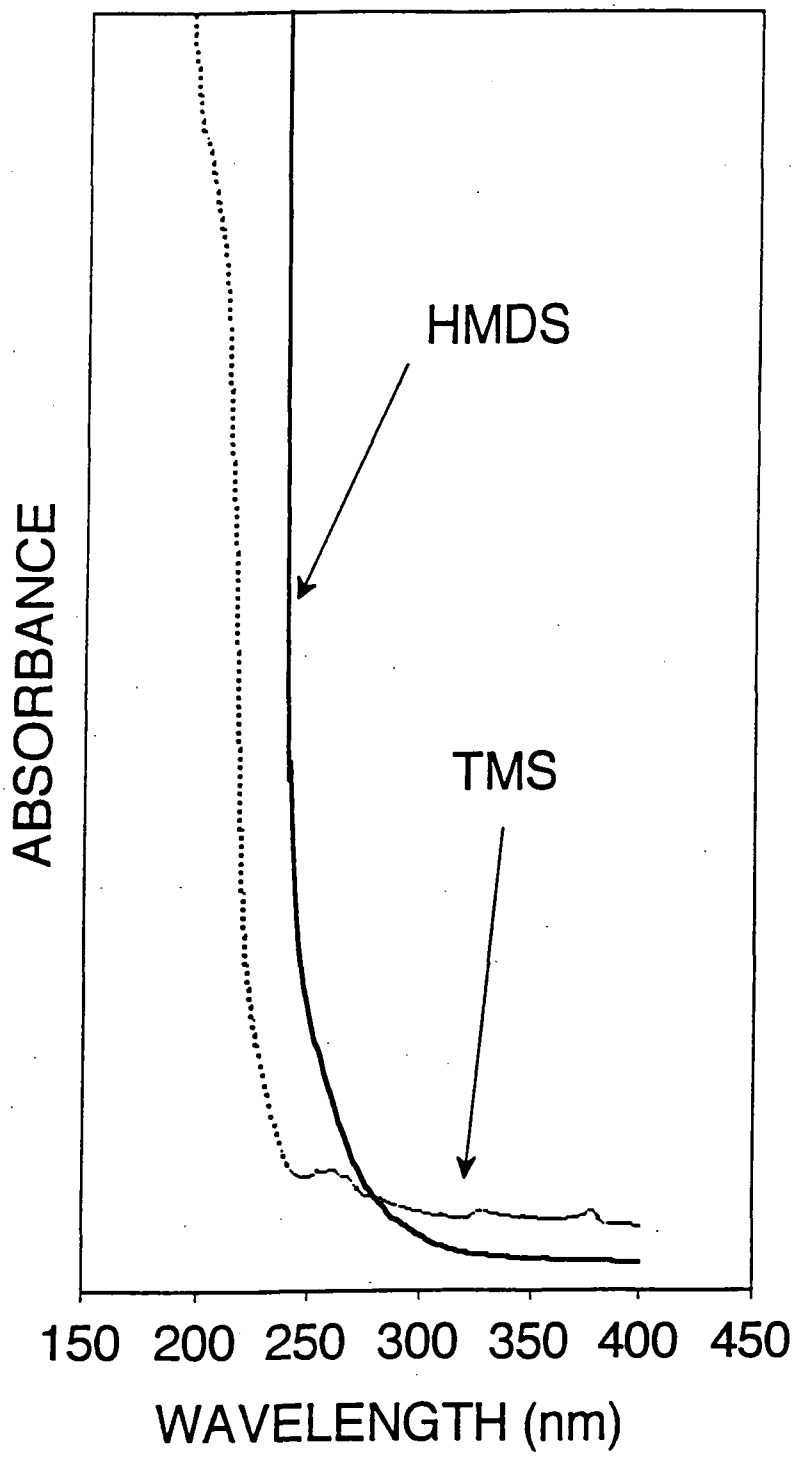

Figure 3: UV absorption spectra of hexamethlydisilane and tetramethlysilane.

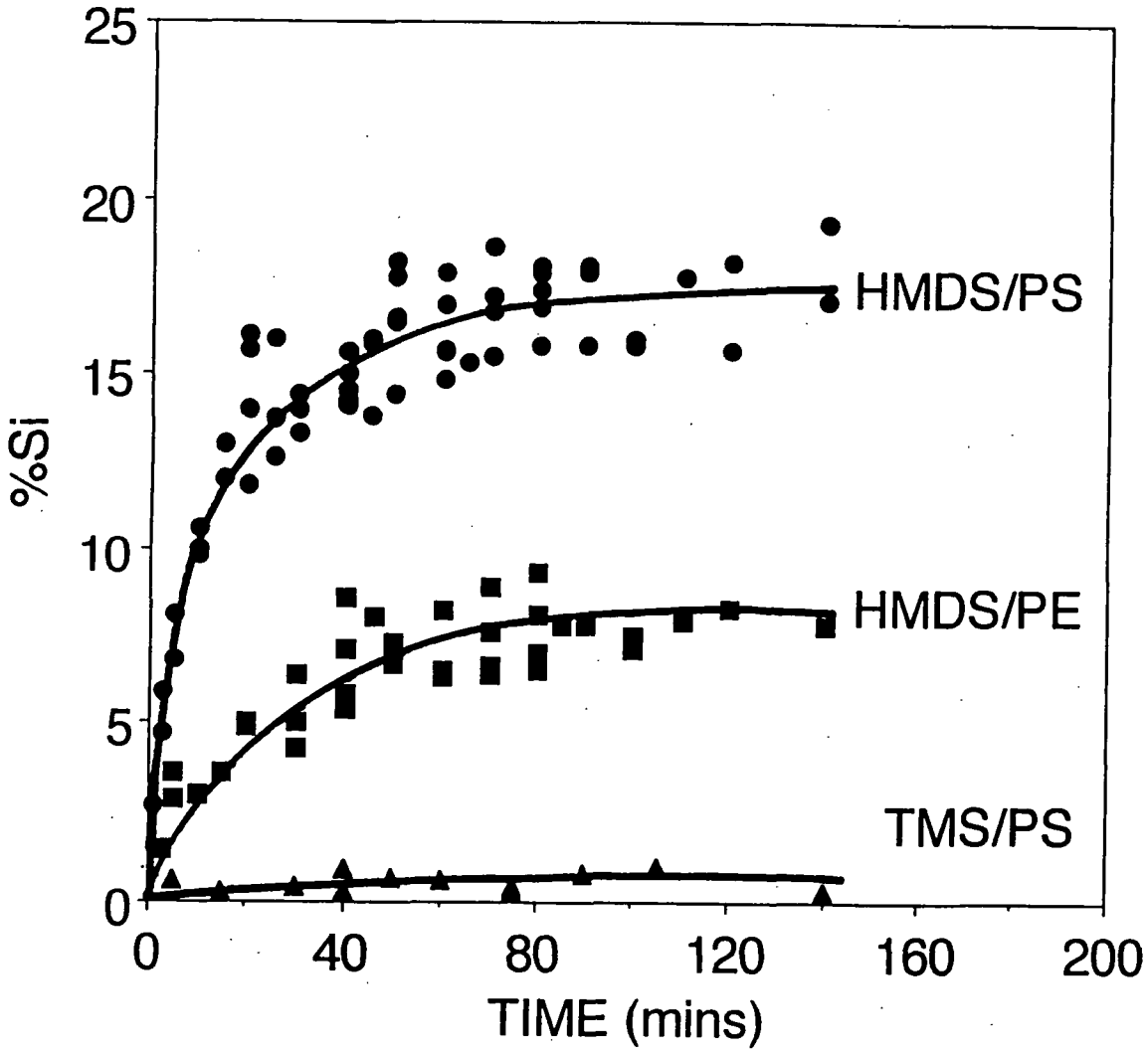

Figure 4: Irradiation induced uptake of silicon for: (a) hexamethyldisilane / polystyrene; (b) hexamethyldisilane / polyethylene; and tetramethylsilane / polystyrene. (N.B. %C + %Si + %O = 100%, as determined by XPS)

In the case of very long exposure times, a thin film of photo-polymerized HMDS material was visible on the quartz window of the reactor; this was easily cleaned by wiping with a tissue soaked in isopropyl alcohol.

Under the given experimental conditions both polystyrene and hexamethyldisilane absorb ultraviolet light, and can therefore simultaneously undergo electronic excitation into a reactive state. The strong UV absorption of hexamethyldisilane may be attributed to the Si-Si bond acting as a chromophore for the σ(Si-Si) $\rightarrow$ σ^*(Si-Si) transition[8]. The photochemical decomposition of hexamethyldisilane leads predominantly to Si-Si bond homolysis and the production of trimethylsilyl radicals[25]:

$$(CH_3)_3SiSi(CH_3)_3 \quad \text{---UV---}> \quad 2(CH_3)_3Si\cdot$$

Once generated, silyl radicals may abstract hydrogen, or add to vinyl or aromatic groups[26]. Therefore one of the most likely reaction products expected would be -Si(CH3)3 functionalities grafted onto the polystyrene surface, i.e. ~C-Si(CH3)3. On this basis, the maximum theoretical value for percentage silicon uptake would be 20%. Experimentally the amount obtained was ~17%, this is fairly close to the value predicted by this simple model. The loss in aromaticity at the polystyrene surface during reaction (as seen by the attenuation in the C(1s) π -π^* shake-up satellite) is consistent with this description.

The polymer surface arising as a result of the process postulated above is very sterically hindered due to the bulky -Si(CH3)3 species, Diagram 9.

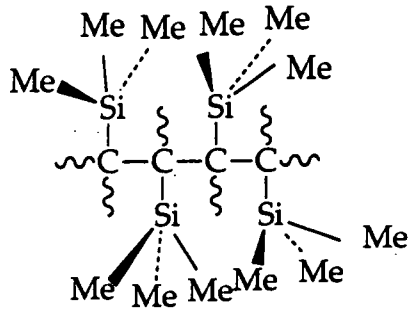

Diagram 9 : Steric restriction of the proposed -(C-Si(CH3)3)n- surface.

Other reaction routes are possible which include polymerisation of a silane upon the polymer surface and a radical reaction between the trimethylsilyl radicals with the unsaturated phenyl rings.

Once generated trimethylsilyl radicals may disproportionate in the gas phase[25,27,28] leading to silanes and highly reactive silenes:

$$2(CH_3)_3Si\cdot \quad \text{---UV---}> \quad (CH_3)_3SiH + (CH_3)_2Si{=}CH_2$$

The latter may subsequently undergo polymerization to give the surface structure illustrated below, Diagram 10.

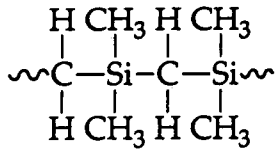

Diagram 10 : Surface structure resulting from the polymerisation of $(CH_3)_2Si{=}CH_2$

The polymerisation might be initiated by the $\cdot SiMe_3$ radical, Diagram 11.

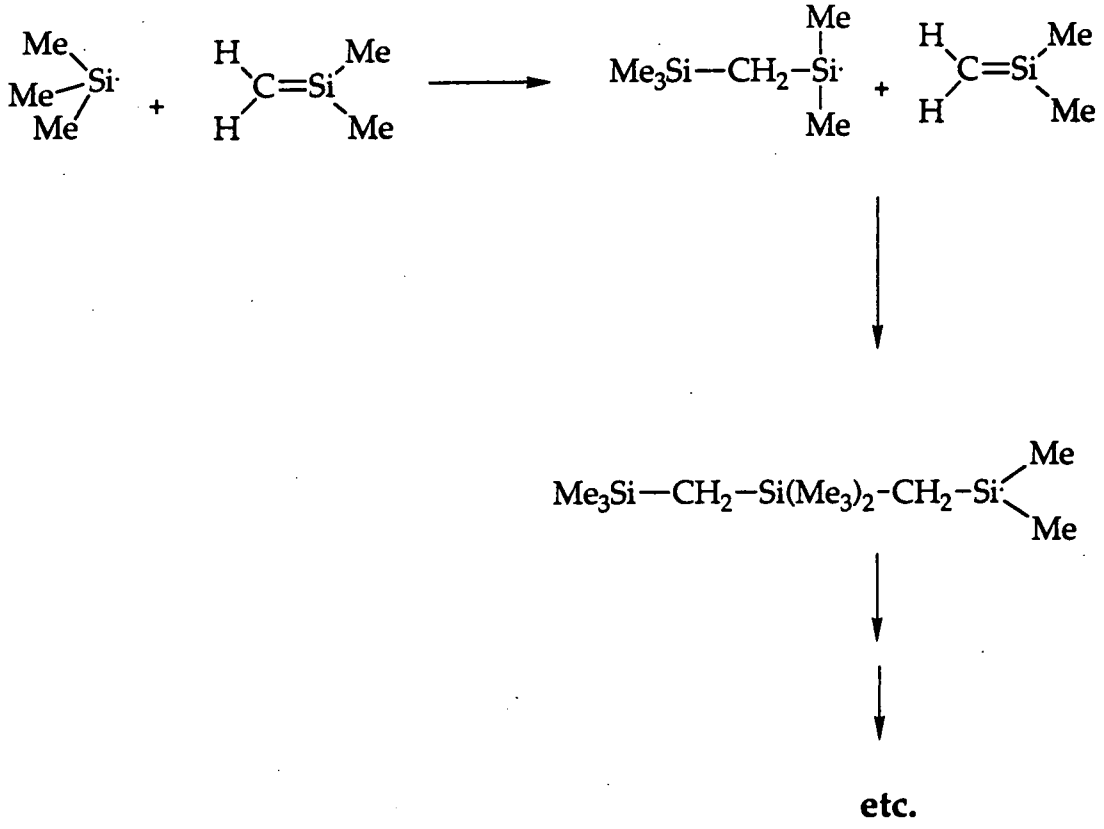

Diagram 11 : Initiation of the free radical addition polymerisation by the trimethylsilyl radical.

It seems reasonable to assume that the free radical attacks the silene at the CH_2 end for steric reasons. Termination may occur by either combination or disproportionation of the end radical[29]. The polymer produced will have a Si : C ratio of 20%.

Trimethylsilyl radicals may undergo a radical reaction with the phenyl groups in polystyrene, Diagram 12.

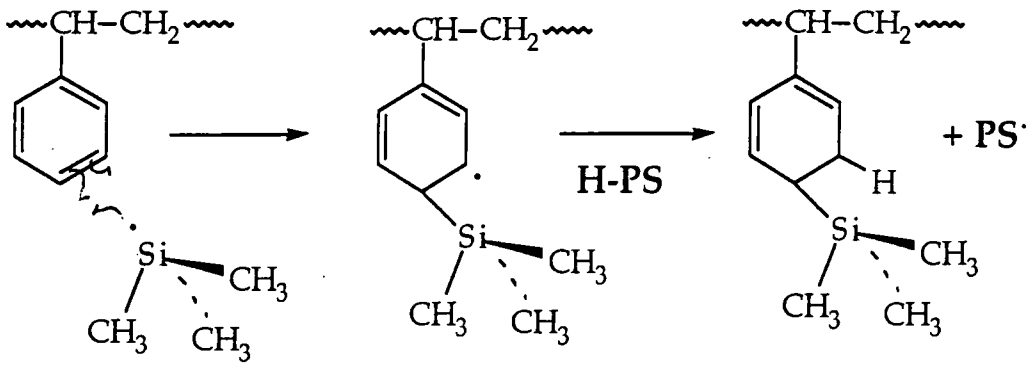

Diagram 12 : Radical reaction of trimethylsilyl radicals with the phenyl groups in polystyrene.

The radical created on the phenyl ring would abstract hydrogen[26] possibly from a neighbouring polystyrene chain. Repetition of this process might lead to a fully reacted phenyl group containing 17 carbon atoms to three silicon atoms, producing Si: C = 15%, Diagram 13.

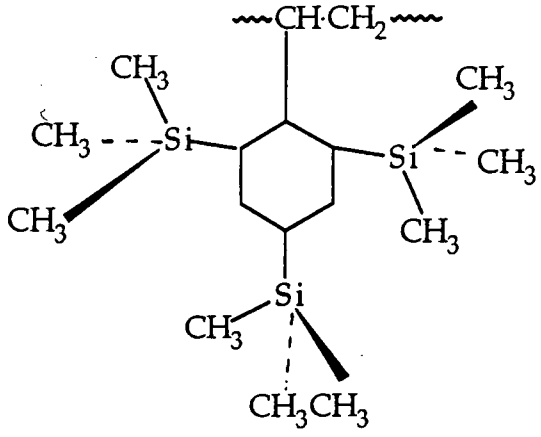

Diagram 13: Phenyl ring of polystyrene fully reacted with trimethylsilyl radicals.

The experimentally determined Si:C ratio of 17%, is consistent with the kinds of reaction postulated above although the evidence is insufficient to make an unambiguous assignment.

The film of polymerised HMDS upon the reactor window is deposited due to local heating of the quartz by the UV source.

3.3 HEXAMETHYLDISILANE / POLYETHYLENE

A weak Si(2p) signal was measurable after UV irradiation of polyethylene under a HMDS environment. The extent of silicon

incorporation into the surface increased towards a maximum value of ~ 7% over the first 40 mins. This trend mirrors the behaviour observed for polystyrene, except that the concentration of surface silicon species is greatly reduced. Again a weak O(1s) signal was measurable following reaction (~ 2%); and there was deposition of organosilicon polymer onto the quartz window.

Polyethylene does not absorb ultraviolet light above 200 nm[23]. Therefore the deposited silicon species must originate from the direct excitation and fragmentation of hexamethyldisilane (as is also found on the quartz window). The extent of reaction of HMDS with polyethylene (%Si = 7%) is much lower than with polystyrene (%Si = 17%) reflecting the enhanced reactivity at the polystyrene substrate.

The trimethylsilyl radicals may react directly with the polyethylene substrate via abstraction of hydrogen atoms, or alternatively disproportionation could occur in the gas phase[25,27,28] leading to silanes and silenes, as mentioned in 3.2 the silenes may undergo photo-polymerization leading to a simple overcoating of the substrate.

Photo-polymerisation of silenes cannot be the only factor effecting the deposition of silicon species upon the polymer surfaces, as one would expect the same extent of silicon incorporation for both polyethylene and polystyrene if this were the case. The increased silylation at the polystyrene substrate could have been a consequence of either the greater reactivity of the polystyrene towards the radicals from HMDS and/or photo-excitation through the phenyl chromophore.

3.4 TETRAMETHYLSILANE / POLYSTYRENE

Only a very small amount of silicon was detected at the polystyrene surface following exposure to UV light in the presence of TMS (~ 0.6%). This value remained constant over the whole range of exposure times, thereby indicating a relative lack of reactivity of polystyrene towards TMS compared with HMDS. Subsequent to reaction, the surface oxygen content was found to be as high as 7%. This was probably due to the photo-activated polystyrene surface reacting with the laboratory atmosphere during transport to the XPS spectrometer. In this case, no polymeric deposit was found on the reactor window following completion of an experiment.

TMS does not absorb strongly over the wavelengths accessible in these experiments (230 - 600 nm, Figure 3). Therefore the only photo-susceptible species in this study will be the polystyrene surface, which upon excitation could react with a TMS molecule, possibly via hydrogen

abstraction (a process which is reported to occur during the photolysis of polystyrene[30,31]):

$$PS\text{-}H \xrightarrow{UV} PS\cdot + H\cdot \xrightarrow{Si[CH_3]_4} PS\text{-}CH_2Si[CH_3]_3 + H_2$$

3.5 TETRAMETHYLSILANE / POLYETHYLENE

Polyethylene was found to be completely inert towards TMS under UV irradiation, even over long exposure times. As neither polyethylene or TMS absorb at the wavelengths used in these studies, no reaction would be expected for this combination of reactants. This is precisely what was found.

4. CONCLUSIONS

Polystyrene and hexamethyldisilane are strongly absorbing in the UV region, and irradiation of this system generates the greatest degree of organosilicon incorporation into the polymer surface, the mechanism cannot be unambiguously assigned. In the case of polyethylene, which is a non-chromophoric substrate, much less surface modification was attained, this can be attributed to either hydrogen atom abstraction by trimethylsilyl radicals at the substrate, or the photo-polymerization of silene (a disproportionation product of trimethylsilyl radicals). Whatever the mechanism polyethylene is less silylated by the reaction conditions than polystyrene. Tetramethylsilane is incapable of absorption at the UV wavelengths employed in these experiments and this leads to only a minor extent of reaction with polystyrene (probably via hydrogen atom abstraction by the photo-excited substrate); and no interactions at all are observed with a polyethylene surface.

It is possible that this photolysis of a HMDS / polystyrene system may prove to be effective for direct photochemical imaging during the production of submicron structures for integrated circuits, since , in principle, the pattern can be generated in one simple step via irradiation through a mask[32].

5. REFERENCES

1) Y.J Wang, C.H Chen, M.L Yeh, G.H. Hsiue, and B.C. Yu; J. Membr. Sci., 53, (1990), 275.
2) D.T. Clark and D. Shuttleworth; J. Polym. Sci. Polym. Chem. Ed., 18, (1980), 27.
3) W.L. Wade; R.J. Mammone; and M. Binder; J. Appl. Polym. Sci., 43, (1991), 1589.
4) B.D. Ratner, D.G. Castner, T.A. Horbett, T.J. Lenk, K.B. Lewis, and R.J. Rapoza; J. Vac. Sci. Technol., A8, (1990), 2306.
5) H. Steinhauser, and G. Ellinghorst; Die Angew. Makromol. Chem., 120, (1984), 177.
6) F.D. Egitto; Pure and Appl. Chem., 62, (1990), 1699.
7) D.T. Clark, and H.S. Munro; Polym. Degrad. and Stab., 3, (1981), 97.
8) T. Veszpremi, M. Feher, E. Zimonyi, J. Nagy, Acta Chim. Hung., 120, (1985), 153.
9) G. Loux, and G. Weill; J. Chem. Phys., 61, (1964), 484.
10) R. C. Jaeger, 'Introduction to Microelecrtonic Fabrication', Addison-Wesley, 1988.
11) R. D. Miller in 'Silicon Based Polymer Science - A Comprehensive Resource', ed J. M. Zeigler and F. W. Gordon, A.C.S., 1990, p431.
12) D. C. Hofer, R. D. Miller and C. G. Wilson, SPIE - Advances in Resist Technology, 469, (1984), 16.
13) P. Trefonas, R. West and R. D. Miller, J. Am. Chem. Soc., 107, (1985), 2737.
14) R. D. Miller and J. Michl, Chem. Rev., 89, (1989), 1359.
15) G. N. Taylor, M. Y. Hellman, T. M. Wolf and J. M. Zeigler, SPIE - Advances in Resist Technology and Processing V, 920, (1988), 274.
16) J. M. Zeigler, L. A. Harrah and A. W. Johnson, SPIE - Advances in Resist Technology and Processing II, 539, (1985), 167.
17) J. L. C. Fonseca and J. P. S. Badyal, Macromolecules, 25, (1992), 4730.
18) V. S. Nguyen, J. Underhill, S. Fridmann and P. Pan, J. Electrochem. Soc., 132, (1985), 1925.
19) R.K. Wells and J.P.S. Badyal; J. Polym. Sci. Polym. Chem. Edn.,30, (1992), 2677.
20) G. Johansson, J. Hedman, A. Berndtsson, M. Klasson, and R. Nilsson; J. Electron Spectr., 2, (1973), 295.
21) M.H. Wood, M. Barber, I.H. Hillier, and J.M. Thomas; J. Chem. Phys., 56, (1972), 1788.
22) D.T. Clark and A. Dilks; J. Polym. Sci. Polym. Chem. Edn., 15, (1977), 15.

23) J. F. McKeller, and N. S. Allen; 'Photochemistry of man-made polymers', Applied Science Publishers Ltd, London, (1979), p.11.
24) A. Gheorghiu, C. Senemaud, H. Roulet, G. Dufour, T. Moreno, S. Bodeur, C. Reynaud, M. Cauchetier, and M. Luce; J. Appl. Phys., 71, (1992), 4118.
25) T. Brix, E. Bastian, P. Potzinger; J. Photochem. Photobiol. A : Chem., 49, (1989), 287.
26) J.W. Wilt, in 'Reactive Intermediates', Ed, R.A. Abramovitch, Plenum (New York), (1983), Chapter 3.
27) G. Raabe, and J. Michl; J. Chem. Rev., 14, (1985), 419.
28) J.A. Hawari, D. Griller, W.P. Weber, and P.P. Gaspar; J. Organomet. Chem., 326, (1987), 335.
29) J. M. J. Cowie, 'Polymers: chemistry and Physics of Modern Materials', Intertext, 1973, Chapter 3.
30) N. Grassie, and N.A. Weir; J. App. Polym. Sci., 9, (1965), 963.
31) J.F. Rabek, and B. Ranby; J. Polym. Sci., Polym. Chem. Edn., 12, (1974), 273.
32) R.D. Miller, D. Hofer, G.N. Fickes, C.G. Willson, E.E. Marinero, P. Trefonas, and R. West; Polym. Eng. Sci., 26, (1986), 1129.

CHAPTER 7

THE PHOTODEGRADATION OF PVC

1. INTRODUCTION

Degradation in PVC can occur thermally or photochemically[1,2,3]. The photochemical process is initiated by chromophoric species which are present as defects in the polymer chain, such as alkene linkages, carbonyl groups, hydroperoxide groups, or impurities in the matrix of the polymer, such as metal salts[2,3,4]. Once initiated the degradation continues via a zipper mechanism to produce short, conjugated polyene chains[2,3,5].

The degradation of PVC alters both its appearance and its mechanical properties[6,7]. Yellowing of the polymer is observed,[2,3,8,9,10,11] when the conjugated polyene sequence length exceeds about 5 units[3,12].

1.1 INITIATION

The reasons for the susceptibility of PVC to UV light are not yet fully understood[12,13]. PVC contains only saturated bonds (C-C; C-H; C-Cl) which absorb at wavelengths of less than 200nm[12,13]. Since PVC has been observed to absorb terrestrial sunlight (which has wavelengths λ>290nm) it must contain some solar radiation absorbing chromophores as either external impurities or functional groups incorporated into the polymer backbone[9,12-16]. These impurities are likely to be introduced at the processing stage, during which the material is subjected to very high thermal and mechanical stress leading to the possibility of the elimination of a small amount of HCl[14,17]. The resultant double bonds and consequent allyl-activated chlorines are potential sites for the initiation of PVC degradation. The actual structural irregularities which result depend very strongly on the method of processing used[16]. The most likely structural defects are alkene linkages, carbonyl and peroxide groups[12]. The order of importance of these photosensitising species is alkenes>carbonyls>peroxides[12].

1.2 MECHANISM

The UV deterioration mechanism for PVC is still unclear[2,3,4,12,16,18]. The way PVC undergoes photodegradation is very dependent on experimental conditions, so that no unique mechanism is expected to operate in all cases[12].

1.2.1 Photolysis

The overall reaction for photolysis may be written:[16]

$$\sim CH_2CHClCH_2CHCl\sim \xrightarrow{h\nu} \sim CH_2CHClCH{=}CH\sim + HCl$$

Which leads eventually to:

$$\sim(CH_2CHCl)_n\sim \xrightarrow{h\nu} \sim CH_2\text{-}CHCl\text{-}(CH{=}CH)_n\text{-}CH_2\text{-}CHCl\sim + nHCl$$

where there is some dispute over possible values of n. Values ranging from 5-10, up to 20 for extended irradiation times[12,16] have been proposed.

The most popular mechanism suggested for the dehydrochlorination of PVC below 200 nm is the free radical mechanism[2] Scheme 1:

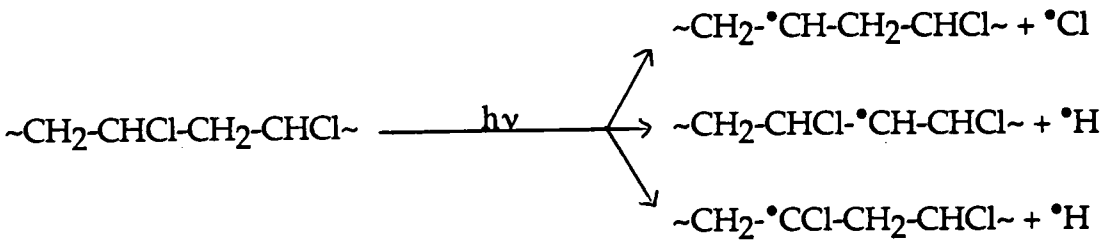

Scheme 1: Initial radical formation in PVC[2].

Above 200 nm the mechanism is more complex as radicals cannot be directly formed via PVC light absorption. However, once radicals are generated on the polymer chain dehydrochlorination would be expected to proceed by the same mechanism.

Any •Cl formed may then abstract a hydrogen atom, Scheme 2:

$$\sim CH_2\text{-}CH^{\bullet}\text{-}CH_2\text{-}CHCl\sim + {}^{\bullet}Cl \longrightarrow \sim CH_2\text{-}CH{=}CH\text{-}CHCl\sim + HCl$$

Scheme 2: HCl formation.

Further dehydrochlorination occurs by the 'zipper' process, Scheme 3:

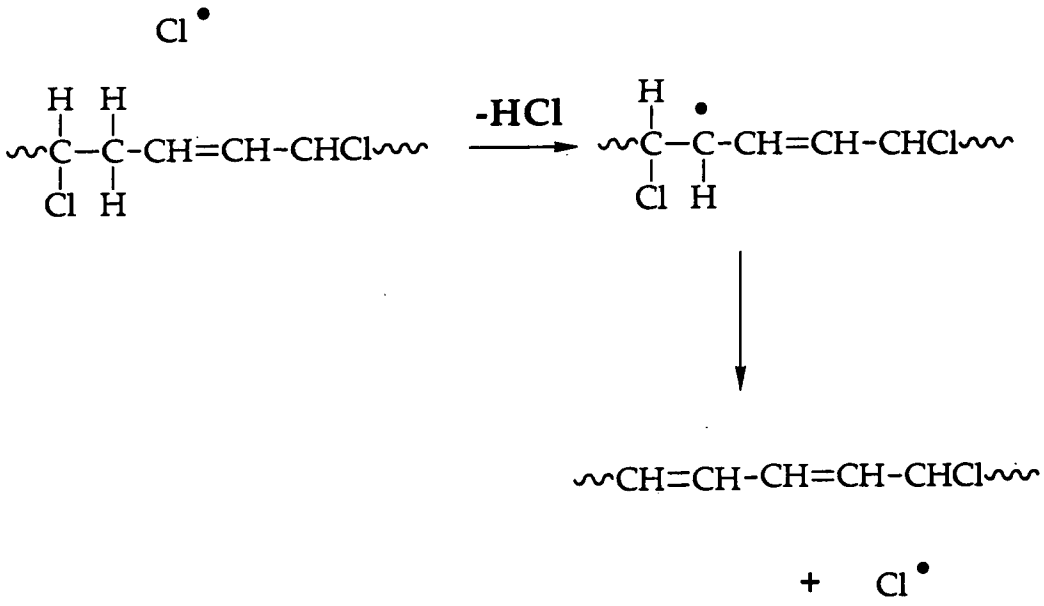

Scheme 3: The 'Zipper' mechanism.
This process is autocatalytic as each dehydrochlorination produces another $Cl^{\bullet}$ radical.

1.2.1.1 Excited Singlet Polyenes

Once polyene structures are formed in the PVC further reactions may occur following absorption of light by these species[10]. This produces singlet polyenes which are known to be short lived species which can undergo various deactivation processes and reactions[10], Scheme 4:

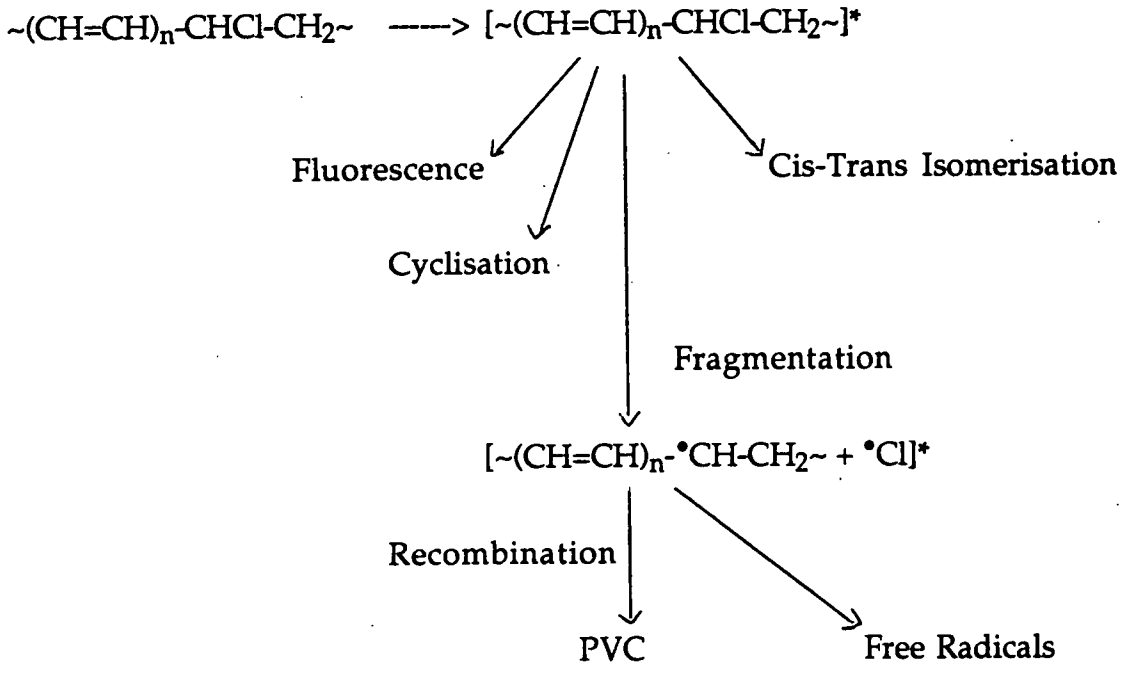

Scheme 4 : Generation and destruction of excited singlet polyenes[10].

A low value for the dehydrochlorination quantum yield is reported which reveals that an overwhelming majority, over 99%, of the excited polyenes disappear by processes other than fragmentation[10]. Photocleavage is expected to mainly involve the weakest linkage, ie. the C-Cl, bond to yield polyenyl and chlorine radicals. These radicals are thought to have limited mobility in a solid polymer at temperatures below Tg, so cage recombination is expected to take place to a large extent. This is highlighted by the observation that dehydrochlorination of PVC develops ten times more effectively in solution than in the solid state[10].

1.2.1.2 Chain Scission and Crosslinking.

The postulated ~•CH-CH_2~ and ~•CCl-CH_2~ species will be susceptible to conventional β scission processes with formation of a double bond at the end of one fragment and a •CHCl~ radical on the other[10], Scheme 5:

~•CH-CH_2-CHCl~ ——> ~CH=CH_2 + •CHCl~

~•CCl-CH_2-CHCl~ ——> ~CCl=CH_2 + •CHCl~

Scheme 5: Unsaturated chain end formation[10].

Recombination of ~•CH-CH_2~ and ~•CCl-CH_2~ will form crosslinks with the possible combinations, Scheme 6:

~CH-CH_2~ ~CH-CH_2~ ~CCl-CH_2~
| | |
~CH-CH_2~ ~CCl-CH_2~ ~CCl-CH_2~

Scheme 6: Crosslinking processes[10].

1.2.2 Photo-oxidation

In the presence of oxygen peroxy radicals may be generated on the polymer[2], Scheme 7:

~•CH-CHCl~ + O_2 ——> ~CH(OO•)-CHCl~

Scheme 7: Peroxy radical formation[2].

which may then abstract a hydrogen atom to give a hydroperoxide, Scheme 8; these two steps being the basis of a possible auto oxidation mechanism.

$$\sim CH(OO^{\bullet})\text{-}CHCl\sim + \sim CH_2\text{-}CHCl\sim \rightarrow \sim CH(OOH)\text{-}CHCl\sim + \sim {}^{\bullet}CH\text{-}CHCl\sim$$

Scheme 8: Hydroperoxide formation[2].

Hydroperoxy groups subsequently decompose under UV irradiation to give carbonyl groups[5].

1.2.2.1 Photo-oxidation Vs Zip Dehydrochlorination

The quantum yield for dehydrochlorination increases in the presence of oxygen therefore the β-chloropolyenyl radical responsible for the zip dehydrochlorination must not be scavenged by oxygen[10].

Scavenging of oxygen by other macro radicals leads to hydroperoxy radicals which may abstract hydrogen to form hydroperoxides which subsequently decompose to produce alkoxy radicals and eventually alcohols and ketones[10].

1.3 EFFECTS OF ADDITIVES ON PHOTODEGRADATION OF PVC

Additives, such as TiO_2 or ZnO are used as pigments[19], and are known to catalyse the photo-oxidation of some polyenes by generating photoactive species[12]. However, TiO_2 has been shown to provide some protection against photodegradation of PVC[12] by retarding the formation of carbonyl groups, hydroperoxides and polyenes.

Organotin compounds are highly efficient stabilisers against PVC thermal degradation, and those in general use have structures of the type $R_nSnX_{(4-n)}$, where R is normally an alkyl group (usually methyl, butyl or octyl) and X is one of a large number of saturated or unsaturated carboxylate (X = R-COO) or mercaptide (X = SR) derivatives[12]. In general sulphur-containing organo-tin compounds offer good protection against thermal degradation but no photoprotection[20], whereas sulphur free organo-tin compounds confer a good degree of photostability and have the advantage, for some applications, of being sulphur free[12,20]. Organo-tin stabilisers act by replacing the labile allylic chlorines in the polymer by more stable groups[12,17] . In addition, organo-tin mercaptides are able to deactivate hydroperoxide groups via decomposition, and function as HCl acceptors (HCl may have a catalytic effect on degradation of PVC)[12].

1.4 LITERATURE REVIEW OF EXPERIMENTAL METHODS FOR MONITORING PVC DEGRADATION

Dehydrochlorination is the proposed mechanism for PVC degradation. The evolution of HCl in the presence of UV has been detected by titration[10,20,21] and conductimetrically[4,18]. Gas chromatography was employed to monitor the evolution of gases from the interaction of ^{60}Co γ radiation and PVC[22]. The experiment was designed to simulate the degradation of PVC jacketing material used in nuclear reactors[22,23]. HCl, H_2, CH_4, CO_2, and CO were detected both in vacuum conditions and in the presence of oxygen.

Several workers have monitored a build up in the rate of HCl production with time to a maximum steady state[18,4]. This effect is thought to be due to initiation by an initial low concentration of photo-sensitising impurities such as carbonyls and hydroperoxides[18]. Tacticity is also said to effect the quantum yield of HCl elimination[15,24]. By studying the literature it seems apparent that this induction period is due to swapping mechanisms[10] from initiation by polymer impurity chromophores to the zipper mechanism leading to polyene sequences which are produced in large amounts and have high absorbancies[10].

XPS has been used to monitor the chlorination and subsequent dehydrochlorination of PVC. In the chlorinated PVC both $\underline{C}H_2$ and $\underline{C}HCl$ peaks were observed in the C(1s) spectrum, however after irradiation with a KrF laser a single sharp component (which was unassigned in the paper but was probably due to carbon not directly attached to chlorine) with a tail at higher binding energies ascribed to the formation of oxidation products at the surface was observed.[25].

Polyene chain lengths have been measured by UV absorbence spectroscopy[20,10]. The position of the polyene absorbence shifts to larger wavelengths as the polyene chain length increases[20,10].

Oxidation of PVC has been monitored by IR[4,5] and by iodometric titration of -OOH groups on the polymer[10].

1.5 APPLICATIONS

Attempts have been made to produce a conducting layer of a polyene sequence on the surface of PVC using photodegradation techniques[25,27].

Irradiation of plasticised PVC with UV light has been shown to reduce or almost prevent plasticiser migration from the polymer into high viscosity oils[28]. This effect is important in foodstuffs and pharmaceuticals packaging to prevent leakage of plasticisers into the contents. The prevention is thought to be due to crosslinking of the polymer surface hence preventing migration of the plasticiser[28].

1.6 SUMMARY

Whichever chromophores are involved in the initiation of PVC degradation during the early stages of exposure to UV light, it is to be expected that the formation and photolysis of the polyene products will become the predominant photochemical reaction owing to the high intrinsic absorption of these chromophores and their large rate of production[12]. The excited polyenes formed stabilise by splitting off an allylic chlorine atom, initiating the zip-dehydrochlorination process through the $Cl^{\bullet}$ radical, and an oxidation process through the polymer backbone radical.

In this chapter, a study of the photodegradation of PVC under different atmospheres by XPS is described, and the dehydrochlorination in vacuum, monitored using a quadrupole mass spectrometer, is reported. Monitoring the species evolved from the polymer surface during UV irradiation may allow a reaction mechanism to be established.

2. EXPERIMENTAL

Unplasticised PVC film(Goodfellows) was degreased in iso-propyl alcohol using an ultrasonic bath for 30 seconds. Elemental analysis and atomic absorption spectroscopy respectively gave 5.37% Ti and < 0.05 % (i.e. beyond the limits of experimental sensitivity) tin by weight in the polymer .

Pure PVC powder (Hydropolymers) was dissolved in tetrahydrofuran (THF) to make a ~ 3% w/w solution. This was subsequently spin coated onto a quartz substrate to form a thin film.

2.1 ULTRAVIOLET IRRADIATION UNDER DIFFERENT ATMOSPHERES

A glass reactor with a quartz port (cut off wavelength 180-200 nm) was used for irradiating the sample. The UV source was an Oriel 200W low pressure Hg-Xe arc lamp operating at 100W which produced a strong line spectrum in the 240-600 nm region.

Samples were positioned facing the quartz window of the reactor. When irradiation under oxygen, nitrogen or argon was required, the gas was passed through the reactor continuously before, during and after UV irradiation at atmospheric pressure.

For irradiation under vacuum conditions a cold trap was added to the system, and a rotary pump used to achieve a base pressure of better than 3 x 10^{-2} Torr. In this case, the system was pumped continuously before, during and after UV irradiation.

For irradiation in air, the reactor was left open to the atmosphere whilst the UV lamp was on.

X-ray photoelectron spectroscopy measurements were made using a Kratos ES300 surface analysis instrument (base pressure ~6 x 10^{-10} Torr). MgKα radiation was used as the excitation source with electron detection in the fixed retarding ratio (FRR) analyser mode. XPS spectra were acquired at an electron take-off angle of 30° from the surface normal. Data accumulation and peak area analyses were performed using an IBM computer. Instrumentally determined sensitivity factors are such that for unit stoichiometry, the C(1s) : O(1s) : Cl(2p) : Sn($2d_{5/2}$) intensity ratios are 1.00 : 0.55 : 0.35 : 0.11 respectively.

An exposure time of 140 minutes was found to result in a significant degree of photodegradation.

2.2 *IN SITU* MASS SPECTROMETRY ANALYSIS

Experiments were carried out in an ultra high vacuum chamber which had a base pressure of 8 x 10^{-10} Torr. This was equipped with a VG SX200 quadrupole mass spectrometer which had been multiplexed to a PC computer. An Oriel 200W low pressure Hg-Xe arc lamp operating at 50 Watts which emitted a strong line spectrum in the 240-600 nm region was used to irradiate the sample through a sapphire window which gave a cut-off wavelength of 141-161 nm. A pure PVC (prepared as described above) sample was inserted into the chamber via a fast insertion lock, and positioned in line with the mass spectrometer and the sapphire window (at an angle of 45° to the vertical).

The acquisition of data was carried out in real time during the photolysis experiment. A total of 200 data points were collected during each run. Initially a shutter was in place to shield the chamber from the UV light. Background spectra were recorded over a number of mass ranges from 1-150 amu. After 10 minutes the shutter was removed and the sample irradiated for 10 minutes before mass spectra were recorded over the same mass ranges. The shutter was replaced and the sample allowed to degas again before this sequence was repeated. Comparison of the spectra obtained by these shutter manipulations indicated the masses whose intensities increased most during irradiation, and these were subsequently monitored with respect to time to produce peak profiles.

3. RESULTS and DISCUSSION

3.1 CLEAN PVC

The analysis of pure PVC (Hydropolymers) by XPS gave a peak in the C(1s) region which could be resolved into two peaks, one at 285.90 eV for Cl-C-C-H and one at 287.00 eV for C-Cl in a ratio of 1:1[29], Spectrum 1a. The Cl(2p) region consisted Cl $2p_{3/2}$ at 200.64 eV and Cl $2p_{1/2}$ at 202.24 eV[29], Spectrum 1b. The chlorine (2p) to carbon (1s) ratio was 0.50 ± 0.01 (allowing for instrumentally determined sensitivity factors) with no oxygen. Unplasticised PVC (Goodfellows) with additives of TiO_2 pigment and an organotin stabiliser showed Cl (2p) : C (1s) of 0.43 ± 0.03 and O (1s) : C (1s) of 0.05 ± 0.01. Tin and titanium were not seen on the polymer surface by XPS. The theoretical value of Cl (2p) : C (1s) in PVC is 0.5

3.2 ULTRAVIOLET IRRADIATION UNDER DIFFERENT ATMOSPHERES

3.2.1 Loss of chlorine / Addition of oxygen (Pure PVC)

Under all conditions a reduction in Cl (2p) : C (1s) was seen by XPS, (Figure 1) for pure PVC. The general trend observed was a reduction of Cl (2p) : C (1s) in the order:

vacuum > nitrogen ~ argon > air ~ oxygen

i.e. vacuum conditions produced the smallest Cl (2p) : C (1s) ratio.

After irradiation under vacuum a shift in the position of the C-H component of the C(1s) peak was observed to 285.02 eV as compared to 285.9 eV in clean PVC. This shift was probably due to the less electronegative

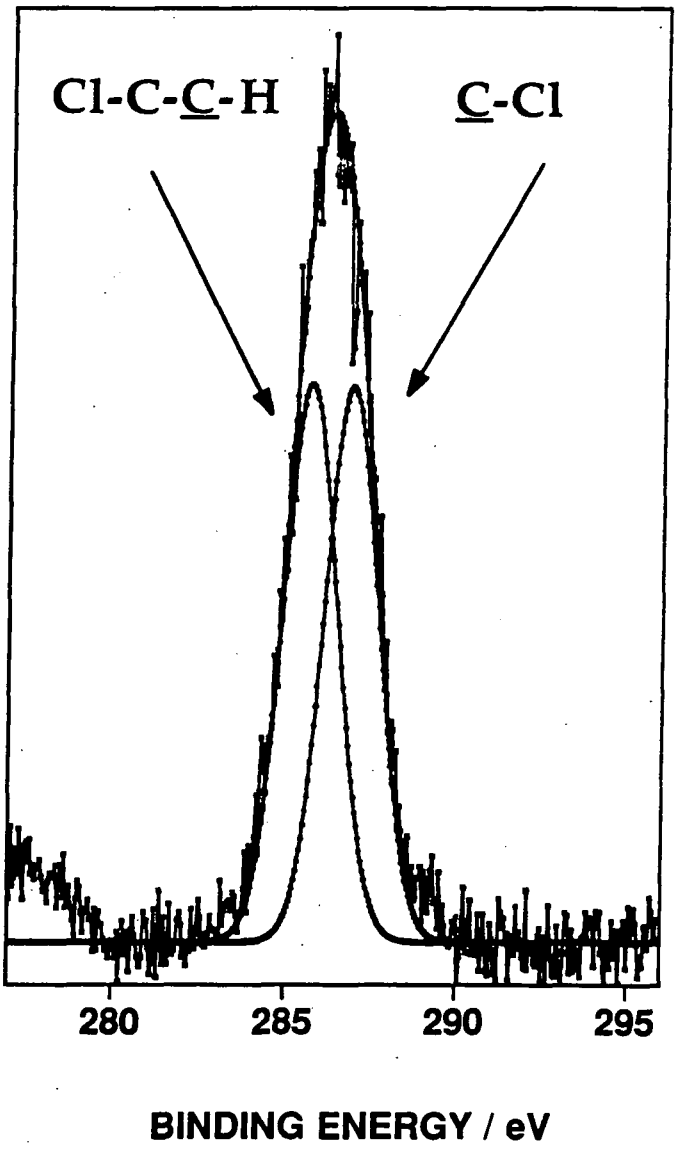

Spectrum 1a : XPS C (1s) region for clean PVC

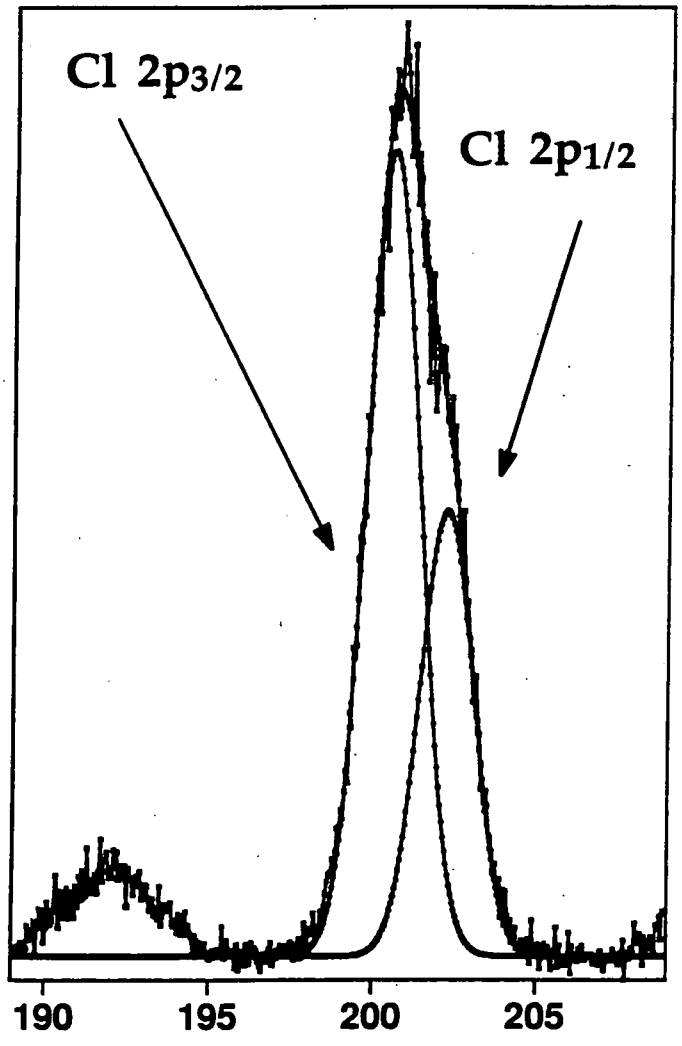

Spectrum 1b : XPS Cl (2p) region for clean PVC

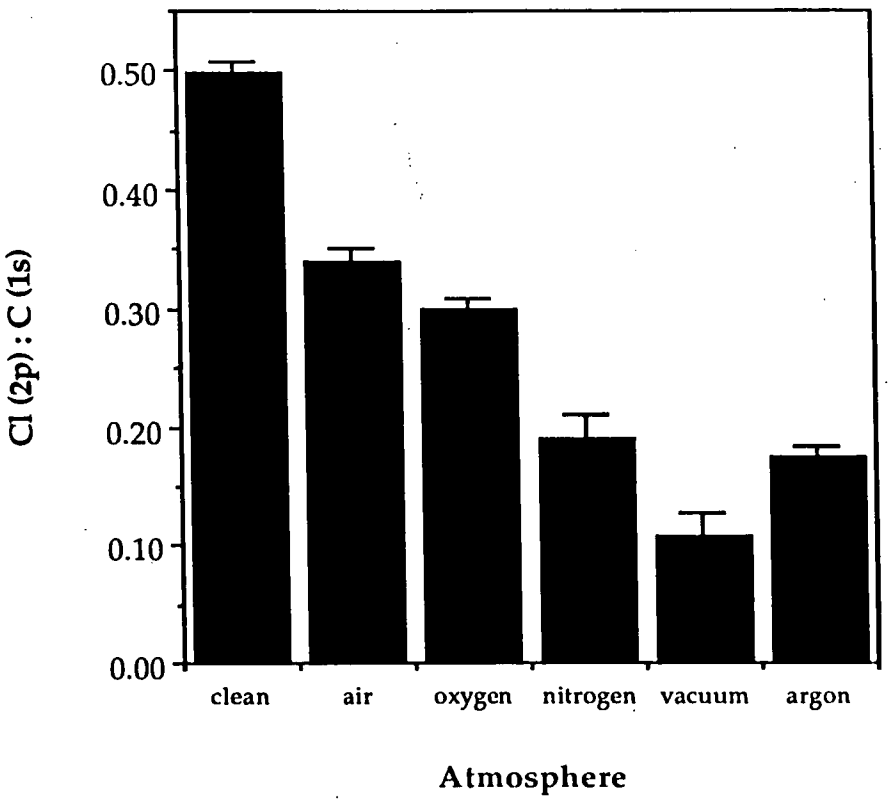

Figure 1: Pure PVC Cl (2p) : C (1s) ratios during photodegradation under different atmospheres as determined by XPS.

environment for the carbons at the surface in UV treated PVC. The C-Cl component of the C(1s) peak was reduced in intensity as compared to the C-H peak, and oxygenated functionalities were observed at 286.6 eV (C-O), 287.9 eV (C=O) and 289.0 eV (O-C=O)[30], See spectra 2a+b.

All conditions resulted in oxygen incorporation into the surface of pure PVC (Figure 2). For pure PVC the trend for oxygen uptake in different atmospheres is:

oxygen> air ~ argon > nitrogen > vacuum

The loss of chlorine is greatest during irradiation under vacuum conditions and oxygen incorporation is smallest. This can be explained as unhindered loss of HCl from the polymer. There are no other species present to react with initiating free radicals once generated. The small amount of oxygen on the modified PVC could have occurred during transfer from the reactor to the XPS spectrometer, or due to a small leakage of air into the reactor (although the leak rate was small, less than 3.12×10^{-3} cm^3min^{-1}).

During irradiation under argon and nitrogen, one may expect similar results as for vacuum conditions as these gases are inert under these experimental conditions. However, less chlorine is lost than under vacuum, and more oxygen incorporation is observed. This observation may be due to a loss of flux of the UV source due to scattering by the argon and nitrogen gases[31]. Upon removal from the reactor, reactive sites still present on the surface may undergo reaction with oxygen in the laboratory atmosphere.

Air and oxygen atmospheres show the least reduction in Cl(2p) : C(1s). Under both of these conditions, free radicals generated in the polymer surface have alternative reaction pathways other than loss of HCl. Reaction with oxygen to form peroxy-type linkages is possible[2]. This is further highlighted in the values of O(1s) : C(1s), which are greatest in the reactions in oxygen and air.

3.2.2 Appearance of tin (unplasicised PVC)

The same trends for loss of chlorine and addition of oxygen were seen with unplasticised PVC (which contained additives of TiO_2 and an unidentified tin compound). Therefore the addition of TiO_2 pigment and a tin stabiliser produces a surface as reactive under ultraviolet light as pure PVC, as far as dehydrochlorination and photo-oxidation is concerned.

Tin was not detected at the surface of clean unplasticised PVC, however upon irradiation a small quantity (< 2% maximum) of tin was

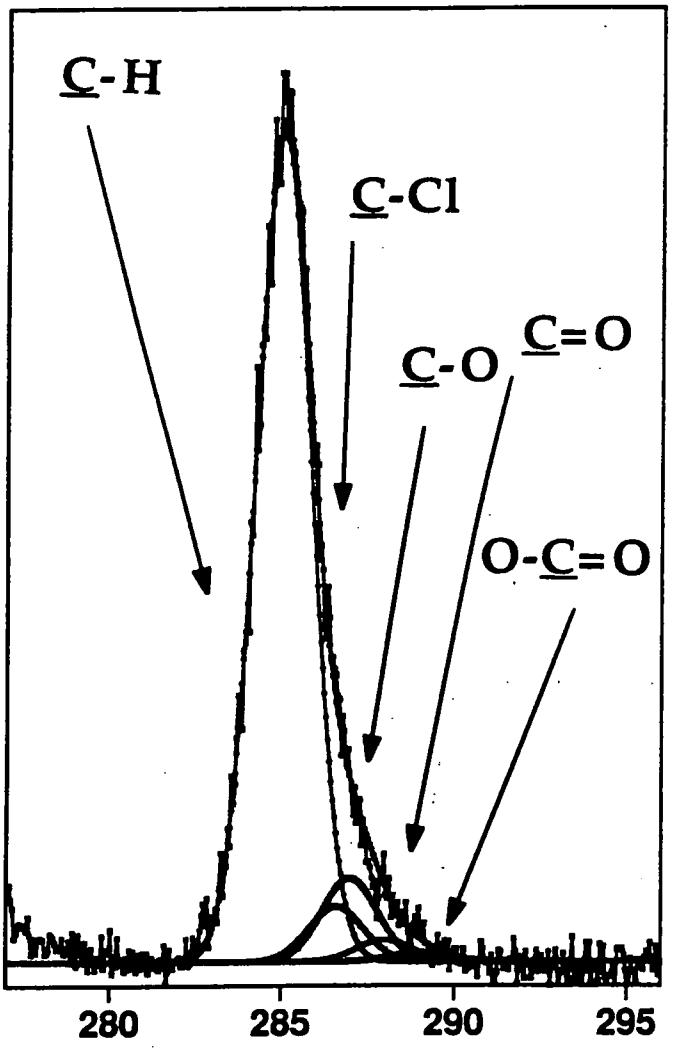

Spectrum 2a : XPS C (1s) region for PVC after 140 min UV irradiation under vacuum conditions.

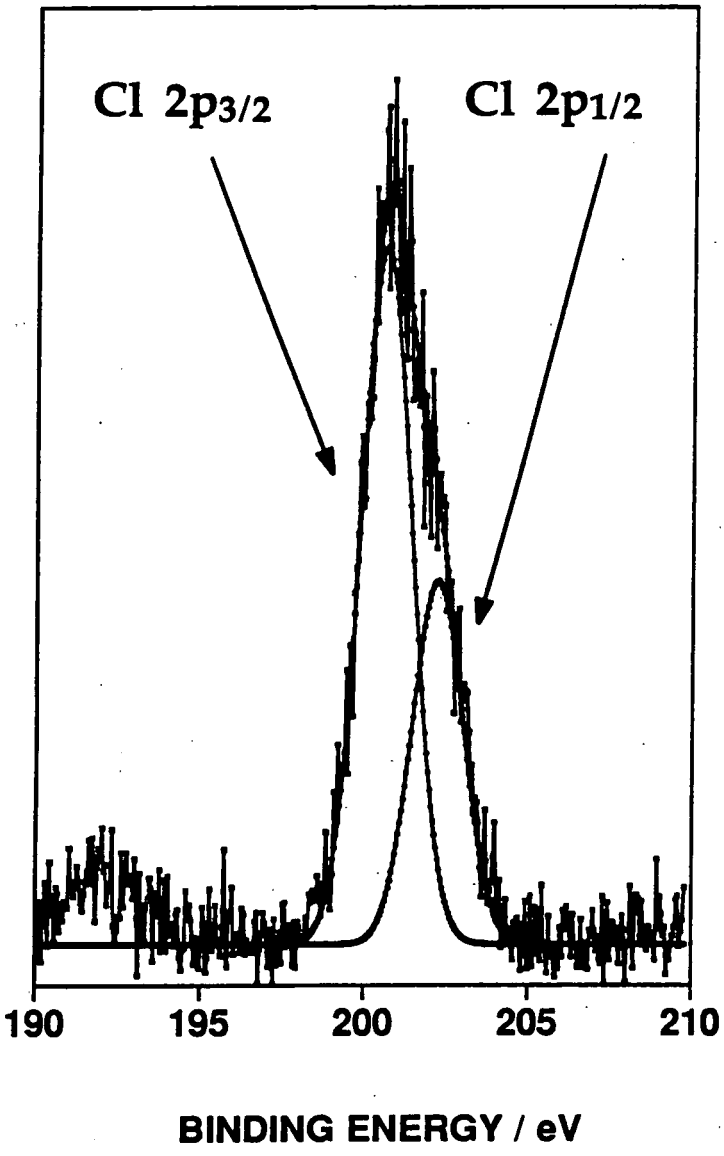

Spectrum 2b : XPS Cl (2p) region for PVC after 140 min UV irradiation under vacuum conditions.

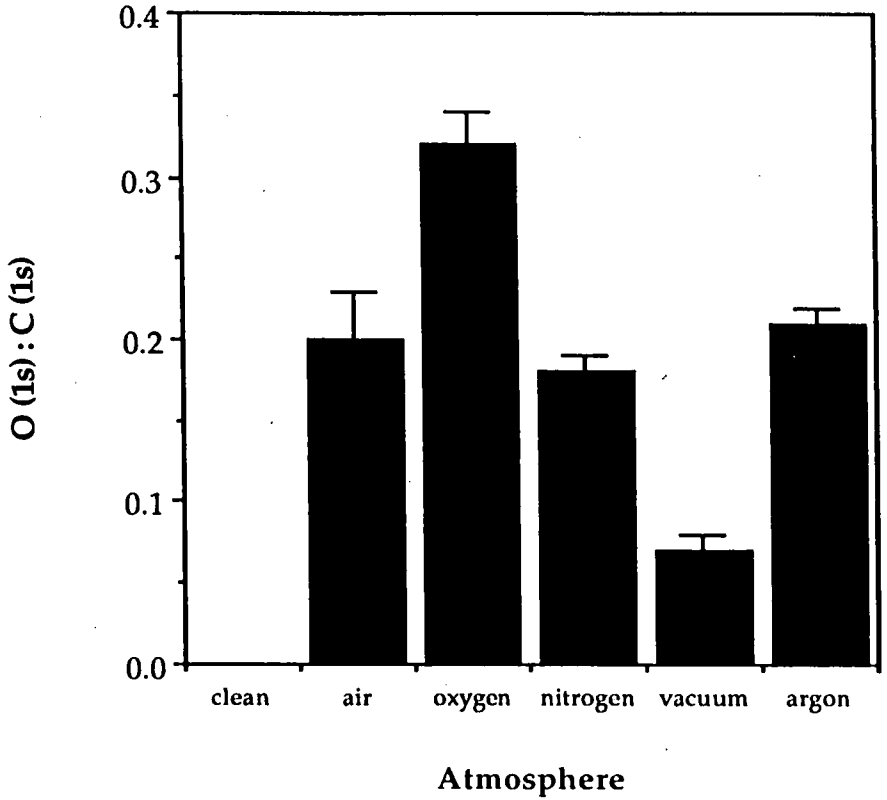

Figure 2: Pure PVC O (1s) : C (1s) ratios during photodegradation under different atmospheres as determined by XPS.

seen. The Sn ($2d_{5/2}$) : C (1s) ratio was plotted as a function of atmosphere (Figure 3). The trend observed was:

argon > air > nitrogen > oxygen > vacuum

No sulphur was seen in elemental analysis of the polymer, therefore the tin containing compound was assumed to be a sulphur-free organo-tin stabiliser. Sulphur-free organotin compounds are efficient stabilisers against thermal and photochemical degradation. TiO_2 is known to catalyse photodegradation by generation of photo-active species[12,19], but has also been observed to provide some photo-protection to PVC[12].

The appearance of tin on the polymer surface after UV irradiation can be explained in two ways:

i) PVC is ablated from the polymer surface during degradation but the tin compound is not, therefore leaving a surface rich in tin.

ii) Tin compounds migrate from the bulk polymer to the surface during irradiation.

Although quantities are very small, it seems certain that most tin appears during irradiation under an argon atmosphere, and least in vacuo. Volatilisation of the tin compounds could be the reason for the results observed in vacuum. In the case of air and oxygen atmospheres tin species may be lost through oxidative attack and subsequent vaporisation. Argon is inert and at positive pressure, so no escape route is present for the tin compounds under these conditions. Also attenuation of the photon flux can cause a build-up of tin in the argon and nitrogen cases.

3.3 *IN SITU* MASS SPECTROMETRY ANALYSIS (PURE PVC)

Upon exposure of pure poly(vinyl chloride) to ultra-violet light, the signals of the following masses were observed (listed in order of decreasing intensity and uncorrected for mass spectrometer sensitivity):

41, 28, 18, 29, 27, 2, 36, 39, 43, 26, 15, 57, 44, 38, 56, 1, 35, 31, 69, 54, 37, 66, 65, 94, 84, 83, 85, 77, 91, 78, 76, 121, 119

However, this order changed during subsequent exposures to ultraviolet light (see later). These masses are assigned in sections 3.3.3 and 3.3.4.

During UV irradiation, all masses show an increase in peak intensity. Most mass signals tail off to the original background level following the shuttering of the UV light (Figure 4, mass 36).

These results demonstrate that most species continue to evolve from the surface after the surface excitation has been terminated, thus the

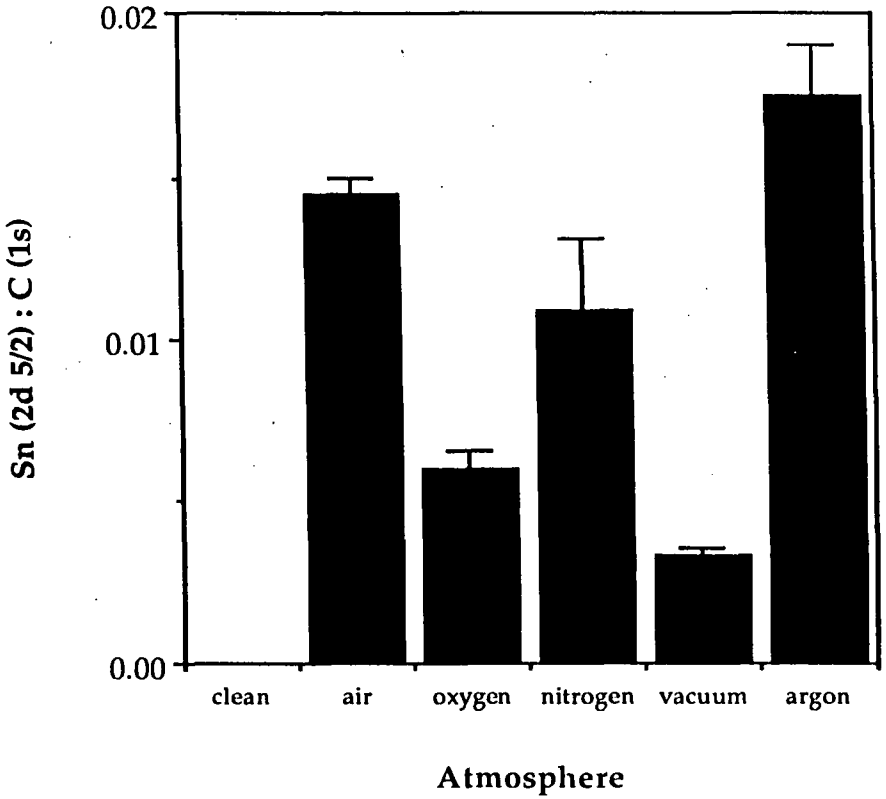

Figure 3: Unplasticised PVC Sn ($2d_{5/2}$) : C (1s) ratios during photodegradation under different atmospheres as determined by XPS.

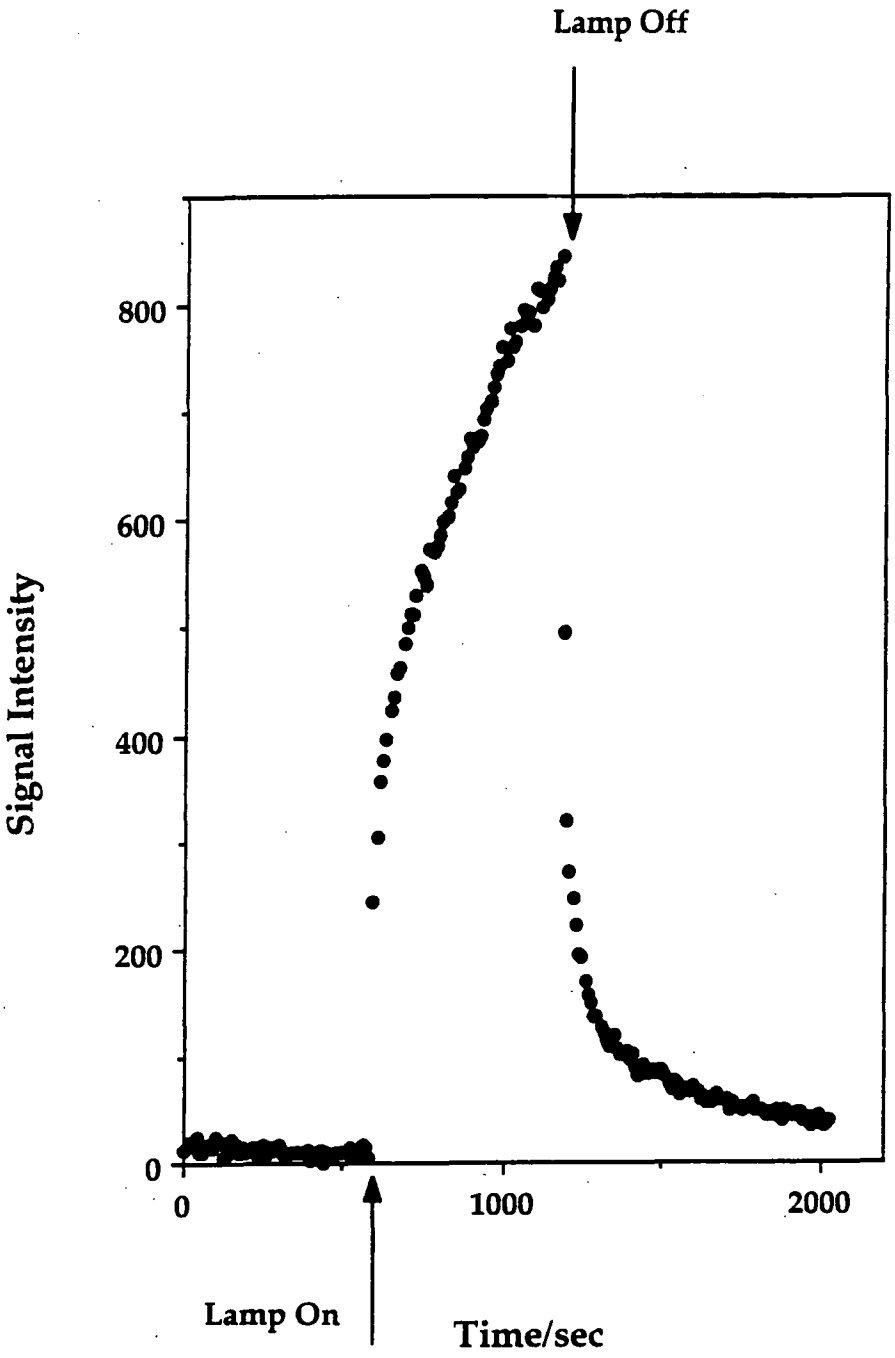

Figure 4: Mass 36 intensity profile for pure PVC (before, during, and after UV irradiation).

polymer surface must take some time to reach a stable state following photolysis. This fits with the hypothesis that the surface remains reactive following irradiation of the polymer for XPS studies, and could react with oxygen from the atmosphere.

3.3.1 Mass 36

The peak corresponding to mass 36 (hydrogen chloride) can be seen to increase significantly during the irradiation of PVC using UV light as do the P+2 isotope masses and those corresponding to its fragmentation in the mass spectrometer (38,37,35)[32]. The intensity profile of this mass (Figure 4) shows the peak dropping away very quickly after the removal of the excitation source.

3.3.2 Mass 41

Initially, the highest intensity peak observed was at mass 41. This mass must be a hydrocarbon molecule as any molecule with chlorine in of mass 41 is not possible (as 41 - 35 = 6, combination of Cl with other atoms to produce mass 41 does not give a sensible molecular species). Mass 41 is assigned to C_3H_5 in these experimental results. This mass corresponds to main chain break-up of the polymer and could be a result of fragmentation of hydrocarbons or chlorocarbons in the mass spectrometer[32]. The peak profile of mass 41 is shown in Figure 5. This fragment also tails off very quickly upon termination of the UV irradiation.

From the results of the XPS experiments it was found that irradiation of PVC using UV light produced a carbon rich surface, therefore to see 41 with a greater intensity than that of mass 36 was unexpected. However, as successive exposures continue, mass 36 becomes the predominant mass species (Figure 6). The same masses were evolved during subsequent exposures but with decreasing intensity except for mass 36 (and corresponding fragmentation products).

This behaviour profile for HCl evolution has been observed previously during photolysis[4,18], and was thought to be due to an initial low concentration of photo-sensitising impurities such as carbonyls and hydroperoxides[18]. Initially impurities must initiate photolysis as PVC does not absorb UV at wavelengths > 200nm[12,13]. Hydrocarbon fragments are initially the major species evolved, which indicates main chain cleavage, and following this radicals left on the polymer chains are likely to crosslink, therefore less fragmentation of the carbon backbone is observed as exposure

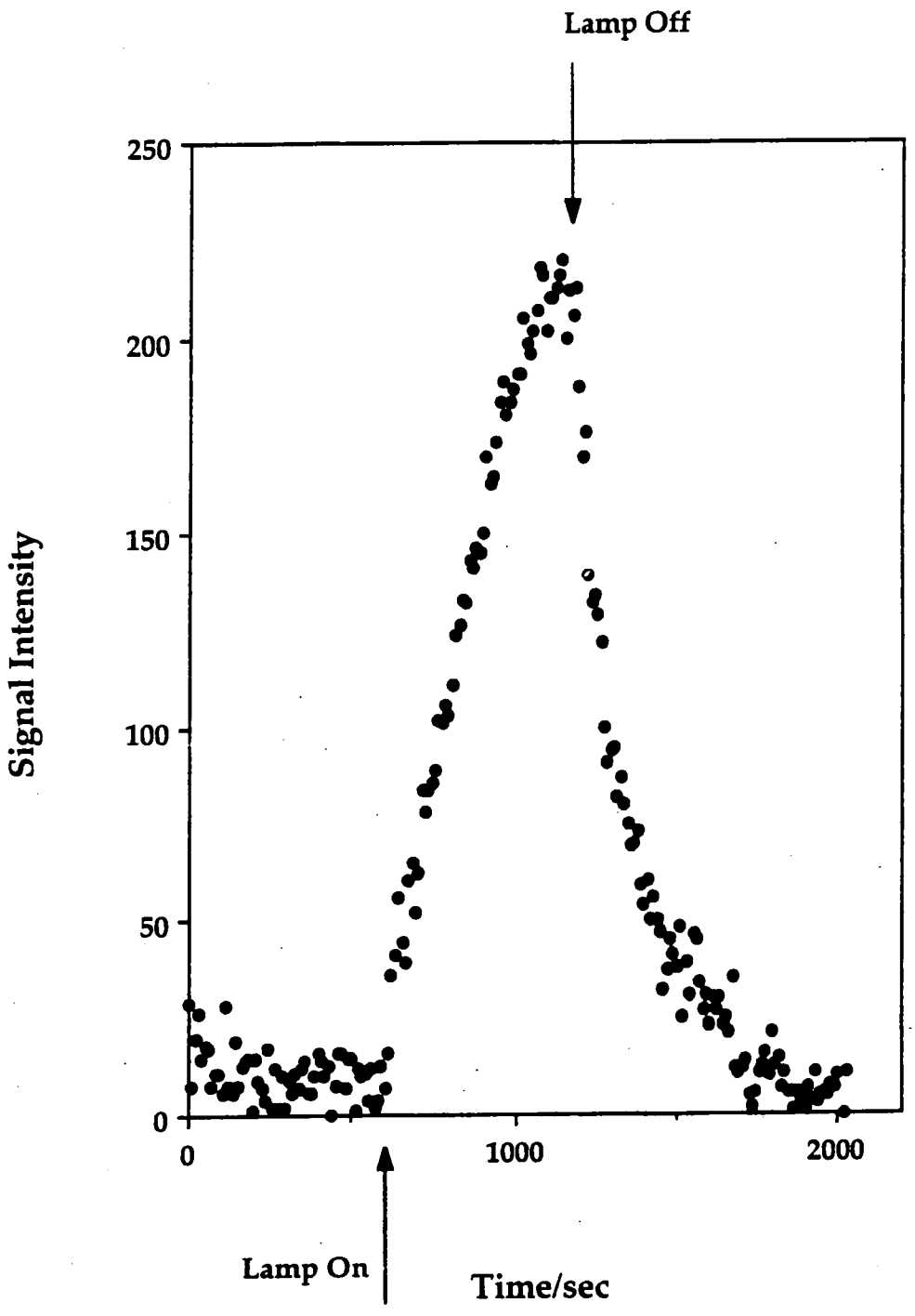

Figure 5: Mass 41 intensity profile for pure PVC (before, during, and after UV irradiation).

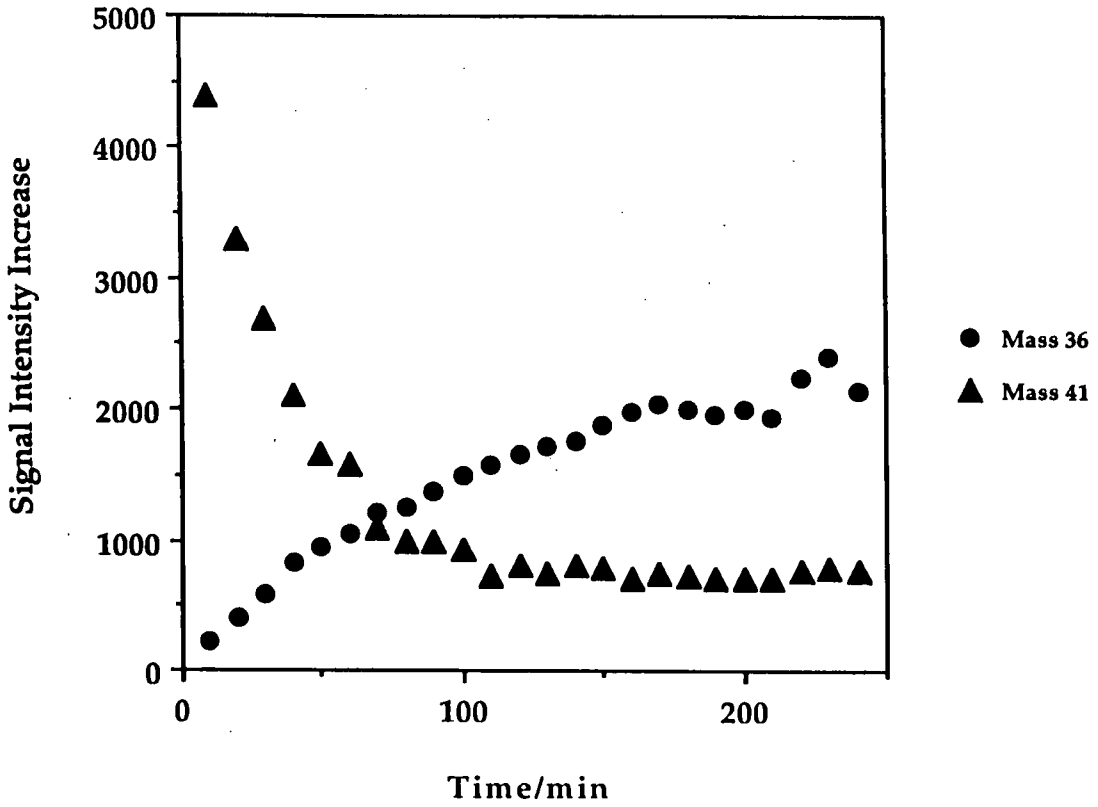

Figure 6: Changes in the signal intensity increase as a function of exposure time for masses 36 and 41 (relative to the same gain).

time increases. Reaction then occurs via HCl elimination forming polyene structures[12,16]. As the concentration of these chromophoric species increase, more UV is absorbed and therefore the rate of HCl production increases. Eventually the system reaches an equilibrium status with more HCl produced than hydrocarbon, i.e breakup of the polymer to produce a new underlying surface and dehydrochlorination equilibrate. The mechanistic description of this process is tentatively addressed in more detail below.

3.3.2.1 Mechanism for Mass 41 Formation

As mentioned in the above section mass 41 is most likely to be the fragment $C_3H_5^+$, the most stable form of which is CH_2=CH-CH_2^+. $C_3H_5^+$ is likely to be formed in the mass spectrometer from C_3H_5· and a possible origin of this radical from PVC is shown in Scheme 9 below:

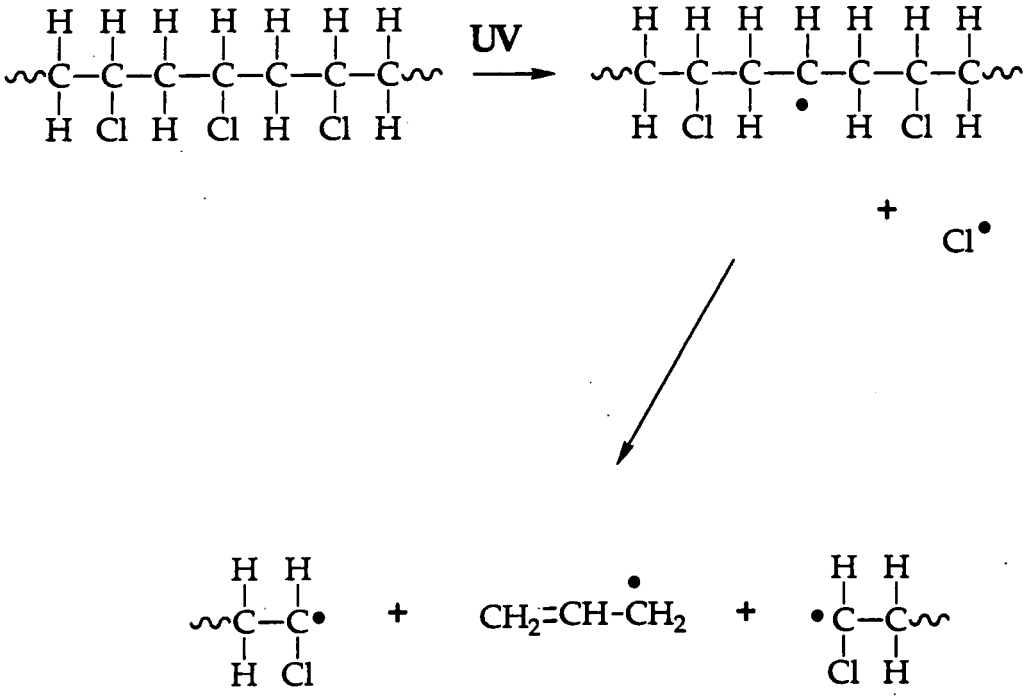

Scheme 9 : A possible mechanism for mass 41 formation.

From the behaviour of the mass profile for mass 41, Figure 6, the reaction to produce this fragment must occur easily in the initial stages of the photochemical reaction but later become inhibited. A possible rationalisation of these observations might be that loops of the polymer chain at the surface initially give rise to the mass 41 species, but as reaction time increases further reactions of the radicals produced on these chains result in crosslinking, producing a surface less susceptible to this mode of fragmentation. Polyenes, formed by dehydrochlorination reactions, are

produced simultaneously, and these chromophores would be expected to increase in concentration with reaction time and also be susceptible to crosslinking. Eventually the predominant reaction would become HCl production.

An alternative mechanism may also be possible. Absorption of light by PVC may lead to formation of a secondary polymer radical with the radical site adjacent to a chlorine-carbon bond, as previously postulated in Scheme 1. The radical produced would be:

$$\sim CH_2\text{-}CHClCH_2\text{-}^{\bullet}C\ Cl\text{-}CH_2\text{-}CHCl\sim$$

Chain scission may then occur to form an unsaturated chain end group and a radical chain end group, as previously postulated in Scheme 5. The resulting species are as follows:

$$\sim CH_2\text{-}CHCl\text{-}CH_2CCl{=}CH_2 \quad + \quad {}^{\bullet}CHCl\sim$$

Absorption of radiation by the chain containing the unsaturated end group may produce another radical, again as previously seen in Scheme 1. Chain scission in the radical produced results in the elimination of a small molecule from the polymer, see Scheme 10 below:

$$\sim{}^{\bullet}CH\text{-}CHCl\text{-}CH_2\text{-}CCl{=}CH_2 \longrightarrow \sim CH{=}CHCl + {}^{\bullet}CH_2\text{-}CCl{=}CH_2$$

Radical 1

Scheme 10: Splitting-off of a small fragment of the PVC chain.

Alternative fragmentation pathways are also possible. Radical 1 is almost identical to 2-chloroprop-1-ene:

$$H_2C{=}CCl\text{-}CH_3$$

indeed 2-chloroprop-1-ene could be formed from Radical 1 by atomic hydrogen abstraction or combination. 2-Chloroprop-1-ene is an isomer of 3-chloropropene, $H_2C{=}CH\text{-}CH_2Cl$, and 1-chloro-1-propene, $ClHC{=}CH\text{-}CH_3$, both of which fragment in the ion source of a mass spectrometer to yield mainly mass 41 by loss of Cl^{32}. 2-Chloroprop-1-ene is expected to show a similar splitting pattern to 3-chloropropene and 1-chloro-1-propene[33]. So splitting-off of Radical 1 from the modified PVC chain followed by hydrogen abstraction or combination to form a chloropropene may be another possible mechanistic description for origin of the mass 41 species.

Fragmentation becomes less likely as time increases as there is a greater probability that the polymer chains are crosslinked and hence restricted. There is not any restriction to HCl elimination as a result of crosslinking. Initially PVC radicals are probably produced by impurity chromophores in the polymer. As reaction time increases, PVC radicals are

formed by absorption and transfer of energy via polyenes, therefore the process is expected to be autoaccelerating.

Unzipping of the polymer back into vinyl chloride monomer units can be dismissed as a significant reaction route, as vinyl chloride does not produce mass 41 in the ioniser of the mass spectrometer[32].

3.3.3 Hydrocarbon fragments

In SIMS studies, the positive ion fragments produced from PVC are the same as those from polyethylene (i.e. $C_nH_m^+$ type clusters)[34]. A wide range of these fragments were observed in our experiments which are believed to have been produced by the break-up of the polymer chain. Masses 15, 29, 43, and 57 are attributed to fragment types C_nH_{2n+1}[34] but it is difficult to assign mechanisms to their formation from PVC due to their saturated nature. C_nH_{2n-1}[34] fragments such as masses 27 and 69 may form by polyene fragmentation.

Other hydrocarbon fragments were observed in these spectra which were not reported in the SIMS spectra of PVC. Fragments of the type C_nH_{2n-1} other than those already mentioned were 28($C_2H_4^+$) and 56($C_4H_8^+$). Other, less hydrogenated, fragments such as masses 39($C_3H_3^+$), 26($C_2H_2^+$), 54($C_4H_6^+$), 66($C_5H_6^+$), 65($C_5H_5^+$) and 94($C_7H_{10}^+$)[35] were also observed which may be produced by the fragmentation of a polyene. Mass 44($C_3H_8^+$) was also detected in these experiments. Masses 28 and 44 can be positively identified as hydrocarbon fragments C_2H_4 and C_3H_8 rather than CO and CO_2 respectively by looking at their fragmentation patterns. CO produces mainly mass 28, whereas C_2H_4 fragments to mass 28 and mass 27 (approximately 60% intensity)[32]. CO_2 produces mainly mass 28, but C_3H_8 has a main mass fragment at 29[32]. Masses 27 and 29 were observed in abundance during these experiments. It is difficult to assign a mechanism to the production of mass 44 as it contains more hydrogen than would be expected from a molecule originating from PVC or a polyene. It is possible that all the saturated hydrocarbon fragments observed do not originate from the PVC but from some agent, such as a detergent molecule, used in the preparation or processing of this polymer.

3.3.4 Other masses

Water (mass 18), molecular and atomic hydrogen (masses 2 and 1 respectively) were also identified during the photolysis. It is possible that the water was introduced into the polymer during processing.

When unplasticised PVC was analysed by *insitu* mass spectrometry, the same fragments were evolved as with pure PVC. Fragments that could be attributed to tin species were not observed. This could be due to two reasons:

i) mass fragments may be out of range of the quadrupole mass spectrometer (maximum mass species observable is 200 amu, tin has a mass of 119 so organotin molecules may be much greater)

ii) the signal of the tin compound was too small and was not detected (due to the decrease in sensitivity of this system towards higher masses)

4. CONCLUSIONS

The greatest degree of dehydrochlorination occurs under vacuum conditions. *In Situ* mass spectrometric analysis shows that there is an induction time for hydrogen chloride evolution. This can be explained as the initiation process of dehydrochlorination switching from photolysis of impurities in the polymer chains to initiation via absorption of UV light through polyene sequences formed in the dehydrochlorination reaction. As dehydrochlorination time increases, the concentration of initiation sites will increase. Hence the gradual build up to maximum HCl production. The decrease in hydrocarbon fragment evolution with increasing exposure time can be thought of as hindrance to main chain cleavage through intermolecular crosslinking.

5. REFERENCES

1) B. Ivan, T. Kelen, F. Tudos, Makromolekulare Chemie-Macromolecular Symposia, 29, (1989), 59-71.
2) J.F. McKellar and N.S. Allen, 'Photochemistry of Man-made Polymers', Applied Science, 1979
3) B. Ranby and J.F. Rabek, 'Photodegradation, Photo-oxidation and Photostabilization of Polymers, Principles and Applications', Wiley-Interscience, 1975
4) L.A. Jian, Z. Dafei, Z. Deren, Polymer Degradation and Stability, 30, (1990), 335-343.
5) L.A. Jian, Z. Dafei, Z. Deren, Polymer Degradation and Stability, 31, (1991), 1-7.
6) R.L. Clough, K.T. Gillen, Radiation Physics and Chemistry-International Journal of Radiation Applications and Instrumentation Part C, 22, (1983), 527-535.
7) A. Gonzalez, J.M. Pastor, J.A. Desaja, J. Appl. Polm. Sci., 38, (1989), 1879-1882.
8) T. Danno, H. Kondoh, K. Furuhata, K. Miyasaka, J. Appl. Polym. Sci., 29, (1984), 3171-3184.
9) A.L. Anrady, N.D. Searle. J. Appl. Polym. Sci., 37, (1989), 2789-2802.
10) C. Decker, M. Balandier, Polymer Photochemistry, 5, (1984), 267-282.
11) P. Simon, P. Cernay, L. Valko, Eur. Polym. J., 25, (1989), 531-533.
12) E.D. Owen, Degradation and Stabilisation of PVC, Elsevier, N.Y, 1984
13) J. F. Rabek, B. Ranby, T.A. Skowronsky, Macromolecules, 18, (1985), 1810.
14) A.L. Anrady, K. Fueki, A. Torikai, J. Appl. Polm. Sci., 39, (1990), 763-766.
15) F. Castillo, G. Martinez, R. Sastre, J.L. Millan, Makromolekulare Chemie-Rapid Communications, 7, (1986), 319-323.
16) S.S. Labana, Ultraviolet Light Induced Reactions in Polymers. ACS Symposium Series, 1976, Chapter 15
17) T. Kelen, Polymer Degradation, Van Nostrand Reinhold, N.Y, 1983
18) F. Castillo, G. Martinez, R. Sastre, J. Millan, V. Bellenger, J. Verdu, Polymer Degradation and Stability, 13, (1985), 211-224.
19) J. F. Rabek, 'Photostabilisation of Polymers-Principals + Applications', Chapter 4, Elsevier, 1990.
20) Z. Vymazal and Z. Vymazalova, Eur. Polm. J., 27, (1991), 1265-1270.
21) P. Simon, A. Gatail and L. Valko, Polymer Degradation and Stability, 29, (1990), 263.

22) A. H. Zahran, E. A. Hegazy and F. M. EzzEldin, Radiat. Phys. Chem., 26, (1985), 25.
23) Radiat. Phys. Chem., 18, (1981), 661.
24) F. Castillo, G. martinez, R. Sastre, J. Millan, V. Bellenger, B. D. Gupta and J. Verdu, Polymer Degradation and Stability, 27, (1990), 1
25) Masashi Shimoyama, Hiroyuki Niino, Akira Yabe, Makromol. Chem., 193, (1992), 569-574.
26) C. Decker, Polymer Preprints, 27, (1986), 42-43.
27) A. Kuczkowski, Physica Status Solidi A-Applied Research, 89, (1985), K109.
28) T. Duvis, G. Karles and C. D. Papaspyrides, J. Appl. Polym. Sci., 42, (1991), 191.
29) G. Beamson and D. Briggs: 'High Resolution XPS of Organic Polymers: The Scienta ESCA300 Database', J. Wiley, Chichester, (1992).
30) D. T. Clark and A. Dilks, J. Polym. Sci., Polym. Chem. Ed., 17, (1979), 957
31) J. Brehm and W. J. Mullin, 'Introduction to the Structure of Matter', Wiley, 1989.
32) A. Cornu and R. Massot, Compilation of Mass Spectral Data, 2nd Ed., Heyden and Son.
33) Personal communication with Dr M. Jones, Durham University Chemistry Department.
34) D. Briggs, A. Brown and J. C. Vickerman, Handbook of Static Secondary Ion Spectrometry, Wiley, 1989.
35) R. M. Silverstein, G. C. Bassler and T. C. Morrill, 'Spectrometric Identification of Organic Compounds', 4th Edn., Wiley, 1981.

APPENDIX 1

ANALYTICAL TECHNIQUES

1. INTRODUCTION

In this chapter, the techniques used in this thesis to analyse sample surfaces and reaction products are outlined.

As described in Chapter 1, polymer surface morphology is different to bulk structure. It is not enough to consider a two-dimensional structure for the polymer surface as chains may lie flat or be oriented in the surface plane or perhaps be normal to it[1]. The surface of a polymer may be considered as being 50-100Å thick[1] and its detailed structure and nature is time and temperature dependant[2,3]. Factors which effect surface composition are briefly outlined below.

Polymers have a range or distribution of molecular weights, MW. As the lower MW fraction of the polymer is likely to be more mobile than the higher MW counterpart, because of their smaller physical size, the lower MW chains may diffuse to the surface region. Therefore the surface of the polymer will effectively have a lower MW than the bulk.

Semi-crystalline polymers have amorphous regions of the bulk interdispersed with crystallites. Crystallites may be formed by adjacent stereo-regular chains and also single polymer chains doubling back on themselves. In the latter case it can be envisaged that loops of amorphous polymer chain will be present at the ends of the crystallites. Two extreme situations could occur at the surface region. The amorphous loops may orient towards the surface so that the polymer appears to be totally amorphous from this viewpoint, or the loops may orient so that the surface appears to be totally crystalline.

Extrusion of polymer melts and also thin film formation could cause preferential orientation of the polymer chains throughout the bulk as well as the surface region.

Initiators used to start the polymerisation process are usually permanently attached to the polymer chain ends. These polar functionalities may affect the surface properties of the polymer if they preferentially aggregate at the surface. Whether this occurs depends upon the nature of the initiator and the nature of the polymer.

Additives which have been included in to the polymer matrix sometimes diffuse to the surface region, see Chapter 1 section 3.1, this migration will obviously alter the surface composition. Another process which will alter the polymer surface characteristics is oxidation which may occur during processing and storage.

Because of the nature of polymers the methods used to characterise their surface must be carefully chosen, the characteristics of the surface must

not change during observation and one must be certain that the surface and not the bulk is being analysed. Standard bulk analysis techniques which are normally used to study polymers, such as nuclear magnetic resonance and transmittance infra-red spectroscopy, are of little use in the analysis of polymer surfaces as the signal due to the surface region is swamped by the signal due to the bulk.

In the work reported in this thesis X-ray Photoelectron spectroscopy (XPS) has been used to study polymer surface modification as, in general, polymer systems are reasonably stable during XPS analysis and time dependence of spectra during typical analysis times is not a major concern[4]. XPS can give information from a depth of < 50 Å in a polymer[5], and is therefore a surface sensitive tool[6]. The theory and experimental setup for XPS is described in this chapter.

When a polymer surface is modified it would be useful not only to analyse the resulting surface but also to monitor any gaseous species emitted from the surface during modification as fragments and molecules may give an insight into mechanistic aspects of the reaction. For these gaseous reaction products to be studied a novel analysis technique was developed, the experimental set-up of which is described in Chapter 3. This technique has the entrance of a mass spectrometer directly above the polymer sample surface enabling species evolved to be detected *in situ*. The theory of mass spectrometry and the experimental instrumentation are described in this chapter.

2. X-RAY PHOTOELECTRON SPECTROSCOPY

A brief review of the background theory to XPS will be given here and the use of XPS in relation to polymer core and valence levels is discussed.

2.1 THEORY

Photoelectron spectroscopy involves the ejection of electrons from atoms or molecules following bombardment by photons[7]. The ejected electrons are called photoelectrons, Scheme 1.

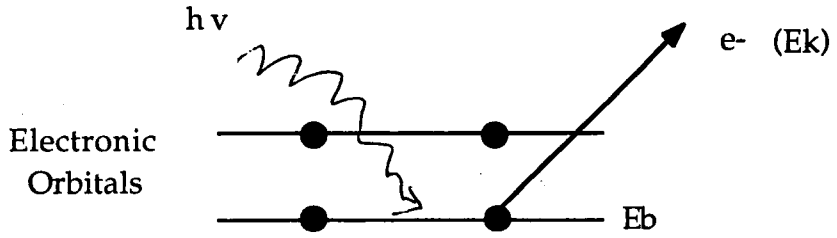

Scheme 1: Ejection of a photoelectron[7].

The effect was observed originally on surfaces of easily ionisable metals such as alkali metals. Bombardment of the surface with photons of tunable frequency did not produce any photoelectrons until the threshold frequency was reached. At this frequency υ_t, the photon energy was just sufficient to overcome the work function Φ of the metal, so that[7]:

$$h\upsilon_t = \Phi$$

At higher frequencies the excess energy of the photon is converted into kinetic energy of the photoelectrons[7]:

$$h\upsilon_t = \Phi + 1/2\ m_e v^2$$

where m_e and v are the mass and velocity of the photoelectrons respectively.

Photoelectron spectroscopy is a simple extension of the photoelectric effect involving the use of higher energy incident photons[3]. The sample surface is irradiated by a source of low energy X-rays under ultra high vacuum (UHV) conditions. Photoionisation takes place in the sample surface, the resultant photoelectrons having kinetic energy (E_k), which is related to the X-ray energy ($h\upsilon$), the binding energy of the electron (E_b) and the material work function Φ by the Einstein relation[6-9]:

$$E_k = h\upsilon - E_b - \Phi$$

Shifts in the core binding energy can be measured and are related to the chemical environment of the atom; the more highly oxidised a species, the greater the binding energy[6]. Valence band levels may also be probed, this will be discussed in more detail later (see 2.4).

Ultra high vacuum (UHV) and a consideration of electron escape depths are both essential for the XPS experiment, the reasons for this are given below.

2.1.1 Ultra High Vacuum

Why does XPS require UHV? XPS observes electrons emitted from a surface upon bombardment with photons. Species travelling from a sample surface towards a detector should encounter as few gas molecules as possible otherwise they will be scattered and not be analysed[7,10]. Vacuum requirements of 10^{-5} - 10^{-6} mbar or less are required for optimum detection[10] as this gives inelastic mean free paths for the electrons of the order of the distances to the analyser. Also few gaseous molecules strike a sample surface at these pressures and therefore UHV conditions also limit surface contamination[10,11].

2.1.2 Electron Escape Depths

XPS involves the detection of electrons ejected from energy levels and the surface sensitivity of this method depends upon the probability of the generated electron escaping from the surface without any further energy loss, and does not depend upon the mode of excitation[11]. The trend of attenuation length vs electron energy is illustrated in Scheme 2[4]. The escape depth of electrons in a solid is related to their attenuation length[4].

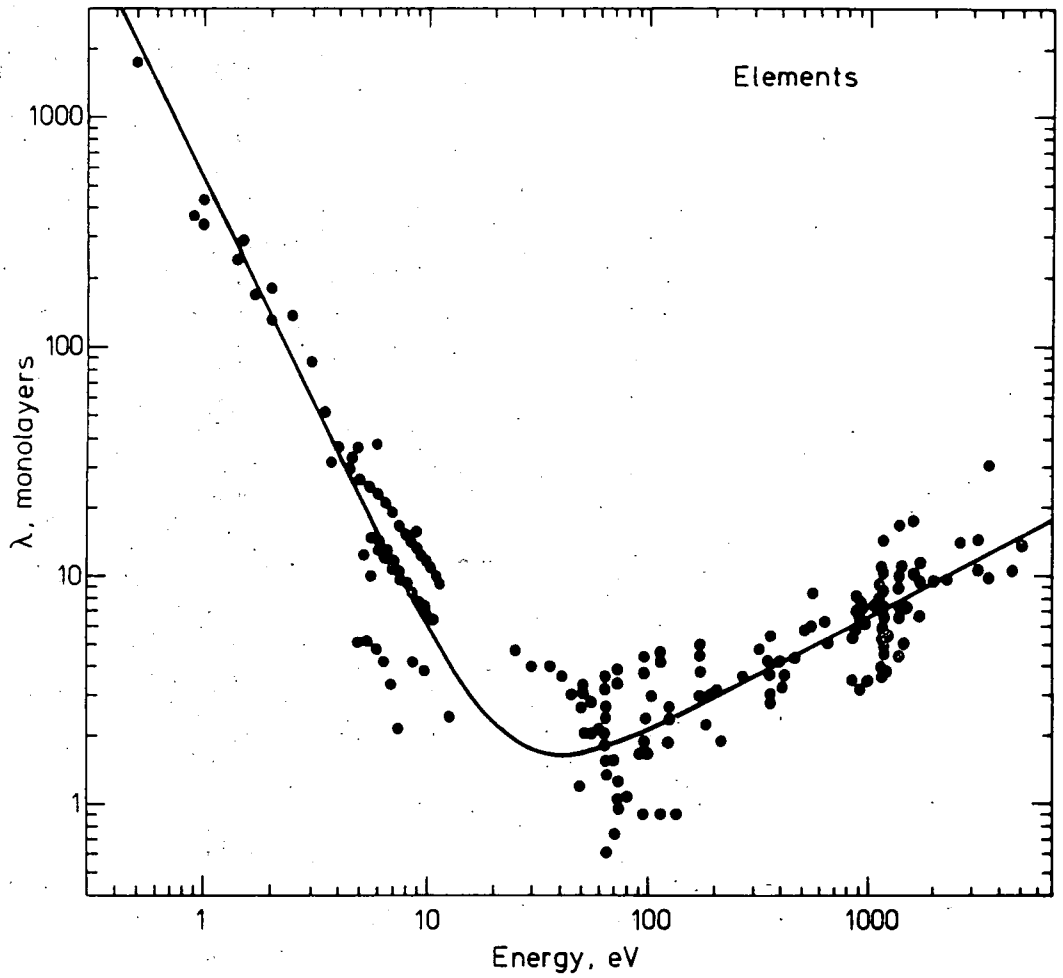

Scheme 2: The dependance of attenuation length upon electron energy[4].

Electrons lose energy when leaving a surface by excitation of lattice vibrations called phonons (10's of meV losses), by electron-electron interactions which excite collective density fluctuations in the electron gas in the solid, known as plasmons (5 - 25 eV losses) and by other single and double particle excitations: loss of energy by raising an electron from its ground state to an empty state (e.g. π-π^* energy level transitions) or ejection of another electron[11].

2.2 EXPERIMENTAL

The equipment used for XPS analysis is shown diagramatically in Scheme 3.

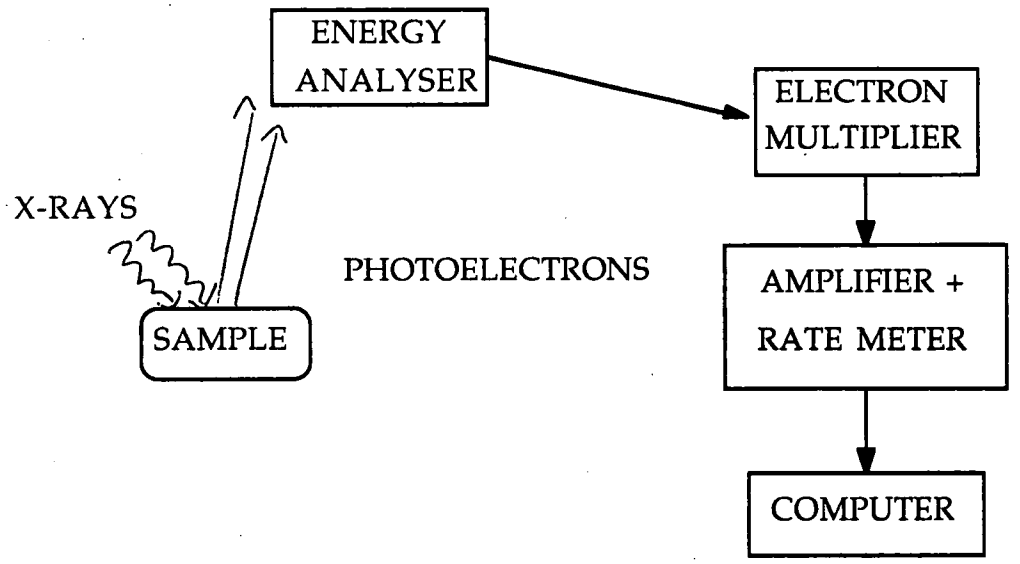

Scheme 3 : XPS experiment schematic.

Electrons ejected from the sample by use of soft X-rays are analysed by an analyser, usually a Concentric Hemispherical Analyser (CHA) and the signal is collected, multiplied and transferred into a signal for the computer.

The equipment used in the work described in this thesis was specified in Chapters 2 and 4. The basic instrumentation is more generally described in the following section.

2.2.1 X-Ray Source

A schematic of a typical X-ray source is shown over[5,12], Scheme 4 over page. The window acts as a barrier to electrons, irradiation, heating effects and other contamination arising from the x-ray source. The anode is at a high positive potential and the filaments at near earth potential. This arrangement is used rather than alternative arrangements, such as the filaments at high negative potential and the anode at earth potential, as in X-ray diffraction, because this arrangement stops other surfaces, such as the window, being bombarded by electrons, which helps to limit contamination[12].

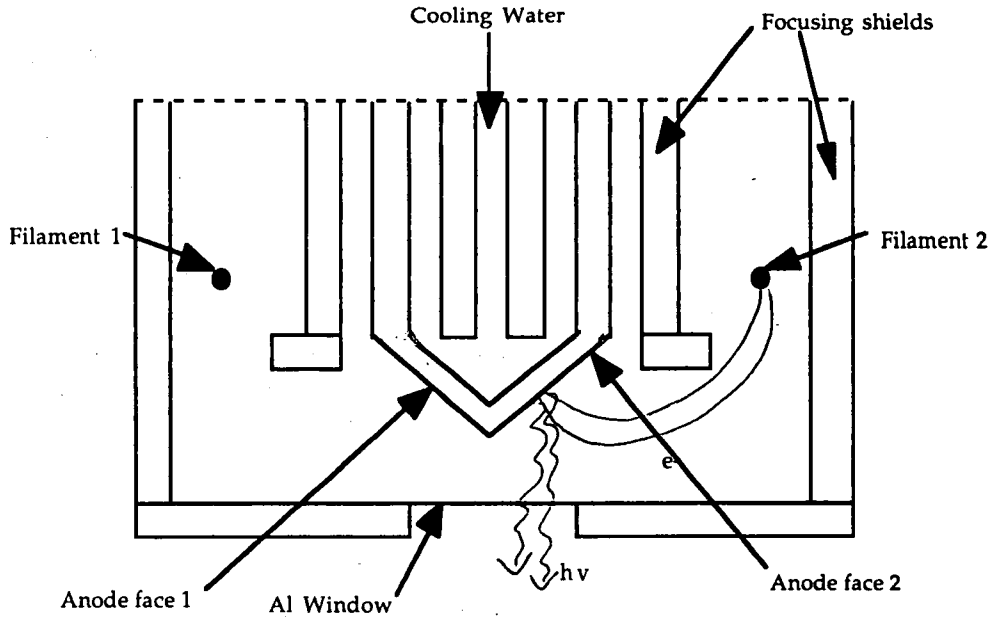

Scheme 4 : Schematic of X-ray Source[13].

Choice of material for a soft X-ray source in XPS depends on two considerations[10], the line width of the X-ray source must not limit the energy resolution required in the analysed spectrum and the characteristic X-ray energy of the source must be high enough so that a sufficient range of core electrons can be photo-ejected[9]. In XPS consideration of these restraints results in the most commonly used anodes in soft X-ray sources being magnesium and aluminium[6,9,10,13].

The soft X-ray source illustrated above has a dual copper anode with a tapered end onto which films of magnesium and aluminium are deposited, one metal on each side of the tapered end, allowing the use of either magnesium or aluminium K_α radiation[12]. There are two semicircular filaments, one for each anode face with a focusing shield of the same potential as the filament so that electrons are focused onto the correct anode surface. The spectrum emitted from the X-ray source is complex and consists a broad continuous background (Bremsstrahlung) on which are imposed the characteristic X-ray lines[12].

2.2.1.1 Monochromatisation of X-rays

Monochromatisation of the X-ray source removes satellite interference, improves signal to background by eliminating the Bremsstrahlung continuum and enables selection of an individual line in the resulting spectrum from the unresolved principal line doublet[12]. Monochromatisation is achieved by dispersion of X-ray energies by

diffraction in a crystal. Only a narrow band of X-ray energies are focussed onto the sample. All other photon energies are dispersed in the crystal and emerge into the spectrometer volume and not onto the sample.

The dispersion is governed by the Bragg relation[12]:

$$n\lambda = 2d\sin\vartheta$$

where:
n is the order of diffraction
λ is the wavelength of the X-rays
d is the crystal spacing
and ϑ is the Bragg angle

Quartz crystals are usually used as they are very suitable for first order diffraction of Al K_α X-rays, λ for X-rays is 0.83 nm, the crystal spacing of the quartz 1010 planes is 0.425 nm and the Bragg angle is therefore 78.5°. The wavelength required from Al K_α emerges at a convenient angle, 78.5°. If another X-ray sorce was used, say Mg K_α, which had a different wavelength, then as λ and ϑ are the only variables in the above equation, the angle at which the X-ray energies would emerge may not be convenient. Spectrometer geometries would have to be altered for a different X-ray source.

Quartz crystals have many advantages over other crystals as they can be easily bent or ground and can be baked to high temperatures without change or distortion.

The most often used set up for monochromisation is fine focussing, see Scheme 5.

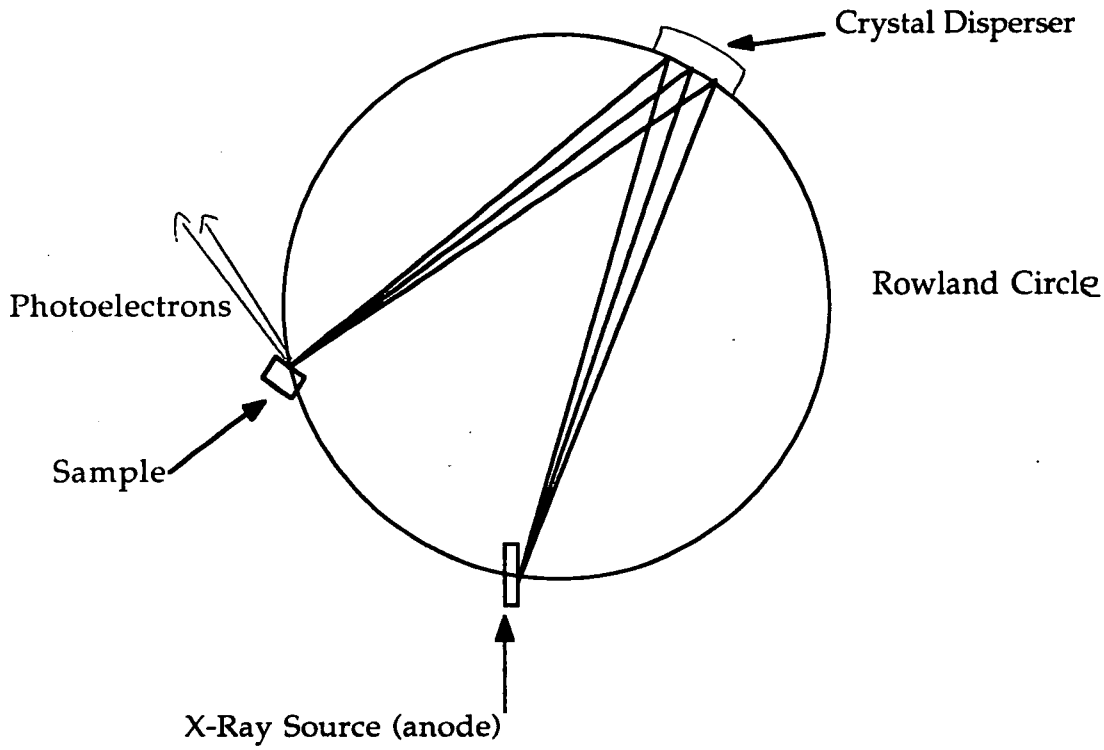

Scheme 5 : X-ray monochromatisation[12].

The quartz crystal is placed on the surface of a Rowland or focussing sphere and ground into the shape of the sphere. The anode is also placed on this circle and irradiated with a sharply focussed electron beam. X-rays are dispersed by diffraction in the crystal and focused at another point on the Rowland circle where the sample is placed. The flux of the X-rays onto the sample is much reduced after monochromatisation, as compared to the unmonochromatised source for the same operating conditions.

2.2.2 Retardation of Electrons

Before entering the analyser electrons are decelerated by a constant factor or ratio usually by a grid near the entrance slit. Photoelectrons must be retarded in energy because of resolution requirements.

There are two definitions of energy resolution:

1) Absolute resolution, ΔE, the full width at half maximum (FWHM) height of a chosen observed peak[12], Scheme 6.

Scheme 6: Absolute resolution.

The width ΔE_B of the peak at its base is sometimes measured and ideally $\Delta E_B = 2\Delta E$

2) Relative resolution, R, which is defined as $R = \Delta E / E_0$ where E_0 is the kinetic energy of the photoelectrons at that peak position[12], Scheme 7.

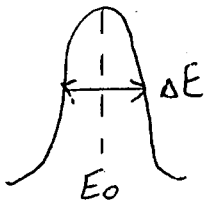

Scheme 7 : Relative resolution.

Relative resolution is usually expressed as a percentage. In summary, absolute resolution can be specified independantly of peak position in a spectrum but the relative resolution, R, can only be specified by reference to a particular kinetic energy.

In XPS, in order to identify differences in chemical states, the same absolute resolution must be applied to any photo-electron peak in the spectrum[5,12]. The natural line widths of Mg K_α and Al K_α X-ray sources are 0.7 eV and 0.85 eV. For the absolute resolution of these lines to be monitored at the maximum available K.E. (1253.6 eV for Mg K_α and 1486.6 eV for Al K_α) a relative resolution of ~ 6×10^{-4} would be required . This resolution is possible but would result in a loss of sensitivity. Therefore it is usual for the K.E.'s of the photo-elecrons to be retarded either to a chosen energy or by a chosen ratio. The pass energy or the ratio is kept constant during the recording of any one spectrum. When the retardation is by a constant relative ratio the retardation mode is termed CRR or FRR. In the other mode the electrons are decelerated to a constant pass energy with constant absolute resolution termed CAT of FAT, constant or fixed analyser transmission. With CAT/FAT the absolute resolution is the same at all points therefore these spectra are easier to quantify, however the signal to noise gets worse towards low kinetic energies. CRR or FRR mode is less easy to quantify but small peaks at low kinetic energies can be detected without difficulty.

2.2.3 Concentric Hemispherical Analyser

In XPS electron energy analysers are of the electrostatic type as electromagnets and permanent magnets are difficult to construct and handle in an UHV environment[10]. The most frequently used analysers are the

cylindrical mirror analyser (CMA) and the concentric hemispherical analyser (CHA)[10,14,16]. The CHA was used as an analyser in the experiments involving XPS in this thesis, and hence this will be discussed in more detail.

Two hemispherical surfaces of inner radius R_1 and outer radius R_2 are positioned concentrically, and a potential ΔV is applied between the surfaces so that the outer is negative and the inner positive[5,12], see Scheme 8.

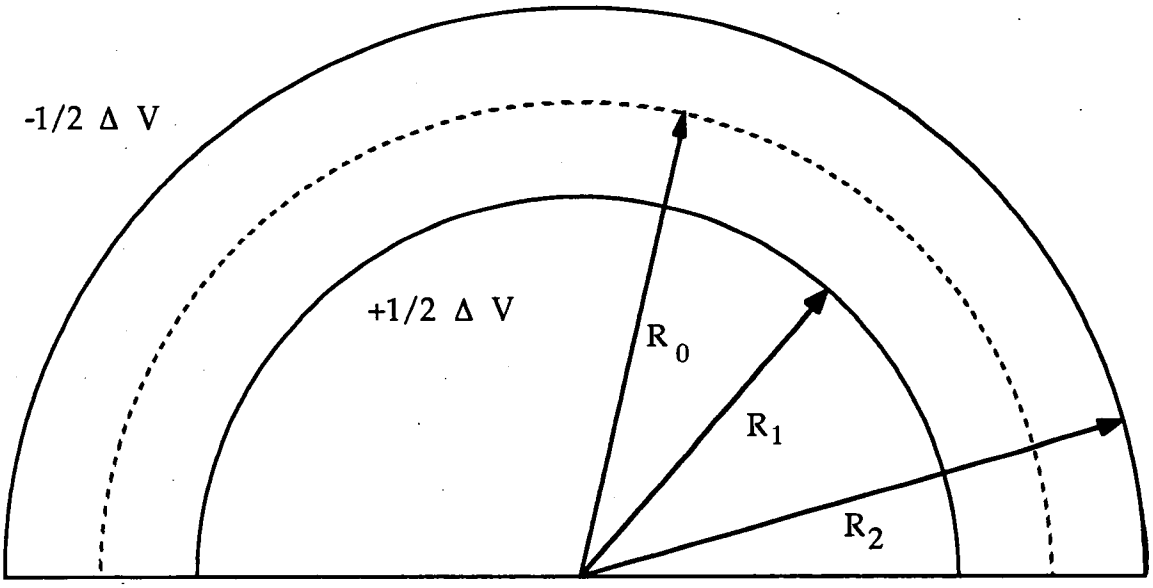

Scheme 8: Concentric hemispherical analyser[12].

R_0 is the median equipotential between the hemispheres and the entrance and exit slits are both centred on R_0.

Scanning is performed by varying the potential of the analyser, and only those electrons with the required energy pass through the analyser without hitting the walls to be detected at the exit slit.

2.3 POLYMER CORE LEVEL XPS

Work on the XPS of polymers was pioneered in the 1970s by Clarks' research group[15]. They studied many polymer systems and also used model compounds to elucidate polymer spectra[15-17].

Samples for XPS analysis are introduced into a UHV system and then manoeuvred so that the X-ray source and the energy analyser are in the correct position[10]. Polymer samples are easily introduced into UHV systems attached to a sample probe by means of double sided adhesive tape[4]. This was the method used in our experiments.

Electrons ejected from a particular core energy level have a specific energy related to their binding energy. By scanning over all possible kinetic

energies (known as a wide scan) it is possible to obtain a spectrum which shows the binding energy features of a particular substance. For example, XPS of a certain substance may show peaks corresponding to the presence of oxygen and carbon over the background spectrum. This wide scan may then be narrowed down to provide a more detailed picture of a particular region.

Non-equivalent atoms of the same element in a solid give rise to core level peaks with measurably different binding energies. This is termed the 'chemical shift'. This non-equivalence of atoms can arise in several ways such as differences in lattice site, difference in formal oxidation state and difference in molecular environment[18]. For example, electronegative and/or electropositive atoms in the vicinity of a particular element result in shifts in peak positions and broadening of the peaks. A hydrocarbon polymer such as polyethylene would be expected to show a peak at ~ 285.0 eV corresponding to C-H, but polypropylene glycol would show both a peak at ~285 eV for C-H and also a peak at 286.6 eV due to C-O, as well as a peak in the O(1s) spectrum.

The physical basis of the chemical shift effect is illustrated by a model called the charge potential model[18]. The atom is considered to be a hollow sphere on the surface of which the valence charge resides. The classical potential inside the sphere is the same at all points. A change in the valence electron charge density changes the potential inside the sphere. Thus the binding energy of all core levels will change by this amount.

2.4 POLYMER VALENCE BAND XPS

Valence band spectra of polymers can give a unique fingerprint of molecular orbitals[19]. Changes in fundamental molecular structure may be observed[20-22]. For polymers valence bands give structural as well as chemical information.

The most common way of measuring the valence band spectrum with X-rays is by using a standard XPS spectrometer equipped with a monochromator[19]. Monochromatisation is needed because satellites of the X-ray source (Al K_α at 10-12 eV with 10% of the intensity of the main line) occur in the valence band region (0-40 eV), and also removal of the Bremsstrahlung continuum improves sensitivity and reliability of fine structures in the spectrum. However monochromatisation gives a weak intensity X-ray source. So in order to obtain a better signal to noise ratio, a complex lens system is used to collect the photo-electrons and data is accumulated for long periods, usually overnight.

The depth probed is approximately 50-60 Å. With insulating samples such as polymers, sample charging distorts the spectrum. This is solved by the use of either an electron flood gun or by using thin polymer films deposited on metal substrates.

The valence band spectra can be analysed by comparison with theoretical simulations of the valence band spectrum or by a fingerprint approach. The electronic band structure of polymers are most often calculated by paramatized semi-empirical techniques because *ab-initio* methods would take far too long to compute. The Valence Effective Hamiltonian (VEH) technique is currently the commonest form used[23-25]. VEH is based on the use of an effective Fock Hamiltonian, F_{eff} , which combines a kinetic term and a summation over all atomic potentials. All parameters entering the atomic potentials are optimised by using model molecules, so that the difference between F_{eff} and the Fock Hamiltonian built from *ab-initio* methods is minimal. VEH is then able to give electron energy levels of *ab-initio* quality. From the band structure, the Density of Valence States (DOVS) can be calculated. The theoretical simulation of the valence band spectrum is obtained by including the effect of relative photoionisation intensities of the crystal orbitals in the DOVS curves.

The above calculations are easily performed using available computer software. Input parameters are simply the geometry of the polymer chain, given by standard experimental structural determination techniques.

A previously uncharacterised valence band structure of a polymer may be solved by comparison with a model compound containing part of the polymer chain in its structure[24], or by considering substituent effects on a simpler, pre-characterised polymer[26]. This is known as the fingerprint approach.

3. MASS SPECTROMETRY

In its simplest form a mass spectrometer uses an electron source to bombard gaseous molecules under investigation and causes them to ionise and then fragment in a predictable way. The result is quantitatively recorded as a spectrum of positive ions.

Mass spectrometers are usually classified according to the method used for separating the ions during analysis, these are Magnetic field deflection, Time of flight (ToF) and Quadrupole techniques. Magnetic field deflection uses a magnetic field to seperate fragments of different masses, while ToF uses the time taken for ions to travel to the detector while being accelerated to the same kinetic energy, and a quadrupole uses 4 electric poles to cause separation. The quadrupole method was used in this thesis (Chapters 3 and 7) and the mass spectrometer used was the SX200 from Vacuum Generators Ltd

3.1 THEORY AND EXPERIMENTAL

Gaseous species entering a quadrupole mass spectrometer are bombarded with a beam of electrons which causes ionization and positive ions form[27-32]. These positive ions are separated on the basis of mass (strictly mass/charge, but the majority of ions are singly charged), and the result is quantitatively recorded as a spectrum of these positively charged ion fragments.

The path of a molecule and the subsequent signals generated in a quadrupole mass spectrometer may be summarised as follows, Scheme 9:

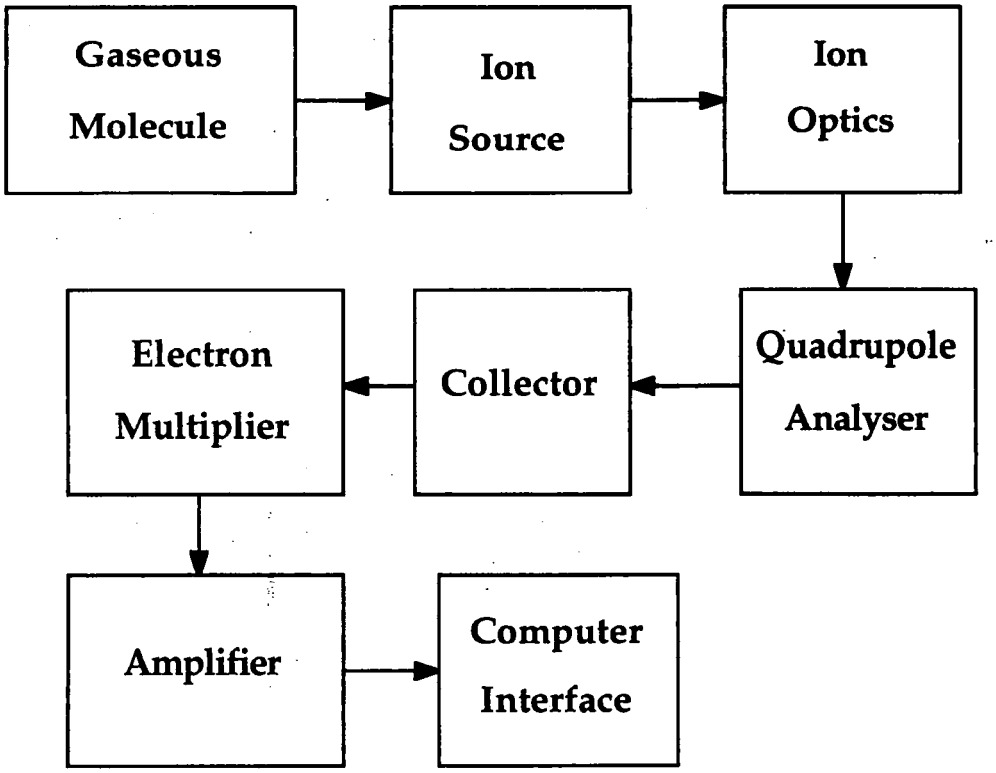

Scheme 9: Schematic of a Quadrupole Mass Spectrometer.

3.1.1 Ion Source

Positive ions are generated in the ion source by the process of electron bombardment. The source consists of a fine cylindrical stainless steel wire mesh cage and a ceramic filament assembly[32]. The filament assembly consists of two filaments diametrically opposite each other and is mounted around the cage[29,32]. This is surrounded by a circular repeller. Ions pass through the source plate, and then a focusing plate before exiting via an earthed plate towards the mass analyser[32].

3.1.2 Mass Analyser

The quadrupole analyser, Scheme 10, consists of four electric poles (stainless steel rods aligned axially and symmetrically)[29,32]. This arrangement produces fields which approximate those from hyperbolic surfaces (which are claimed to give the best performance)[31,32]. The hyperbolic surfaces may be described by the equation[33]:

$$x^2 - y^2 = \pm C \quad \text{where C is a constant.}$$

No magnetic field is used.

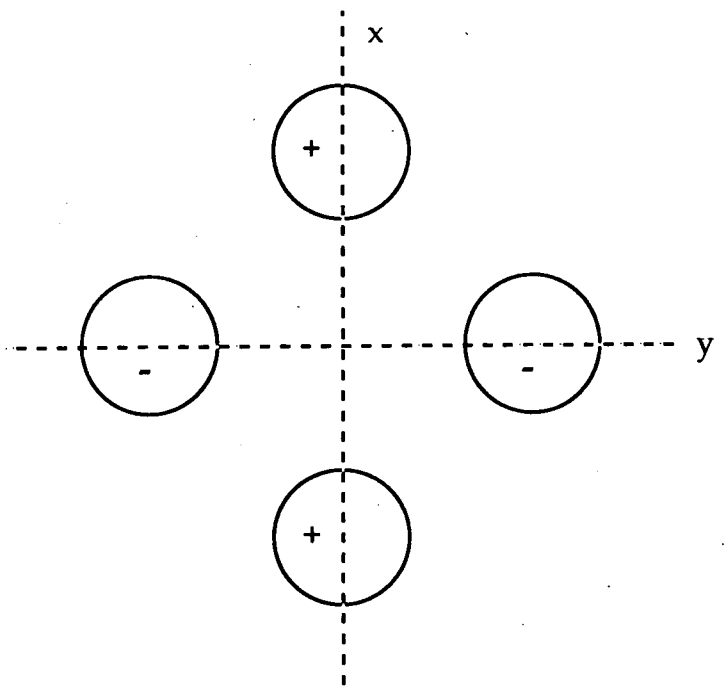

Scheme 10: Schematic of a Quadrupole Analyser[27].

Opposite rods are connected to the same potential, which can be described by[33]:

$$P(t) = \pm [U + V\cos(2\pi ft)]$$

where U is a D.C. voltage and V is the peak amplitude of a radio frequency voltage at frequency f. To the other pair of electrodes a potential of opposite sign is applied[33]. V and U are chosen so that ions of a given e/m will have stable trajectories. The mass resolution, $m/\Delta m$, is given by[33]:

$$m/\Delta m = 0.126/(0.16784-U/V)$$

By making U/V equal to 0.16784 in theory infinite mass resolution may be obtained. In practice U/V is altered so that unit mass resolution is obtained throughout the spectral range, however this gives poor transmission and hence sensitivity for higher mass signals. In order to have equal sensitivity over the whole mass range the resolution is decreased with increasing mass number.

Ions are focused to enter the analyser at a constant velocity in the z-direction (parallel to the poles) but acquire oscillations in the x- and y-directions due to the oscillating radio frequency/d.c voltage applied to the poles[27]. A "stable oscillation" allows an ion to travel the entire length of the quadrupole without striking the poles. Transmitted ions strike the detector which feeds output to an external amplifier. This oscillation is dependent on the mass/charge ratio of the ion, the mass being in this case between 1 a.m.u and 200 a.m.u[29].

3.1.3 Ion Detector

In the SX200 quadrupole mass spectrometer either a Faraday Cup detector or an electron multiplier is used as the ion detector. Which is used depends upon the pressure in the vacuum system (Faraday 10^{-5} - 10^{-11} mbar, SEM (Semiconductor Electron Multiplier) 10^{-7} - 10^{-13} mbar)[29], and the scan speed of the spectrum. The bandwidth of the amplifiers used limit the scan speeds in the Faraday mode[29].

The quadrupole mass spectrometer is interfaced to an IBM compatible computer as shown in Scheme 11:

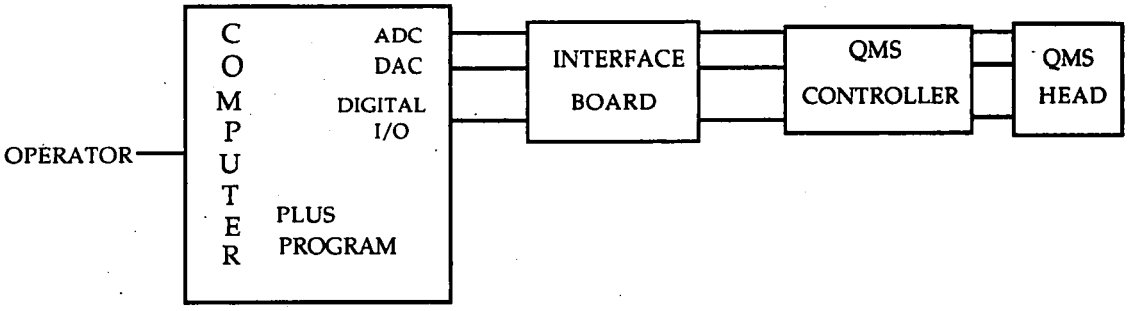

QMS = Quadrupole Mass Spectrometer.

ADC = Analogue to Digital Converter.
Reads mass spectrometer output for peak selected by program.

DAC = Digital to Analogue Converter.
Provides voltage which determines the mass to be observed.

Digital I/O = Digital Input/Output.
Mainly controls the gain setting of the quadrupole mass spectrometer.

Scheme 11. Interfacing of Quadrupole Mass Spectrometer.

3.2 RELATED TECHNIQUES

Secondary Ion Mass Spectroscopy (SIMS) and Thermal Desorption are methods of surface analysis which use mass spectrometry. In SIMS the surface of a sample is bombarded with a beam of primary ions (usually Ar^+) having energies of several keV[34]. Atoms and molecules are knocked (sputtered) out of the target and may emerge in their ground states, as excited particles, or as positive or negative ions. A fraction of these are

passed into a mass spectrometer where the charged ions are separated according to their mass to charge ratio. The resulting spectrum is characteristic of the sample under inversigation.

For thermal desorption the sample under investigation is heated and molecules are evolved from the surface and detected by mass spectrometry[35,36]. With gas chromatography mass spectrometry (GC-MS) mixtures of molecules are separated by a GC column before mass spectral analysis, which makes spectral identification much simpler as spectra are recorded as a function of the molecular retention times on the particular column and so usually spectra of pure compounds emerge if resolution is great enough.

TD-GC-MS has been used to study the volatiles held within a polymer matrix such as stabilisers, plasticisers and virgin polymer resin[35]. The temperatures used for desorption (~150°C) are not high enough to decompose the polymer.

4. SUMMARY

The analysis techniques used in this thesis have been breifly discussed with relation to theoretical and experimental considerations.

5. REFERENCES

1) H. Sperling, 'Introduction to Physical Polymer Science', 2nd edn., Wiley Interscience, 1992.
2) J. D. Andrade in 'Polymer Surface Dynamics', ed. J. D. Andrade, Plenum, New York, 1988.
3) V. D. Fedotov and H. Schneider, 'Structure and Dynamics of Bulk Polymers by NMR Methods', Springer-Verlag, 1989, Chapter 4.
4) D. Briggs in 'Practical Surface Analysis' ed. D. Briggs and M. P. Seah, Vol 1, Second Edition, Wiley, (1990), p436.
5) N. J. Chou in 'New Characterisation Techniques for Thin Polymer Films', Wiley, 1990, Chapter 11.
6) H. Hantsche, Scanning, 11, (1989), 257-280.
7) J. M. Hollas, 'Modern Spectroscopy', Wiley, (1987), p260.
8) A. D. Baker and D. Betteridge, 'Photoelectron spectroscopy - chemical + analytical aspects' Pergamon press, 1972, p7.
9) A. B. Christie in 'Methods of surface analysis - techniques and applications', ed J. M. Walls, 1989, Cambridge University press, p127.
10) J. C. Riviere in 'Practical Surface Analysis' ed. D. Briggs and M. P. Seah, Vol 1, Second Edition, Wiley, (1990), p19.
11) M. Prutton, 'Surface Physics', Oxford University Press, 1983.
12) J. C. Riviere in 'Practical Surface Analysis' ed. D. Briggs and M. P. Seah, Wiley, (1983).
13) T. A. Carlson, 'Photoelectron + Auger Spectroscopy', Plenum press, 1975, p15.
14) J. D. Carette and D. Roy in 'Topics in Current Physics - Electron Spectroscopy for Surface Analysis', ed. H. Ibach, 1977, p13.
15) D. T. Clark and H. R. Thomas, J. Polym. Sci, Polym. Chem. Ed., 16, (1978), 791.
16) D. T. Clark and H. R. Thomas, J. Polym. Sci, Polym. Chem. Ed., 14, (1976), 1671.
17) D. T. Clark and H. R. Thomas, J. Polym. Sci, Polym. Chem. Ed., 16, (1976), 1701.
18) D. Briggs and J. C. Riviere in 'Practical Surface Analysis' ed. D. Briggs and M. P. Seah, Vol 1, Second Edition, Wiley, (1990), Chapter 3.
19) J.J. Pireaux, J. Riga and J.J. Verbist, in 'Photon, Electron and Ion Probes for polymer Structure and Properties', ed. by D.W. Dwight, T.J. Fabish and H.R. Thomas, p. 169, ACS Symposium Series 162 (1981).
20) R.K. Wells, I.W. Drummond, K.S. Robinson, F.J. Street and J.P.S. Badyal, Chemical Communications, 6, (1993).

21) R.K. Wells, I.W. Drummond, K.S. Robinson, F.J. Street and J.P.S. Badyal, Polymer, 34, (1993), 3611.
22) R.K. Wells, I.W. Drummond, K.S. Robinson, F.J. Street and J.P.S. Badyal, Journal of Adhesion Science and Technology, 7, (1993), 1129.
23) M. Chtaib, J. Ghijsen, J.J. Pireaux, R. Caudano, R.L. Johnson, E. Orti, J.L. Bredas, Phys. Rev. B, 44, (1991), 10815.
24) R. Lazzaroni, N. Sato, W.R. Salaneck, M.C. Dos Santos, L.J. Bredas, B. Tooze, D.T. Clark, Chem. Phys. Lett., 175, (1990), 175.
25) E. Orti, J.L. Bredas, J.J. Pireaux, N. Ishihara, J. Elect. Spect. Rel. Phenom., 52, (1990), 551.
26) K. Seki in 'Optical Techniques to Characterize Polymer Systems', ed. by H. Bassler, p115, Elsevier, 1989.
27) R. M. Silverstein, G. C. Bassler and T. C. Morrill, 'Spectrometric Identification of Organic Compounds', Fourth Edition, Wiley (1980)
28) D. Briggs, A. Brown, J.C. Vickerman, 'Handbook of Static Secondary Ion Mass Spectrometry', Wiley (1989)
29) Micromass SX-200 Quadrupole Mass Spectrometer Instrument Manual, Vacuum Generators Ltd.
30) K. L. Busch in 'Ion Spectroscopies for Surface Analysis', ed. A. W. Czanderna and D. M. Hercules, 1991, Plenum Press, New York, p166.
31) J. D. Morrison in 'Gaseous Ion Chemistry and Mass Spectrometry', ed. J. H. Futrell, 1986, Wiley + Sons, p117.
32) Micromass QX-200 Quadrupole Mass Spectrometer Instrument Manual, Vacuum Generators Ltd.
33) R. Jede, O. Ganschow and U. Kaiser in 'Practical Surface Analysis' ed. D. Briggs and M. P. Seah, Vol 2, Second Edition, Wiley, (1990),Chapter 2.
34) R. Jede, O. Ganschow and U. Kaiser, 'Practical Surface Analysis', ed. D. Briggs and M. P. Seah, Vol 2, Second edn., Wiley, (1990), p19
35) P. J. Tayler, D. Price, G. Milnes, J. H. Scrivens, T. G. Blease, Int. J. Mass and Ion Proc., 89, (1989), 157
36) D. D, Beck and N. Somers, J. Vac. Sci. Tech., A10, (1992), 3216.

APPENDIX 2

SEMINARS, COURSES AND CONFERENCES ATTENDED

UNIVERSITY OF DURHAM - BOARD OF STUDIES IN CHEMISTRY COLLOQUIA, LECTURES AND SEMINARS

24. 10. 90	Dr. M. Bochmann (University of East Anglia) Synthesis, Reactions and Catalytic Activity of Cationic Titanium Alkyls.
1. 11. 90	Dr. N. Logan (Nottingham University) Rocket Propellants.
7. 11. 90	Dr. D. Gerrard (British Petroleum) Raman Spectroscopy for Industrial Analysis.
8. 11. 90	Dr. S. K. Scott (Leeds University) Clocks, Oscillations and Chaos.
14. 11. 90	Prof. T. Bell (SUNY, Stoney Brook, U.S.A.) Functional Molecular Architecture and Molecular Recognition.
29. 11. 90	Prof. D. Crout (Warwick University) Enzymes in Organic Synthesis.
5. 12. 90	Dr. P. G. Pringle (Bristol University) Metal Complexes with Functionalised Phosphines.
31. 1. 91	Dr. D. Lacey (Hull University) Liquid Crystals.
6. 2. 91	Dr. R. Bushby (Leeds University) Biradicals and Organic Magnets.
7. 2. 91	Dr. J. Markham (I.C.I. Pharmaceuticals) D.N.A. Fingerprinting.
17. 10. 91	Dr. J. A. Salthouse (University of Manchester) Son et Lumiere - a demonstration lecture.
31. 10. 91	Dr. R. Keeley (Metropolitan Police Forensic Science) Modern Forensic Science.
20. 11. 91	Dr. R. More O' Ferrall (University College, Dublin) Some Acid Catalysed Rearrangements in Organic Chemistry.
28. 11. 91	Prof. I. M. Ward (IRC in Polymer Science, University of Leeds) The SCI Lecture: The Science and Technology of Orientated Polymers.
4. 12. 91	Prof. R. Grigg (Leeds University) Palladium-Catalysed Cyclisation and Ion-Capture Processes.
5. 12. 91	Prof. A. L. Smith (ex-Unilever) Soap, Detergents and Black Puddings.
11. 12. 91	Dr. W. D. Cooper (Shell Research) Colloid Science: Theory and Practice.

22. 1. 92	Dr. K. D. M. Harris (St. Andrews University) Understanding the Properties of Solid Inclusion Compounds.
30. 1. 92	Dr. M. Anderson (Sittingbourne Research Centre, Shell Research) Recent Advances in the Safe and Selective Control of Insect Pests.
12. 2. 92	Prof. D. E. Fenton (Sheffield University) Polynuclear Complexes of Molecular Clefts as Models for Copper Biosites.
13. 2. 92	Dr. J. Saunders (Glaxo Group Research Limited) Molecular Modelling in Drug Discovery.
20. 2. 92	Prof. E. Vogel (University of Cologne) *The Musgrave Lecture* Porphyrins: Molecules of Interdisciplinary Interest.
26. 2. 92	Prof. M. L. Hitchman (Strathclyde University) Chemical Vapour Deposition.
5. 3. 92	Dr. N. C. Billingham (University of Sussex) Degradable Plastics-Myth or Magic.
18. 3. 92	Dr. H. Maskill (Newcastle University) Concerted or Stepwise Fragmentation in a Deamination-Type Reaction.
22. 10. 92	Professor A.G. Davies (University College, London) [RSC Ingold-Albert Lecture] The Behaviour of Hydrogen as a Pseudometal
22. 10. 93	The Ingold-Albert Lecture Prof. A. Davies (UCL) - The Behaviour of Hydrogen as a Pseudometal
5. 11. 93	Dr. C. Ludman (Durham) Explosions, a Demonstration Lecture
11. 11. 92	Professor D. Robins (Glasgow University) Pyrrolizidine Alkaloids: Biological Activity, Biosynthesis and Benefits
18. 11. 92	Dr. R. Nix (Queen Mary College, London) Characterisation of Heterogeneous Catalysts
9. 12. 92	Dr. A.N. Burgess (ICI Runcorn) The Structure of Perfluorinated Ionomer Membranes
13. 5. 93	Professor J.A. Pople (Carnegie-Mellon University, Pittsburgh) [RSC Boys-Rahman Lecture] Applications of Molecular Orbital Theory

CONFERENCES ATTENDED:

September 1991:	Polymer IRC Club Meeting, Durham University.
April 1992:	Macro Group UK Meeting, Durham University.
August 1993:	11th International Symposium on Plasma Chemistry, Loughborough University

EXAMINED LECTURE COURSES:

October 1990 - April 1991:

'Solids and Surfaces' - Dr J. P. S. Badyal and Dr N. D. S. Canning.

'Synthetic Polymers' - Prof. W. J. Feast.